Australasian Physical & Engineering Sciences in Medicine (2019) 42:285–401
https://doi.org/10.1007/s13246-019-00724-x

EPSM2018 ABSTRACTS

EPSM 2018, Engineering and Physical Sciences in Medicine

29–31 October 2018, Adelaide Convention Centre, Adelaide, Australia

KS01 The relative biological effectiveness of clinical proton therapy beams

H. Paganetti

Massachusetts General Hospital

The proton RBE varies among cell lines, tissues, endpoints, as well as with beam-quality. Experimental data do show a trend towards an increase in RBE as α/β of the linear-quadratic model decreases. Furthermore, one would also expect the RBE to increase as dose decreases. The RBE also increases with increasing linear energy transfer (LET). Phenomenological models are capable of predicting the RBE as a function of these parameters but input parameters for these models are solely based on cell survival data obtained in vitro. It is unclear if in vitro relationships can be translated to in vivo endpoints even for tumor control. Furthermore, to define normal tissue complications, the endpoint of cell survival may not be appropriate at all. Patient specific radiosensitivity is poorly understood and clinical evidence that RBE variations indeed matter in patients is scarce. Consequently, proton therapy uses a generic RBE of 1.1. However, variations in RBE are considered indirectly in proton therapy. In treatment planning, some qualitative consideration is given towards variable RBE values by, for instance, avoiding specific beam angles or reducing the dose to critical structures for a limited number of fractions. The current clinical focus is on mitigating potential impacts of proton RBE uncertainties.

This presentation will summarize our current knowledge of RBE variations as a function of normal tissue and tumor endpoints, as a function of dose, and as a function of energy deposition characteristics. Uncertainties with respect to in vivo RBE predictions will be discussed and implications in treatment planning will be outlined. Further, the current clinical evidence supporting a change in current clinical practice will be reviewed. Strategies to improve a treatment plan by redistributing the LET away from critical structures will be introduced as a way to move forward until more biological data become available.

KS02 Radiopharmaceutical therapy: the role of dosimetry in treatment optimization

G. Sgouros

Johns Hopkins University

Radiopharmaceutical therapy involves the delivery of radiation directly to tumor cells or to the tumor microenvironment. This is typically accomplished using radionuclides that are conjugated to targeting vehicles such as antibodies, peptides, small molecules, engineered nanostructures or, in some cases, by the biological properties of the unconjugated radionculides (e.g., radium chloride targeting of bone tumor, radioiodine targeting of thyroid malignancies).

Treatment optimization, in the context of RPT, may be defined as selecting the most appropriate amount of activity to administer to deliver a cytotoxic tumor absorbed dose without exceeding normal organ absorbed dose tolerance limits. Since RPT agents are administered systemically,

their optimization has proceeded by adopting the chemotherapy paradigm wherein optimization is based on an empirical process of administering different levels of activity on a per body weight or body surface area basis in a series of multi-center, multi-arm trials and then evaluating outcome for each administered activity level. This approach does not take advantage of the inherent distinction between RPT and chemotherapy agents. There is substantial experience in radiotherapy to relate tumor and normal organ absorbed doses to response and toxicity outcomes. This prior experience, coupled with the ability to image tumor and normal organ RPT agent localization in patients over time (by SPECT/CT or PET/CT, for example) may be used to calculate the corresponding absorbed doses and thereby implement absorbed dose-based optimization.

Absorbed dose-based treatment optimization could be implemented, for example, to help stratify patients based on the tumor or normal absorbed dose. In turn this could depend upon tumor burden or the clearance kinetics in individual patients. Early studies of new RPT agents should incorporate dosimetry to determine the potential impact of patient variability on absorbed dose. Ideally such studies could help identify and validate absorbed dose surrogates. Dosimetry-based treatment planning in such a scenario could be considered a biomarker that would help identify patients that most likely to benefit by RPT while also providing some guidance on the most appropriate administered activity for a given patient or population of patients. In this sense, dosimetry-based treatment optimization is a precision medicine approach to implementing RPT.

IS01 Do we now have the biomarkers to Identify Individuals with extreme normal tissue radiotoxicity?

O. Martin

Division of Radiation Oncology, Peter MacCallum Cancer Centre, Melbourne, VIC, Australia

Despite continual improvement in the efficacy of radiotherapy, its success is still limited by the inability to accurately identify prior to treatment, those patients who will suffer severe normal tissue toxicity due to high intrinsic radiosensitivity. While acute radiation side-effects are usually healed, the late adverse effects can be deemed more critical due to their persistent and often progressive nature and can produce severe and debilitating effects that can be fatal. Accordingly, the doses prescribed in current practice are largely based on the clinically determined tolerance of the normal tissues in the radiation field, and have evolved empirically to limit the proportion of patients who will suffer severe adverse reactions to about 1–5% of cases. Identification of radiosensitive individuals prior to commencing radiotherapy is essential for the development of personalized treatment in radiation oncology. Presently, radiosensitivity can only be predicted for the very small number of patients who have one of the rare phenotypic syndromes associated with mutations in DNA repair genes. A long-standing goal in radiation oncology is to identify markers that enable the prediction of individuals who are radiosensitive but do not exhibit a syndromic phenotype, so that therapy can be tailored to each patient. Several methodologies have been applied to develop functional assays based on measurements of *in-vitro* radiation response to predict clinical response. Chromosomal aberrations and clonogenic survival are the classical, most reliable endpoints to predict cellular radiosensitivity. However, they are not suitable for routine clinical use - they are time-consuming relative to the general urgency to commence radiotherapy. Numerous recent publications tested the gamma-H2AX assay as an attractive predictive functional assay that could identify highly radiosensitive individuals. There is a major discrepancy in these reports, however, no attempt has been done to analyse the causes of this discrepancy. Very rarely statistical criteria and the predictive power of the functional assays have been analysed. I will compare currently available functional assays that could be suitable for a large prospective evaluation of radiosensitivity in patients prior to commencing radiotherapy.

O001 Voxel-wise association of dose distributions with urinary toxicity in prostate cancer radiotherapy: results from the TROG 03.04 RADAR trial

M. Marcello[1,2], A. Haworth[3], A. Steigler[4], A. Kennedy[1], D. J. Joseph[1,5], J. W. Denham[6], M. A. Ebert[1,2]

[1]Department of Radiation Oncology, Sir Charles Gairdner Hospital, Western Australia, Australia. (20739859@student.uwa.edu.au [presenting author]), (Angel.Kennedy@health.wa.gov.au), (David.Joseph@health.wa.gov.au), (Martin.Ebert@health.wa.gov.au). [2]School of Physics and Astrophysics, University of Western Australia, Western Australia, Australia. [3]School of Physics, University of Sydney, New South Wales, Australia. (annette.haworth@sydney.edu.au). [4]Prostate Cancer Trials Group, Faculty of Health, University of Newcastle, Callaghan, New South Wales, Australia. (Allison.Steigler@newcastle.edu.au). [5]School of Surgery, University of Western Australia, Western Australia, Australia. [6]School of Medicine and Public Health, University of Newcastle, Callaghan, New South Wales, Australia. (Jim.Denham@newcastle.edu.au)

Introduction The purpose of this study was to utilize high-quality prostate radiotherapy clinical trial data to identify anatomically-localised regions where 3D dose-variation is associated with urinary toxicity.
Method The TROG 03.04 RADAR trial (1) tested the impact of duration of androgen deprivation on outcomes for prostate cancer patients receiving dose-escalated external beam radiation therapy (EBRT). The trial incorporated a plan-review process (2) in which planned 3D dose distributions, time-to-event data and other relevant subject-specific variables were recorded. Approximately 680 EBRT RADAR participant dose distributions were deformably registered onto a single exemplar. From these 680 subjects, 596 and 656 were available for analysis with dysuria and haematuria endpoints respectively. Voxel-wise Cox regression modelling was used to identify regions where 3D dose-variation was associated with the above urinary toxicities. These toxicities were defined combining both acute and late presentation.
Results Voxel-wise Cox regression modelling revealed regions where increases in dose were correlated with urinary toxicity. In particular, increased dose to the urethra was associated with increased dysuria (Figure 1) and increased dose to the bladder walls with haematuria. The results are consistent with proposed pathophysiological effects of increased radiation dose to these organs. For example, Blaivas et al(3) have proposed that substantial dose to the urethra can cause stricture formation, which could be causing irritation during urination, leading to dysuria presentation in the subject. It must be noted that the correlations are with planned dose and not actual dose.
Conclusion Voxel-wise association identified anatomical regions where dose variation is correlated with urinary toxicity. These organ sites become candidates for dose variation sensitivity in regards to urinary toxicity incidence.

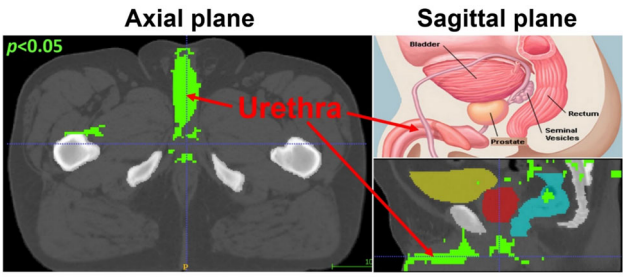

Figure 1 P-value map imposed onto exemplar CT with anatomical structures. The map shows regions where subjects with increased dose experienced a significantly higher ($p<0.05$) incidence of dysuria, as a result of the voxel-wise Cox regression analysis. These regions appear to directly coincide with the penile urethra.

References

1. Denham JW, Joseph D, Lamb DS, Spry NA, Duchesne G, Matthews J, et al. Short-term androgen suppression and radiotherapy versus intermediate-term androgen suppression and radiotherapy, with or without zoledronic acid, in men with locally advanced prostate cancer (TROG 03.04 RADAR): An open-label, randomised, phase 3 factorial. Lancet Oncol [Internet]. Elsevier Ltd; 2014;15(10):1076–89.
2. Ebert MA, Haworth A, Kearvell R, Hooton B, Coleman R, Spry N, et al. Detailed review and analysis of complex radiotherapy clinical trial planning data: Evaluation and initial experience with the SWAN software system. Radiother Oncol. 2008;86(2):200–10.
3. Blaivas JG, Weiss JP, Jones M. The pathophysiology of lower urinary tract symptoms after brachytherapy for prostate cancer. BJU international. 2006;98(6):1233–7.

Acknowledgements This work was supported by NHMRC grant APP1077788.

O002 Clinical translation of linac generated microbeam radiation therapy (MRT)

N. Suchowerska[1], A. D. Esteves[2], V. Peng[3], E. C. Mackonis[2], L. Delaney[2], D. McKenzie[3]

[1]VectorLAB, Radiation Oncology, Chris O'Brien Lifehouse. (natalka.suchowerska@lh.org.au [Presenting author]). [2]Radiation Oncology, Chris O'Brien Lifehouse. (Ana.Esteves@lh.org.au), (Elizabeth.Mackonis@lh.org.au), (Lyndal.Delaney@lh.org.au). [3]School of Physics, University of Sydney. (vpen0255@uni.sydney.edu.au), (David.McKenzie@sydney.edu.au)

Introduction The periodic high frequency spatial modulation, characteristic of synchrotron microbeam irradiations, can be approximated using a micro-multileaf collimator in a linac generated 6MV beam. We have previously reported that this technique achieves 30% more cytotoxicity than than a uniform field of the same average dose. This provides an opportunity for the therapeutic advantages of microbeam radiotherapy (MRT) to be translated into routine clinical practice.
Method Treatment plans were calculated using the Varian Eclipse™ planning system to deliver a prescribed average dose to the PTV either using uniform fields or spatially modulated fields, where the period of the modulation is 5mm and the beam width 2.5mm. The treatment was delivered on a Varian Novalis™ TX to cancer cell lines located in a customised CTDI phantom. The survival fraction for each plan and each cell line were compared.
Results Optimisation of a 7 field prostate plan for modulations with a period of 5mm was poorly achieved. Even with 'fluence painting' post-optimisation, the planned peak to valley ratio was compromised. The treatment time to deliver 3.5Gy with 7 fields was 20 min, significantly longer than the original single field treatment time (Peng 2017). These exposure constraints impact the cytotoxicity outcomes, with no improvement in cancer cell killing observed.
Conclusion A serious barrier to the clinical translation of this technique is that treatment planning and delivery systems are not designed or optimised to deliver periodic modulated radiation fields with high peak to valley ratio (PVR) and high spatial frequency.
Since our single field exposure *invitro* studies have yielded such compelling results with the Varian mMLC, the next step is collaboration with the manufacturer to drive the required software changes.
Acknowledgements We acknowledge The Prostate Cancer Foundation of Australia project grant funding

Reference

1. Peng V, Suchowerska N, McKenzie D R, Grid therapy using high definition multileaf collimators: realizing benefits of the bystander effect, Acta Oncologica, Vol56[8], 1048–1059, 2017

O003 A Pre-clinical image-guidance protocol for large animal radiotherapy studies at the Australian synchrotron

M. Barnes[1], L Day[1], J. Livingstone[2], D. Hausermann[2], D. Pelliccia[1], J. Crosbie[1]

[1]School of Science, RMIT University, Melbourne, Australia. (micah.barnes@student.rmit.edu.au Presenting author]), (liam.day@rmit.edu.au), (daniele.pelliccia@rmit.edu.au), (jeffrey.crosbie@rmit.edu.au). [2]IMBL, Australian Synchrotron, Melbourne, Australia. (jayde.livingstone@synchrotron.org.au), (daniel.hausermann@synchrotron.org.au)

Introduction A successful pre-clinical small animal image-guided synchrotron MRT study has been carried out on the Imaging and Medical Beamline (IMBL) at the Australian Synchrotron [1]. To date, all synchrotron radiotherapy studies on IMBL have been carried out in Hutch 2B; an experimental hutch equipped to deliver sub-millimetre alignment for small animals. The purpose of this study was to test the feasibility of providing equivalent sub-millimetre treatment accuracies in Hutch 3B for large animals. The technical challenges of delivering accurate, image-guided synchrotron radiotherapy in Hutch 3B on IMBL are discussed.
Method The Large Animal Positioning System (LAPS) in Hutch 3B on IMBL (pictured in Figure 1) was used for positioning a lamb cadaver. A 5x5 cm^2 broad-beam field was planned on a diagnostic quality CT scan in the Eclipse™ treatment planning system. An in-house image-guidance program, *SyncMRT*, was used to align the lamb cadaver to the treatment plan. Treatment accuracies were verified with film.

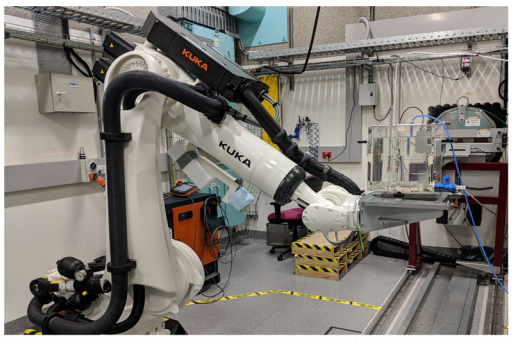

Figure 1: The Long Arm Animal Positioning System (LAPS) in Hutch 3B on IMBL at the Australian Synchrotron.

Results A lamb cadaver was successfully aligned and treated in Hutch 3B on IMBL (Figure 2); the treatment was repeated three times. For each treatment, the entire tumour volume was covered in the 5x5 cm^2 field, thus demonstrating that treatments on large-animals with modest margins is possible.

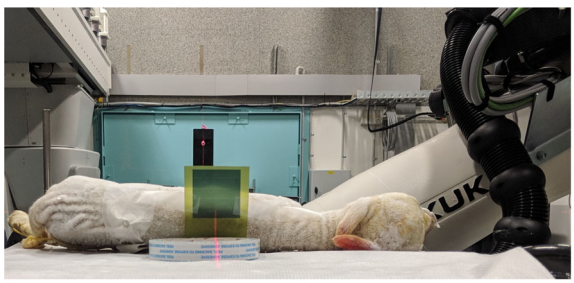

Figure 2: An image-guided synchrotron broad-beam treatment on a lamb cadaver in Hutch 3B on IMBL.

Conclusion There are mechanical challenges using LAPS for radiotherapy purposes; overcoming these require further technical development. Once fixed, sub-millimetre accuracies for alignment on

LAPS with large animals will be possible. Hutch 3B is not far away from satisfying the technical requirements to support a veterinary trial for image-guided synchrotron radiotherapy.

References

1. Livingstone, J., et. al. Preclinical radiotherapy at the Australian Synchrotron's Imaging and Medical Beamline: instrumentation, dosimetry and a small-animal feasibility study (2017). J. Synchrotron Rad. 24, 854–865.

O004 Synchrotron radiotherapy planning of a large animal cadaver using a commercial treatment planning system and a custom Monte Carlo dose calculation algorithm

L. Day[1], O. Algethami[1], M. Barnes[1], J. Livingstone[2], M. Donzelli[3], M. Klein[2], D. Hausermann[2], S. Bartzsch[4], S. Ryan, J. Crosbie[1]

[1]School of Science, RMIT University, Melbourne, Australia. (liam.day@rmit.edu.au [Presenting author]), (s3507645@student.rmit.edu.au), (micah.barnes@rmit.edu.au), (jeffrey.crosbie@rmit.edu.au). [2]Imaging and Medical Beamline, Australian Synchrotron, Melbourne, Australia. (Jayde.Livingstone@synchrotron.org.au), (Mitzi.Klein@synchrotron.org.au), (Daniel.Hausermann@synchrotron.org.au). [3]ID17 Biomedical Beamline, European Synchrotron Radiation Facility, Grenoble, France. (donzelli@esrf.fr). [4]Institute of Innovative Radiotherapy, Helmholtz-Centre, Neuherberg, Germany. (stefan.bartzsch@tum.de). [5]Faculty of Veterinary & Agricultural Science, University of Melbourne, Melbourne, Australia. (stewart.ryan@unimelb.edu.au)

Introduction Recent interest in animal radiotherapy of common household pets (such as dogs or cats) using synchrotron light at the Australian Synchrotron has necessitated preliminary trials on large animal cadavers in Hutch 3 of the Imaging and Medical Beamline (IMBL). The trials include all stages of the treatment delivery process, including CT simulation, treatment planning, patient positioning, dose delivery, and dose verification. Treatment planning is facilitated by the Eclipse treatment planning system (TPS) provided by Varian Medical Systems, Inc. and a custom Monte Carlo dose calculation algorithm [1].
Method A synchrotron radiation 5x5 cm^2 field was planned on a lamb cadaver CT in Eclipse. The cadaver was positioned on the Synchrotron's Large Animal Positioning System (LAPS) according to the plan and treated.

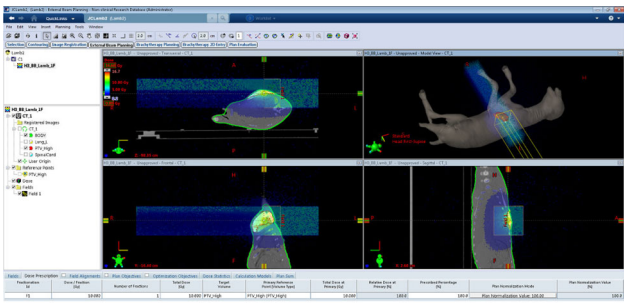

Eclipse synchrotron radiotherapy plan treating a mock-tumour in a lamb cadaver.

For dose verification, additional plans were produced on Solid Water® and liquid water tank geometries. Calculated doses were verified against ionisation chamber measurements for a number of fields.

Results A planned 5x5cm^2 synchrotron radiation field was successfully delivered to a mock-tumour target in a large animal cadaver at Hutch 3 of the IMBL.

Lamb cadaver on LAPS post treatment with synchrotron radiotherapy.

Measured doses for single field plans in Solid Water® and liquid water were all found to agree with dose calculations to within 3%. Larger fields (produced via re-adjustment of the LAPS position between field fractions) were found to disagree by $\sim$ 10%. Corrections to the mechanical motion of the LAPS and further refinements to the algorithm is expected to bring planned doses for larger fields into agreement.
Conclusion Eclipse has been used to plan synchrotron radiotherapy fields on a large animal cadaver in Hutch 3 at the Australian Synchrotron's IMBL. For single fields the plans show excellent agreement with measurements in water, and, provided that limitations in the LAPS are addressed, this preliminary study highlights the feasibility in delivering synchrotron radiotherapy as part of a veterinary trial for live animal patients.

References

1. Donzelli M, Bräuer-Krisch E, Oelfke U, Wilkens J, Bartzsch S (2018) Hybrid dose calculation: a dose calculation algorithm for microbeam radiation therapy. Phys Med Biol 63(4):045013. https://doi.org/10.1088/1361-6560/aaa705

O005 Comparison of radiographic skeletal survey and tin filtration CT

C. Boyd[1], M. Korlaet[2], L. Kruse[2], B. Drever[2], K. Hickson[1]

[1]SA Medical Imaging Physics, Adelaide, SA, Australia, 5000. (chris.boyd2@sa.gov.au [Presenting author]), (kevin.hickson@sa.gov.au). [2]Dr Jones & Partners Medical Imaging, Adelaide, SA, Australia. (mishelle.korlaet@drjones.com.au), (lars.kruse@drjones.com.au), (bradley.drever@drjones.com.au)

Introduction The current clinical standard for imaging of myeloma requires a digital radiographic skeletal survey (DR-SS) [1]. Recently published literature has suggested that MRI or CT, either as part of FDG PET/CT or Whole Body CT (WBCT) provides better information in many patients [2]. Compared to DR-SS, WBCT has relatively high radiation doses [3], although results have shown improved prognostic utility and diagnostic accuracy [1, 3, 2]. In this study, we investigated the effect tin filtration CT has in specific orthopaedic and haematological applications compared to DR-SS and the overall radiation dose.
Method The Siemens™ Somatom® FORCE CT allows implementation of tin (Sn) filtration, resulting in shaping of the energy spectrum. By removal of low energy photons through the use of Sn, patient dosimetry and image characteristics are dramatically changed from conventional aluminium only filtration. A qualitative image quality assessment was performed comparing Sn filtration CT images against DR-SS.
Comparative dose estimates were performed for the current clinical protocol of DR-SS using PCXMC [4]. Normalised CTDI

measurements were performed, and from this, a custom scanner profile was created on ImPACT [5]. Dose estimates were then performed using ImPACT for a "standard patient" using machine parameters intended for clinical use, including 150 kVp, 0.6 mm of Sn filtration and 30 reference mAs.

Results Using acquisition protocol and parameters specific to the site being investigated yielded a DR-SS dose of 0.94 mSv. Based on standardised patient parameters, the ImPACT dose was calculated to be 1.0 mSv. Qualitative results show radiographer and radiologist preference for performing and reviewing a CT series compared to a DR-SS.

Conclusion Tin filtration, 150 kVp, CT skeletal survey requires comparable radiation exposure to Digital Radiographic Skeletal Surveys. This study has identified a radiologist preference for Tin filtration CT with increased clinical outcomes to be further investigated.

References

1. A. Andrew Chantry, M. Kazmi, S. Barrington, V. Goh, N. Mulholland, M. Streetly, M. Lai and G. Pratt, "Guidelines for the use of imaging in the management of patients with myeloma," *British Journal of Haematology,* vol. 178, pp. 380–393, 2017.
2. S. Suntharalingam, C. Mikat, A. Wetter, N. Guberina, A. Salem, P. Hell, M. Forsting and K. Nassenstein, "Whole-body ultra-low dose CT using spectral shaping for detection of osteolytic lesion in multiple myeloma," *European Journal of Radiology,* 2018.
3. J. Hillengass, L. Moulopoulos, S. Delorme, V. Koutoulidis, J. Mosebach, T. Hielscher, M. Drake, S. Rajkumar, B. Oestergaard, N. Abildgaard, M. Hinge, T. Plesner, Y. Suehara, K. Matsue, N. Withofs, J. Caers, A. Waage, H. Goldschmidt, M. Dimopoulos and e. al., "Whole-body computed tomography versus conventional skeletal survey in patients with multiple myeloma: a study of the International Myeloma Working Group," *Blood Cancer Journal,* vol. 7, no. 8, p. 599, 2017.
4. M. Tapiovaara and T. Siiskonen, *PCXMC,* Helsinki: Säteilyturvakeskus (STUK), 2008.
5. Impactscan.org, *ImPACT CTDosimetry Software v1.0.4,* London: Impactscan.org, 2011.
6. Australian Government, "Availability and accessibility of diagnostic imaging equipment around Australia," Senate Community Affairs Committee, Canberra, 2018.
7. Siemens Healthcare, "System Owner Manual: Dosimetry and imaging performance report | C2-058.660.01.03.02," Siemens Healthcare, Erlangen, Germany, 2015.

O006 Acceptance and initial validation of Philips IQon Spectral CT

D. J. Serra[1], D. A. Carrick[1], T. Ireland[2]

[1]Gold Coast University Hospital, Biomedical Technology Services, QLD. (daniel.serra@health.qld.gov.au [Presenting author]), (deborah.carrick@health.qld.gov.au). [2]BTS Central, Biomedical Technology Services, QLD. (timothy.ireland@health.qld.gov.au)

Introduction The first Philips IQon spectral CT scanner in Australia was installed and commissioned at Gold Coast University Hospital in May 2018.

The Philips IQon uses a multi-layered "NanoPanel Prism" detector to simultaneously measure both high and low energy photons, and interpolates these spectral measurements to attain imaging results such as monoenergetic images (MonoE), iodine concentration images, virtual non-contrast images, iodine no water images and effective atomic number (Zeff) maps.

Method Routine acceptance testing was extended to perform validation of the spectral results. The validity of MonoE was assessed using the sensitometry (linearity) section of a Catphan600. The accuracy of Zeff maps were validated using the same sensitometry section of the Catphan, in conjunction with a radiotherapy Electron Density phantom with various tissue-equivalent material inserts. Iodine concentration samples ranging from 0.5 mg/mL to 15 mg/mL were produced to verify accuracy of results when imaged both in air and in a phantom.

Results The energy of the monoE reconstruction agreed with the measured effective energy to within 5% for energies of 40–140 keV and within 7% for 160–200 keV. The measured Zeff agreed with reported values to within 5% for 7 inserts and 10% for 2 inserts in the Catphan, and to within 10% for 7 inserts and 30% for 1 insert (lung inhale) in the ED phantom. Iodine concentration quantification (15–0.5 mg/ml) measured at various CTDI, kVp and phantom locations was underestimated by 20–66%, with the poorest accuracy at lower iodine concentrations.

O007 A tool to aid protocol naming regularization across multiple CT scanners

K. P. L. Ewert, P. Ratnakanthan, Z. Brady

Radiology Department, Alfred Health, Melbourne, Australia. (K.Ewert@alfred.org.au [Presenting author]), (P.Ratnakanthan@alfred.org.au), (Z.Brady@alfred.org.au)

Introduction The growing adoption of patient dose management software has increased the data available to medical physicists but introduces the obstacle of inter-scanner comparisons. In CT, a key difficulty is the differences in protocol naming across vendors, facilities, and departments. Data collection and analysis can be made simpler by standardizing the protocol naming nomenclature across scanners, and this process can be aided by using a program designed to aid a user (e.g. supervising radiographers) in creating standardization names and pairing them to protocols on other scanners. This standardization would also assist in the auditing and comprehension of the CT protocol parameters [1].

Method A facility wide nomenclature was established that describes different protocol scanning types, pathologies, and contrast phases. Exhaustive lists of currently programmed protocol names were extracted from six CT scanners, and fed into a combined database. A program was written (VBA and Excel) that takes single protocol names and prompts the user to select the appropriate scanning features and automatically generates names according to the established nomenclature. These changes are fed back to the database to be exported and used as a summary of necessary protocol names to be edited on the modality.

Results Over 1380 idiosyncratic protocol names were examined and assigned an improved descriptor matching the constraints of the nomenclature. The consequent regularization of protocol names across scanners then reduced the sum total of unique protocol names.

Conclusion The regularization of protocol names has improved protocol recognition for staff working across multiple scanners, with the potential advantage of avoiding unnecessary patient exposure when protocol selection errors are made. Additionally, the introduced systematic naming will in future aid any auditing processes (including dose surveys) and categorization of patient doses in dose reporting software.

References

1. Cody DD, Fisher TS, Gress DA, Layman JR, McNitt-Gray MF, Pizzutiello JR, Fairobent LA. AAPM medical physics practice guideline 1. a: CT protocol management and review practice guideline. Journal of applied clinical medical physics. 2013 Sep;14(5):3–12.

O008 Large cohort retrospective CT dosimetry

Z. Brady[1,2], A. Forsythe[2], C. Lee[3], B. E. Moroz[3], A. Berrington de González[3], J. D. Mathews[2]

[1]Radiology Department, Alfred Health, Australia. (z.brady@alfred.org.au [Presenting author]). [2]Melbourne School of Population and Global Health, The University of Melbourne, Australia. (annaf@unimelb.edu.au), (mathewsj@unimelb.edu.au). [3]Division of Cancer Epidemiology and Genetics, National Cancer Institute, National Institutes of Health, US. (leechoonsik@mail.nih.gov), (morozb@mail.nih.gov), (berringtona@mail.nih.gov)

Introduction It is not common in Australia for diagnostic imaging medical physicists to work with epidemiologists and statisticians. However, the pooling of our diverse skills provides an expert team to investigate the shape of the radiation dose response curve in the low dose range relevant to diagnostic imaging. In our analysis of low dose risks from CT scans performed on young people, complex retrospective dosimetry was necessary.
Method We used de-identified Medicare records between 1985 and 2005 to create a cohort of 11.6 million young Australians of whom 688,260 had at least one funded CT scan while aged less than 20 years. Historical data on representative volumetric computed tomography dose index ($CTDI_{vol}$) values was obtained from the literature, manufacturer manuals, Australian surveys and hospital protocols. A regression model was developed to predict an input $CTDI_{vol}$ matrix for each region examined by year of age and by calendar year. This matrix was input into the National Cancer Institute dosimetry system for CT (NCICT) [1] using paediatric phantoms to calculate mean organ doses.
Results Except in very young children (< 5 years) CT use more than doubled in the study period. Most scans were of the brain or face (70%). For a single phase head scan the sex- and age-averaged brain dose was 48 mGy in 1985 (range 33–68 mGy) reducing to 26 mGy (18–37 mGy) in 2005. Dose to the bone marrow from a head scan in 1985 was approximately 10 mGy, which halved by 2005. Figure 1 shows the dose distribution, including scatter, for three common scans.
Conclusion Collaborative research between different scientific and medical fields is essential if we are to fully understand and quantify excess risks caused by ionising radiation from medical imaging. Undertaking large scale retrospective dosimetry for historical cohorts is an important part of epidemiological research.

References

1. Lee C, Kim K, Bolch W, Moroz B, Folio L. (2015) NCICT: a computational solution to estimate organ doses for pediatric and adult patients undergoing CT scans. Journal of Radiological Protection 35(4):891–909.

Acknowledgements This study was supported by project grants 509190 and 1027368 from the National Health and Medical Research Council.

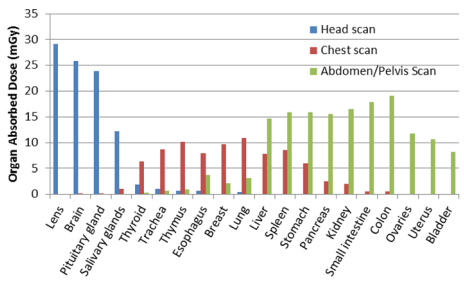

Figure 1: Organ absorbed dose (mGy) for a 10 year old female undergoing CT scans of the head, chest and abdomen/pelvis in 2005.

O009 Dose reduction using sinogram affirmed iterative reconstruction (SAFIRE) software for dedicated paediatric computed tomography (CT) protocols

J. A. Miller, T. Markwell, L. Sim, J. Baines, S. Zawlodzka

Radiation Oncology – Princess Alexandra Hospital Raymond Terrace (ROPART), South Brisbane, Queensland, Australia. (Julie-Anne.Miller@health.qld.gov.au [Presenting author]), (Tim.Markwell@health.qld.gov.au), (Lucy.Sim@health.qld.gov.au), (John.Baines@health.qld.gov.au), (Sylwia.Zawlodzka-Bednarz@health.qld.gov.au)

Introduction For paediatric radiotherapy patients, imaging dose arising from Computed Tomography (CT) simulation is of concern given the life expectancy of these patients and the associated relative risks of secondary induced cancers. In our clinic, paediatric body and head CT scan protocols utilise the Filtered Back Projection (FBP) algorithm.
Method Three Siemens Sinogram Affirmed Iterative Reconstruction (SAFIRE)[1] algorithm strengths (S2, S3 and S4) were compared with the clinically standard FBP protocol on a Siemens Definition AS Open 20 slice CT scanner operating at 120 kVp. In this phantom study, the image quality metrics (noise and spatial resolution) were measured using the CATPHAN 600 phantom. Contrast to Noise Ratio (CNR)[2] was calculated using measurements from the CIRS 62 electron density phantom.
The dose reduction due to SAFIRE was compared against FBP, whilst maintaining comparable noise level in the CATPHAN water module. Improvements in image quality were also evaluated by maintaining the same imaging dose.
Results Image quality (CNR and noise) improved with increasing SAFIRE strength. There was no change in spatial resolution due to algorithm choice. The CT number was within ±5 HU agreement with the corresponding FBP scan. Table 1 shows the maximum dose reduction achievable with SAFIRE, whilst maintaining the same noise level as FBP.

Table 1: Dose reduction using SAFIRE

Protocol	Settings	Dose reduction (%)
Brain	3mm slices with smooth body kernel	46
High Definition Brain	0.6mm slices with sharp head kernel	46
Cranio-Spinal	2mm slices with smooth body kernel	36

Conclusion The SAFIRE algorithm can be used to lower the dose, while retaining image quality or improving the image quality relative to the FBP at the same dose.

References

1. Grant K. and Raupach R., (2012) Siemens Healthcare SAFIRE: Sinogram Affirmed Iterative Reconstruction whitepaper.
2. Hobson et. al, (2014) Using the American College of Radiology (ACR) CT accreditation phantom for routine image quality assurance on both CT and CBCT imaging systems in a radiotherapy environment, Journal of Applied Medical Physics, 15(4), 2014.

O010 Towards low-dose iterative cone-beam CT reconstruction

E. M. Cai[1,2,3], M. Byrne[1], B. Archibald-Heeren[1], G. Liu[1], P. Metcalfe[3], A. Rosenfeld[3], Y. Wang[2,3]

[1]Radiation Oncology Centre, Wahroonga. (emma.cai@icon.team [Presenting author]), (mikel.byrne@roc.team), (ben.archibald-heeren@roc.team), (guilin.liu@roc.team). [2]Icon Cancer Centre, Revesby. (yang.wang@icongroup.global). [3]Centre of Medical Radiation Physics, University of Wollongong. (metcalfe@uow.edu.au), (anatoly@uow.edu.au)

Introduction Cone-Beam CT is being increasingly used in routine radiation therapy for image guidance and adaptive dose assessment. Iterative reconstruction algorithms have been shown to improve image quality over FDK while simultaneously reducing dose to patients. This work explores the use of CERN's open source TIGRE toolbox [1] for low dose CBCT reconstruction.
Method CBCT of a Catphan was acquired using head mode (full-fan half-trajectory) on a Varian TrueBeam. Every second projection image was used for further processing. Air normalisation, kV output normalisation and lag correction were applied to the raw projection data. TIGRE toolbox was implemented in Matlab for image reconstruction. Conjugate-gradient least-squares (CGLS) algorithm was run using FDK result as initial estimate. After the first round of reconstruction, a novel first-order, empirical beam hardening correction method was implemented. The model decouples the beam hardening effect from bowtie filter and the imaging object, then compensates for both and estimates the monochromatic equivalent projections based on object geometry. CGLS was run a second time with beam hardening corrected projections.
Results Varian reconstruction using 500 projections, FDK and CGLS reconstruction using 250 projections are compared in figure 1. As the number of projections decreased, FDK suffered from increased noise while CGLS achieved similar SNR. Beam hardening correction was shown to improve HU uniformity and reduce cupping artefact.

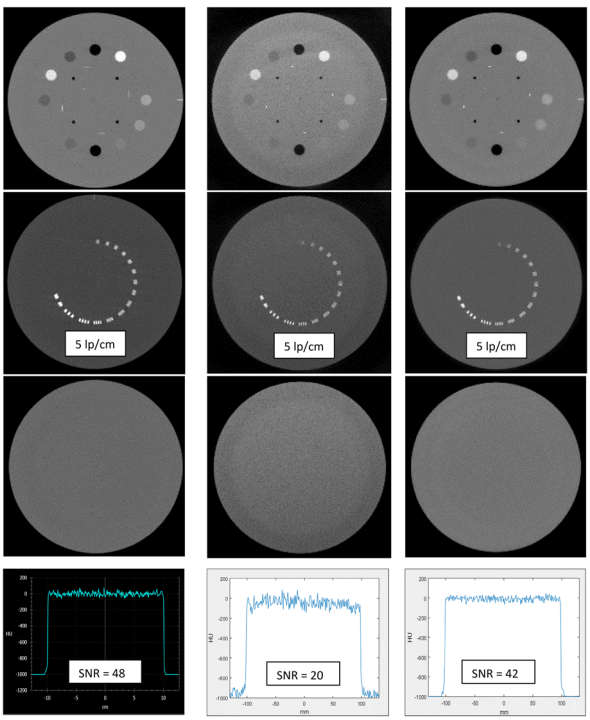

Figure 1.Catphan reconstruction result. left: Varian reconstruction using 500 projections; middle: FDK reconstruction using 250 projections; right: CGLS reconstruction with beam hardening correction using 250 projections. Top three rows: HU, high contrast resolution and uniformity section. Bottom row: midline horizontal profile indicated by the dotted blue line in the uniformity image.

Conclusion This work presented the application of an open source toolbox and an empirical beam hardening correction method for iterative CBCT reconstruction. Implementation of iterative methods may lead to significant imaging dose reduction.

References

1. Biguri A, Dosanjh M, Hancock S, Soleimani M (2016) TIGRE: a MATLAB-GPU toolbox for CBCT image reconstruction. *Biomed. Phys. Eng. Express.*

IS02 Medical device usability observations through the use of in-situ simulation

M. Sheedy

Medical Physics & Bioengineering, Canterbury District Health Board, Christchurch, New Zealand. (michael.sheedy@cdhb.health.nz [Presenting author])

Introduction The use of simulation is common place in clinical environments for strengthening teamwork and communication as well as teaching skills based tasks. It is also a useful tool for observing device usability and highlighting potential issues. In-situ simulation is particularly good as it allows the medical device to be used in its typical environment. By minimising or highlighting medical device usability errors, a much safer clinical space can be created for patients and staff.
Method In-situ simulations are simulated medical events that occur in a typical clinical space such as an emergency department trauma bay. Regular scenarios are run which have learning objectives for clinical components and can involve the use of real medical devices. Technical observations of the usability of medical devices are made and fed back to clinical educators. These observations are based on actual devices and interactions with it in context to its clinical use.
Results The use of simulation at the Canterbury District Health Board has found a number of medical devices with usability issues. These are either inherent device issues or created due to the environment they are used in. Simulation has highlighted device labelling issues in some devices creating confusion about proper device use. There have also been equipment positioning issues creating additional challenges for clinical procedures such as intubating. Physiological waveforms on monitors were also found to be different colours in different clinical areas creating potential confusion of information.
Conclusion In-situ simulation enables safe observations of how equipment is used in the clinical environment. By highlighting medical devices usability issues then the issue can be rectified or training put in place to educate staff in its proper use. Ideally potential issues would be identified in the procurement process so that medical device issues are known before large scale deployment throughout the hospital.

IS03 Visual electrophysiology: an insight into sight

E. Shelva

Sir Charles Gairdner Hospital

Clichéd as 'the window to the soul', the eye is compact, compartmental, of small volume, and respects the blood-brain barrier. As such, it offers many unique opportunities for research and advancement in diagnosis and treatment of eye diseases, including high resolution diagnostic imaging modalities, gene-based therapies and prosthetic implants. Evaluation of these technologies requires sensitive and reliable measures of visual function.

Visual electrophysiology is unique in its ability to provide objective measures of the function of various cell types, metabolic activity and axonal connections involved in the process of vision. It utilises highly specialised electrodes which are placed at strategic sites on or near the eye, or on the scalp, to record electrical activity in response to specific photic stimulation.

Test protocols such as the electrooculogram, electroretinogram and visual evoked potential target specific structural elements to provide important diagnostic information on rod and cone photoreceptors, pigment epithelial, bipolar, amacrine and ganglion cells, and optic nerve pathways. These procedures are applied routinely in subspecialty clinics for inherited retinal disease, neuro-ophthalmology, paediatric ophthalmology, functional visual disturbance, and early detection of drug-related toxicity. Research applications include monitoring treatment effects and assessment of ocular safety in clinical drug trials.

The eloquence of visual electrophysiology in determining aetiology of eye disease, measuring its progression and evaluating response to treatment speaks for itself.

We would like to acknowledge the dedication and generosity of ophthalmologists, Drs Douglas Candy, Jane Khan and Steve Colley who have devoted years of their own time to report on the hundreds of patients annually, with no financial benefit whatsoever to themselves.

O11 Evaluation of the routine use of IO-TOE in non-valve cardiac surgery

I. R. Smith[1], R. B. Garlick[2], J. S. Keys[2], J. T. Rivers[3]

[1]Physical Sciences, St Andrew's War Memorial Hospital, Brisbane, Australia. (ismith@sawmh.com.au [Presenting author]). [2]Cardiac Surgery, St Andrew's War Memorial Hospital, Brisbane, Australia. (garlick.bruce@gmail.com), (jkeysie@hotmail.com). [3]Queensland Cardiovascular Group, Brisbane, Australia. (johnr@qcg.com.au)

Introduction Intra-operative transoesophageal echocardiograpy (IO-TOE) contributes to improved outcomes for patients undergoing valve related surgery, however, debate continues concerning it's benefit in non-valve cases. In this study we evaluate a single site experience with IO-TOE in cardiac surgery.

Methods Data for 4116 cardiac surgery procedures, comprising 1584 isolated Coronary Artery Bypass Graft (CABG): 1687 Valve Only, 712 CABG+Valve and 133 Other Cardiac procedures performed between Nov-08 and Dec-17 were analysed. Propensity score based analysis was used to quantitatively assess the impact of IO-TOE on a range of acute peri- and post-operative process measures and outcomes including major adverse cardiac and cerebrovascular events (MACCE).

Results Use of IO-TOE was associated with a 'transient' increase in bypass duration; however, there was no discernible increase in the major negative consequences linked to prolonged time on bypass. Although an increase in intraoperative variations was noted this was potentially linked to improved detection with IO-TOE. Knowledge of these findings did not translate to improved outcomes. Across all surgery types, IO-TOE was linked to increased adverse events such as pulmonary complications (OR 1.5). A similar pattern of outcomes is shown for isolated CABG cases, although none achieve significance. There is no evidence of reduction in MACCE following CABG involving IO-TOE (OR 1.0). Longer term, there does not appear to be any survival advantage associated with IO-TOE in CABG.

Conclusion Expanded use of IO-TOE in CABG is largely argued on the ability to identify and respond to unexpected findings not evident during pre-operative assessment or arising during surgery. The quality of pre-operative workup at the study site may negate any advantage gained through use of IO-TOE. The outcome of this study questions the value of routine IO-TOE in CABG.

O12 Supervised machine learning of prostate cancer in the peripheral zone using multiparametric MRI

N. Gholizadeh[1], J. Simpson[2,3], S. Ramadan[1,4], D. Lee[2,3], P. Lau[4,5], P. B. Greer[2,3]

[1]Faculty of Health and Medicine, The University of Newcastle, Australia. (Neda.gholizadeh@uon.edu.au [Presenting author]), (saadallah.ramadan@newcastle.edu.au). [2]Faculty of Science, The University of Newcastle, Australia. (John.Simpson@calvarymater.org.au), (Danny.Lee@newcastle.edu.au), (peter.greer@newcastle.edu.au). [3]Calvary Mater Newcastle, Radiation Oncology, Australia. [4]Hunter Medical Research Institute (HMRI) Imaging Centre, Australia. [5]Calvary Mater Newcastle, Radiology, Australia. (Peter.lau@hnehealth.nsw.gov.au)

Introduction Multiparametric MRI (mp-MRI) combines anatomical with different functional techniques to achieve improved accuracy or tissue characterization and is routinely applied in the study of prostate cancer [1]. The increased number of images generated during mp-MRI increases image interpretation time and interpretation difficulty [2]. Machine learning has the potential to improve the efficiency and consistency of prostate mp-MRI interpretation and aid the accuracy of prostate lesion detection and delineation and provide a consistent response to treatment evaluation [3]. The purpose of this study was to develop and evaluate a machine learning system for peripheral zone (PZ) prostate cancer using mp-MRI including T2WI, diffusion weighted imaging (DWI) and diffusion tensor imaging (DTI).

Method Twelve high-grade prostate cancer patients signed written consent prior to participating in this study. Cancer and healthy region of interests (ROI)s were outlined in the peripheral zone (PZ) by a radiologist. A total of 192 different features were extracted from within cancer and healthy ROIs from the mp-MRI images. The dataset was divided into two parts, a training set (10 patients) and testing set (2 patients). Principle component analysis (PCA) was used for dimension reduction. A nonlinear support vector machine (SVM) using a Radial Basis Function (RBF) was used to generate a model for classifying as either tumour or healthy tissue. The testing data set was used to validate the optimised classification model and the accuracy, sensitivity, specificity of the model was measured.

Results The classifier achieved an area under the ROC curve of 0.902. Figure 1 shows an example of machine learning output. The accuracy, sensitivity and specificity of the model using the testing data set are summarized in Table 1.

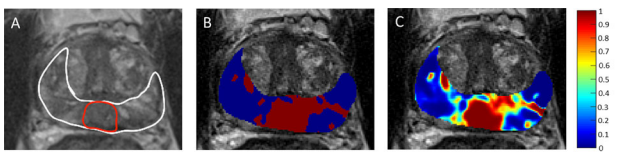

Figure 1. A) Axial T2WI of a prostate cancer patient with delineation of peripheral zone (white) and cancer (red) regions with B) corresponding output of RBF-SVM and C) probability map of RBF-SVM.

Table 1. Accuracy, sensitivity, specificity, precession and recall results of RBF-SVM classifier for two testing patient dataset.

	%Accuracy	%Sensitivity	%Specificity
test 1	92.9	98.9	87.7
test 2	88.8	91.4	83.7

Conclusion This study demonstrated the ability of T2WI, DWI and DTI to accurately PZ prostate cancer diagnosis using RBF-SVM. The output potentially provides valuable tool to aid physicians for prostate cancer diagnosis.

References

1. Delongchamps NB, Beuvon F, Eiss D, Flam T, Muradyan N, Zerbib M, Peyromaure M, Cornud F (2011) Multiparametric MRI is helpful to predict tumor focality, stage, and size in patients diagnosed with unilateral low-risk prostate cancer. Prostate cancer and prostatic diseases 14 (3):232
2. Assefa D, Keller H, Menard C, Laperriere N, Ferrari RJ, Yeung I (2010) Robust texture features for response monitoring of glioblastoma multiforme on T1-weighted and T2-FLAIR MR images: a preliminary investigation in terms of identification and segmentation. Med Phys 37 (4):1722–1736. https://doi.org/10.1118/1.3357289
3. Niaf E, Rouvière O, Lartizien C Computer-aided diagnosis for prostate cancer detection in the peripheral zone via multisequence MRI. In, 2011. pp 79633P-79633P-79638

O13 First in world clinical implementation of REspiratory Adaptive Computed Tomography (REACT) reduces imaging artefacts

N. Morton[1], J. Sykes[2,3], J. Barber[2,3], J. Kipritidis[4], C. Hofmann[5], P. Keall[1], R. O'brien[1]

[1]ACRF Image X Institute, Faculty of Medicine and Health, University of Sydney, Australia. (nmor8420@uni.sydney.edu.au [Presenting author]), (paul.keall@sydney.edu.au), (ricky.obrien@sydney.edu.au). [2]Blacktown Cancer and Haematology Centre, Sydney West Cancer Network, Blacktown Hospital, Australia. (Jonthan.sykes@health.nsw.gov.au), (Jeffrey.barber@health.nsw.gov.au, f.lastname@gmail.com). [3]Institute of Medical Physics, School of Physics, The University of Sydney, Australia. [4]Northern Sydney Cancer Centre, Royal North Shore Hospital, Northern Sydney Health District, Australia. (John.kipritidis@sydney.edu.au). [5]Siemens AG, Imaging and Radiotherapy Department, Florchheim. (hc.hofmann@siemens-healthineers.com)

Introduction Respiratory Adaptive Computed Tomography (REACT) system aims to mitigate motion errors which currently occur in up to 90% of 4DCT images. Errors are caused by inconsistent patient breathing, and have deleterious effects on tumour delineation and functional imaging. The REACT system identifies changes to a patient's breathing cycle and gates the beam in real-time. This investigation implements the REACT method on a clinical CT scanner for the first time and quantifies its effect on reducing imaging artefacts.

Method Three respiratory traces were simulated on CIRS dynamic thorax phantom. Phantom motion was detected using the Varian Real-time Position Management system and fed to our in-house REACT software. The software detects irregularities in the breathing trace and prospectively gates CT scans accordingly. Each set of images was acquired for peak inhale and visually compared to the peak inhale phase of conventional 4DCT. The total volume difference to the phantom ground truth was calculated.

Results Image artefacts were visually found in all three conventional scans. These artefacts were reduced in two of three real-time triggered images. The total volume error as compared to the phantom ground truth was reduced by 81% and 27% in two cases and increased by 11% in on case.

Conclusion The REACT, real-time, respiratory-triggered CT method, was successfully integrated with a clinical CT scanner for the first time. The results showed a reduction in imaging errors in comparison to conventional 4DCT techniques, complementing results from previous in silico studies. This is the first step in introducing patient specific imaging, creating clearer images for clinical use.

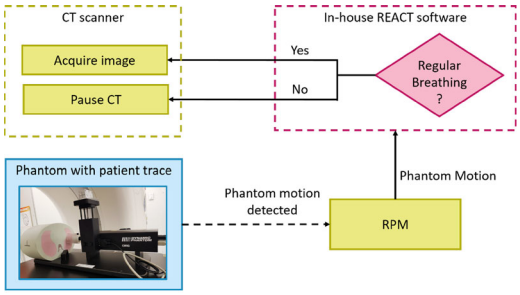

Figure 1: Workflow of experimental setup and real-time gating of the CT scanner.

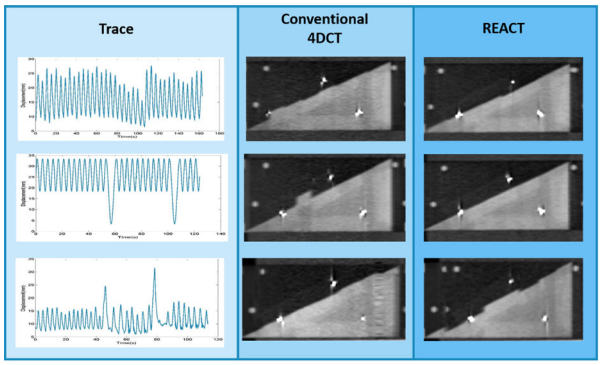

Figure 2: Images of phantom film insert. Conventional 4DCT vs REACT method.

O14 Initial phantom validation of Hounsfield Unit corrected cone beam CT for adaptive radiotherapy

S. Lydiard[1], G. Bengua[1], J. Sandison[1], S. Andersson[2], R. Nilsson[2]

[1]Radiation Oncology Department, Auckland City Hospital, Auckland, New Zealand. (slydiard@adhb.govt.nz [Presenting Author]), (gerardb@adhb.govt.nz), (jsandison@adhb.govt.nz). [2]RaySearch Laboratories AB, Stockholm, Sweden. (sebastian.andersson@raysearchlabs.com), (rasmus.nilsson@raysearchlabs.com)

Introduction Calculating dose accurately on cone beam CT (CBCT) is challenging; CBCT intensity-electron density relationship is not easily established and is dependent on imaging protocol and patient anatomy. An algorithm that converts CBCT intensities to the same scale as CT intensities and corrects for shading artefacts is being

developed in the RayStation (RaySearch Laboratories) treatment planning system. This Hounsfield Unit (HU) correction tool allows the use of the CT HU to electron density relationship for CBCT dose calculations. We report the first results of this technique for prostate on an anthropomorphic phantom.

Method The pelvis of the phantom was imaged using CT and a total of six CBCT imaging protocols across two CBCT systems. Images were imported into RayStation for subsequent analysis. Deformable registrations between the CT and CBCTs were generated. The prostate, bladder, rectum and left femoral head were contoured on each image set or propagated from the CT. The HU correction tool was used to create a corrected CBCT (corr_CBCT). A VMAT plan prescribing 80Gy to the prostate was calculated on the CT, the bulk density overridden original CBCTs (bd_CBCTs), and the corr_CBCTs. Voxel-based analysis of the HU distribution and dose metrics for pelvis structures in the CBCTs were compared to the CT.

Results The absolute differences and standard deviations in the mean HU for pelvis structures compared to the CT were considerably smaller on the corr_CBCTs than CBCTs (Table 1). The difference in CT mean doses ranged from 0.1–2 Gy for bd_CBCT and 0.2-1.5 Gy for corr_CBCT.

Table 1: Average and standard deviations of HU differences between CT, CBCT, and corr_CBCT for average HU in pelvis structures.

	Intensity Difference (HU)	
	CT - CBCT	*CT - corr_CBCT*
Prostate	-302 ± 172	-11 ± 7
Bladder	237 ± 178	2 ± 2
Rectum	-17 ± 122	-10 ± 14
Left Femoral Head	-359 ± 248	-4 ± 78

Conclusion The CBCT HU correction tool improved the CBCT HU agreement with CT for the investigated pelvis structures, irrespective of imaging protocol or CBCT system. This resulted in a closer mean dose estimate for pelvis structures. Retrospective investigation on clinical datasets is underway to further assess the clinical usefulness of this tool.

O15 Validation of the DirectDensity™ reconstruction algorithm for conversion of CT numbers to mass-density and its application in radiotherapy treatment planning

M. Lawson[1], D. Wilkinson[2], A. Ceylan[2], P. Metcalfe[1]

[1]Centre for Medical Radiation Physics, University of Wollongong, NSW, Australia. (ml387@uowmail.edu.au [Presenting author]), (metcalfe@uow.edu.au). [2]Illawarra Cancer Care Centre, Wollongong Hospital, NSW, Australia. (Dean.Wilkinson@health.nsw.gov.au), (Abdurrahman.Ceylan@health.nsw.gov.au)

Introduction A Computed Tomography (CT) Number (#) to density calibration curve is required for radiotherapy treatment planning to accurately calculate the dose distribution within an anatomical CT data set. The CT# to density calibration curve is tube energy-dependent and so for simplicity, often only a single kilovoltage-peak (kVp) tube setting is used for all radiotherapy patient scans.

SIEMENS developed a novel CT reconstruction algorithm known as DirectDensity™ (DD) that performs a two-material decomposition of the raw CT images into effective water and bone thickness components yielding a DD CT image with CT# values that are independent of tube voltage [1].

Method CT# to mass-density calibration curves were generated on a SIEMENS SOMATOM Confidence CT for tube voltages 70–140 kVp. Comparison of CT#s with and without DD were performed for known tissue analogue materials.

To assess dose calculation accuracy of DD CT images for treatment planning, a CIRS anthropomorphic head and neck phantom was scanned at 80, 120 and 140 kVp. DD CT data sets were generated for all energies and compared with a standard 120 kVp 'control' scan. A common VMAT plan was calculated on each CT data set using Pinnacle[3] treatment planning system and dose-volume statistics calculated for a common set of target volumes and organs-at-risk.

Results Experimental DD CT#s showed high correlation to the expected identity line with an $R^2 > 0.98$ for all energies indicating energy-independence (Figure 1).

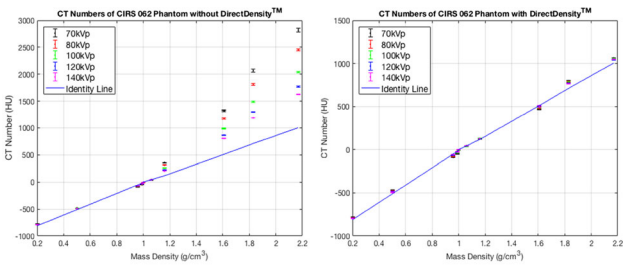

(Figure 1: CT numbers vs mass density for known tissue analogues with and without DirectDensity™)

For the VMAT plan, target volume V95% and organ-at-risk mean dose varied by less than 0.5% between the DD data sets to the control scan. The image quality of DD CT data sets was non-inferior in terms of spatial resolution, contrast and uniformity.

Conclusion DirectDensity™ provides options for optimising tube voltage during CT simulation, whilst maintaining dose calculation accuracy for radiotherapy treatment planning.

References

1. Ritter A. and Mistry N. (2016) Direct Density: Technical principles and implications for radiotherapy, SIEMENS Healthineers, SIEMENS Healthcare GmbH, Germany.

O16 Evaluation of dual energy CT and iterative metal artefact reduction (iMAR) for artefact reduction in radiotherapy applications

P. Lim[1], J. Barber[1,2], J. Sykes[1,2]

[1]School of Physics, University of Sydney, Australia. (plim3421@uni.sydney.edu.au [Presenting author]), (Jeffrey.barber@health.nsw.gov.au) (jonathan.sykes@health.nsw.gov.au). [2]Radiation Oncology, Blacktown Hospital, Sydney West Cancer Network, Australia

Introduction The number of patients with metal implants is continually increasing due to aging population and high success rates of orthopaedic implants. Metal artefacts pose a constant problem in Single Energy Computed Tomography (SECT) images used for radiotherapy. Virtual Monoenergetic (VME) images constructed with dual energy CT (DECT) scans can be used to reduce beam hardening artefacts. Dual energy metal artefact reduction (DE-MAR) is compared and combined with iMAR to determine optimal imaging strategies for patients with metal implants.

Method SECT and DECT scans were performed on a Siemens Somatom AS-64 Slice CT scanner. Images were acquired of a

modified CIRS pelvis phantom with a 20mm stainless steel rod and VME images reconstructed at 100, 120, 140 and 190 keV. These were post-reconstructed with and without the iMAR algorithm. Artefact reduction was measured using: 1) the difference in HU with and without MAR for 4 regions of interest (ΔHU); 2) the total number of artefact pixels (N_{art}), defined as pixels with a difference (between images with metal rod and without) exceeding a threshold; 3) the mean pixel intensity difference of the artefact pixels (I_{art}).

Results

DE-MAR, SECT + iMAR and DE-MAR + iMAR were compared. ΔHU (relative to SECT) was 19.8% in DE-MAR_{120keV}, 7.6% in SECT + iMAR and 8.2% in DE-MAR_{120keV} + iMAR images. N_{art} was lowest for DE-MAR_{190keV} + iMAR. I_{art} was lowest for SECT+ iMAR.

Conclusion Both SECT + iMAR and DE-MAR + iMAR offer successful MAR for phantom simulating unilateral hip implant. DE-MAR gives minimal artefact reduction over iMAR alone. However, there are limitations in the metrics used which have scope for improvement.

O17 The most likely path of protons in heterogeneous media and its application to proton computed tomography

M. D. Brooke[1], S. N. Penfold[2,3]

[1]CRUK/MRC Oxford Institute for Radiation Oncology, University of Oxford, UK. (mark.brooke@oncology.ox.ac.uk [Presenting author]). [2]Department of Physics, University of Adelaide, Australia. (scott.penfold@adelaide.edu.au). [3]Department of Medical Physics, Royal Adelaide Hospital, Australia.

Introduction Multiple Coulomb scattering (MCS) poses a challenge in proton CT (pCT) image reconstruction. The assumption of straight trajectories is replaced with the Bayesian most likely path (MLP). Current MLP-based pCT reconstruction approaches assume a water scattering environment. In this work, an MLP formalism taking into account the inhomogeneous composition of the human body has been proposed, which is based on the accurate determination of scattering moments in heterogeneous media.

Method Monte Carlo simulation was used to compare the inhomgeneous MLP formalism to the homogeneous water approach. An MLP-Spline-Hybrid method was investigated for improved computational efficiency and a metric introduced for assessing the accuracy of MLP estimates. Anatomical materials have been catalogued based on their relative stopping power (RStP) and relative scattering power (RScP) and a relationship between these two values was investigated.

Results A bi-linear correlation between RStP and RScP was shown. When compared to Monte Carlo proton tracks through a water cube with thick bone inserts using TOPAS, the inhomogeneous formalism predicted proton paths to within 1.0 mm on average for beams ranging from 230 to 210 MeV incident energy. The improvement in accuracy over the conventional MLP ranged from 5% for a 230 MeV beam to 17% for 210 MeV. There was no noticeable gain in accuracy when predicting 190 MeV proton paths through a more clinically relevant phantom consisting of 1 cm bone inserts and a 2 cm air cavity. Implementation of a new MLP-Spline-Hybrid method greatly reduced computation time while suffering negligible loss of accuracy.

Conclusion An inhomogeneous MLP formalism has been proposed, which has predicted Monte Carlo proton paths to equal or greater accuracy than the current water-based formalism. Improvements are most noticeable at lower beam energies. There is scope to implement catalogued RScP and RscP into iterative pCT reconstruction.

Acknowledgements M D Brooke is supported by a John Monash Scholarship and a Clarendon Fund Scholarship. This work was supported by Cancer Research UK grant number C2195/A25197, through a CRUK Oxford Centre DPhil Prize Studentship.

O18 Assessing reproducibility of breath-hold SBRT using intrafraction cone-beam CT

P. O'Connor, E. Brown, D. Pryor, E. Eaves

Radiation Oncology, Princess Alexandra Hospital, Brisbane, Australia. (Patrick.OConnor2@health.qld.gov.au [Presenting author])

Introduction The commissioning of XVI Intrafraction has facilitated the introduction of breath-hold gated stereotactic body radiotherapy (SBRT). Intrafraction cone beam CT (CBCT) enables imaging of patient anatomy during patient VMAT treatment, as opposed to imaging in-between treatment fields or post treatment. A means of intrafraction imaging is a pre-requisite for breath-hold SBRT, to visualise any unpredictable target volume motion associated with patient breath-hold. Intrafraction CBCT registration results have been collected and are presented to demonstrate the reproducibility of patient positioning under breath-hold.

Method Intrafraction CBCTs from several SBRT patients have been collected. Breath-hold was achieved using the Elekta Automatic Breathing Control (ABC) system. Planning target volume (PTV) margins with ABC were 8mm craniocaudally and 5mm radially. Positional couch shifts were applied if results were out of prescribed tolerance (2 mm) from a CBCT vs planning CT registration. Average couch shifts for each breath-hold type (either Deep-inspiration (DIBH) or End-expiration (EEBH)) are presented here as an indication of reproducibility.

Results A total of 24 out of 50 fractions had an intrafraction couch move based off the results from the CBCT during treatment. Average shifts from intrafraction CBCT was found to be 0.2, 0.1, 0.1 mm for DIBH and 0.5, 0.1, 0.0 mm for EEBH in the Sup/Inf, Left/Right and Ant/Post directions respectively. Qualitatively, image quality was degraded on the intrafraction CBCT from noise introduced by MV scatter. However, the prescribing RO was satisfied with image quality in all cases, including visualization of abdominal targets and adjacent organ-at-risk (OAR).

Conclusion Intrafraction CBCT has been a successful addition to the SBRT programme and breath-hold with ABC for these patients has been shown to be reproducible. More patients are now eligible for SBRT thanks to in-treatment target and OAR visualisation provided by XVI Intrafraction, coupled with the advantages of using breath-hold to manage motion.

KS03 Modelling secondary electron emissions

M. Dingfelder, J. Teller, J. L. Shinpaugh

Department of Physics, East Carolina University, USA. (dingfelderm@ecu.edu [Presenting author]), (tellerja04@students.ecu.edu), (shinpaughj@ecu.edu)

Introduction Ionizing radiation produces secondary electrons. General radiation transport calculations often neglect these low energy (below 100 eV) electrons and deposit the energy locally. Only high energy electrons, often referred to as delta rays, may be considered. On the other hand, detailed (or event-by-event) track structure simulations follow all secondary particles until total stopping and rely on reliable interaction cross sections for these low energy electrons.

These codes are often used to model the physical and chemical stages of radiation action with matter and the initial radiation damage to biological systems. Low-energy electron transport can be tested by modelling and measuring secondary electron yields from thin condensed targets like metal foils or amorphous solid water after proton impact.
Method The dielectric formalism within the first Born approximation has been used to calculate inelastic interaction cross sections for electrons and protons with liquid water, copper, and gold. Transport models for proton and electron transport have been implemented into the MC track structure code PARTRAC. Secondary electron emission yields have been simulated and measured for amorphous solid water targets frozen on thin copper and gold foils. Different transport models for *bulk* and *surface* transport, as well as geometrical and size factors have been considered.
Results Simulated secondary electron emission yields for AWS and copper follow the trends of the experimental data well. Yields for electron emissions below 50 eV, however, are sensitive to elastic cross sections and details of the transport model.
Conclusion Low-energy electron transport in condensed media is still a challenge for detailed track structure simulation codes. Interaction cross-sections, transport models, and target geometry need to be adequately and carefully considered.
Acknowledgements We thank the organizers for conference travel funding.

O19 4D cellular model of tumour growth, radiation track structures, DNA damage induction and cell death

J. C. Forster[1,2], M. J. J. Douglass[1,2], W. M. Phillips[1,2], E. Bezak[1,3]

[1]Department of Physics, University of Adelaide, Australia. (Jake.Forster@adelaide.edu.au [Presenting author]), (mdouglass@adelaide.edu.au), (WendyMichelle.Phillips@sa.gov.au), (Eva.Bezak@unisa.edu.au). [2]Department of Medical Physics, Royal Adelaide Hospital, Australia. [3]Cancer Research Institute for Health Research and the School of Health Science, University of South Australia, Australia.

Introduction Stochastic radiotherapy models have the potential for greater accuracy and utility than analytic models. A model was developed that simulates head and neck squamous cell carcinoma i) cellular tumour growth with angiogenesis, ii) tumour irradiation with track structure, iii) induction of DNA damage in cells and iv) cell survival probability.
Methods 3D ellipsoidal cells containing nuclei occupied randomised, non-overlapping positions [1, 2]. Cells proliferated amidst a chaotic network of blood vessels. The cellular geometry was voxelised (2 μm voxels) and imported into Geant4 [3] for irradiation. Geant4-DNA was used to simulate direct-type and indirect effects [4, 5]. Water radiolysis and chemical tracks were simulated along segments of physical tracks inside nuclei (Figure 1). Direct events (ionisations and excitations > 10.79 eV) and hydroxyl radical interactions were spatially clustered in nuclei to predict DNA damage, including double-stand breaks (DSBs), in a pO_2-dependent fashion [6]. Incongruent DSB ends could misrejoin [7] and misrejoining events could cause cell death.
1224 cells in a cubic volume $(0.2\ \text{mm})^3$ were irradiated by X-rays from a 6 MV linac. Doses up to 1 Gy were simulated, followed by DNA damage induction and DSB misrejoining.
Results The mean number of misrejoining events per cell, and thus cell survival probability, were mostly quadratic with dose up to 1 Gy (survival $\alpha/\beta \sim 0.13$ under full oxia, ~ 0 under anoxia). A DSB yield of 30/Gy/cell and a non-lethal misrejoining probability of 50% gave an OER_{DSB} of 4.5, SF2 under full oxia of 53% and OER of 4.6.
Conclusion By inference, the linear component of low-LET cell survival curves may receive a larger contribution from DSB unrejoining than from misrejoinings between DSBs produced by the same electron track.

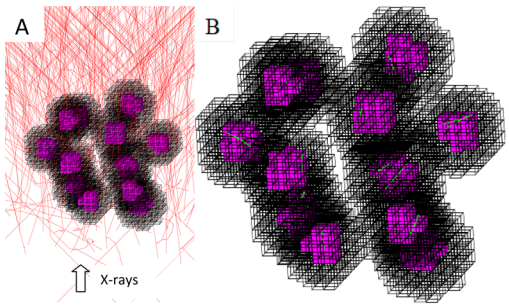

Figure 1: Example simulation of multicellular irradiation. Panel A: electron tracks (red). Panel B: hydroxyl radicals (green) lining electron tracks through nuclei.

References

1. Forster JC, Douglass MJJ, Harriss-Phillips WM, Bezak E (2017) Simulation of head and neck cancer oxygenation and doubling time in a 4D cellular model with angiogenesis. Sci Rep 7:11037
2. Forster JC, Douglass MJ, Harriss-Phillips WM, Bezak E (2017) Development of an in silico stochastic 4D model of tumor growth with angiogenesis. Med Phys 44:1563–1576
3. Allison J, Amako K, Apostolakis J et al (2016) Recent developments in Geant4. Nucl Instrum Methods Phys Res A 835:186–225
4. Bernal MA, Bordage MC, Brown JMC et al (2015) Track structure modeling in liquid water: A review of the Geant4-DNA very low energy extension of the Geant4 Monte Carlo simulation toolkit. Phys Med 31:861–874
5. Incerti S, Ivanchenko A, Karamitros M et al (2010) Comparison of Geant4 very low energy cross section models with experimental data in water. Med Phys 37:4692–4708
6. Forster JC, Douglass MJ, Harriss-Phillips WM, Bezak E (in press) Radiat Res
7. Tello Cajiao JJ, Carante MP, Bernal Rodriguez MA, Ballarini F (2017) Proximity effects in chromosome aberration induction by low-LET ionizing radiation. DNA Repair (Amst) 58:38–46

O20 New theoretical atomic radiation library for medical applications

T. Kibédi[1], B. Q. Lee[2], A. E. Stuchbery[1]

[1]Department of Nuclear Physics, The Australian National University, Canberra, Australia. (tibor.kibedi@anu.edu.au [Presenting author]), (andrew.stuchbery@anu.edu.au). [2]Department of Oncology, Oxford University, Oxford, United Kingdom. (boon.lee@oncology.ox.ac.uk)

Introduction Unstable atomic nuclei release excess energy through various radioactive decay processes by emitting neutrons, alpha- and beta-particles or electromagnetic radiation. In some cases, including internal conversion and electron capture, the atom remains ionised after the nuclear decay event. Atomic relaxation occurs rapidly by the emission of X-rays and Auger electrons.
While these atomic radiations usually only carry a fraction of the available nuclear decay energy, because of their high cross section to interact with matter, they are important for nuclear dosimetry. Since

the early 70s, when the use of Auger electrons for cancer therapy was first suggested by Bloomer and Adelstein [1], considerable advances have been made in understanding the radiobiological effect of low-energy electrons. In contrast to nuclear radiations, the experimental data on low-energy atomic radiations are scarce, therefore in most cases, theoretical transition energies and rates are used to evaluate the absorbed energy dose. Unfortunately, these calculations are based on several very different physical assumptions and approximations resulting very different emission rates [2].

Method Recently, we have proposed an Auger-cascade model [2, 3] to provide more realistic theoretical descriptions of atomic radiations after nuclear decay. The model is based on a full Monte Carlo approach to treat the stochastic nature of the creation of the initial vacancy in the nuclear decay process and the subsequent propagation of vacancies.

Results To achieve reasonable accuracy, a large number of decays need to be calculated. To reduce the CPU time drastically we are have developing a new data base, which will contain pre-calculated atomic radiation spectra for Z = 6–100 systems for each initial vacancy location, thus allowing quick evaluation of the full energy spectrum. The new model calculations have been successfully tested in evaluating dose point kernels and *S* values for commonly used radioisotopes [4].

Conclusion In comparison to (MIRD) RADTAB the new library offers a more detailed and realistic emission spectra of atomic radiations from nuclear decay, which could improve the accuracy of the nuclear dosimetry calculations for Auger electrons.

References

1. W.D. Bloomer and S.J. Adelstein, Nature **265** (1977) 620
2. B.Q. Lee, T. Kibédi, A.E. Stuchbery, K.A. Robertson, Comp. and Math. Meth. in Medicine (2012) 651475
3. B.Q. Lee, H. Nikjoo, J. Ekman, P. Jönsson, A.E. Stuchbery, T. Kibédi, Int. J. of Rad. Biol. **92** (2016) 1
4. N. Falzone, B.Q. Lee, J.M. Fernández-Varea, C. Kartsonaki, A.E. Stuchbery, T. Kibédi, K.A. Vallis, Phys. Med. Biol. **62** (2017) 2239

O21 Monte Carlo model development for evaluation of efficacy of proton boron fusion therapy for glioblastoma

L. Moghadassi[1], E. Bezak[2,3]

[1]GenesisCare, Tennyson Centre, Adelaide, Australia. (Leyla.moghaddasi@adelaide.edu.au [Presenting author]). [2]Department of Physics, University of Adelaide, Australia. [3]Cancer Research Institute and School of Health Sciences, University of South Australia, Australia. (Eva.Bezak@unisa.edu.au)

Introduction Glioblastoma (GBM) tumours are notorious for high fatality rate. Proton-Boron-Fusion Therapy (PBFT) is based on proton fusion reaction with labelled ^{11}B in a tumour (Boron Uptake Region (BUR)). The reaction results in a compound nucleus ^{12}C which splits into three α-particles. Primary advantages of PBFT are: (1) emission of three high LET α-particles, achieving good therapeutic outcome; 2) proton beams are relatively easy to produce. The purpose of this work is to develop a Geant4 Monte Carlo (MC) model for use in PBFT, demonstrate the accuracy and reliability of the Geant4 proton interaction models and investigate the feasibility of PBFT for potential application in radiotherapy of GBM.

Methods The GEANT4 (v. 10.04) GBM-PBFT model was designed as a cylindrical phantom with 16cm diameter and 10cm height and irradiated with monoenergetic proton beam with energies 80, 90 and 100 MeV at 50cm distance from water surface. Percentage depth dose curves (PDDs) were calculated in water and boron phantoms to test the accuracy of Columbic and nuclear stopping powers via range calculations in water and boron, respectively. PDDs were also calculated with BUR inserted at several depths in the phantom to examine the change in the intensity of Bragg-peak. The results were validated against SRIM software and IAEA EXFOR.

Results The accuracy of Geant4 physics model (QGSP_BIC_AllHP) to model proton fusion reaction was validated. Although insertion of 11B increased the energy deposited within BUR, the absorbed dose was found lower than that in water. The increase in energy deposited is due to PBFT reaction as well as increased electronic stopping power in boron. However, the PBFT cross-section for protons in the Bragg-peak itself ($\sim$ 0.5 MeV) is too low to increase the intensity of the absorbed dose.

Conclusion These in-silico results suggest that PBFT may not be useful for treatment of GBM.

O22 Validation of Monte Carlo imaging beam data from a TrueBeam x-ray imaging system

L. A. Gilling[1,2], O. Ali[2], S. Marsh[1]

[1]Department of Physics and Astronomy, University of Canterbury, New Zealand. (luke.gilling@waikatodhb.health.ac.nz [Presenting author]), (steven.marsh@canterbury.ac.nz). [2]Onocology Department, Waikato Hospital, Hamilton, New Zealand. (omer.ali@waikatodhb.health.nz)

Introduction Concomitant dose from CBCT-based image guided radiotherapy has become an increasingly active area of research due to the potential increase in secondary cancer risk over a complete course of radiotherapy. A variety of deficiencies exist in quantifying kV dose in current treatment planning systems. This work has therefore attempted to simulate TrueBeam x-ray imaging system (XI) beam data using the GATE simulation toolkit for the purpose of radiotherapy treatment planning.

Method The GATE simulation toolkit (version 8.1) was used to simulate the x-ray source, geometry and physics involved in the operation of the XI source arm. The x-ray source was modelled from simulated spectral data (Figure 1). To validate the relative dose distribution from the model, depth dose and profile curves simulated in water were compared to physical measurements made with ion chambers and radiochromic film. Due to restrictions in radiochromic film size, validation measurements using this dosimeter type were performed in 10 × 10 cm field sizes.

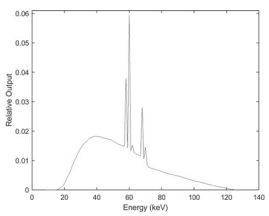

Figure 1 The simulated 125 kV photon energy spectrum from the Truebeam x-ray imaging system tube.

Results Analysis of the water phantom simulations showed good agreement with physical measurements. GATE and ion chamber results agree to within 5% up to a depth of 150 mm (Figure 2).

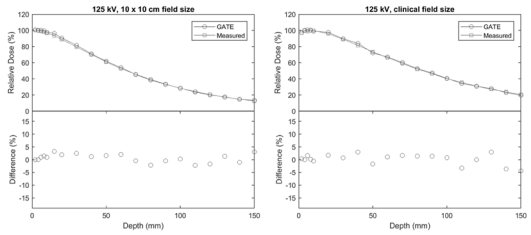

Figure 2 Plots showing depth dose curve deviations between GATE and measured data for a 10 x 10 cm field size and clinical field size.

Conclusion The results of this study represent an independent validation of imaging beam data using the GATE toolkit for the XI system. Results from water phantoms show good agreement with physical measurements within an accuracy of ± 5%. These preliminary results show GATE can be an effective toolkit in estimating effective dose from CBCT imaging during RT.

References

1. Verhaegen F, Nahum A E, Van De Putte S, Namito Y (1999) Monte Carlo modelling of radiotherapy kV X-ray units. Phys Med Biol 44:1767–1789. https://doi.org/10.1088/0031-9155/44/7/315
2. Ding GX, Duggan DM, Coffey CW (2007) Characteristics of kilovoltage x-ray beams used for cone-beam computed tomography in radiation therapy. Phys Med Biol 52:1595–1615. https://doi.org/10.1088/0031-9155/52/6/004
3. Marchant TE, Joshi KD (2016) Comprehensive Monte Carlo study of patient doses from cone-beam CT imaging in radiotherapy. J Radiol Prot 37:13–30. https://doi.org/10.1088/1361-6498/37/1/13
4. Li XA, Ma CM, Salhani D (1997) Measurement of percentage depth dose and lateral beam profile for kilovoltage x-ray therapy beams. Phys Med Biol 42:2561–2568. https://doi.org/10.1088/0031-9155/42/12/019
5. Abolaban FA (2011) On board cone beam CT for treatment planning in image guided radiotherapy. Dissertation, University of Surrey
6. Hill R, Healy B, Holloway L, Kuncic Z, Thwaites D, Baldock C (2014) Advances in kilovoltage x-ray beam dosimetry. Phys Med Biol 59:183–231. https://doi.org/10.1088/0031-9155/59/6/R183

O23 Monte Carlo verification of radiotherapy treatment plans: Vancouver Island Centre experience

S. F. Zavgorodni

BC Cancer Agency, Vancouver Island Centre, Victoria, Canada. (szavgorodni@bccancer.bc.ca [Presenting author])

Introduction Independent verification of treatment planning dose calculations is an essential part of radiotherapy quality assurance program. As of August 2015 our department implemented Monte Carlo (MC) based verification of VMAT and IMRT as well as complex conformal plans.
Method Vancouver Island MC system [1, 2] is used for routine verification of clinical VMAT / IMRT and conformal plans. "Quick MC" option within the system includes "Fast Jaw Tracking" (FAJT) [3] combined with VCU particle DMLC [4] models for particle transport through the linac head. VMC++ code is used for particle transport through the phantom produced from patient CT dataset. MC simulation times are of the order of 5–10 min for majority of cases. MC dose distribution is imported to the planning system (Eclipse), compared to AAA dose and kept as a part of the patient record. A summary of the dose comparison is also written to Excel spreadsheet.
Results Over 2700 plans have been verified using our MC system. Overall agreement of mean PTV dose between AAA and MC across all treatment sites was − 0.5% (SD = 1.4%), ranging from − 16.1 to + 6.6%. Site-specific mean PTV dose agreement for abdomen, breast & chest-wall, brain, esophagus, head & neck, lung and pelvis was within ± 1% (SD = 1%). As expected, the worst agreement between AAA and MC calculations was observed for lung-SABR plans with mean PTV dose difference of − 3.1%, SD = 2.9%, ranging from − 16.1 to + 4.0%.
Conclusion MC verification of the treatment plans has shown to be efficient and reliable process. It highlighted deficiencies in commercial planning algorithms in the regions of heterogeneity and allowed to make appropriate corrections.

References

1. S. Zavgorodni, K. Bush, C. Locke and W. Beckham, "Vancouver Island Monte Carlo (VIMC) system for radiotherapy treatment planning dosimetry and research," Radiother. Oncol. 84, Supplement 1, S49 (2007).
2. K. Bush, R. Townson and S. Zavgorodni, "Monte Carlo simulation of RapidArc radiotherapy delivery," Phys. Med. Biol., N359–370 (2008).
3. R. Townson, H. Egglestone and S. Zavgorodni, "A fast jaw - tracking model for VMAT and IMRT Monte Carlo simulations," J. Appl. Clin. Med. Phys. (2018).
4. J. V. Siebers, P. J. Keall, J. O. Kim and R. Mohan, "A method for photon beam Monte Carlo multileaf collimator particle transport," Phys. Med. Biol. 47, 3225 (2002).

O24 Optimisation of CT dose in nuclear medicine

J. Crocker

The Alfred Hospital, Melbourne. (j.crocker@alfred.org.au [Presenting author])

Introduction The use of CT in nuclear medicine has been steadily increasing for several years, however until 2017 no national DRLs for CT use in nuclear medicine had been published. Optimisation of CT dose with reference to the existing diagnostic CT DRLs was not considered appropriate as the diagnostic image quality objective is different to nuclear medicine. It was discovered that nuclear medicine CT doses at The Alfred were higher than the newly published DRLs for several scan types.
Method A survey was of current CT parameters used in nuclear medicine was conducted. Several variations to factors such as slice thickness, noise index, and the use of iterative reconstruction were investigated on both an anthropomorphic phantom and a Catphan®. Proposed changes to settings were then performed in phantom and approved for clinical use by nuclear medicine physicians. This process was repeated iteratively, with a 'cooling-off' period between each adjustment to allow physicians to become accustomed to the new image appearance in patient scans.
Results Through adjustment of scan settings, CT DLP was reduced in several scan categories by an average of 50% initially. After

physicians became accustomed to lower dose scans, they reported no change in the overall diagnostic quality of hybrid images and in many cases allowed further CT dose reduction. In some cases CT DLP has now been reduced by as much as 75%. Physicians who had previously been accustomed to higher dose scans reported that lower image quality did not affect the interpretation and utility of the CT as it is used in nuclear medicine.
Conclusion CT dose in nuclear medicine has been significantly reduced, and the perception of acceptable image quality has altered among nuclear medicine physicians. There is additional scope for dose reduction through adjustment of parameters specific to the patient or clinical indication.

O25 Problems, pitfalls and solutions in the radiation safety requirements for a new tertiary children's hospital: part II: nuclear medicine facilities

J. Atkinson, S. Crossley, M. McGibbons, T. Rourke, L. Maddox

Medical Technology & Physics, Sir Charles Gairdner Hospital, Australia. (Janette.Atkinson@health.wa.gov.au [Presenting author])

Introduction The Perth Children's Hospital (PCH) opened in May–June 2018. It is Western Australia's new $1.2 billion dedicated paediatric hospital and replaces Princess Margaret Hospital. At EPSM2017, problems and solutions were presented relating to laser safety, shielding and warning lights. PCH's design and construction is complex and radiation safety requirements are not always understood by those performing the construction. Medical Physics services commenced towards completion of the hospital and consequently there were multiple radiation safety related problems. In addition to those previously presented, there were problems with the plumbing and ventilation for Nuclear Medicine requiring resolution.
Method PCH has a SPECT/CT and provisions for future use of PET imaging, but currently there are no facilities to provide radioisotope therapies at PCH. A delay and decay radioactive waste tank has been installed for nuclear medicine plumbed waste. In preparation to have the hospital registered for the use of radioactive substances, the nuclear medicine facility design and radiation safety requirements were reviewed with areas of concern identified. Plans to correct non-compliances were created, reviewed and sent to the regulator for approval.
Results Non-compliance with requirements included:

- Ventilation drawings showed air exhaust from the nuclear medicine precinct being recycled to the Medical Imaging department and did not satisfactorily exhaust to the atmosphere.
- The waste line from the waste tank to the main sewer was joined by two other waste lines. This line was not labelled as radioactive, however if the tank auto pumped during weekdays when patient toilets were in use the waste would need to be considered radioactive according to the limits from the Western Australian Radiation Safety (General) Regulations 1983 [1].

Conclusion The ventilation and plumbing problems were ultimately resolved. If these issues were identified prior to construction corrective measures that impact cost and completion time could have been prevented.

References

1. Radiation Safety Act 1975, Radiation Safety (General) Regulations 1983. State Law Publisher www.slp.wa.gov.au. Accessed 1 Jan 2016.

O26 IAEA conference on accidental and unintended exposures in nuclear medicine

P. A. Marks, T. E. Beveridge, P. D. Thomas

Medical Imaging Section, ARPANSA. (paul.marks@arpansa.gov.au [Presenting author]), (toby.beveridge@arpansa.gov.au), (peter.thomas@arpansa.gov.au)

Introduction With the rise in nuclear medicine procedures performed around the world, there is a need to avoid any related accidental or unintended radiation exposure. Practitioners from all fields of nuclear medicine met in May 2018 at the International Atomic Energy Agency (IAEA) in Vienna to discuss how to ensure the safety of patients, health workers and the public in nuclear medicine. It is estimated that over 30 million nuclear medicine procedures are performed annually. This represents a new procedure starting every second somewhere in the world.
Method The aim of the three-day meeting was to share experiences, learn from past incidents and prepare guidelines on how to avoid accidents in the future. Discussions focused not only on incidents but also included near misses, which occur more frequently than accidents.
Results Describing and categorising incidents is the first step towards identifying procedures for their prevention. There is a need for subsequent reporting, so that trends can be understood and conclusions drawn. Accurate and timely reporting is therefore a primary goal and an important part of the process.
It was proposed that radionuclide therapy be included in Safety in Radiation Oncology (SAFRON), an integrated voluntary and anonymous reporting and learning system covering radiotherapy incidents and near misses, run by the IAEA and designed to support the sharing of safety-related information.
Conclusion The meeting highlighted the importance of strengthening safety culture in nuclear medicine for the prevention of incidents and accidents. The need to address unsafe conditions by increasing awareness and alertness, develop comprehensive operating procedures, training and understanding, and clearly defining responsibilities is paramount.
A report drawing on the results and discussion from the meeting will be published to give guidance on safety measures and support national authorities and hospitals in ensuring safety of patients, staff and the public.

O27 Lessons learnt from a non-standard outpatient administration of 9.2 GBq of Iodine-131

L. E. Wilkinson

Department of Medical Engineering & Physics, St. Vincent's Hospital Melbourne. (luke.wilkinson@svha.org.au [Presenting author])

Introduction A non-standard administration of 9.2 GBq of 131I was conducted on a hospital outpatient on a semi-rural property who had low mobility and high care needs. The level of radioactivity administered exceeded the normally guidance level for outpatient administrations of 131I by over a factor of ten.
Method Key radiation exposure pathways and legislative issues were identified and addressed through a collaborative effort from Medical Physicists, Nuclear Medicine Technologists and the State Regulator. This included modelling potential radiation exposure to the patient's primary carer, consideration of transport of the radioisotope to the patient property, disposal via the domestic septic system and the process of gaining regulatory authorisations to conduct this procedure.

Results From personal monitoring provided to the primary carer, carer exposure was measured as being approximately 400 microsieverts from the treatment. Time dependent exposure from assisting with basic toiletry needs and transporting the patient to and from the hospital for post-treatment imaging at 96+ h are identified and quantified. Exposure from transporting the patient via car is estimated as being 6–10 microsieverts per hour of transport for a patient body burden of approximately 200 MBq of ^{131}I. Administrative controls minimising access to the septic system and patient were also required to minimise potential exposure.

Conclusion Outpatient administrations of large quantities of ^{131}I can be undertaken but to do this the patient/carer have to meet criteria regarding level of knowledge and compliance that can be expected of the patient/carer team. Additionally to do this a range of specialised equipment has to be provided to the carer and specialised documentation/procedures addressing a range of potential medical and domestic emergencies has to be provided to the carer and state regulatory body.

O28 Assessing amount of radioactive effluents from nuclear medicine procedures released to public sewerage

J.-H. Kim[1,2], J. Burrage[1,2]

[1]Medical Engineering & Physics, Royal Perth Hospital. (Jung-Ha.Kim@health.wa.gov.au [Presenting author]), (John.Burrage@health.wa.gov.au). [2]Clinical Physics, Fiona Stanley Hospital

Introduction A major hospital in WA, performing more than 7000 nuclear medicine exams per year, was recently assessed in terms of its annual discharge of radioactivity into the sewer. It was of importance to estimate this in order to ensure its compliance to the regulatory requirement[1], in an absence of the means of directly measuring the radioactive discharges, or holding tanks.

Method Total administered activity was determined by combining annual statistics of all nuclear medicine exams with protocol information, including the type of radiopharmaceutical, administered activity, post-injection scanning time and the requirements of voiding for the scan. Biological half-lives of radiopharmaceuticals were directly referenced or calculated from data in the literature (i.e. ICRP publications[2–3], or other sources[4–10]), and used to estimate the amount of radioactivity discharged to public sewer. To simplify the calculation, several assumptions were made in determining the probability of the patient voiding at the department. A measure of the total annual discharged radioactivity defined in the Regulations as the "score" was calculated as the sum of the radioactivity from various radioisotopes weighted by their exempt quantities provided in the Regulations[1].

Results Table 1 shows the estimated annual score of total radioactivity discharged to public sewer from FSH, which is about 40 times higher than the allowable WA limit set out in the Regulations[1] (100 000).

Conclusion The results suggest that the radioactivity from the hospital exceeded the regulatory limit. Due to the relatively short half life of the radioisotopes, a temporary exemption was granted while a review of the existing regulations is performed. Aside from checking regulatory compliance, the exercise also indicated the importance of considering mitigating strategies, such as delay tanks, when planning for larger institutions, since the total annual radioactive discharge may be significant.

Table 3 Estimated annual score for amount of radioisotopes discharged to public sewer from FSH using the exempt quantities of radioactive substances provided in Schedule V of the Regulation[1].

Study type	Isotope	Total activity to sewer (MBq)	Exempt quantity (MBq)	Score
Nuc Med	I-123	167	0.004	41750
	Tc-99m	537773	4	134443
	Ga-67	6554	0.004	1638500
	I-131*	600	0.04	15000
PET	F-18	49626	40	1241
	Ga-68	8898	0.004	2224500
Total				4 055 434

*Assumed to have come solely from I-131 therapy inpatients, based on measured annual discharged quantities at FSH.

References

1. Radiation Safety (General) Regulations 1983, Government of Western Australia.
2. ICRP Publication 53 (1988) Radiation Dose to Patients from Radiopharmaceuticals. Ann ICRP 18.
3. ICRP Publication 128 (2015) Radiation Dose to Patients from Radiopharmaceuticals: A Compendium of Current Information Related to Frequently Used Substances. Ann ICRP 44.
4. Sattari A et al. (2001) Urinary excretion and external radiation dose from patients administered thallium-201 and technetium-99M methoxy isobutyl isonitrile. Radiat Prot Dosimetry, 59–61.
5. Azarbar S et al. (2015) A phase I-II, open-label, multicenter trial to determine the dosimetry and safety of 99mTc-sestamibi in pediatric subjects. J Nuc Med, 728–736.
6. Vallabhajosula S et al. (1989) Technetium-99m ECD: a new brain imaging agent: in vivo kinetics and biodistribution studies in normal human subjects. J Nuc Med, 599–604.
7. Atkins H et al. (1980) A Comparison of Tc-99m-labeled Human Serum Albumin and In Vitro Labeled Red Blood Cells for Blood Pool Studies. Clin Nuc Med, 166–169.
8. Moran J K et al. (1999) Optimization of urinary FDG excretion during PET imaging. J Nuc Med, 1352–1357.
9. Hermann K et al. (2015) Biodistribution and Radiation Dosimetry for a Probe Targeting Prostate-Specific Membrane Antigen for Imaging and Therapy. J Nuc Med, 855–861.
10. Kwekkeboom D J et al. (2001) [177Lu-DOTA0,Tyr3]octreotate: comparison with [111In-DTPA0]octreotide in patients. Eur J Nuc Med, 1319–1325.

O29 Challenging experiences with iodine-131 therapy patients

T. Rourke, L. Maddox, S. Rodgers, L. Grigoroff, J. Atkinson, M. McGibbons

Medical Technology & Physics, Sir Charles Gairdner Hospital, Australia. (Tegan.Rourke@health.wa.gov.au [Presenting author])

Introduction Iodine-131 is used to treat several diseases, including hyperthyroidism (400–600 MBq, NaI), thyroid cancer (1–7 GBq, NaI) and neuroendocrine tumours (6–20 GBq, mIBG). Patients who are treated with more than 600 MBq I-131 are usually isolated from the general public as inpatients during their therapy. Additionally, patients have restrictions on their activities for several days after they have reached the discharge limit [1]. Unfortunately, sometimes circumstances do not allow patient contact to be restricted to radiation workers, for example when patients need unexpected medical intervention, or planned treatments for existing conditions.

Method During several unusual I-131 cases, efforts were made to minimise radiation doses, and measure them where possible. Non-radiation worker staff and the patients' family members were given radiation safety advice to help keep their doses as low as reasonably achievable, and reassure them about treating radioactive patients.
Res ults Several unusual patients are discussed, including:

- A seizure due to hyponatraemia;
- Atrial fibrillation requiring High Dependency Unit admission;
- A possible emergency hip replacement;
- Patients requiring dialysis;
- Paediatric patients with complex needs;
- Patients with extremely slow clearance rates due to extensive metastases

Conclusion The radiation doses to radiation workers, non-radiation worker staff, and family members were managed. As the population increases and ages, and more patients with comorbidities are treated, we expect these unusual cases to become more frequent.

References

1. "Discharge of Patients Undergoing Treatment with Radioactive Substances" (2002) ARPANSA Radiation Protection Series.

O30 Suitability of vendor-recommended small field output factors in a post-TRS-483 world

T. Kairn[1,2]

[1]Royal Brisbane and Women's Hospital, Herston, Australia. (t.kairn@gmail.com [Presenting author]). [2]Queensland University of Technology, Brisbane, Australia

Introduction In recent decades, there has been a rapid growth in published knowledge of small field dosimetry, culminating in the November 2017 publication of the IAEA's small field dosimetry protocol, TRS-483 [1]. In addition to absolute dosimetry guidance, the protocol provides recommendations for the performance of relative dosimetry measurements, including a carefully curated list of small field correction factors for use when measuring output factors with diodes and other small-volume dosimeters [1]. Such correction factors, or advice to use correction factors, were not included in the older small field dosimetry protocols (eg. IPEMB report 103 [2]) that may have been used by treatment planning system vendors to generate data that is still used to evaluate user measurements (eg. Brainlab iPlan/Elements) or pre-populate the treatment planning system (eg. Elekta GamaKnife).
Method A set of output factors (total scatter factors) were measured for HD-MLC-defined fields produced by a Varian Truebeam STx linac, operating in 6 MV and 6 MV FFF modes. The small field measurements were set up using an established method [3], completed using a PTW 60017 unshielded diode and daisy-chained with an Exradin A16 micro-ionisation chamber which was used for all measurements in larger fields. Result with and without corrections for diode over-response were compared with Brainlab reference data and further verified using radiochromic film measurements in liquid water.
Results Measurement results for fields larger than 1×1 cm^2, where the required correction factors are close to or equal to unity, fell within the vendor's range of recommended values. The measurement results for the smallest field, 0.5×0.5 cm^2, agreed with the vendor's reference data only when the diode over-response factor was not used, suggesting that the vendor's data was produced with reference to an older dosimetry protocol. Film results confirmed the corrected diode measurements.
Conclusion Whether vendor reference data is produced by uncorrected diode measurements, Monte Carlo simulations benchmarked against uncorrected diode measurements, or other sources, uncritical reliance on vendor-recommended small field output factor data produced before November 2017 has become questionable, in this post-TRS-483 world.

References

1. International Atomic Energy Agency. *Dosimetry of Small Static Fields Used in External Beam Radiotherapy, an International Code of Practice for Reference and Relative Dose Determination*. IAEA Technical Reports Series No. 483. Vienna (2017)
2. Aspradakis MM, Byrne JP, Palmans H, et al. *IPEM Report 103: Small field MV photon dosimetry* (2010)
3. Kairn T, Charles PH, Cranmer-Sargison G, et al. Clinical use of diodes and micro-chamber to obtain accurate small field output factor measurements. *Australas. Phys. Eng. Sci. Med.* **38**: 357–367 (2015)

O31 Implementing the newly released IAEA TRS-483 code of practice for Small Field dosimetry

J. E. Morales[1], R. Hill[2], J. V. Trapp[3]

[1]Department of Radiation Oncology, Chris O'Brien Lifehouse, Australia and School of Chemistry, Physics and Mechanical Engineering, Queensland University of Technology, Australia. (johnny.morales@lh.org.au [Presenting author]). [2]Department of Radiation Oncology, Chris O'Brien Lifehouse, Australia and Institute of Medical Physics, School of Physics, University of Sydney. (robin.hill@lh.org.au). [3]School of Chemistry, Physics and Mechanical Engineering, Queensland University of Technology, Australia. (j.trapp@qut.edu.au)

Introduction There has been extensive research in small field dosimetry and to date, several passive detectors such as radiochromic film and TLDs have been proposed as reference dosimeters. Recently the IAEA published the TRS-483 code of practice (COP) for small fields and includes published correction factors for a range of detectors, beam energies and field sizes. This work provides an analysis of the suitability of these correction factors a range of dosimeters.
Method All measurements were performed on a Varian Trilogy linear accelerator using the 6 MV SRS X-ray beam mode. The field sizes investigated ranged from 5×5 mm^2 to 40×40 mm^2 as defined at the isocentre using the 2.5 mm width MLCs. The detectors used were a PTW Diode E, an IBA SRS diode, a PTW Diamond and PTW microDiamond detector. The methodology in the TRS-483 COP was followed by which the uncorrected dose readings were corrected using the published k correction factors for the specific detector and field size.
Results The table below shows the field output factors obtained when corrections were applied. The total measurement uncertainty using the ISO GUM technique was determined to be within 1%.

MLC defined Field Size (mm^2)	microDiamond	Diamond	Diode E	IBA SRS
5	0.592	0.605	0.585	0.581
10	0.724	0.724	0.720	0.717
20	0.803	0.797	0.801	0.802
30	0.844	0.835	0.842	0.842
40	0.876	0.868	0.875	0.874

Conclusion It was expected that the final readings would converge to the same field factor after corrections are applied. However, this is not case with differences of up to 4% for the 5 mm field size is attributed to the source data used to calculate the k correction factors and inappropriate reference detectors. At this stage, it is recommended verify field output factors with an independent detector which does not require any correction factor.

O32 Evaluation of the IAEA TRS-483 protocol for the dosimetry of small static fields using multiple detectors

C. L. Smith, C. P. Oliver, D. J. Butler

Primary Standards Dosimetry Laboratory, Medical Radiation Services Branch, ARPANSA, Australia. (clare.smith@arpansa.gov.au [presenting author]), (chris.oliver@arpansa.gov.au), (duncan.butler@arpansa.gov.au)

Introduction The first international code of practice for the dosimetry of small static fields in radiotherapy (IAEA TRS-483) was recently released. Eleven detectors have been used to determine the field output factors (OF) for the Elekta stereotactic conical collimator system at the Australian Radiation Protection and Nuclear Safety Agency (ARPANSA) following the code of practice to evaluate its consistency.
Method The stereotactic cones had nominal diameters of 5, 7.5, 10, 15 and 50 mm and were attached to the ARPANSA Elekta Synergy linac (6 MV WFF X-ray beam). Two sets of measurements were completed from which the average 'corrected' (using factors from the protocol) and 'uncorrected' OF values were obtained for the following detectors; PTW diodes; SRS 60018, electron 60017 and photon 60016, ionisation chambers; Pinpoint 31014, Pinpoint 3D 31016, and micro-diamond 60019 (x3) and the Wellhöfer/IBA diodes; EFD and PFD and CC04 ionisation chamber.
Results The corrected OF values showed good agreement between all detectors and cone sizes. Comparisons relative to the Micro-diamond detector (Figures 1 a & b) gave a maximum difference of 2.3 % (SRS diode, 5 mm cone) (Figure 1b), which was -3.2 % for the uncorrected OF. In all other cases the corrected OF values differed by < 1.8 %. For the uncorrected OF values, the maximum difference was 4.0 % (PFD diode, 15 mm cone, relative to the Micro-diamond as shown in Figure 1a), which reduced to 1.2 % when corrected. Further analysis of all the detectors and cone sizes used showed a relative standard deviation (RSD) of ≤ 0.85 % (corrected) and ≤ 1.7 % (uncorrected), and for the estimated standard deviation of the mean (ESDM) ≤ 0.3 % (corrected) and ≤ 0.6 % (uncorrected).

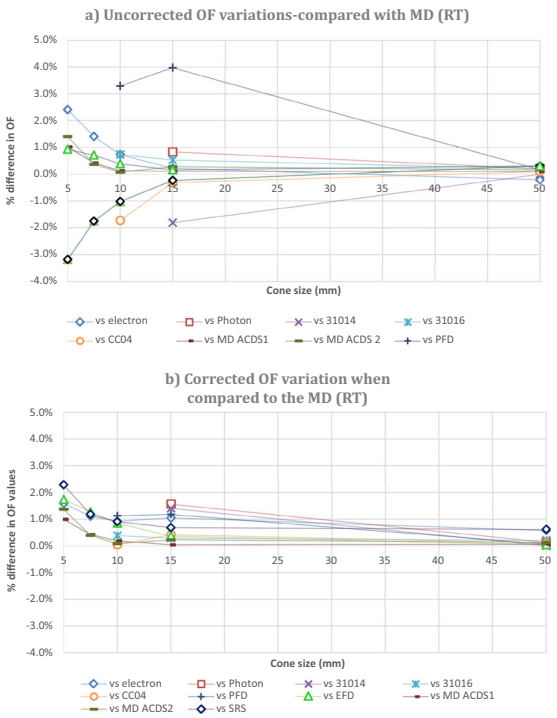

Figure 1 a & b: The OFs for the detectors investigated relative to the Micro-diamond, uncorrected (a), and corrected (b).

Conclusion Using the methods and correction factors detailed in the IAEA TRS-483 protocol, good agreement for the corrected OF was obtained for all eleven detectors investigated.

O33 Measurement of tissue-maximum ratio and percentage depth-dose profiles in small fields

S. B. Crowe[1,2], E. Whittle[2,3], C. Jones, T. Kairn[1,2]

[1]Royal Brisbane & Women's Hospital, Herston, Australia. (sb.crowe@gmail.com [Presenting Author]), (t.kairn@gmail.com). [2]Queensland University of Technology, Brisbane, Australia. [3]Biomedical Technology Services, Herston, Australia. (emma.whittle@health.qld.gov.au). [4]Princess Alexandra Hospital, Wooloongabba, Australia. (catherine.jones@health.qld.gov.au)

Introduction Radiotherapy treatment planning systems and independent dose checking software require measured tissue-maximum ratio (TMR) and/or percentage depth dose (PDD) profiles as part of the beam configuration data that is used to calculate dose. For systems that are used to for stereotactic radiosurgery (SRS) treatments of small cranial lesions, beam configuration must include accurate measurements in small radiation fields [1]. Small field TMR or PDD measurements can be obtained using small-field-suitable dosimeters such as diodes [2]. The aim of this study was to evaluate whether accurate TMR or PDD measurements might also be obtained using relatively large volume ionisation chambers that are otherwise unsuitable for small field measurements.
Method PDDs and TMRs were measured for a 1×1 cm^2 MLC-collimated field from an Elekta linac using an IBA BluePhantom 3D water tank with dosimeters of different active volumes, listed in table 1. The PDD measurement procedure followed published recommendations [2], and the diode measurements were regarded as the "gold standard" for comparisons.

Table 1. Dosimeters used for PDD and TMR measurements

Detector	Active Volume (cc)
PTW diode E, 60017	0.00003
PTW diode SRS, 60018	0.0003
Exradin A16 chamber	0.007
PTW Semiflex, 31010	0.125
PTW farmer, 30013	0.6

Results The area of the radiation field at the depth of the dosimeter varied between 1×1 cm^2 and 1.3×1.3 cm^2 during each PDD measurement, but remained very close to 1×1 cm^2 during each TPR measurement. The resulting differences in the amount of phantom scatter reaching each dosimeter during each measurement led to important differences and similarities between the dosimeter measurements. The largest disagreement in PDD profiles existed between diode and Farmer chamber measurements with a mean difference of 11% beyond maximum dose depth. However, diode and Farmer chamber TPR measurements at the same range of depths differed by a mean of only 0.5%.
Conclusion While the uncritical use of ionisation chambers for small field dosimetry is entirely inadvisable, the geometry of TPR measurements may allow accurate measurement data to be obtained using dosimeters that are unsuitable for other small field applications.

References

1. T. Kairn, P. H. Charles, S. B. Crowe, J. V. Trapp, "Effects of inaccurate small field dose measurements on calculated treatment doses", *Australasian Physical and Engineering Sciences in Medicine* **39**(3): 747–753 (2016)

2. S. Khoei, M. West, T. Kairn, "Measurement of percentage depth-dose profiles in very small fields", *IFMBE Proceedings* **68/3**: 557–560 (2018)

O34 ACDS preliminary audit results on small field output factors

A. Montaseri[1], A. Alves[2], C. Davey[2], F. Kadeer[2], J. Kenny[2], M. Shaw[2,3], J. Supple[2], J. Lye[2]

[1]Peter MacCallum Cancer Centre. (Atousa.Montaseri@petermac.org [Presenting author]). [2]Australian Clinical Dosimetry Service, ARPANSA, Melbourne VIC Australia. (Andrew.Alves@arpansa.gov.au), (Cate.Davey@arpansa.gov.au), (Fayz.Kadeer@arpansa.gov.au), (John.Kenny@arpansa.gov.au), (Jeremy.Supple@arpansa.gov.au), (Jessica.Lye@arpansa.gov.au). [3]Genesis Cancer Care, Melbourne VIC Australia. (Maddison.Shaw@arpansa.gov.au)

Introduction ACDS level Ib audit includes a field trial on small field output factors. This is a fundamental component which contributes in the results of higher level audits where small fields are measured such as SABR audit.

Method Measurements are done at facility SSD and depth. ACDS measures 6MV and 6FFF output factors (OF) as a direct ratio to 10x10 cm^2 reference field with a PTW microdiamond (model 60019). Detector dependent small field correction factors ($k_{Q_{clin},Q_{msr}}^{f_{clin},f_{msr}}$) are sourced from TRS483 table 26 to correct ACDS OF measurements (1). Facility states which detector they have used and whether or not $k_{Q_{clin},Q_{msr}}^{f_{clin},f_{msr}}$ has been applied. The percentage difference between the facility stated and ACDS measured OF is calculated.

Results Figure 1 shows audit results where the facility has not corrected for $k_{Q_{clin},Q_{msr}}^{f_{clin},f_{msr}}$ and figure 2 shows audit results where the facility results have been corrected. At very small field 0.5 × 0.5 cm^2, the discrepancy between ACDS and facilities reduces from 5.7% ± 1.2% to 0.6% ± 1.2% when the OF is corrected. At 1 × 1 cm^2, applying $k_{Q_{clin},Q_{msr}}^{f_{clin},f_{msr}}$ reduces the standard deviation of data from 2.9 to 1.6%. At larger field sizes no significant change in discrepancy between ACDS measured output factors and the facility stated values is observed. Similarity of results for 6MV flat and 6FFF is noticed. Overall discrepancy between ACDS and facility output factors decreases with $k_{Q_{clin},Q_{msr}}^{f_{clin},f_{msr}}$ corrections applied.

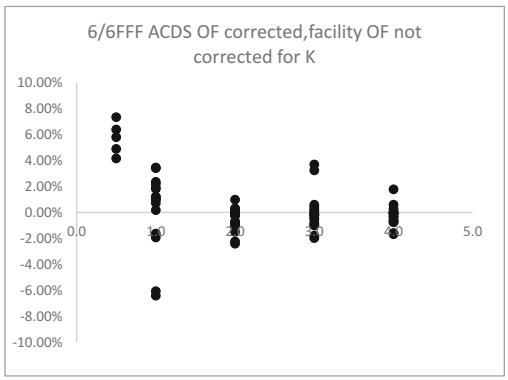

Figure 1: the results from small field audit. Only ACDS OF is corrected for K

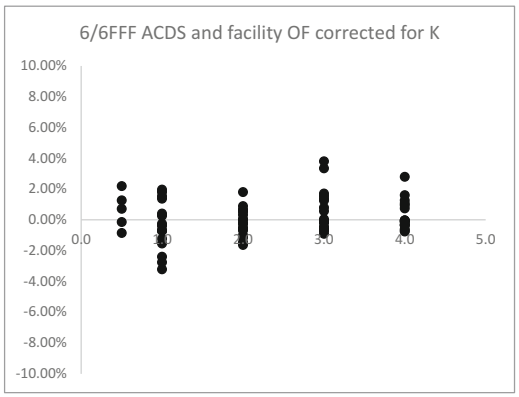

Figure 2: the results from small field audit. The Facility OF corrected for K

Conclusion ACDS level Ib small field trail is still being developed and needs more data on all field sizes in order to assess consistency of output factor measurements all over Australia. Early indications are that applying TRS483 improves consistency of small field output factors.

References

1. INTERNATIONAL ATOMIC ENERGY AGENCY, Dosimetry of Small Static Fields Used in External Beam Radiotherapy (TRS 483): An International code of Practice for Reference and Relative Dose Determination, IAEA 2017

O35 Development of a dedicated phantom for multi-target single-isocentre SRS end-to-end testing

J. Poder, R. Brown, H. Porter, R. Gupta, A. Ralston

St George Cancer Care Centre, Kogarah, NSW, Australia, 2217. (Joel.Poder@health.nsw.gov.au [Presenting author]), (Ryan.Brown@health.nsw.gov.au), (Harry.Porter@health.nsw.gov.au), (Rashmi.Gupta@health.nsw.gov.au), (Anna.Ralston@health.nsw.gov.au)

Introduction Stereotactic radiosurgery (SRS) is now becoming the standard of care in the treatment of patients with multiple brain metastases. Furthermore, the role of SRS has recently expanded to include the treatment of multiple cranial metastases with a single isocentre (MTSI) using multi-leaf collimators (MLCs). The aim of this project was to design and manufacture a cost-effective end-to-end (E2E) phantom for quantifying the geometric and dosimetric accuracy of our MLC based SRS technique

Method A Perspex Multi-Plug device from a Sun Nuclear ArcCheck phantom (Sun Nuclear, Melbourne, Florida) was enhanced to make it more applicable for MTSI SRS E2E testing. All steps in the SRS chain were analysed using the phantom, from magnetic resonance imaging (MRI) distortion and MRI-CT image registration accuracy, through to quantifying the dosimetric accuracy of the plan using radiochromic film and an ionization chamber, and the coincidence of linear accelerator MV/kV isocentres using Winston-Lutz testing (WLT).

Results The dedicated E2E phantom successfully quantified the geometric and dosimetric accuracy of the MTSI SRS technique at our centre. MRI distortions were less than 0.5 mm, and the average MRI-CT registration accuracy was within 0.4 mm. Point dose measurements were within 5% and comparison of planar film doses to the

planning system dose distributions, performed using gamma analysis, resulted in pass rates greater than 97% (4%/1mm gamma criteria). WLT showed MV/kV coincidence to be within 0.6 mm on central axis and within 1 mm for off-axis distances up to 60 mm.
Conclusion A novel, versatile and cost-effective phantom for comprehensive E2E testing of MTSI SRS treatments was developed, incorporating multiple detector types and fiducial markers. The phantom is capable of quantifying the accuracy of each step in the MTSI SRS planning and treatment process.

O36 3D printing of bone scaffolds: prediction of elastic properties and improvement of biological integration

G. Katsifis[1], D. R. McKenzie[1], A. D. Esteves[2], N. Suchowerska[2], A. Wang[3], T. Shearing[4], A. Ruys[4]

[1]School of Physics, University of Sydney. (gkat2146@uni.sydney.edu.au [Presenting author]), (david.mcKenzie@sydney.edu.au). [2]VectorLAB, Radiation Oncology, Chris O'Brien Lifehouse. (Ana.Esteves@lh.org.au), (natalka.suchowerska@lh.org.au). [3]Center for Advanced Materials Technology, University of Sydney. (hong.j.wang@sydney.edu.au). [4]School of Aerospace, Mechanical and Mechatronic Engineering, University of Sydney. (trevor.shearing@sydney.edu.au), (andrew.ruys@sydney.edu.au)

In medicine, bone sometimes needs to be surgically removed. The replacement can be a piece of bone transplanted from another part of the body or a metal implant such as titanium. Substituting bone from other parts of the body disadvantages the patient by opening a new surgical site. Metal implants such as titanium, although having favourable properties, are not mechanically compatible with tissue. Furthermore, radiotherapy patients may receive enhanced radiation doses at the implant-tissue interface, leading to further complications. The aim of this project is to create a 3D printed scaffold to temporarily support the region of interest while bone regrows and mineralises around and within the scaffold. Predicting the elastic properties of additively manufactured (3D printed) objects is essential for applications that require specific mechanical properties such as the mandible or the femur. Some applications require objects that possess high mechanical rigidity and strength for one type of applied stress, but may not have a specific requirement for another applied stress. We report on the feasibility of using PEEK as a material for constructing the scaffold. The structural implants must possess high linear elastic moduli and strength for the relevant stress. The symmetry of the object's microstructure is used to determine how many independent quantities are required to predict the linear elastic response of a body. We perform this analysis on our PEEK scaffold and show that it can be described as a cylindrically isotropic structure with 6 independent constants. We confirm by testing with an INSTRON machine that our 3D printed PEEK scaffold has much higher strength than the same structure printed in ABS. We also show that the PEEK structure recruits bone cells better than the ABS, allowing it to integrate more rapidly and gain additional strength from the biologically produced material.

O37 Continued development of a dynamic thorax phantom for clinical QA

T. L. Ackerly[1,2], M. Geso[2], C. Wen[3]

[1]Alfred Radiation Oncology, Alfred Health, VIC 3004 Australia. [2]School of Biomed. & Health Sciences, RMIT University, VIC 3083 Australia. (trevor.ackerly@wbrc.org.au [Presenting author]), (moshi.geso@rmit.edu.au). [3]INWENTECH, Melbourne, VIC 3150 Australia. (wen.inwentech@bigpond.com)

Introduction Confirmed to be the 1st breathing phantom with expandable chest and deformable organs, the dynamic phantom, ChestPhan4D is being continuously developed by Australian institutions, following its recognition of winning the ACPSEM David Robinson Innovation Award 2016 and securing IP protection globally. This paper describes the development process of an inventive medical device.
Method Through collaboration between a leading design firm and an artistic crafting workshop under government financial support, the dynamic phantom was architecturally designed as an electro-mechanical, computer-driven and remote-controlled device by a Melbourne based designer. Deformable organs included in the phantom, e.g. heart, lung and breasts were digitally modelled and artistically fabricated by craft-and-design engineers. 3D printing technology was employed to produce the human-like heart with great detail. Clinical validation for functions and features of the phantom were conducted on CT and 4DCT in clinical environment. An advanced prototype was constructed and can be used for clinical research purposes.
Results The phantom can produce chest expansion and contraction, the skin and breast are deformable, the heart and lung behave alike to human movement when simulating free-breathing and DIBH modes. Built-in fiducial marks and tumour structures can represent and thus simulate the clinical targets in SBRT and DIBH treatment process, hence the phantom, ChestPhan4D can be used as an end-to-end pre-clinical verification before real treatment for SBRT of lung cancer and DIBH of left breast cancer.
Conclusion A clinical orientated purposely-built dynamic phantom has been built and is available for clinical research and training projects. With continued improvement, this Australian invention and design will be commercialized and can clinically benefit many patients by undertaking advanced radiotherapy treatment with higher standards globally.

References

1. Keall et al. (2006) The management of respiratory motion in radiation oncology report of AAPM Task Group 76 Med. Phys. 33 10, 3874–900
2. Willoughby et al. (2012) Quality assurance for nonradiographic radiotherapy localization and positioning systems: Report of Task Group 147 Med. Phys. 39 (4)
3. P Steidl et al. (2012) A breathing thorax phantom with independently programmable 6D tumour motion for dosimetric measurements in radiation therapy Phys. Med. Biol. 57 2235–2250

O38 Acoustic noise for conventional and open split-bore magnet MRI

B. Dong[1], R. Rai[1,2], G. P. Liney[1,2]

[1]Ingham Institute for Applied Medical Research, Liverpool, Australia. [Bin.Dong@health.nsw.gov.au [Presenting author]). [2]Liverpool Cancer Therapy Centre, Liverpool, Australia. (Robba.Rai@health.nsw.gov.au), (Gary.Liney@health.nsw.gov.au)

Introduction An open split-bore magnet MRI was developed for an MRI guided radiotherapy system MRI-Linac. Since the unique design of the magnet, the acoustic noise level due to the gradient pulsing during the scan is unknown. This work measured the acoustic noise of

the scan from the open split-bore magnet in comparison with a conventional close bore magnet MRI.

Method To measure the acoustic noise level, a sound level meter (Extech 407730) was setup at various test positions while a series of pulse sequences were scanned and the maximum sound level was recorded accordingly. The acoustic noise was measure at the following positions, the bore entry of a conventional MRI (Siemens Skyra 3.0T).

- the control room of the 3T MRI
- the gap between the two halves of the open split-bore magnet (Agilent 1.0T)
- in the bunker but outside the RF cage inline and perpendicular to the magnet bore direction

Results The measurement results are listed below, all measurements in dB(A) using the 'A' weighting for human ear response.

Table 1. Results of sound pressure level measurements in conventional MRI 3.0T

	TE (ms)	TR (ms)	Bore	Control Room
Background				47.3 to 55.9
TSEq (noise cancellation)			66.6	53.9
TSE	97	6350	67.6	53.6
PETRA	0.07/3.3	2250	84.5	55.1
FL	4.6	689	**97.2**	55.6
EPI	98	6400	**104.6**	55.1
Pre-scan			**105.0**	
ASL (EPI)	13	2800	**107.7**	57.4

Table 2. Results of sound pressure level measurements in open split-bore MRI 1.0T

	TE (ms)	TR (ms)	Bore (dB)	Bunker (side panel) (dB)	Bunker (inline panel) (dB)
Background			64.5	58.6	57.6
TSE	13	3000	82.8 & **97.4-99.6***	58.8	60.8
FL	10	100	**87.8**	59.5	62.4
TrueFISP	1.9	3.9	**107.8**	71.1	84.1

*range of values with repeat scans comparing triaxial & sagittal plane and at both gap and bore.

Highlighted values which exceed recommended guidelines for hearing protection.

Conclusion Acoustic materials used in RF cage of 3T reduces the scan noise to background levels in all cases. Noise cancellation employed on 3T did not provide any significant reduction. Noise in MRI-Linac bunker is greater than background level for all scans and in some cases the noise in the bunker can exceed the noise experienced inside the 3T scanner and hearing protection could be considered. In conclusion, MRI-Linac is generally noisier than the 3T scanner and similar maximum levels were recorded for the loudest sequence.

O39 Investigation of Frequency Domain Near-Infrared Spectrometry (FD-NIRS) parameters as indicators of severity for Hypoxic Ischemic Encephalopathy (HIE)

D. E. Forster[1], E. Koumoundouros[2,3], V. Saxton[2], J. Holberton[2]

[1]The University of Melbourne, Parkville VIC, Australia. (danielle.forster@themedicalroom.com [Presenting Author]). [2]The Mercy Hospital for Women, Heidelberg VIC, Australia. [3]The University of Melbourne, Parkville VIC, Australia.

Introduction The severity of Hypoxic-Ischemic Encephalopathy (HIE) resulting from perinatal asphyxia can be difficult to assess in the first 72 h whilst infants undergo hypothermia treatment (1). Current protocol involves an MRI post-cooling to assess brain injury, which is beyond the window of intervention. Frequency-Domain Near Infrared Spectrometry (FD-NIRS) allows quantification of oxy- and deoxy-Haemoglobin (HBO and HBR respectively) (2, 3). Cerebral oxygenation saturation ($rScO_2$), the ratio of HBO to Total Haemoglobin (HBT), HBO and HBR were investigated as indicators of HIE severity and outcome during hypothermia treatment.

Method HBO and HBR were measured using an OxiplexTS (ISS Inc). 40 Control infants and 6 HIE infants were recruited from The Mercy Hospital for Women. Control infants (mean post-natal age 37 (range 1–98) h, gestation 39+3/7 (range $37^{+6/7}$–$41^{+4/7}$) and birthweight mean 3414 g (2850–4760 g)) were monitored for 5–10 mins. 6 HIE neonates with mean gestation 39 weeks (range $36^{+5/7}$–$41^{3/7}$) and birthweight 3016 g (range 2440–4230 g) were continuously monitored from admission to the Mercy Hospital for Women to until they returned to normal temperature (84 hrs).

Results $rScO_2$ was generally higher in the HIE group (as shown in Fig.1) than to the Controls and this was significantly different in the time periods of 24–36, 48–60 and 72+ h. HBO was significantly higher in the time period 24–36 h, and HBR significantly lower in the 36–60 h period. In case study analysis of the 6 HIE infants, HBO concentration was significantly higher (2 infants) and lower (1 infant) during cooling in the infants with poor outcome at 2 years of age (2 infants) or death (1 infant). Whereas infants with HBO concentrations significantly similar to the Control group prior to re-warming (3 infants) had normal outcomes at 2 years.

Conclusion Results indicate HBO may be an indicator of the severity of HIE during hypothermia treatment and therefore warrants further research.

Acknowledgements All the staff of Mercy Hospital for Women NICU for their ongoing support of the Optimising Cooling for HIE (OCHIE) research project.

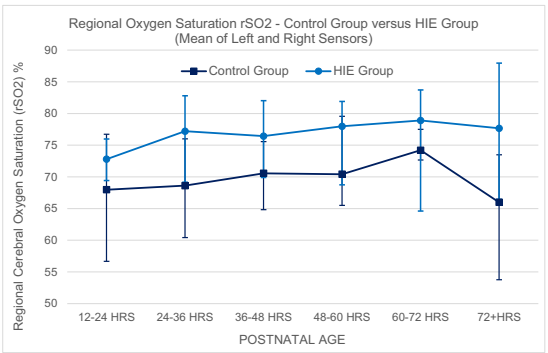

Figure 1. *Mean rScO2 of the left and right sensors in the Control group vs HIE group by Post-Natal Age.*

References

1. Higgins RD, Raju T, Edwards AD, Azzopardi DV, Bose CL, Clark RH, et al. Hypothermia and Other Treatment Options for Neonatal Encephalopathy: An Executive Summary of the Eunice Kennedy Shriver NICHD Workshop. J Pediatr. 2011 11;159(5):851,858.e1.
2. Elwell CE, Cooper CE. Making light work: illuminating the future of biomedical optics. PHILOSOPHICAL TRANSACTIONS OF THE ROYAL SOCIETY A-MATHEMATICAL PHYSICAL AND ENGINEERING SCIENCES. 2011;369(1955): 4358–79.
3. Franceschini MA, Thaker S, Themelis G, Krishnamoorthy KK, Bortfeld H, Diamond SG, et al. Assessment of infant brain development with frequency-domain near-infrared spectroscopy. Pediatr Res. 2007 05;61(5):546–51.

O40 Additive manufacture of gyroid structures: a method to fabricate low Hounsfield-equivalent AM materials

R. Tino[1,2], M. Leary[1,2], E. Ungureanu[3], M. Brandt[1,2], T. Kron[2,3]

[1]RMIT Centre for Additive Manufacture, School of Aerospace, Mechanical and Manufacturing Engineering, RMIT University. (s3487718@student.rmit.edu.au [Presenting Author]), (martin.leary@rmit.edu.au), (milan.brandt@rmit.edu.au). [2]ARC Training Centre in Additive Biomanufacturing, www.additivebiomanufacturing.org, Melbourne, VIC Australia 3001. [3]Physical Sciences, Peter McCallum Cancer Centre, Melbourne, VIC Australia 3000. (Elena.Ungureanu@petermac.org), (Tomas.Kron@petermac.org)

Introduction This work provides first insights on determining the feasibility of fabricating Radiation Dosimetry Phantoms (RDP) using Gyroid structures as the geometric basis for Additive Manufacture (AM). Gyroids are triply periodic minimal surfaces and exhibit unique geometric attributes including the ability to self-tessellate to fill space while allowing varying relative density.

Current AM literature offers limited guidance and validation in highlighting the inhomogeneity of AM-RDPs, especially with low radiopacity. There exist significant opportunities in the quality assurance of these phantoms pertaining to imaging quality and treatment planning of the patient.

Methodology Gyroid structures with differing geometric attributes were 3D-printed using High-Impact Polystyrene. Geometric attributes varied in the experiment are cell numbers and wall thickness. Computed Tomography (CT) (Philips Big Bore) was applied to acquire HU using standard medical protocol of 140 kVp at 3 mm slice thickness. Relative density was evaluated theoretically from the mathematical Gyroid definition (Fig. 1a). Eclipse treatment-planning system was then used to determine mean HU for each volume.

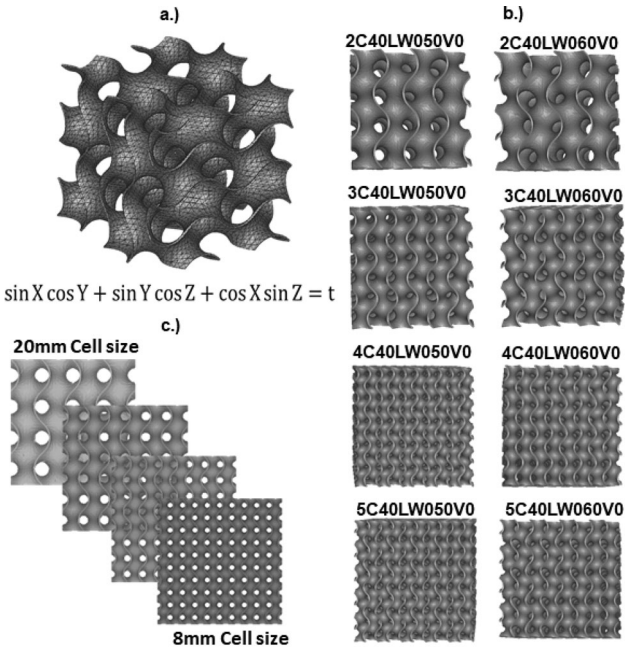

Figure 1 a.) Gyroid mesh structure defined by local Cartesian coordinate X, Y, Z according to specified Isovalue, t b.) STL models of the gyroid geometries where: 2C = Cell number, 40L = Bulk Size, W050 = Wall Thickness, V0 = Isovalue c.) Decreasing gyroid cell size: 2 cell (20mm), 3 cell (13.3mm), 4 cell (10mm), 5 cell (8mm)

Results Samples were successfully manufactured with observed manufacturing artifacts. However, these artifacts appear to have little influence on their observed HU. Varying the Gyroid geometric attributes allows control over the imaged HU. This can be seen with the linear relationship between increasing relative density and mean HU (Fig. 2b) from − 900 to− 700, emulating the lung tissue [1]. For large cell size samples, the Gyroid is visible in the CT image (Fig. 2a.left). For smaller cell size, the Gyroid is less visible due to the partial volume effect [2] observed from the low porous sample (Fig. 2a.right)

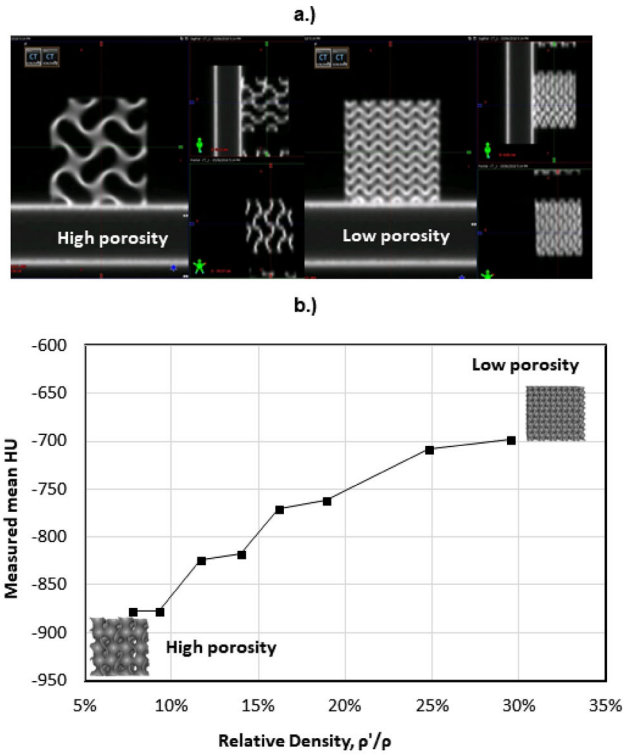

Figure 2 a.) Eclipse treatment planning software to measure mean HU of each sample volume through interpolation b.) Decreasing Gyroid porosity shows linearity between increased relative density and mean HU

Conclusion This research confirms that Gyroid structures provide a feasible candidate for RDP manufacture, specifically for the lung tissue's low varying density. This AM strategy is clinically useful as the variable structure provides a basis for the manufacture of anthropomorphic phantoms using available AM technologies.

References

1. Kalender, W.A., *Computed tomography: fundamentals, system technology, image quality, applications*. 2011: John Wiley & Sons.
2. Soret, M., S.L. Bacharach, and I. Buvat, *Partial-Volume Effect in PET Tumor Imaging*. Journal of Nuclear Medicine, 2007. 48(6): p. 932–945.

Acknowledgements This research was conducted by the Australian Research Council Industrial Transformation Training Centre in Additive Biomanufacturing (IC160100026), www.additivebiomanufacturing.org

O41 Comparison of the diagnostic performances of diffusion parameters in diffusion weighted imaging and diffusion tensor imaging of prostate cancer

N. Gholizadeh[1], P. B. Greer[2,3], J. Simpson[2,3], D. Lee[2,3], P. Lau[4,5], S. Ramadan[1,5]

[1]Faculty of Health and Medicine, The University of Newcastle, Australia. (Neda.gholizadeh@uon.edu.au [Presenting author]), (saadallah.ramadan@newcastle.edu.au). [2]Faculty of Science, The University of Newcastle, Australia. (peter.greer@newcastle.edu.au), (John.Simpson@calvarymater.org.au), (Danny.Lee@newcastle.edu.au). [3]Calvary Mater Newcastle, Radiation Oncology, Australia. [4]Calvary Mater Newcastle, Radiology, Australia. (Peter.lau@hnehealth.nsw.gov.au). [5]Hunter Medical Research Institute (HMRI) Imaging Centre, Australia.

Introduction Diffusion weighted imaging (DWI) measures isotropic water diffusion quantified by the apparent diffusion coefficient (ADC) and is routinely used in prostate cancer (PC) diagnosis [1,2,3]. Diffusion tensor imaging (DTI) measures anisotropic water diffusion and has been extensively used for neural assessment. The most used quantitative DTI parameters are mean diffusivity (MD) and fractional anisotropy (FA) [4] however DTI also yields several parameters that have not been evaluated in the diagnosis of prostate cancer. In this work, nine DTI parametric maps were generated based on eigenvalues including: MD, FA, diffusion mode, axial diffusivity (AD), volume ratio (VR), linear, planar, spherical anisotropy (Cl, Cp and Cs respectively) and radial anisotropy (RA) [5]. The objective of this study was to evaluate and compare the diagnostic capability of DWI parameters to DTI parameters in prostate cancer.

Method Twelve high grade prostate cancer patients signed written consent prior to participating in this study. Cancer and healthy region of interests (ROI)s were outlined in the peripheral zone (PZ) by a radiologist. The sensitivity, specificity of DWI, DTI using FA+MD and DTI using the total parameter space was quantitatively evaluated. An area under receiver operating characteristic (ROC) curve was used to evaluate the diagnostic performance.

Results Quantitative parameters from DWI and DTI for the ROIs and the corresponding p-values are summarized in Table 1.

Table 1. Mean ± standard deviation of the DWI and DTI quantitative parameters for peripheral zone at healthy and cancer region of interests.

Parameters	Healthy	Cancer	p-value
ADC ($\times 10^3 mm^2/sec$)	1.52 ± 0.33	1.08 ± 0.17	0.000
MD ($\times 10^3 mm^2/sec$)	1.45 ± 0.36	0.99 ± 0.25	0.000
FA	0.25 ± 0.08	0.32 ± 0.10	0.002
RA	0.15 ± 0.02	0.17 ± 0.03	0.001
VR	0.88 ± 0.06	0.80 ± 0.07	0.000
	0.08 ± 0.01	0.10 ± 0.02	0.000
	0.16 ± 0.03	0.20 ± 0.03	0.000
	0.77 ± 0.09	0.70 ± 0.07	0.002
Mode	0.03 ± 0.15	0.03 ± 0.16	0.972
AD	1.64 ± 0.26	1.28 ± 0.28	0.000

The diagnostic performance of the quantitative DWI (sensitivity/specificity = 71.1%/89.4%), DTI using FA and MD (sensitivity/specificity = 83.1%/76.9%) and DTI using total quantitative parameters (sensitivity/specificity = 84.2%/88.7%) yielded an area under the ROC curve of 0.850, 0.834 and 0.865, respectively (Figure 1).

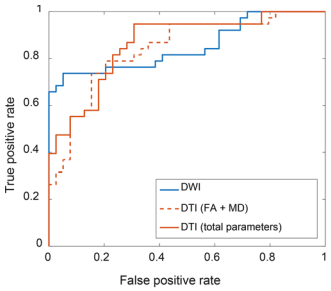

Figure 1. ROC curves of DWI (area = 0.849), MD + FA parameters of DTI (area = 0.834) and DTI using total quantitative parameters (area = 0.865) for cancer vs healthy regions.

Conclusion Our results suggest that new DTI parameters improve the sensitivity, specificity and diagnostic performance of DTI for prostate cancer diagnosis. However, there was no significant difference between DWI and DTI using total quantitative parameters performance.

References

1. Tanimoto A, Nakashima J, Kohno H, Shinmoto H, Kuribayashi S (2007) Prostate cancer screening: The clinical value of diffusion-weighted imaging and dynamic MR imaging in combination with T2-weighted imaging. Journal of Magnetic Resonance Imaging 25 (1):146–152. https://doi.org/10.1002/jmri.20793
2. Le Bihan D, Mangin JF, Poupon C, Clark CA, Pappata S, Molko N, Chabriat H (2001) Diffusion tensor imaging: concepts and applications. Journal of magnetic resonance imaging 13 (4):534–546
3. Gibbs P, Pickles MD, Turnbull LW (2006) Diffusion imaging of the prostate at 3.0 tesla. Investigative radiology 41 (2):185–188
4. Kim CK, Jang SM, Park BK (2012) Diffusion tensor imaging of normal prostate at 3 T: effect of number of diffusion-encoding directions on quantitation and image quality. Br J Radiol 85 (1015):e279–283. https://doi.org/10.1259/bjr/21316959
5. Sinha S, Sinha U (2004) In vivo diffusion tensor imaging of the human prostate. Magnetic resonance in medicine 52 (3):530–537

KS04 Health device cybersecurity: a rapidly evolving landscape

T. Cooper

Trusted Solutions Foundry, Inc.

Until recent years, designers and health and medical devices gave little if any consideration to the security of their devices, let alone the role they might play in managing the overall cybersecurity of an organization. This is exacerbated by the fact that many systems run core operating software that is 5–10 or more years old, with little support for addressing identified security vulnerabilities. There are many incidents of ransomware or horizontal attacks that came from a humble little device sitting in the corner of an exam room, that is discovered and exploited. This session will provide a brief overview of the challenges presented by health device cybersecurity, and then review the standardization and industry efforts to address the problem, providing guidance for those who are either developing new products or are struggling with how to manage 10,000's of devices deployed both inside a healthcare facility as well as with patients out in the wild.

O42 Rethinking cancer: developing the role of physicists in oncology research

M. A. Ebert[1], R. Jeraj[2]

[1]Department of Radiation Oncology, Sir Charles Gairdner Hospital and Department of Physics, University of Western Australia, Perth, Australia. (Martin.Ebert@health.wa.gov.au [Presenting author]).
[2]Department of Medical Physics, University of Wisconsin, Madison WI, USA, and Faculty of Mathematics and Physics, University of Ljubljana, Slovenia. (rjeraj@wisc.edu)

Introduction An international effort is underway to revitalise the role physicists have in cancer research. Conversely, it is in the interests of clinical physicists to ensure they participate in and contribute to cancer research in order to maintain relevance and facilitate achieving the objectives of the global cancer research mission. Efforts are being made within the Australasian region to rethink how physicists can participate in cancer research to greatest effect.
Method A forum on 'Rethinking Cancer' prior to the Engineering and Physical Sciences in Medicine (EPSM) in 2017 focused on: identifying areas which physicists can contribute to;

- provoking relevant physics research;
- identifying barriers currently impeding physicists contributing to cancer research;
- engaging the community, stakeholders and collaborators.

Subsequently, concepts have been discussed for ways to address the issues, appropriately challenge clinical and academic physicists, adequately prepare and enrich the workforce and generate suitable environment and culture.
Results Strategies have been developed that focus on particular issues and from these strategies a shortlist of action items has been identified. These actions revolve around the concepts of:

- encouraging inter-disciplinary understanding and scope;
- expanding medical physics' research horizons;
- developing promotional materials and challenges for the (non-medical) physics and allied community;
- encouraging inter-disciplinary and community engagement via EPSM and other meetings.

One highlighted issue is the importance of a clear description of the medical physics duality – either as a research discipline or clinical profession. There is also a need to tightly engage with international medical physics efforts (e.g., AAPM's Provocative Questions, Expanding Horizons initiatives).
Conclusion The developed strategies form an ongoing process to further the role of physicists in cancer research and all stakeholders are invited to contribute to that process.
Acknowledgements This abstract is submitted on behalf of a large number of individuals who have been participating in this program.

KS05 Current advances in clinical radiation biology aad risk of second cancers following radiation therapy

L. Marcu

The University of Oradea

Innovative therapeutic strategies over the last decade have led to significantly improved survival outcomes among cancer patients. These new strategies that helped revolutionize our approach to therapy are built not only upon technical advances in the field of medical physics but also on strong radiobiological foundations that broadened our understanding of cancer on a molecular level. The latest trends in radiobiology show a shift from a macrolevel to a microlevel evaluation of tumour properties owing to the increasing interest in a more personalised treatment approach.

This talk revisits the radiobiological aspects behind radiotherapy that lead to treatment resistance and failure, covering both traditional factors as well as novel parameters that influence tumour control. The modern Rs of radiobiology will be discussed in the context of novel therapeutic strategies and their impact on clinical practice.

Radiobiological principles also serve in understanding the underlying processes behind second cancers that may occur after the radiotherapy of the primary tumour. The topic of second cancer risk is highly debated nowadays and undoubtedly there is a large epidemiological evidence supporting this risk. It is becoming critical for future studies to strengthen epidemiology by including radiobiological considerations into the big picture. This talk will also tackle the factors that impact second cancer risk, viewed from a radiobiological perspective.

KS06 Future health: Charting the 10-year journey to the 2028 Olympic Games in Los Angeles

T. Cooper

Trusted Solutions Foundry, Inc.

What an opportunity: The Olympic Games in Southern California in 10 years! Given the uniqueness of the region, none of the usual "legacy" projects fit: no stadiums to build, L.A. already has plenty of freeways, and because the 1984 games there were profitable, youth sports programs today are funded by the LA84 Foundation. Consider the creation of a "digital health legacy"—public/private infrastructure that will support state-of-the-art health, wellness and healthcare for everyone in the region—resident and visitor—and can be showcased during the Games. What might that "future health" state look like? What of today's emerging innovative technologies can we advance into common use? And how will care delivery models be changed to meet the challenges of this digital health future? Will the interoperability and standardization issues that have historically held back widespread implementation and use of digital healthcare technology, similarly plague integration of a new generation of knowledge-based technologies integrating IoT, predictive analytics, AI and machine learning, genomic and proteomic content, etc.? What architectures should be considered and what role will disruptors play like Apple, Google, Amazon, Microsoft, and others? This session will explore these questions and more as a team in Southern California works to chart a 10-year journey to establish a digital health legacy by the 2028 Games. How hard can it be? And what could possibly go wrong?!

O43 Development of a simple method for calculating breast dose from radio-guided occult lesion localisation using iodine-125 seeds (ROLLIS)

A. J. Reed, J.-H. Kim, J. W. Burrage

Medical Engineering Physics, Royal Perth Hospital, WA, Australia. (Anita.Reed@health.wa.gov.au [Presenting author]), (Jung-Ha.Kim@health.wa.gov.au), (John.Burrage@health.wa.gov.au)

Introduction Radio-guided occult lesion localisation using iodine-125 seeds (ROLLIS) for surgical removal of impalpable breast lesions has been increasingly used as an alternative to hook-wire localisation.

This study aims to provide a simple technique to estimate the absorbed breast dose to patients undergoing the ROLLIS procedure.
Method The transverse plane dose rates as a function of distance of the I-125 seed (IsoAid, IAI-125A) were obtained from the supplement to the TG-43U1 [1]. These data were used to calculate the dose rate to voxels in a breast modelled as a voxelised hemisphere. The dose rate to each voxel within the breast was calculated using values interpolated from the transverse plane dose rate data set and the radial distance of each voxel from the seed position. Two scenarios were simulated: (i) One seed at the centre of lesion; and (ii) Two seeds bracketing the lesion. As a volume of tissue is excised from the breast (lesion + margin), the mean dose to the breast was calculated excluding this excision volume which is modelled as a sphere with its centre at the centre of the lesion. Absorbed doses were calculated for a range of breast and lesion sizes.
Results The calculated post-excision absorbed dose rates to a breast from the ROLLIS procedure ranged from 0.0097 to 0.0466 $mGy{\cdot}MBq^{-1}\ h^{-1}$. The post-excision absorbed breast dose depends on many factors including breast size, lesion size, seed number, seed activity and the time in situ.
Conclusion The feasibility of using this technique to estimate the absorbed dose to the breast from ROLLIS procedure has been demonstrated. Based on clinical data collected, the absorbed dose to the breast for a typical ROLLIS patient would be approximately 0.3 mGy. Lookup tables were compiled to make absorbed dose to the breast simpler to evaluate for future ROLLIS patients.

References

1. Rivard MJ, Butler WM, De Werd LA et al (2007) *Supplement to the 2004 update of the AAPM Task Group No. 43 Report.* Med Phys **34**: 2187–2205.

O44 HDR brachytherapy source tracking: sensitivity of plan quality dose metrics to source position measurement uncertainties

M. D. Hanlon[1], R. L. Smith[2], V. Panettieri[2], R. D. Franich[1]

[1]School of Science, RMIT University, Melbourne, Australia (Maximilian.Hanlon@rmit.edu.au [Presenting author]), (Rick.Franich@rmit.edu.au). [2]Alfred Health Radiation Oncology, The Alfred, Melbourne, Australia. (Ryan.Smith@alfred.org.au), (v.panettieri@alfred.org.au)

Introduction Correct delivery of an HDR brachytherapy treatment can be confirmed with source tracking by comparing measured dwell positions and times to the plan [1]. Dose metrics derived from the re-calculated plan can be used to assess the impact of any observed differences. Understanding the sensitivity of dose metrics to measurement uncertainties in the source tracking system is critical, and can guide the selection of suitable dosimetric indicators and action level thresholds.
Method For 10 clinical patient plans, planned dwell positions were altered by applying random shifts between 1–10 mm per dwell to simulate a source tracking data-log subject to random (Type A) uncertainties of various magnitudes. The dose distribution arising from the new dwell coordinates was calculated with an independent TG-43-based dose calculation engine. Plan quality dose metrics were calculated and compared to those of the original plan. Re-calculations were repeated 10 times for each degree of shift to assess the mean effect.
Results Plan metrics relating to the PTV (PTV D90, V100%, V150%, V200%) generally showed insensitivity to random dwell position shifts up to 5 mm, with D90 and V100% changing from ideal to acceptable or unacceptable above this. OAR dose metrics showed greater sensitivity, with the urethra D10 becoming unacceptable from 3–5 mm, depending on initial values. In some plans, steep dose gradients in or near urethra contour showed that urethral D10 can also be hyper-sensitive to differences in dose-grid interpolation.

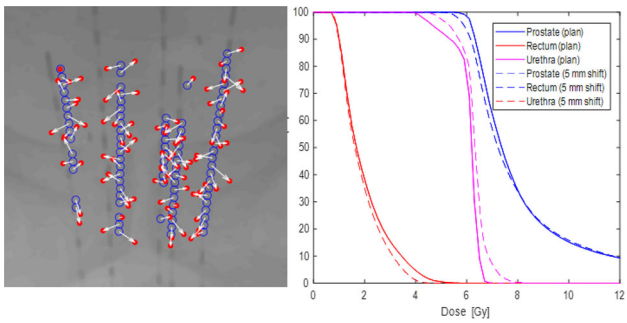

Figure 1: (Left) Coronal radiograph of patient of HDR implant with radiopaque markers inside a subset of catheters. Blue circles represent planned dwell positions, red markers represent dwell positions randomly shifted by 0-5 mm with white arrows between. (Right) DVH representation of a patient plan with no changes (solid lines) and with a 5 mm maximum random shift applied to each dwell (dashed)

Conclusion Knowledge of the quantitative dependence of plan dose quality metrics on random uncertainties in source position tracking should be used to drive the degree of accuracy and precision required of such systems to meet clinical objectives.
For these prostate plans, the source tracking system should have the ability to resolve source position to within 3 mm for sensitivity to urethral D10 constraint.

References

1. Smith, R. L., Hanlon, M., Panettieri, V., Millar, J. L., Matheson, B., Haworth, A., & Franich, R. D. (2017). An integrated system for clinical treatment verification of HDR prostate brachytherapy combining source tracking with pretreatment imaging. *Brachytherapy*.

O45 A study of longitudinal seed deployment accuracy for LDR prostate implants using a new transrectal ultrasound phantom

M. W. Jennings[1,2], T. P. Rutten[1,2]

[1]Department of Radiation Oncology, Royal Adelaide Hospital, Adelaide, Australia. (matthew.jennings@adelaide.edu.au [Presenting author]), (thomas.rutten@sa.gov.au). [2]Department of Physics, University of Adelaide, Australia

Introduction Transrectal ultrasound (TRUS) imaging is useful for guiding needle insertion and seed strand deployment in LDR prostate implant procedures, but it can suffer from artefacts and image quality degradation introduced by the metal needles. Longitudinal errors in seed deployment can result in an underexposed prostate, overexposure to the urethra or penile bulb, or seeds accidentally implanted into the bladder. The objective of this study was to test the longitudinal accuracy of needle insertion and seed deployment at the Royal Adelaide Hospital in order to improve LDR prostate implant quality.
Method A new phantom was constructed to simulate implantation (see Figure 1). The transparent phantom contains a water-filled balloon surrounded by gelatin with a cavity running through its posterior. The balloon simulates a patient's bladder and the cavity permits insertion of a TRUS probe. The user inserts needles into the phantom via a rubber membrane and deploys seed strands within the gelatin

under TRUS guidance. The phantom's lateral faces are precisely etched at 5 mm intervals for the user to measure longitudinal positions of strands after deployment. The phantom's transparency allows the user to observe etchings on both faces to avoid parallax error. Simulations of implants using the phantom were first conducted by physicists and then one of our prostate implant urologists.
Results TRUS images accurately reflected true needle-tip positions within the QA phantom, with an average deviation of + 0.5 mm (where '+' indicates the inferior direction). However, initial seed deployment results yielded unacceptably high average errors between deployed and planned strand position of + 4.1 mm. Subsequent investigation highlighted a systematic error in the urologist's deployment technique. Correcting this technique significantly improved longitudinal accuracy of strand deployment to an average error of + 1.5 mm.
Conclusion The new phantom has proved valuable for assessing and subsequently improving LDR prostate implant accuracy.

O46 EyeCheck: development of a system for fast QA of low dose rate brachytherapy eye plaques

T. Brennen[1], J. Poder[1], D. L. Cutajar[1], G. Cohen[2], A. Damato[2], M. Petasecca[1], A. B. Rosenfeld[1]

[1]Centre for Medical Radiation Physics, University of Wollongong, AUS. (tjb790@uowmail.edu.au [Presenting author]), (joel.poder@health.nsw.gov.au), (deanc@uow.edu.au), (marcop@uow.edu.au), (anatoly@uow.edu.au). [2]Memorial Sloan Kettering Cancer Care Centre, New York, USA. (damatoa@mskcc.org)

Introduction Ocular melanomas are often treated using LDR brachytherapy seeds places posteriorly on the eye sclera by the means of a metallic plaque. Fast and accurate quality assurance (QA) measures do not exist, with visual inspection by a physicist being common practice. A novel approach utilising gamma camera imaging techniques with a high resolution Medipix device is presented.
Method The QA system developed consists of a single cone pinhole tungsten collimator. Situated directly below the pinhole at a variable distance is a Medipix detector, allowing for adjustment of magnification and FoV for varying plaque sizes. A computer algorithm developed in MATLAB has been designed to provide automatic seed detection and extraction from the images, as shown in Figure 1. It is then possible to assess each seeds activity and verify the configuration within the plaque.

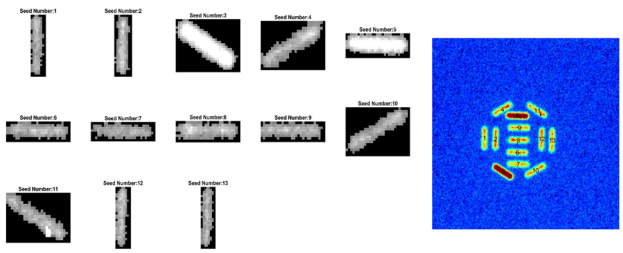

Figure 1: Each seed is extracted from the image (left) and given a label as to its position in the plaque image (right).

Results Measurements with various plaque sizes, activities (uniform and non-uniform loading), and miss loading scenarios have been undertaken. This work has shown the successful development and application of a system, that when coupled with an algorithm for performing automatic seed extraction from high resolution images of eye plaques (of ranging diameters; 12, 14, 16, 18, 20, and 22 mm COMs plaques), has the capabilities to be used as a complete QA system for eye plaque verification.
Conclusion It has been demonstrated that it is possible to use a solid state silicon pixelated detector, Medipix, to perform QA for eye plaque brachytherapy. An algorithm for automatic seed extraction has been developed for use with a digital QA system for the developed system. It is envisaged that further development of the system will allow for verification of vendor plaques and absolute calibration of preloaded seeds.

References

1. Vajidic C. M, Kricker A *et al* (2003), "Incidence of ocular melanoma in Australia from 1990 to 1998.", *International Journal of Cancer* 105: 1:117–122

O47 A Leipzig-style applicator for HDR skin brachytherapy: caveats & corrections

P. Reich[1], C. Bridger[2], A. Santos[1]

[1]Department of Medical Physics, Royal Adelaide Hospital, South Australia. (paul.reich@sa.gov.au [Presenting Author]). [2]School of Physical Science, University of Adelaide, South Australia. (a1687402@student.adelaide.edu.au), (alexandre.santos@sa.gov.au)

Introduction During the commissioning of a Leipzig-style applicator the dose measured at the skin surface and beyond were found to be systematically greater than predicted by our treatment planning system and Monte Carlo data published in the literature. A published study on the Leipzig-style applicator also reported higher doses than expected and concluded the primary cause was source sag due to gravity inside the applicator [1]. The purpose of our study was to validate the source sag hypothesis by ruling out set-up error and measurement reproducibility and to apply any necessary corrections during treatment.
Method Reproducibility and set-up error in the delivered dose was evaluated using film with the Leipzig-style applicator positioned in two orientations: treatment cone facing up and facing down, repeated five times in each orientation. In addition, repeated measurements were performed by varying the degree of bend in the source guide tube (SGT) connection between the applicator and afterloader. All measurements were performed using calibrated Gafchrmic^{TM} EBT^{3} film at 3 mm depth in a Solid Water phantom. The effective source position in the treatment planning system was subsequently corrected to account for source sag during treatment.
Results Set-up error was ruled out as the primary cause of the known discrepancies. Reproducibility in delivered dose was within ± 3 %. Varying the curvature in the SGT did not have a statistically significant impact on the delivered dose. The discrepancy between measurement and treatment planning system was less than ± 5 % after applying an offset to the source position in our treatment planning system.
Conclusion Source sag due to gravity within the Leipzig-style applicator was confirmed to be the primary cause of discrepancy between measurement and treatment planning system. The source offset in the planning system was subsequently modified to account for source sag during treatment.

References

1. Jeong J, Barker CA, Zaider M, Cohen GN (2016) Impact of source position on high-dose-rate skin surface applicator dosimetry. Brachytherapy 15:650–660.

O48 BrachyView: Development of an algorithm for real-time automatic seed detection and reconstruction

T. Brennen[1], D. L. Cutajar[1], S. Alnaghy[1], J. Bucci[2], A. Bece[2], L. Galli[3], M. Favoino[3], F. Carriero[3], M. Lerch[1], A. B. Rosenfeld[1], M. Petasecca[1]

[1]Centre for Medical Radiation Physics, University of Wollongong, AUS. (tjb790@uowmail.edu.au [Presenting author]), (deanc@uow.edu.au), (sa641@uowmail.edu.au), (mlerch@uow.edu.au), (anatoly@uow.edu.au), (marcop@uow.edu.au). [2]St George Cancer Care Centre, St George Hospital, Kogarah, Australia. (joseph.bucci@health.nsw.gov.au), (andrej.bece@health.nsw.gov.au). [3]Advanced Computer Systems Pty Ltd, Rome, Italy. (luca.galli@acsys.it), (marco.favoino@acsys.it), (francesco.carriero@acsys.it)

Introduction BrachyView is a novel in-body imaging system developed with the objective to provide real-time intraoperative dosimetry for LDR prostate brachytherapy treatments. The system can reconstruct the 3D positions of seeds after their implantation by the means of a high-resolution pinhole gamma camera[1].
Previous work has shown the BrachyView probes capabilities to identify 100% of the seeds and reconstruct seeds 75% of seeds' positions within 1 mm of their nominal positions determined by CT[1] by an operator based procedure. This work presents the development of a real-time fully automatic seed reconstruction algorithm that has been developed and tested in MATLAB.
Method The algorithm proposed utilises a local feature detector, speeded up robust features (SURF), to perform detection of brachytherapy seeds 2D projections. An automatic frame alignment and subtraction procedure is utilised, allowing for increased accuracy and elimination of the previously subjective manual procedure. The complete algorithm architecture is shown in Figure 1.

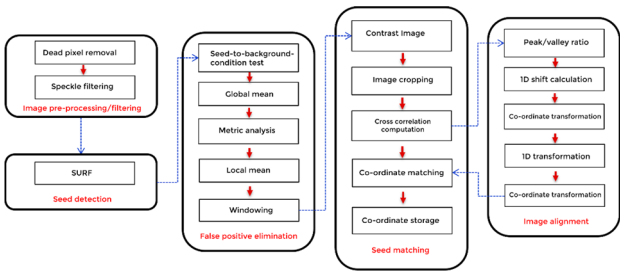

Figure 1: Automatic detection software architecture.

Results The algorithm has been tested using the experimental results obtained with 98 I-125 brachytherapy seeds implanted into a prostate gel phantom. It is able to correctly identify and match 94% of the implanted seeds, as shown in Figure 2. False positive detection removal has shown to be extremely effective with 90 false positives reduced to 1 with the processes outlined in Figure 1. With an average computation time of 2.75 seconds per needle.

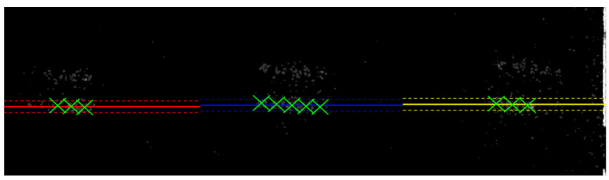

Figure 2: Automatic alignment and background subtraction has been performed, image pre-processing and false positive elimination.

Conclusion It is the authors' belief that with integration of the proposed algorithm with the current in-house C++ software, the accuracy of the 3D reconstruction calculations will be improved, providing a highly accurate and robust method for automatic seed reconstruction for use as an intra-operative dosimetry tool for LDR prostate brachytherapy treatments.

References

1. Alnaghy S, Cutajar D. L, Bucci J. A et al (2016), BrachyView: Combining LDR seed positions with transrectal ultrasound imagining in a prostate gel phantom, European Journal of Medical Physics 34:55–64

O49 Global comparison of targeted alpha vs targeted beta therapy for cancer: In vitro, in vivo and clinical trials

B. J. Allen[1], L. Marcu[2,3], E. Bezak[4,5]

[1]School of Medicine, University of Western Sydney, Locked Bag 1797, Penrith NSW 2751, Australia. (bja1940@outlook.com [Presenting author]). [2]Department of Physics, Faculty of Science, 1 Universitatii street, University of Oradea, 410087, Romania. [3]School of Health Sciences, University of South Australia, Australia. (Loredana@marcunet.com). [4]Cancer Research Institute and School of Health Sciences, University of South Australia, Australia. [5]Department of Physics, University of Adelaide, Australia. (Eva.Bezak@unisa.edu.au)

Introduction Targeted therapy for cancer is a rapidly expanding and successful approach to the management of many intractable cancers. However, most immunotherapies fail in the longer term and there continues to be a need for improved targeted cancer cell toxicity, which can be achieved by radiolabelling the targeting vector with a radioisotope. Such constructs are successful in using a gamma ray emitter for imaging. However, this is often not the case for beta emitters is used for therapeutic applications. The new approach is to use the short range and highly cytotoxic alpha radiation from alpha emitters to achieve improved efficacy and therapeutic gain.
Methods This paper reviews available experimental and theoretical comparisons of efficacy and therapeutic gain for alpha and beta emitters labelling the same targeting vector in the published literature.
Results Comparative results are given for in vitro cytotoxicity, in vivo toxicity and therapeutic efficacy for tumour growth inhibition and regression. Evaluation of preclinical data and clinical trials show that alpha radiation is better suited to the treatment of microscopic or small-volume disease since their short range and high energies potentially offer more efficient and specific killing of tumour cells, while sparing distant normal cells
Conclusion The overall conclusion is that targeted alpha therapy is superior to targeted beta therapy in every case. As such, the application of targeted alpha therapy in clinical settings should be expanded with high priority.

IS04 Radiomolecular imaging & molecular radiotherapy: some novel emerging 'niche' roles in targeted cancer diagnosis & treatment

R. I. Price

Dept of Medical Technology & Physics, Sir Charles Gairdner Hospital, Australia & School of Physics, University of Western Australia. (Roger.price@health.wa.gov.au)

Introduction The SNMMI has defined molecular imaging (MI) as the 'visualization, characterization, and measurement of biological processes at the molecular and cellular levels in humans and other living systems'. Considerable advances this century have been made in the version where the reporter signal is provided by a targeting PET or SPECT radioisotope ('radioMI)', usually as robustly-bound cargo on a biomolecule that is stable under physiological conditions and which systemically targets a specific tumour-cell population. Increasingly, this is combined with a 'theranostic' strategy where (guided by the quantitative radioMI) the same cell-selective molecular ligand is used subsequently to deliver a β^- or β-emitting cytotoxic agent of the same or chemically-similar elemental species to the tumour cells. This 'molecular radiotherapy' (MRT) is applicable to a restricted class of cancers, in addition to its traditional use in the thyroid; haematological; neuroendocrine, metastatic prostate, paediatric neuroblastoma and bone metastases. However its extension to further applications covered by traditional approaches such as external beam radiation therapy (EBRT) faces formidable challenges, including targeting specificity, radiopharmacokinetics, delivered-dose estimation (tumour-tissue vs. tissues-to be-spared), and the interpretation of calculated 'mean absorbed doses' in terms of beneficial (target) and detrimental (non-target) biological effects when compared with more comprehensive EBRT-based data. To advance the scope and effectiveness of radioMI and MRT (and particularly their combination), improved understanding of MRT dose-efficacy/detriment relationships and new targeting radiomolecular agents must be formulated. This short review highlights some emerging possibilities.

Method Since MRT requires systemic administration and is not restricted by accurate geometric targeting (i.e., only its molecular specificity), dose is estimated by MIRD or related schemas, underpinned by Monte Carlo data from standard phantoms [1]. Injected activities (MBq) are pragmatically based on limiting side-effects. However there seems considerable scope for model-based dosimetry such as the biologically effective dose (BED) for providing a common dose-vs-effect platform for MRT acting alone, comparing MRT and EBRT outcomes [1, 2] or (in selected cases) for hybrid MRT+EBRT therapies [1, 3]. For delivering precision therapies, development and meaningful clinical deployment of new radiomolecular agents (e.g., theranostic combinations such as 18F-PSMA [PET/CT] and 225Ac-PSMA [targeted alpha-therapy]) depend on innovations and breakthroughs along the entire 'supply chain'. These include advances in cyclotron technologies; reliable reactor-based therapy-isotope productions; avid, rapid and specific targeting biomolecular platforms and strategies; advances in synthetic radiochemistry; and innovations in imaging such as total-body PET/CT [4]. Many such advances are 'in the pipeline' and some are reflected in early clinical trials. New combinations of physics, engineering and radiochemistry expertise are incubating a new professional class, the 'radiopharmaceutical scientist' (RPS), for which a training program has recently been formulated in Australia under ACPSEM management.

Conclusion Emerging multidisciplinary opportunities for delivering effective 'niche' precision-medical radiopharmaceutical-based treatments within the cancer management spectrum are being driven by rapid advances in radioMI and MRT, served by a new class of professionals, the RPS.

References

1. Bolch WE et al., 2009 MIRD pamphlet No. 21 *Journal of Nuclear Medicine* **50** 477–84
2. Wessels BW et al., 2008 MIRD pamphlet No. 20 *Journal of Nuclear Medicine* **49** 1884–99
3. Bodey R et al., 2003 *Cancer Biotherapy and Radiopharmaceuticals* **18** 89–97
4. Cherry et al., 2018 *Journal of Nuclear Medicine* **59** 3–12

O50 Dead time characterisation for quantitative SPECT of 177Lu and 90Y

C. D. Pain, G. J. O'Keefe, S. J. Gong

Department of Molecular Imaging and Therapy, Austin Health, Vic. (cameron.pain@austin.org.au [Presenting author])

Introduction The following work aims to characterise the count-rate dependence of gamma camera sensitivity for quantitative SPECT of the therapeutic isotopes and . Deadtime corrections are necessary for accurate quantitation at high count rates. Planar sensitivity measurements on a GE Discovery 670 Pro for varying amounts of activities are presented.

Method Sensitivity variation for was compared to the Sorenson deadtime model [1] by measuring count rate as a function of activity with an initial activity of 1.5 GBq and a set up described in NEMA NU 1 2007 measurement of planar sensitivity [2]. The planar sensitivity was measured at activities of 258 MBq, 721 MBq and 1950 MBq for and activities of 228 MBq, 720 MBq and 2160 MBq for.

Results Deadtime effects for are well approximated by a linear fit in the count rate region investigated as shown in Figure 1.

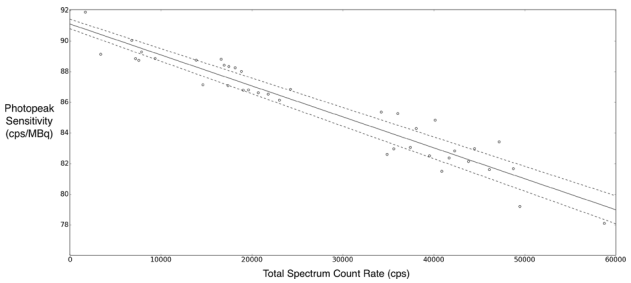

The planar sensitivities for and at specified count rates are shown in Table 1.

Table 1: Planar sensitivities for and .

Count Rate (cps)	Sensitivity (cps/MBq)	Count Rate (cps)	Sensitivity (cps/MBq)
6705	7.92	3522	4.61
17479	7.52	9591	4.39
45249	7.33	26118	4.123

Conclusions The dead time effects for have been shown to decrease sensitivity linearly as a function of total spectrum count rate. Sensitivity values of and also show a relative decrease consistent with the curve. Future work will involve finer sampling of the and sensitivity data to confirm whether the normalised describes dead time effects of all three isotopes. Volume sensitivity curves will also be produced for comparison.

References

1. Sorenson. J. A, 1975, Deadtime characteristics of Anger Cameras, J Nucl Med Vol. 16(4), pp. 284–288
2. NEMA, 2007, NEMA NU 1 Performance Measurements of Gamma Cameras

O51 Quality assurance for a CyberKnife® system: the power couple

G. Biasi[1], S. Alhujaili[1,2], S. Guatelli[1], M. A. Ebert[3,4], T. Kron[5,6], A. B. Rosenfeld[1], M. Petasecca[1]

[1]Centre for Medical Radiation Physics, University of Wollongong, Wollongong, Australia (gb446@uowmail.edu.au [Presenting author]). [2]Radiology and Medical Imaging Department, College of Applied Medical Sciences, Aljouf University, Saudi Arabia. [3]Department of Radiation Oncology, Sir Charles Gairdner Hospital, Perth, Australia. [4]School of Physics and Astrophysics, University of Western Australia, Perth, Australia. [5]Peter MacCallum Cancer Centre, Melbourne, Australia. [6]Sir Peter MacCallum Cancer Institute, University of Melbourne, Melbourne, Australia

Introduction The CyberKnife® robotic unit delivers x-ray radiotherapy with sub-mm accuracy. Codes of Practice [1, 2] dedicated to small-field dosimetry prescribe the use of suitable detectors, but none of the commercially available options is ideal. For example, recommended diodes require correction factors [3]; their angular-dependence prevents their use for patient-specific quality assurance (QA) if non-isocentric beams are employed; sub-mm resolution is achievable only by scanning with single detectors [2]. We report on two devices which would fill the technological gap.

Method The *Octa* is a 2D detector (Figure 1) [4]. Its 512 sub-mm diodes are arranged with sub-mm pitch along 4 crossing linear arrays. Its potential for machine-specific QA was investigated with output factors (OFs), off-axis ratios, PDDs and TMRs measurements. A PTW SRS diode was considered as benchmark. Investigated field sizes were between to diameter.

The *Edgeless* is an angular-independent single diode-detector (side) [5]. Its potential for patient-specific QA was investigated with plans delivered to a lung phantom, in static and dynamic conditions (Figure 2). EBT3 films and the Multiplan® treatment planning system (TPS) were considered as benchmarks.

Results The *Octa* was correction-free for OFs measurements. Its diodes' layout allowed for OF and 4 off-axis ratios to be measured simultaneously. Central-axis PDDs and TMRs distributions were accurate within and respectively. Its potential for accurate positional-verification of a dynamic aperture collimator (Iris™) was shown. Dose measurements by the *Edgeless* agreed within and with TPS and EBT3 films respectively. The potential for its use in an array of single devices was shown.

Conclusion The integrated use of two real-time devices, a 2D array detector dedicated to machine-specific QA and an angular-independent single diode dedicated to patient-specific QA was shown to be appropriate for a comprehensive CyberKnife-dedicated QA.

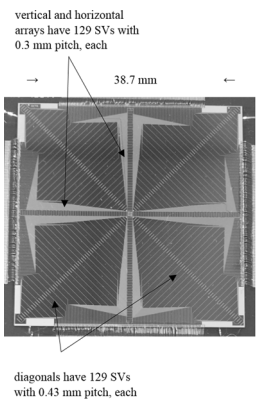

Figure 1. The Octa, a 2D monolithic silicon array detector dedicated to machine-specific QA. It has 512 diode-sensitive volumes (SVs) arranged with sub-mm pitch along 4 crossing linear arrays.

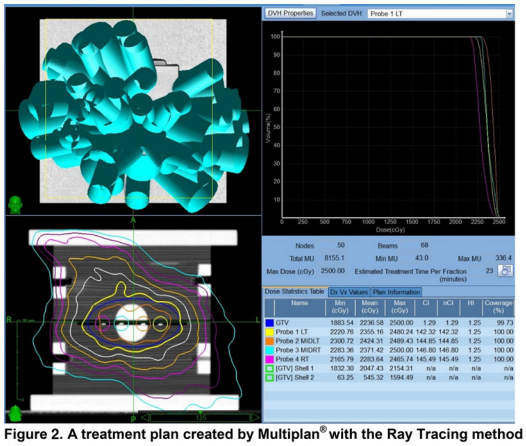

Figure 2. A treatment plan created by Multiplan® with the Ray Tracing method for the lung phantom. Edgeless-diodes, numbered from 1 to 4, are shown at their position inside the heterogeneous timber phantom (left lower panel): two diodes were placed inside the spherical solid water target volume and two diodes were placed in the surrounding timber.

Acknowledgements We would like to acknowledge the Gross Foundation and the National Health and Medical Research Council of Australia (grant APP 1123376) for financial support. We would like to thank G. Grogan, B. Hug and J. Lane at the Sir Charles Gairdner Hospital for access to their CyberKnife®. S. Alhujaili is supported by the Aljouf University. We would like to thank Dr V. Perevertaylo for useful discussions and support with detector fabrications.

References

1. IAEA (2017) Technical Reports Series No.483 - Dosimetry of Small Static Fields Used in External Beam Radiotherapy
2. ICRU (2017) ICRU Report 91 - Prescribing, Recording, and Reporting of Stereotactic Treatments with Small Photon Beams
3. Francescon P, Beddar S, Satariano N, Das IJ (2014) Variation of k for the small-field dosimetric parameters percentage depth dose, tissue-maximum ratio, and off-axis ratio. Med Phys 41:101708 . https://doi.org/10.1118/1.4895978
4. Biasi G, Petasecca M, Guatelli S, et al (2018) A novel high-resolution 2D silicon array detector for small field dosimetry with FFF photon beams. Phys Medica 45:117–126. https://doi.org/10.1016/j.ejmp.2017.12.010
5. Petasecca M, Alhujaili S, Aldosari a. H, et al (2015) Angular independent silicon detector for dosimetry in external beam radiotherapy. Med Phys 42:4708–4718. https://doi.org/10.1118/1.4926778

O52 Sensitivity of EPID dosimetry to delivery errors for pre-treatment verification of lung SBRT VMAT plans

T. Alharthi[1,2,3,4], S. Arumugam[3,5], P. Vial[1,3,4,5], L. Holloway[1,3,4,5,6], D. I. Thwaites[1]

[1]Institute of Medical Physics, School of Physics, The University of Sydney, Sydney, New South Wales, Australia. (talh5880@uni.sydneuy.edu.au [Presenting author]), (philip.vial@health.nsw.gov.au), (Lois.Holloway@health.nsw.gov.au), (david.thwaites@sydney.edu.au). [2]School of Medicine, Taif University, Taif, Saudi Arabia. [3]Liverpool and Macarthur Cancer

Therapy Centers, Liverpool, NSW, Australia. [4]Ingham Institute for Applied Medical Research, Sydney, NSW, Australia. [5]South Western Sydney Clinical School, University of New South Wales, Sydney, NSW, Australia. (Sankar.Arumugam@sswahs.nsw.gov.au). [6]Centre for Medical Radiation Physics, University of Wollongong, Wollongong, NSW, Australia.

Introduction Stereotactic body radiotherapy SBRT involves the delivery of substantially larger doses over fewer fractions compared to conventional radiotherapy. Dosimetry verification and patient-specific quality assurance (QA) tests are particularly important in such a complex treatment to ensure accurate treatment delivery [1, 2]. The aim is to study the sensitivity of an Electronic Portal Imaging Device (EPID) in detecting delivery errors for VMAT lung SBRT using the Collapsed Arc method.
Method Baseline VMAT plans and plans with intentionally introduced errors were generated for 15 lung SBRT patients. Three types of errors were introduced by modifying collimator angles, multi-leaf collimator (MLC) field sizes and MLC shifts by ± 5°, ± 2°, and ± 1° or mm. A total of 103 plans were measured with EPID on an Elekta Synergy Linear Accelerator (Agility MLC) and compared to both the original treatment planning system (TPS) Collapsed Arc dose matrix and the no-error baseline EPID measurements. Gamma analysis was performed using the OmniPro-I'mRT (IBA Dosimetry) software and gamma criteria of 1%/1 mm, 2%/1 mm, 2%/2 mm, and 3%/3.
Results When the error-introduced EPID measured doses were compared to the TPS matrices, the majority of simulated errors were detected with gamma tolerance of 2%/1 mm and 1%/1 mm. When the error-introduced EPID measured doses were compared to the baseline EPID measurements, all the MLC field size and MLC shift errors, and ± 5° collimator errors were detected using 2%/1 mm and 1%/1 mm gamma criteria.
Conclusion This work demonstrates the feasibility and effectiveness of the collapsed arc technique and EPID for pre-treatment verification of lung SBRT VMAT plans. The EPID was able to detect the majority of MLC errors and the larger collimator errors with sensitivity to errors depending on the gamma tolerances.

References

1. Benedict SH, Yenice KM, Followill D, Galvin JM, Hinson W, Kavanagh B, Keall P, Lovelock M, Meeks S, Papiez L, Purdie T. Stereotactic body radiation therapy: the report of AAPM Task Group 101. Medical physics. 2010 Aug 1;37(8):4078–101.
2. Giglioli FR, Clemente S, Esposito M, Fiandra C, Marino C, Russo S, Strigari L, Villaggi E, Stasi M, Mancosu P. Frontiers in planning optimization for lung SBRT. Physica Medica: European Journal of Medical Physics. 2017 Dec 1; 44:163–70.

O53 Investigating the advantages of reducing respiratory motion for tomotherapy stereotactic ablative body radiotherapy (SABR) deliveries

Y. Hu[1], B. Archibald-Heeren[2], M. Byrne[2], E. Cai[3], Y. Wang[3]

[1]Radiation Oncology Centres Gosford, Gosford, Australia. (yunfei.hu@roc.team [Presenting author]). [2]Radiation Oncology Centres Wahroonga, Wahroonga, Australia. (ben.archibald-heeren@roc.team), (mikel.byrne@roc.team). [3]ICON Cancer Centre Revesby, Revesby, Australia(emma.cai@icon.team), (yang.wang@icon.team)

Introduction TomoTherapy can provide highly accurate SABR deliveries, but without any effective motion management techniques. Shallow breathing has been identified as one possible motion management solution on TomoTherapy, which has been made possible with the BreatheWell audiovisual biofeedback (AVB) device, whose implementation requires comprehensive verification and validation. This paper investigated the potential advantages of performing shallow breathing during TomoTherapy SABR delivery.
Method Healthy volunteers were randomly selected, whose breathing waveforms were recorded under normal breathing and shallow-breathing conditions by the Varian RPM system. The subject's shallow breathing was guided by the BreatheWell device, which provided AVB to the patient to help controlling the breath. These waveforms were then imported to the 4-dimensional QUASAR phantom to investigate whether shallow breathing was able to effectively reduce target's breathing motion among various individuals. A dosimetric study was also performed using the same phantom, whose cylindrical insert was designed to move at different speeds and amplitudes. SABR plans were generated, delivered and measured on the phantom with ion-chamber and Gafchromic EBT3 film as the dosimeters. The planning statistics and the measurement results of the insert moving at different amplitudes and speeds were compared.
Results Results from healthy volunteers suggested that performing shallow breathing using the BreatheWell device can effectively reduce the target's respiratory motion amplitude. Dosimetric study results demonstrated that by reducing the target's motion, in addition to improved target dose coverage, dose to surrounding organ-at-risks (OARs) was also reduced due to a reduced planning margin. Gamma analysis results also indicated that with reduced target motion, the delivery accuracy of the plan was also significantly improved, possibly due to reduced dose blurring and MLC interplay effect.
Conclusion It was found that for TomoTherapy SABR deliveries, by reducing the targets respiratory motion through shallow breathing, target coverage, organ-at-risk (OAR) sparing and delivery accuracy were improved.

O54 Assessment of intra-fraction prostate motion and delivered dose accuracy in prostate SBRT using an in-house real-time position monitoring system

S. Arumugam[1,2,3], M. Udovitch[1], A. Xing[1,2,3], L. Holloway[1,2,3,4,5], M. Sidhom[1,2]

[1]Liverpool and Macarthur Cancer Therapy Centres, Liverpool, NSW, Australia. (Sankar.Arumugam@health.nsw.gov.au [Presenting author]), (Mark.Udovitcg@health.nsw.gov.au), (Aitang.Xing@health.nsw.gov.au), (Lois.Holloway@health.nsw.gov.au), (Mark.Sidom@health.nsw.gov.au). [2]Ingham Institute for Applied Medical Research, Sydney, NSW, Australia. [3]South Western Sydney Clinical School, University of New South Wales, Sydney, NSW, Australia. [4]Institute of Medical Physics, School of Physics, The University of Sydney, Sydney, New South Wales, Australia. [5]Centre for Medical Radiation Physics, University of Wollongong, Wollongong, NSW, Australia

Introduction To assess and correct the intra-fraction prostate motion in prostate Stereotactic Body Radiation Therapy (SBRT) using an in-house real-time position monitoring system.
Materials and methods An online x-ray image based position monitoring system, SeedTracker, was developed to monitor the position of radiopaque markers implanted in prostate. The SeedTracker system is currently being used at Southwestern Sydney Local Health District to monitor the prostate position of the patients treated within PROMETHEUS trial (UTN: U1111-1167-2997). To date the system is successfully used for the position verification of 54 patients. The difference in dose delivered between the treatment with and

without real-time monitoring and position corrections were assessed by introducing the observed position deviations, at the respective time of delivery, in treatment plans and recalculating the dose.

Results The mean (σ) treatment time and dose delivery time of individual SBRT fractions are 32.4(12.6) mins and 5.5(2.3) mins respectively. In 17% of treatment fractions the position deviations were observed at the start of treatment delivery just before turning on the treatment beam and 80% of time this occurred at the first treatment fraction. The continuous drift in prostate position during the treatment delivery, which resulted in the gating event, was observed in 15% of the treatment fractions and 40% of these events are multiple occurrences in the same fractions. The transient excursion of prostate position occurred in 5% of the treatment fractions. The retrospective dose reconstruction study showed that the D98 to prostate would have decreased by a maximum 12% compared to the planned D98 in some cases if real-time position monitoring had not been performed and position corrections were not under taken.

Conclusion The real-time position monitoring of prostate SBRT was successfully achieved using an in-house system and the developed system shown to improve the accuracy of treatment delivery.

O55 End-to-end dosimetry audits of stereotactic ablative radiotherapy

M. Shaw[1,2,6], A. Alves[1], C. Davey[1], S. Keehan[3], F. Kadeer[1], J. Kenny[1,4], J. Supple[1], N. Hardcastle[3], J. Lehmann[2,5], M. Geso[2], J. Lye[1]

[1]Australian Clinical Dosimetry Service, ARPANSA, Melbourne VIC Australia. (Maddison.Shaw@arpansa.gov.au [Presenting author]), (Andrew.Alves@arpansa.gov.au), (Cate.Davey@arpansa.gov.au), (Fayz.Kadeer@arpansa.gov.au), (John.Kenny@arpansa.gov.au), (Jeremy.Supple@arpansa.gov.au), (Jessica.Lye@arpansa.gov.au). [2]RMIT University, Melbourne VIC Australia. (Joerg.Lehmann@calvarymater.org.au), (Moshi.Geso@rmit.edu.au). [3]Physical Sciences, Peter MacCallum Cancer Centre, Melbourne VIC Australia. (Stephanie.Keehan@petermac.org), (Nick.Hardcastle@petermac.org). [4]Health STEM Solutions, Melbourne VIC Australia. [5]Calvary Mater Hospital, Newcastle NSW Australia. [6]Genesis Cancer Care, Melbourne VIC Australia

Introduction Stereotactic Ablative Radiotherapy (SABR) refers to radiotherapy treatment deliveries which give a high dose of radiation to an extra-cranial tumour, with high geometric precision (1). The risk to patients is increased with SABR techniques due to the increased dose per fraction, and as such specialised planning, treatment and QA practices are needed to ensure patient safety (1). Independent on-site audits are recommended by current SABR guidelines (1–3).

Method The Australian Clinical Dosimetry Service (ACDS) began field trials of SABR audits in March 2018. An end-to-end dosimetry audit was developed using a customised CIRS® humanoid thorax phantom. The audit planning cases include lung, spine and soft tissue targets, with delivery modality being at the discretion of the treating facility. The audit planning guidelines follow current SABR clinical trials: TROG SAFRON II (5), TROG/CCTG SC24 (6) and ICR/TROG CORE (7). Measurements were taken using Gafchromic EBT3 Film and a PTW 60019 microDiamond. Film was analysed using FilmQA Pro and in-house Matlab software.

Results To date, a total of 18 SABR plans have been included in the audit. Figure 1 shows the point dose variation in the first field trials. Large variations are seen in the vertebrae hard bone measurement point (average -5.5%, standard deviation 2.0) and the out of field spinal cord measurement point (average 1.9%, standard deviation 6.0).

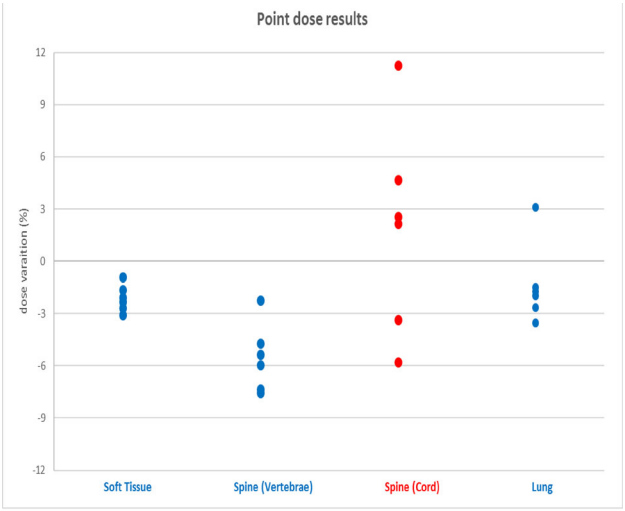

Figure 1. Point dose variations

Film localisation accuracy within the phantom has been verified to < 0.5 mm. The distance-to-agreement in the sagittal and coronal planes was analysed at the 50% isodose level. Figure 2 shows the results of a VMAT spine plan with maximum discrepancies of 0.21 mm (A–P) and 0.33 mm (L–R).

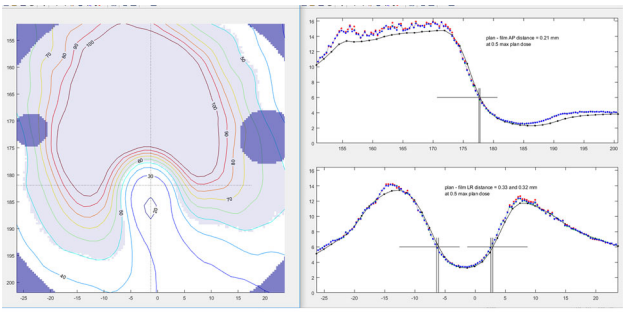

Figure 2. Example results of SABR spine audit plan

Film analysis metrics such as gamma criteria, absolute dose and isodose line agreement will be explored.

Conclusion The ACDS is developing a comprehensive audit for SABR treatments. Large discrepancies between calculated and measured dose in different medium such as bone are to be further explored.

References

1. Guidelines for safe practice of stereotactic body (ablative) radiation therapy. Faculty of Radiation Oncology, The Royal Australian and New Zealand College of Radiologists. (2015)
2. Solberg TD, Balter JM, Benedict SH et al. Quality and Safety Considerations in Stereotactic Radiosurgery and Stereotactic Body Radiation Therapy. PRO (2011) 2(1), pp 2–9.
3. Stereotactic Ablative Body Radiation Therapy (SABR): A resource. UK SABR Consortium. Version 4.0 (2013).
4. TRS-483 Dosimetry of Small Static fields used in external beam radiotherapy: An international code of practice for reference and relative dose determination. IAEA and APPM 2017.

5. SAFRON II – Stereotactic Ablative Fractionated Radiotherapy versus Radiosurgery for Oligometastatic Neoplasia to the Lung: A Randomised Phase II Trial (TROG 13.01/ALTG 13.001). Trans-Tasman Radiation Oncology Group, Australasian Lung Cancer Trials Group. Amendment 4 (2016).
6. SC24 – A randomised phase III study comparing stereotactic body radiotherapy (SBRT) versus conventional palliative radiotherapy (CRT) for patients with spinal metastases (TROG 17.06). Canadian Cancer Trials Group, Trans-Tasman Radiation Oncology Group.
7. CORE - A randomised trial of COnventional care versus Radioablation (stereotactic body radiotherapy) for Extracranial oligometastases: Radiotherapy planning and delivery guidelines. The Institute of Cancer Research, Trans-Tasman Radiation Oncology Group. Volume 1.1 2016.

O56 An assessment of motion management strategies in liver SABR

N. Hardcastle[1], E. Ungureanu[1], A. Yeo[1], C. Markham[2], R. Thomas[2], S. Chander, J. Chu[3]

[1]Physical Sciences, Peter MacCallum Cancer Centre, Melbourne, Australia. (nick.hardcastle@petermac.org [Presenting author]), (elena.ungureanu@petermac.org), (adam.yeo@petermac.org). [2]Radiation Therapy, Peter MacCallum Cancer Centre, Melbourne, Australia. (cathy.markham@petermac.org), (roshini.tomas@petermac.org). [3]Division of Radiation Oncology, Peter MacCallum Cancer Centre, Melbourne, Australia. (sarat.chander@petermac.org), (julie.chu@petermac.org)

Introduction Liver stereotactic ablative body radiotherapy is an emerging treatment for primary liver cancer and liver metastases. High rates of local control with acceptable toxicity can be achieved if sufficient tumour dose is reached, while limiting surrounding liver dose. The liver moves with respiration; reduction of respiratory motion results in reduced healthy liver treated and potential increased tumour dose. We recently implemented a motion reduction protocol and report on the compliance rates and liver positional stability from the first year in use.

Method The protocol contains three strategies – voluntary exhale breath hold (VEBH), abdominal compression (AC) and free breathing (FB). An assessment session is performed prior to simulation CT on the linac (Figure 1). In this session we assess compliance and reproducibility of VEBH using superior-inferior liver dome position on anterior-posterior fluoroscopy. If VEBH is not reproducible we use fluoroscopy to assess effect of AC on motion; if AC reduces motion this is used with an internal target volume (ITV), otherwise the patient is treated in FB with an ITV. The VEBH compliance, liver dome position reproducibility and reduction of liver dome motion with AC have been assessed.

Results From June 2017 to June 2018, 21 patients have been simulated following this procedure. VEBH was used in 14 patients (66.7%), AC in 5 patients (23.8%) and FB in 2 patients (9.5%). Liver dome position variation in those that could achieve VEBH was within 4 mm for 13/14 patients (Figure 2). In non-VEBH patients, AC reduced liver dome motion by 1.6–22.5 mm. One patient could not comply with VEBH at treatment and was subsequently treated with AC.

Conclusion We have shown that reproducible VEBH can be achieved in approximately two-thirds of liver SABR patients. AC resulted in variable reductions in liver motion and should be assessed on a per patient basis.

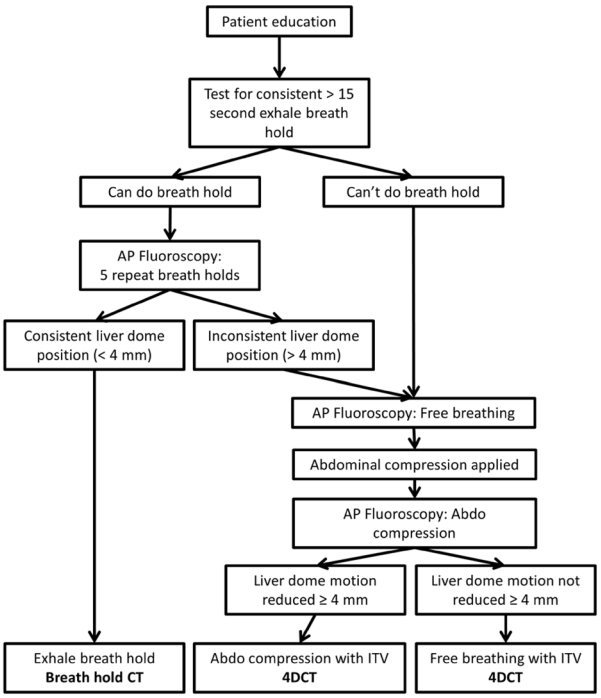

Figure 1: Motion management assessment workflow

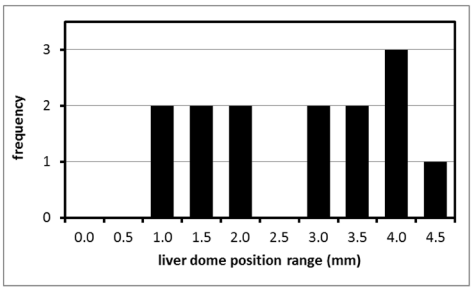

Figure 2: Frequency of liver dome superior-inferior position range in repeat breath-holds for 14 VEBH patients

O57 Stereotactic ablative body radiotherapy (SABR) in NSW: where are we now?

E. R. Claridge Mackonis[1], N. Hardcastle[2], M. Shaw, J. Lye[3], A. Haworth[4]

[1]Department of Radiation Oncology, Chris O'Brien Lifehouse, Australia. (elizabeth.mackonis@lh.org.au [Presenting author]). [2]Physical Sciences, Peter MacCallum Cancer Centre, Australia. (nick.hardcastle@petermac.org). [3]ACDS, ARPANSA, Australia. (maddison.shaw@arpansa.gov.au), (Jessica.lye@arpansa.gov.au). [4]Institute of Medical Physics, University of Sydney, Australia. (Annette.haworth@sydney.edu.au)

Introduction Stereotactic ablative body radiotherapy (SABR) is an established technique for the treatment of a variety of sites, in particular lung, liver and spine [1]. Data from overseas and anecdotal evidence suggest that use of SABR is rising but little information is available about its uptake in Australia. To address this, New South Wales (NSW) radiotherapy centres were surveyed on their use of SABR.

Method A survey was sent to all public and private radiotherapy centres in NSW. The survey questionnaire contained questions regarding the techniques used for SABR, treatment units used, number of patients treated and for which sites, image guidance used and confidence of the staff in the SABR treatment technique.
Results Responses from nine centres were received at time of writing. Experience in delivering a SABR service ranged from none (not yet commissioned) to 2007 years. Most sites that have a SABR service include lung with liver and spine being the most common additional clinical sites.
The most common treatment technique was multiple-arc VMAT. CBCT is used by all sites with 4D-CBCT used by most sites. Both Elekta and Varian linacs are used for SABR in NSW.
Conclusion There clearly exists a range of experience in using SABR techniques, however once established for one treatment site, expansion to other treatment sites appears to follow quickly. Future studies will investigate barriers to introducing a new SABR service, and possible networked solutions to facilitate rapid roll out of new techniques in a safe and efficient manner.

References

1. Foote M, Bailey M, Smith L, Siva S, Hegi-Johnson F, Seeley A, Barry T, Booth J, Ball D, Thwaites D (2015) Guidelines for safe practice of stereotactic body (ablative) radiation therapy. J Med Imaging Radiat Oncol 59 (5):646–653. https://doi.org/10.1111/1754-9485.12336

O58 Small field dosimetry using film in plastic phantoms: a Monte Carlo study

P. H. Charles[1,2]

[1]Radiation Oncology, Princess Alexandra Hospital, Brisbane, Australia. [2]Science & Engineering Faculty, Queensland University of Technology, Brisbane, Australia.
(Paul.Charles@health.qld.gov.au)

Introduction Small field dosimetry presents many challenges not seen in larger fields, including electronic disequilibrium. The material properties of the detector therefore have a large effect on the dose measured by that detector. While there is now a large body of literature on the effects of detector material on small field dosimetry, to date there is little on the effect of the phantom material. Solid alternatives to water for small field dosimetry are desirable for patient specific dosimetry of stereotactic treatments. Film is the dosimeter of choice in plastic phantoms because it avoids the large setup uncertainties associated with point dosimeters. However, unlike other detectors, there is little work on how the material makeup of film affects small field dosimetry. This study aims to address both problems mentioned above.
Method EBT3 film was simulated using realistic dimensions and material properties of the active layer and Polyester film base with the Monte Carlo code DOSXYZnrc. The film was simulated perpendicular to the beam at a depth of 5 cm in a cubic (20 cm^3) water phantom. The source was a previously modelled 5 × 5 mm^2 square 6 MV beam from a Varian 21iX. CAX profiles (with a resolution of 0.1 mm) and point doses were extracted.
The above simulation was repeated for film in the following plastic materials: Plastic Water, Virtual Water, RW3, Solid Water and Perspex. For initial validation, simulations were also performed in a phantom with the same geometry, but entirely water.
Results The output factor in film was the same as in pure water within the simulation uncertainty (~ 1.5%). Table 1 displays the output factor as measured in the various plastic phantoms. The profile measurements were all in agreement, except for some variations outside the field edge of up to 5 % (local dose) in RW3 and 10% in Perspex.

Table 1. Output factors for a 5 x 5 mm^2 field (normalised to 30 x 30 mm^2) simulated in film in various phantom materials.

Material	Output factor	Difference from water (%)
Water	0.643	-
Perspex	0.660	2.7
Plastic Water	0.638	- 0.7
Virtual Water	0.651	1.3
Solid Water	0.650	1.1
RW3	0.648	0.8

Conclusion Film is adequately water equivalent for small field dosimetry. All water equivalent plastics simulated in this study can be used as water substitutes in very small fields. Perspex however should not.

O59 Applying the spatial resolution limits of the Octavius 1500 detector array to TPS dose calculations in order to isolate causes of low gamma pass rates in patient specific quality assurance

C. Noble, S. F. E Liu, B. Perrett, P. O'Connor, P. Charles

Radiation Oncology, Princess Alexandra Hospital, Brisbane, Australia. (Christopher.Noble@health.qld.gov.au [Presenting author]), (Saufan.liu@health.qld.gov.au), (Ben.Perrett@health.qld.gov.au), (Patrick.OConnor2@health.qld.gov.au), (Paul.Charles@health.qld.gov.au)

Introduction The Octavius 1500 ion chamber array (PTW, Freiburg, Germany) in combination with the Octavius 4D phantom and VeriSoft software is currently used for patient specific quality assurance (PSQA). An increasing number of complex, highly modulated treatment plans that regularly yield gamma pass rates of less than 95% (3%/3mm) have been encountered during PSQA. These low gamma pass rates can potentially be due to the detector array having insufficient spatial resolution to measure highly modulated fields.
Method A large flat field, with a jaw edge at the isocenter at a collimator angle of 5°, was used to acquire a 2D dosemap on an Octavius 1500 array. The dose map was then used to calculate an edge spread function (ESF) and a line spread function (LSF). The combined spatial resolution of the Octavius array and linac was then derived by fitting a Gaussian to the LSF. A point spread function (PSF) with this linewidth was then applied to the dosegrid from the TPS to match the resolution of the Octavius array.
Results The LSF function of the Octavius array was found to fit well with a Gaussian lineshape with a full width half maximum (FWHM) of 9mm. This is comparable to the dimensions of the ion chambers (4.4 mm) and the spacing of the ion chambers (7.1 mm). A selection of highly modulated treatment plans were selected with gamma pass rates less than 95%. Applying this PSF function to the 3D dosegrid from the TPS improved the gamma pass rate in all cases to more than 95%.
Conclusion Many routine VMAT plans are highly complex and have dose gradients that exceed the spatial resolution of the Octavius1500 detector array. Further research is necessary to establish protocols for dealing with these plans.

O60 A study on the dose to contralateral breast with electronic compensators and conventional tangential fields

P. Ramachandran, A. Smith, J. Hughes, B. Howard, P. Lonski, G. Osboure, J. Hagekyriakou, D. Taylor, T. Kron

Peter MacCallum Cancer Centre, VIC.
(Ramachandran.Prabhakar@petermac.org [Presenting author]), (Amanda.Smith@petermac.org), (Jeremy.Hughes@petermac.org), (Beth.Howard@petermac.org), (Peta.Lonski@petermac.org), (Glenn.Osbourne@peterrmac.org), (Jim.Hagekyriakou@petermac.org), (David.Taylor@petermac.org), (Tomas.Kron@petermac.org)

Background Radiation dose to the contralateral breast (CLB) after radiotherapy (RT) treatment has potential to induce secondary breast cancer [1, 2, 3]. Subsequently, amidst the introduction of new technology in breast cancer RT management, CLB dose must be considered. Electronic compensation (eComp) has been implemented at the Peter MacCallum Cancer Centre to provide an alternative method to conventional 3d-conformal RT (ConRT) planning and delivery. The aim of this ethics approved study was to measure and compare contralateral breast dose for patients undergoing tangential field radiotherapy with eComp and ConRT fields.
Methods Forty patients undergoing tangential field breast radiotherapy were included in this study. 20 patients utilised eComp tangential irradiation. The remaining 20 patients were planned with ConRT tangential fields. Four sets of TLDs were placed on the CLB at 3 cm from the medial tangential fields (Pt1), areola (Pt3), midway (pt2) between Pt1 and Pt3 and at the axilla. The doses were measured with (TLD domes) and without (TLD strips) build-up. Contralateral breast doses were assessed with both treatment techniques. The mean dose to CLB was also calculated on the Eclipse™ (Varian Medical Systems) treatment planning system and correlated to the measured dose.
Results Our preliminary results show that the mean dose measured at 3 cm from the medial tangential border for eComp and ConRT techniques with strips were 9.79 ± 1.31% and 10.75 ± 1.74% of the prescription dose respectively. The dose at pt2 was almost half that of the dose at pt1. The dose measured with strips was almost twice that measured with domes. On an average, the eComp patients received 20% more monitor units as compared to ConRT.
Conclusion Contralateral breast dose is dependent on the proximity of the medial tangential field edge to the CLB, which is very patient specific. Our study shows that CLB dose with eComp and ConRT is comparable.

References

1. Boice J. D.Jr., Harvey E. B., Blettner M., Stovall M., Flannery J. T. Cancer in the Contralateral Breast after Radiotherapy for Breast Cancer. N Eng J Med 1192;326, 781–785.
2. Clarke M, Collins R, Darby S, Davies C, Elphinstone P, Evans V, Godwin J, Gray R, Hicks C, James S, MacKinnon E, McGale P, McHugh T, Peto R, Taylor C, Wang Y; Early Breast Cancer Trialists' Collaborative Group (EBCTCG). Effects of radiotherapy and of differences in the extent of surgery for early breast cancer on local recurrence and 15-year survival: an overview of the randomised trials. Lancet. 2005;366(9503): 2087–106.
3. Travis LB, et al. Breast cancer following radiotherapy and chemotherapy among young women with Hodgkin disease. JAMA. 2003;290:465–75.

O61 SABR Pre-treatment verification using PTW 60019-microDiamond Detector

N. Esen[1,2], P. Ramachandran[1,2], M. Geso[2,3]

[1]Medical Radiations Science, RMIT University, Melbourne, Australia. [2]Peter MacCallum Cancer Centre, Melbourne, Australia. (nsikanjesus@yahoo.com [Presenting author]). [3]Medical Radiations Science, RMIT University, Melbourne, Australia

Introduction The increasing interest in stereotactic ablative radiotherapy (SABR), otherwise called stereotactic body radiation treatment (SBRT) is one of the most chosen treatment approaches for early-stage cancer treatment. This technique is increased to treatment sites like lung, Spine, Scapula, Sternum, etc. It was the aim of this work to evaluate the performance of the PTW 60019-microDiamond detector for 6 MV beams delivered with ClinaxTH 21ix and explore the feasibility of using this detector for pre-treatment verification of the dose delivered to patients during SABR.
Method Prior to the utilization of PTW60019-microDiamond detector for SABR pre-treatment verification, the dosimeter was considered for dose linearity, energy, directional and dose rate dependence in 6 MV x-ray beam. *Dose 1* Electrometer was used to read the charge signal of microDiamond detector. An indigenous Rod phantom made of Perspex (*Peter MacCallum Cancer Centre, Melbourne, Australia*) was used to perform SABR pre-treatment patient verification while the statistical analysis of the linear fit was done using OriginPro 2018.
Results Three treatment sites (sternum, spine, and scapula) was considered, the average measured and plan dose was recorded for PTW60019-microDiamond (17.76 ± 0.65 % and 17.68 ± 0.63) respectively. The linear response of the detector indicates excellent relationship linear fit with $R^2 = 1$ for 6 MV and $R^2 = 0.9987$ 18 MV and no significant difference with dose rate, and energy was observed for the detector. PTW60019-microDiamond percentage difference between the measured and the planned dose was 2%.
Conclusion: The performance of PTW 60019-microDiamond has been verified for the purpose of this work. The measured and plan dose is consistent with the excellent agreement. This study confirmed that microDiamond is a valuable dosimeter for SABR pre-treatment verification.
Keywords: PTW60019, microDiamond, SABR, pre-treatment verification

O62 Assessment of an EPID based in-vivo dosimetry solution

L. K. Webb[1], P. H. Charles[1,2]

[1]Radiation Oncology, Princess Alexandra Hospital, Brisbane, Australia. (Luke.Webb@health.qld.gov.au), Paul.Charles@health.qld.gov.au). [2]Science & Engineering Faculty, Queensland University of Technology, Brisbane, Australia

Introduction The ever increasing complexity of modern radiotherapy heightens the importance of in-vivo dosimetry. This is typically performed using equipment like film, diodes or thermo-luminescent dosimeters; however, these are time consuming methods. Electronic portal image detector (EPID) based dosimeters offer the ability to perform in-vivo measurements without the need for extra equipment or setup time. This study assesses the error detection, limitations and usability of EPIgray EPID based in-vivo dosimetry.
Method The ability of EPIgray to detect errors was assessed using 200 mm thickness of plastic water @ 90cm SSD with a 5 cm, 10 cm,

15 cm and 20 cm field size and 100 MU. The thickness of plastic water, field size and dose delivered were all then independently changed to determine the software's ability to identify changes in patient thickness, field size and dose respectively. EPIgray's capacity to correctly handle multiple delivery types was evaluated by delivering VMATs, Hybrid IMRT and wedged tangents to an anthropomorphic phantom. A series of 3 patients (H&N, Chest and Prostate) were then imaged per fraction for a period of two weeks to evaluate the software in a clinical workflow.
Results EPIgray was able to detect changes in patient size, with an error of 5% per 1 cm deviation in thickness, and the dose delivered with errors proportional to the change in MU. However, the software was not able to detect induced field size errors. The software was correctly able to handle all treatment delivery types tested. It was simple to use clinically and only required the treatment therapists to extend the EPID panel to the nominal position and start an acquisition before treatment began.
Conclusion The EPIgray software has shown to be a suitable tool for in-vivo dosimetry utilising the EPID panel. The software is capable of determining significant dose delivery errors or changes in patient thickness/positioning.

IS05 Metal nanoparticle radiosensitizers are entering clinical use, but how do they work?

I. Kempson

The University of South Australia

Metallic nanoparticles are recognised for enhancing the effects of ionizing radiation on the radiobiological impact on cells. Opportunities exist to improve the therapeutic ratio in radiotherapy by delivering such nanoparticles specifically to cancerous cells. While metallic nanoparticles have entered several radiotherapy human trials up to Phase III, elucidating the actual mechanisms of increasing radiosensitization of cells has remained elusive. Motivated to understand the structure-function relationship of nanoparticle physico-chemical properties on radiosensitization, we developed a cross-correlative methodology to quantify the nanoparticle uptake in cells along with biological markers. The degree of heterogeneity greatly complicates such studies, however, analysis of relatively large cell-populations has enabled extraction of various sub-populations that elude to understanding the mechanisms involved. Here, we will review the clinical status of metallic nanoparticle radiosensitization and then present our research into identifying the underlying mechanisms. We observe that low numbers of nanoparticles can actually lead to a protective effect and that the propensity of cells to be sensitized by nanoparticles can vary greatly through the cell cycle phases. The research is offering intriguing insight into the role of physical, chemical and biological mechanisms of radiosensitization. The processes are intricately entwined and are a complex mix of both synergistic, but also antagonistic, mechanisms. Resulting paradigm shifts in our basic understanding of radiosensitization will have impactful implications on how nanoparticle formulations translate into clinical use and the clinical considerations for how they can deliver the best patient outcomes.

O63 Investigations into the combined effects of gold nanoparticles and ionising radiations on cancer cell migration

E. Shahhoseini[1], B. Feltis[2], M. Nakayama[2], M. Geso[2]

[1]Discipline of Medical Radiation, School of Health and Biomedical Sciences, RMIT University, Bundoora, Victoria, Australia. (elham.shahhoseini@rmit.edu.au). [2]Discipline of Pharmaceutical Science, School of Health and Biomedical Sciences, RMIT University, Bundoora, Victoria, Australia. (bryce.feltis@rmit.edu.au), (masao.nakayama@rmit.edu.au), Moshi.geso@rmit.edu.au [Presenting author])

Introduction Cell migration is a key physiological ability in wound healing, organ regeneration and cancer metastasis[1,2]. This ability in cancer cells enables them to invade the normal tissues in their vicinity. A few studies have revealed the suppressed cancer cell migration in the presence of gold nano-particles (AuNPs)[3–6]. In addition, alteration on cytoskeleton properties by x-irradiation has been reported[7]. However, the close investigation for the effects of AuNPs on cancer cell migration have not been previously performed and the effects of AuNPs combined with X-ray irradiation also remained unclear. In this in vitro study, we investigated the effects of AuNPs on the cell migration for two types of cancer cells to determine the cellular response to the AuNPs. Furthermore, we investigated the combined effects of AuNPs and X-ray on cell migration.
Method Two cancer cell line; A549 (lung) and DU145 (prostate) were treated with various scenarios i.e. A) control with no AuNPs and no radiation, B) with and without AuNPs and no radiation, C) with and without radiation and no AuNPs and, D) with 1 mM AuNPs combine with 5 Gy of 6MV x-ray. Scratch test assay and CytoSmart® image system was used to observe and measure the cells' movements.
Results The results of scratch tests show that the cancer cells treated with AuNPs filled.
The gaps about 25% slower than the control groups. This indicates the inhibitory effects of the AuNPs on the cancer cells. The greatest inhibitory effects on cells' motility was obtained from group D (the combination of 5 Gy of 6 MV x-ray and 1mM AuNPs) which was about 31% slower than the control groups.
Conclusion Decrease in cell migration speed can be attributed to the fact that the presence of high atomic number nanoparticles such as gold, can disorder the normal metabolism of the cancer cells.

References

1. Hulkower, K. I. & Herber, R. L. Cell migration and invasion assays as tools for drug discovery. *Pharmaceutics* **3,** 107–124 (2011).
2. Claire Wells and Maddy Parsons. *Cell Migration*. **769,** (2011).
3. Gupta, A. K. & Gupta, M. Cytotoxicity suppression and cellular uptake enhancement of surface modified magnetic nanoparticles. *Biomaterials* **26,** 1565–1573 (2005).
4. Wadhwa, S. *et al.* Comparative in vitro cytotoxicity study of carbon nanotubes and titania nanostructures on human lung epithelial cells. *J. Hazard. Mater.* **191,** 56–61 (2011).
5. Ahamed, M. Toxic response of nickel nanoparticles in human lung epithelial A549 cells. *Toxicol. In Vitro* **25,** 930–936 (2011).
6. Wang, H.-J. *et al.* Zinc oxide nanoparticle disruption of store-operated calcium entry in a muscarinic receptor signaling pathway. *Toxicol. Vitro Int. J. Publ. Assoc. BIBRA* **24,** 1953–1961 (2010).
7. Panzetta, V. *et al.* X-rays effects on cytoskeleton mechanics of healthy and tumor cells: X-Rays Effects on CSK Mechanics of Healthy and Tumor Cells. *Cytoskeleton* **74,** 40–52 (2017).

O64 Radiosensitisation with gadolinium-based nanoparticles: towards a pre-clinical investigation on the Australian MRI-linac

H. L. Byrne[1], G. Le Duc[2], O. Tillement[3], F. Lux[3], G. Liney[4], T. Roberts[4], Z. Kuncic[1]

[1]School of Physics, The University of Sydney, Sydney, Australia. (hilary.byrne@sydney.edu.au), (zdenka.kuncic@sydney.edu.au). [2]NH Theraguix, 43 boulevard du 11 novembre 1918, F69100 Villeurbanne, France. [3]Institut Lumière-Matière, Université Claude Bernard Lyon 1, CNRS UMR5306, 69622 Villeurbanne, France. [4]Ingham Institute for Applied Medical Research, Liverpool, Australia. (gary.liney@health.nsw.gov.au [Presenting author]), (tara.roberts@westernsydney.edu.au)

Introduction Brain cancer is the leading cause of childhood cancer death, with little progress in extending survival times over the last 20 years [1].

Our industry collaborators, nhTheraguix, have created a gadolinium-based nanoparticle shown to give a synergistic enhancement of the therapeutic effect of radiotherapy, increasing survival times compared to radiotherapy alone in pre-clinical studies [2, 3, 4]. Gadolinium provides strong positive contrast in magnetic resonance (MR) images aiding target delineation and confirming the uptake of nanoparticles.

Method We report on the progress of pre-clinical investigations at the Australian MRI-Linac. This unique facility combines a linear accelerator for therapeutic delivery of radiation with a custom-designed 1 T magnet, allowing MR images to be taken during treatment.

Fischer 344 rats were implanted with 9L glioma cells by stereotaxic injection into the right caudate nucleus at 10 weeks old. Seventeen days after surgery, T1-weighted images were taken on the Australian MRI-linac before and after intravenous administration of contrast agent, identifying the tumour. A trial irradiation achieved a 2x2.5 cm field for whole brain irradiation over a source-to-isocentre distance of 2.4 m.

Results The brain tumour can clearly be seen enhancing in the post-contrast T1-weighted image (see figure 1), showing a mass in the front right brain hemisphere. The presence of a large tumour in this area was confirmed ex-vivo.

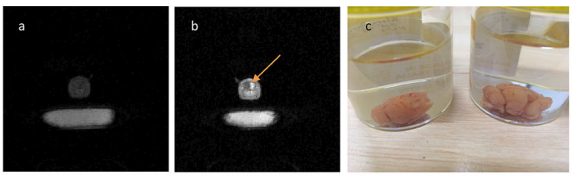

Figure 1. Images taken on the Australian MRI-linac, axial slice through the rat head a) pre-contrast. b) immediately post-contrast, arrow indicates tumour. Note: the white area below the rat on the image is the gel heating pad used to maintain the animal's temperature under anaesthesia. c) tumour visible ex-vivo.

Conclusion Images taken on the Australian MRI-linac allowed the identification of a rat brain tumour enhanced with contrast agent. This work enables a full pre-clinical investigation of the radiosensitising properties of gadolinium based nanoparticles, laying the groundwork for a clinical trial.

References

1. AIHW (2014) Cancer in Australia, an Overview. Australian Institute of Health and Welfare.
2. Le Duc G, Miladi I, Alric C, Mowat P, Bräuer-Krisch E, Bouchet A, Khalil E, Billotey C, Janier M, Lux F, Epicier T, Perriat P, Roux S, Tillement O (2011) Toward an Image-Guided Microbeam Radiation Therapy Using Gadolinium-Based Nanoparticles. ACS Nano 5, 9566–9574. https://doi.org/10.1021/nn202797h
3. Verry C, Dufort S, Barbier EL, Montigon O, Peoc'h M, Chartier P, Lux F, Balosso J, Tillement O, Sancey L, Le Duc G (2016) MRI-guided clinical 6-MV radiosensitization of glioma using a unique gadolinium-based nanoparticles injection. Nanomedicine 11, 2405–2417. https://doi.org/10.2217/nnm-2016-0203
4. Detappe A, Kunjachan S, Sancey L, Motto-Ros V, Biancur D, Drane P, Guieze R, Makrigiorgos GM, Tillement O, Langer R, Berbeco R (2016) Advanced multimodal nanoparticles delay tumor progression with clinical radiation therapy. Journal of Controlled Release 238, 103–113. https://doi.org/10.1016/j.jconrel.2016.07.021

O65 Monte Carlo investigation of radiolysis yield enhancement due to gold nanoparticles for proton therapy: Effects of LET, nanoparticle size and coating

D. Peukert[1,2], M. Douglass[3,4], I. M. Kempson[1], E. Bezak[4,5]

[1]Future Industries Institute, University of South Australia, Australia. (dylan.peukert@mymail.unisa.edu.au [Presenting author]), (ivan.kempson@unisa.edu.au). [2]Division of ITEE, University of South Australia, Australia. [3]Department of Medical Physics, Royal Adelaide Hospital, Australia. [4]Department of Physics, University of Adelaide, Australia. (Michael.Douglass@sa.gov.au). [5]Cancer Research Institute and School of Health Sciences, University of South Australia, Australia. (Eva.Bezak@unisa.edu.au)

Introduction Gold nanoparticles (GNPs) are being investigated as a method to enhance radiation damage in cells following radiotherapy. While GNPs were not expected to enhance proton radiotherapy, experimental measurements contradict this and indicate that radiolysis contributes to the enhancement [1–3]. Proton radiotherapy allows improved healthy tissue sparing over photon radiotherapy and can be further improved with GNP radiosensitisers. In this work, radiolysis enhancement was evaluated for a variety of GNP sizes, coatings and proton energies to aid the optimisation of nanoparticle design.

Method The radiolysis yield was modelled in two stages. First, protons were modelled incident on the nanoparticle using Geant4 [4, 5] low energy physics models and secondary particles emitted from the nanoparticle were scored in a phase space file. In the second stage, radiolysis was modelled in water with the file as particle source using Geant4 DNA [6–9] physics and chemistry models. The radiolysis and dose enhancement factors (REF, DEF) were found from the ratio of the yields and dose for the nanoparticle and equivalent water nanoparticle. The enhancement was calculated for a variety of nanoparticle types, sizes, coatings and proton energies.

Results Figure 1 shows the effect of proton energy on enhancement for a 50 nm GNP and Figure 2 shows the effect of silica coating thickness on enhancement for a 15 nm GNP. The enhancement peak for 5 MeV protons corresponds to the maximum total energy of secondary electrons. The peak occurs due to the electron yield decreasing and the mean energy increasing with increasing proton energy. The enhancement reduction with coating thickness is due to the absorption of electrons produced in the gold within the coating.

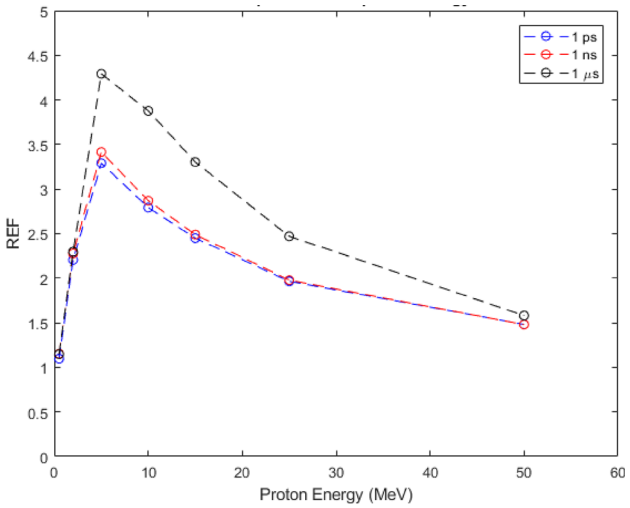

Figure 1. Plot of enhancement energy dependence.

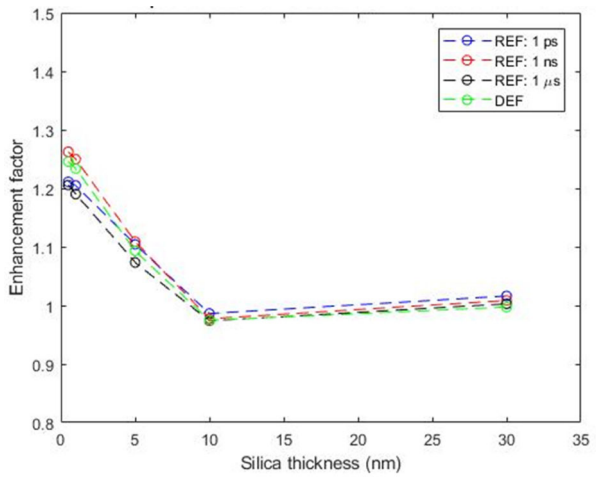

Figure 2. Plot of enhancement coating thickness dependence.

Conclusion This study provides information to aid the optimisation of nanoparticle design.

Acknowledgements
We thank UniSA and the Future Industries Institute for research and conference funding.

References

1. Kim J-K, Seo S-J, Kim H-T, et al (2012) Enhanced proton treatment in mouse tumors through proton irradiated nanoradiator effects on metallic nanoparticles. Phys Med Biol 57:8309–8323 . https://doi.org/10.1088/0031-9155/57/24/8309
2. Li S, Penninckx S, Karmani L, et al (2016) LET-dependent radiosensitization effects of gold nanoparticles for proton irradiation. Nanotechnology 27: . https://doi.org/10.1088/0957-4484/27/45/455101
3. Peukert D, Kempson I, Douglass M, Bezak E (2018) Metallic nanoparticle radiosensitisation of ion radiotherapy: A review. Phys Medica 47:121–128 . doi: https://doi.org/10.1016/j.ejmp.2018.03.004
4. Agostinelli S, Allison J, Amako K, et al (2003) GEANT4 - A simulation toolkit. Nucl Instruments Methods Phys Res Sect A Accel Spectrometers, Detect Assoc Equip 506:250–303 . https://doi.org/10.1016/s0168-9002(03)01368-8
5. Allison J, Amako K, Apostolakis J, et al (2016) Recent developments in Geant4. Nucl Instruments Methods Phys Res Sect A Accel Spectrometers, Detect Assoc Equip 835:186–225 . doi: https://doi.org/10.1016/j.nima.2016.06.125
6. Bernal MA, Bordage MC, Brown JMC, et al (2015) Track structure modeling in liquid water: A review of the Geant4-DNA very low energy extension of the Geant4 Monte Carlo simulation toolkit. Phys Medica 31:861–874 . https://doi.org/10.1016/j.ejmp.2015.10.087
7. Incerti S, Ivanchenko A, Karamitros M, et al (2010) Comparison of GEANT4 very low energy cross section models with experimental data in water. Med Phys 37:4692–4708 . https://doi.org/10.1118/1.3476457
8. Karamitros M, Mantero A, Incerti S, et al (2011) Modeling radiation chemistry in the Geant4 Toolkit. Prog Nucl Sci Technol 2:503–508
9. Karamitros M, Luan S, Bernal MA, et al (2014) Diffusion-controlled reactions modeling in Geant4-DNA. J Comput Phys 274:841–882 . https://doi.org/10.1016/j.jcp.2014.06.011

O66 Influence of equivalent-square field size of SRS field dose calculations using iPlan, AAA and AXB

A. Kejda[1], T. Moodie[2], G. Trompp[2], Romuald Gajewski[2]

[1]Blacktown Cancer and Haematology Centre, Blacktown Hospital, Australia. (Alannah.Kejda@health.nsw.gov.au [Presenting author]).
[2]Crown Princess Mary Cancer Centre, Westmead Hospital, Australia. (Trevor.Moodie@health.nsw.gov.au), (Gavin.Trompp@health.nsw.gov.au), (Romuald.Gajewski@health.nsw.gov.au)

Introduction Stereotactic Radiosurgery (SRS) delivers ablative radiation doses to the central nervous system. SRS treatments at Crown Princess Mary Cancer Centre (CPMCC) are created with iPlan and verified with physical measurements. This study aims to evaluate the small field accuracy of Eclipse using Analytic Anisotropic Algorithm (AAA) and Acuros External Beam (AXB) algorithm, and to assess their feasibility as an independent SRS verification tool.

Method Prior to use, optimal source spot size and dosimetric leaf gap (DLG) for small fields were determined in AAA and AXB models by matching measured and calculated profiles of 1x1 cm jaw- and MLC-defined fields, respectively. 75 SRS fields created in iPlan were measured using an IBA Razor Diode in a water phantom. The SSD and depth of the diode were adjusted per field to reproduce treatment conditions, all fields were delivered at gantry zero. Plans were imported into Eclipse, mapped to a water phantom and recalculated using both AAA and AXB (dose to water) with a grid size of 0.1 cm.

Results SRS plan QA tolerance is 2%, both iPlan and AXB calculated doses were within 2% of measured (Figure 1). AAA underestimated the dose for fields with an equivalent-square less than 15 mm and became more pronounced with decreasing field size.

Conclusion Preliminary results suggest AXB can be used to verify iPlan SRS treatments. AAA is not suitable for dose calculation of fields with an equivalent-square of less than 15 mm as deviation from measurements exceeded the 2% plan tolerance. Future work includes using TRS 483 to review measurement data of small field diode dosimetry. More fields will be measured before using AXB as an independent verification tool.

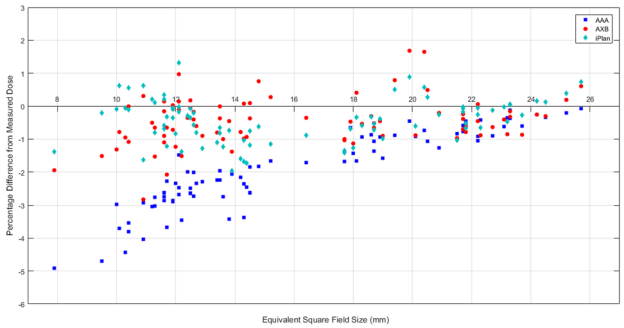

Figure 1. Graph of equivalent-square field size and percentage difference between dose measured and calculated by iPlan, AAA and AXB for SRS fields

O67 Evaluation of a new hybrid vmat-imrt multi-criteria optimisation plan generation algorithm

M. E. Spalding, A. Walsh, H. Clarke, T. Aland

ICON Group, Australia. (myles.spalding@iconplan.global [Presenting author]), (anthony.walsh@roc.team), (hayley.clarke@roc.team), (trent.aland@roc.team)

Introduction To evaluate the Varian 'Fast Hybrid Multi-criteria optimisation (MCO) Volumetric modulated Arc therapy (VMAT)' (H-MCO) tool for both its dosimetric accuracy and calculation time. This is a new function within V15.6 of the Varian Eclipse treatment planning system that allows VMAT optimisation and dose calculation using the graphical processing unit (GPU). In versions prior to V15.6 VMAT MCO calculations were only possible using central processing unit (CPU) not GPU (N-MCO).
Method The study consisted of a cohort of 53 patients representing a range of anatomical treatment sites; bladder (5), brain (6), gynaecological (5), head and neck (5), lung (7), mediastinum (7) prostate (6), oesophagus (7) and rectum (5). Each case was planned to that of a clinical standard (Base) which was compared to a H-MCO and N-MCO approach. The study analysed plan calculation time data, dose to organ at risk (OAR) and target coverage.
Results Large time savings were found using the H-MCO technique when compared to N-MCO, 5 to 40 times faster or up to 75 min time saving (average of 25 mins). Negligible dosimetric differences were found between the H-MCO and N-MCO approach for the cohort of patients evaluated.

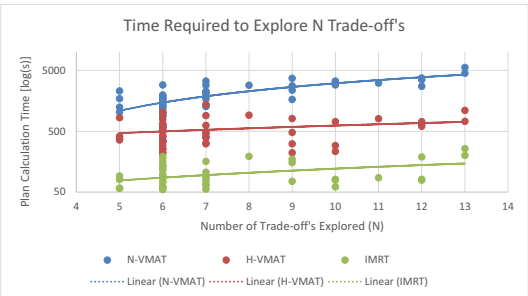

Figure 1: Plot of the time required to calculate the plan in the case of the native-VMAT (N-VMAT), Hybrid-VMAT (H-VMAT) and IMRT.

Conclusion Negligible dosimetric change between the two techniques whilst significant time saving factors were observed with the GPU enabled approach. We have shown that the H-MCO technique has been safely implemented and is ready for clinical use.
Acknowledgements Stephen Thompson, Varian Medical Systems, USA. stephen.thompson@varian.com

O68 Comparison of two flattening filter free (FFF) beams for lung SBRT: analysis of beam modelling and delivery efficiency

M. Mundayadan Chandroth[1], A. Venning[1], B. Chick[1], B. Waller[2]

[1]Mid North Coast Cancer Institute, Port Macquarie, Australia. (Mahesh.Chandroth@ncahs.health.nsw.gov.au [Presenting author]), (Tony.Venning@ncahs.health.nsw.gov.au), (Brendan.Chick@ncahs.health.nsw.gov.au), (Brett.Waller@ncahs.health.nsw.gov.au). [a]Medical Physics Specialist. [b]Senior Medical Physics Specialist

Introduction FFF beams have shown to improve treatment delivery efficiency in SBRT. Our clinic is equipped with 6MVFFF and 10MVFFF beams. This study evaluated the accuracy of beam modelling, dose calculation accuracy in the presence of lung equivalent media, treatment time comparison and the suitability of these beams for lung SBRT treatments.
Method Beams were commissioned on Elekta® linac and were modelled in Monaco® TPS for Monte Carlo (MC) algorithm. The validation is performed in water, in low density tissue equivalent slabs and CIRS E2E SBRT phantom®. A set of treatment plans with simple geometries were created and dose calculated. Five clinical 6MVFFF SBRT lung VMAT plans were recalculated on the E2E phantom. By retaining the segments and scaling the MU, these plans were recalculated for 10MVFFF for same dose. Dose measurements were performed using ion chamber and EBT3 films and compared against Dm and Dw calculations. Peripheral dose to the tumour was assessed using normoxic polymer gel and EBT3 films. The treatment times were compared.
Results In water, calculated dose (Dc) agreed to delivered dose (Dd) for fields down to 2 × 2cm^2. With decrease in the electron density of the medium and increase in beam energy, the dose agreement becomes poor, about 15% for 10XFFF for 2 × 2cm^2 (Table 1). For the SABR plans, point dose at the centre of the lung tumour in E2E SBRT phantom agrees better for 6XFFF (3.1%) compared to 10XFFF (5.5%). On the periphery, the films and GEL shows that Dc overestimates the Dd, more for 10XFFF than 6XFFF. 10XFFF plans deliver faster by 2.7 s/Gy of prescription Table (2).
Conclusion For lung SABR treatments, 6XFFF plan have dosimetric advantage compared to 10XFFF plans but delivers slower. The minimal treatment time advantage of 10XFFF beam should be weighed against the uncertainty on the tumour peripheral dose for lung SBRT.

Table 1

Water	Beam ID	SSD	FS	MU	Expected dose(cGy)	Monaco Dw (cGy)	Monaco Dm(cGy)	Measured dose(cGy)	% diff (Exp - Mon)	% diff (Mea - Mon)	% diff (Mea - exp)	Dw/Dm
	6XFFF	90	2	200	163.6	166.4	166.4	165.9	-1.7	-0.3	1.4	1.000
		90	3	200	173.8	175.2	175.2	174.9	-0.8	-0.2	0.6	1.000
		90	10	200	200.0	200.6	200.6	200.2	-0.3	-0.2	0.1	1.000
	10XFFF	90	2	200	164.0	164.8	164.8	165.9	-0.5	0.7	1.1	1.000
		90	3	200	177.0	178.3	178.3	178.8	-0.7	0.3	1.0	1.000
		90	10	200	200.0	199.2	199.2	200.0	0.4	0.4	0.0	1.000
Exhale lung - RED 0.5	Beam ID	SSD	FS	MU	Dm	SD(cGy)	Dw	SD(cGy)	Dose Meas (cGy)	% diff(Dw Vs Meas)	% diff(Dm Vs Meas)	Dw/Dm
	6XFFF	90	10	200	256.1	1.3	252.8	1.3	255.5	1.0%	-0.3%	0.987
	10XFFF	90	10	200	246.0	1.5	242.5	1.5	248.9	2.6%	1.2%	0.986
	6XFFF	100	10	200	211.1	1.3	208.4	1.3	210.5	1.0%	-0.3%	0.987
	10XFFF	100	10	200	202.6	1.4	199.7	1.4	205.1	2.7%	1.2%	0.986
	6XFFF	90	3	200	226.9	1.6	224.0	1.6	228.8	2.1%	0.8%	0.987
	10XFFF	90	3	200	211.3	1.6	208.2	1.6	217.7	4.4%	2.9%	0.985
	6XFFF	90	2	200	205.2	1.9	202.6	1.8	207.6	2.4%	1.1%	0.987
	10XFFF	90	2	200	185.5	1.5	182.8	1.5	192.2	4.9%	3.5%	0.985
Inhale lung - RED 0.2	Beam ID	SSD	FS	MU	Dm	SD(cGy)	Dw	SD(cGy)	Dose Meas (cGy)	% diff(Dw Vs Meas)	% diff(Dm Vs Meas)	Dw/Dm
	6XFFF	90	10	200	256.5	1.9	257.5	1.9	255.8	-0.7%	-0.3%	1.004
	10XFFF	90	10	200	240.5	1.7	240.7	1.7	244.9	1.7%	1.8%	1.001
	6XFFF	100	10	200	212.0	1.1	212.9	1.1	211.3	-0.7%	-0.3%	1.004
	10XFFF	100	10	200	198.7	1.7	198.9	1.7	202.7	1.9%	2.0%	1.001
	6XFFF	90	3	200	192.5	2.1	193.3	2.1	209.0	7.5%	7.9%	1.004
	10XFFF	90	3	200	172.5	1.8	172.7	1.9	191.5	9.8%	9.9%	1.001
	6XFFF	90	2	200	159.5	1.1	160.1	1.1	180.7	11.4%	11.7%	1.004
	10XFFF	90	2	200	138.3	1.1	138.5	1.1	161.0	14.0%	14.1%	1.001

Table 2

PLAN ID	BEAM ID	TOTAL DOSE(cGy)	#	DOSE/# (cGy)	MU	NO OF SEG	CALC DOSE(cGy)	STD(cGy)	MEAS DOSE(cGy)	% DIFF	Tx time (sec)	diff	diff/Gy
Patient 1	6XFFF	5000	5	1000	1918.23	73	1360.7	30.5	1403.9	-3.2	150	35	3.5
	10XFFF	5000	5	1000	2015.70	73	1360.7	27.9	1440.8	-5.9	115		
Patient 2	6XFFF	3500	5	700	2217.03	183	882.0	7.1	894.3	-1.4	155	31	4.4
	10XFFF	3500	5	700	2269.79	183	882.0	9.6	906.6	-2.8	124		
Patient 3	6XFFF	4800	4	1200	2385.47	154	2158.1	27.1	2226.8	-3.2	175	25	2.1
	10XFFF	4800	4	1200	2569.80	154	2158.1	29.8	2302.2	-6.7	150		
Patient 4	6XFFF	5000	5	1000	1955.22	166	1462.4	23.6	1511.1	-3.3	160	10	1.0
	10XFFF	5000	5	1000	2077.23	166	1462.4	20.0	1538.5	-5.2	150		
Patient 5	6XFFF	4800	4	1200	2106.92	103	1769.8	14.2	1849.1	-4.5	145	28	2.3
	10XFFF	4800	4	1200	2223.91	103	1769.8	17.6	1859.1	-5.0	117		
	6XFFF average									-3.1		average diff	
	10XFFF average									-5.1		26	2.7

References

1. B Prendergast, J Fiveash, R Popple, G Clark, E Thomas, D Minnich, R Jacob, S Spencer, J Bonner, M Dobelbower (2013) Flattening filter – free linac improves treatment delivery efficiency in stereotactic body radiation therapy, J Appl Clin Med Phys 14.
2. Stathakis S, Esquivel C, Gutierrez A, Buckey CR, Papanikolaou N (2009) Treatment planning and delivery of IMRT using 6 and 18MV photon beams without flattening filter, Appl Radiat Isot.1629–37
3. Ong CL, Verbakel WFAR, Dahele M, et al (2012) Fast arc delivery for stereotactic body radiotherapy of vertebral and lung tumors. Int J Radiat Oncol Biol Phys. 137–43.
4. Vassiliev ON, Kry SF, Chang JY, Balter PA, Titt U, Mohan R (2009) Stereotactic
5. radiotherapy for lung cancer using a flattening filter free Clinac. J Appl Clin Med Phys 10:2880
6. G Xiong, D.W.O. Rogers (2008) Relationship between %dd(10)x and stopping- power ratios for flattening filter free accelerators: A Monte Carlo study. Med. Phys 35.
7. W. O. Rogers and C. L. Yang, (1999) Corrected relationship between %dd_10_x and stopping-power ratios, Med. Phys. 26
8. Fippel M (1999) Fast Monte Carlo dose calculation for photon beams based on the VMC electron algorithm Med. Phys. 26
9. A J Venning, B Hill, S Brindha, B J Healy, C Baldock (2005) Investigation of the PAGAT polymer gel dosimeter using magnetic resonance imaging, Phys.Med.Biol 3875-3888

O69 Multisite analysis of over 10,000 radiotherapy treatment plans in a large radiotherapy centre

J. Hughes, P. Ramachandran, D. Taylor, T. Kron

Physical Sciences, Peter MacCallum Cancer Centre, VIC, (Jeremy.Hughes@petermac.org [Presenting Author]), (Ramachandran.Prabhakar@petermac.org), (David.Taylor@petermac.org), (Tomas.Kron@petermac.org)

Introduction Pre-treatment plan checks are routinely performed at all radiotherapy centres for patients undergoing radiotherapy. In this study, we analysed over 10,000 external beam treatment plans exported to Mobius3D^{TM} (Mobius Medical Systems), a 3D treatment dose verification system, and the results of our analysis are summarised.

Method All patients included in this study were planned on Eclipse 3D treatment planning systems at the five different Peter MacCallum Cancer Centre campuses. The plans include 3D-conformal radiotherapy (3D-CRT), intensity modulated radiation therapy (IMRT), and volumetric modulated radiation therapy (VMAT). The plans were exported to our Mobius3D server and using in-house software, over 10,000 treatment plans were extracted from the Mobius3D database and analysed. The treatment plans were mainly categorised by treatment site, modality, beam energy, the total dose computed, machine model, number of fields, and passing status of the DVH, Target, and Gamma checks.

Results Preliminary results show that of the over 10,000 individual treatment plans uploaded to Mobius3D, 66.4% passed all of the DVH, Target, Gamma, and deliverability checks while 33.6% of these individual treatment plans failed at least one of the aforementioned checks. Head and Neck plans (which made up roughly 23.0% of the cohort) had the highest rate of Mobius3D check fails (57.0%). Spine treatment plans (which made up roughly 9.6% of the cohort) had the lowest rate of Mobius3D check fails (20.5%). The treatment plans were categorised as either IMRT (24.9%), 3D-CRT (60.6%), or VMAT (11.8%). 77.8% of 3D-CRT plans passed all Mobius3D checks, 43.7% of all IMRT plans passed all Mobius3D checks, and 56.8% of all VMAT plans passed all Mobius3D checks.

Conclusion Our study shows an independent MU check software incorporating DVH, Target, Gamma, and deliverability checks would help the clinic to identify issues associated with the DVH, target volumes, MUs, treatment accessories/parameters, and avert errors that would not have been picked on the primary treatment planning system.

O70 Assessing the impact of AXB in breast treatments

A. Kejda[1], N. Nahar[2], T. Wang[2], S. Ashworth[2], J. Sykes[1]

[1]Blacktown Cancer and Haematology Centre, Blacktown Hospital, Australia. (Alannah.Kejda@health.nsw.gov.au [Presenting author]), (Jonathan.Sykes@health.nsw.gov.au). [2]Crown Princess Mary Cancer Centre, Westmead Hospital, Australia. (Najmun.Nahar@health.nsw.gov.au), (Tim.Wang1@health.nsw.gov.au), (Simon.Ashworth@health.nsw.gov.au)

Introduction Acuros External Beam (AXB) is a calculation algorithm utilising the linear Boltzmann transport equation (LBTE) to calculate treatment plans accurately in regions of heterogeneous tissue. Radiotherapy of the breast is often made difficult because of the presence of lung and air bordering the target volume. In this study, breast plans calculated with the default Anisotropic Analytic Algorithm (AAA) and Acuros External Beam (AXB) dose calculation algorithm were compared to quantify dosimetric differences.

Method Twenty 6MV breast plans, generated and optimised using Eclipse with AAA were recalculated using AXB, reporting dose to water. The plan metrics used to evaluate the algorithms were D99%, D98%, D95%, D90%, D50%, D1%, D2cc and mean heart dose.

Results Statistically significant differences between AAA and AXB were not found for the above plan metrics, except D2cc (t-test $P < 0.0001$), where AXB mean dose was approximately 1 Gy higher (Figure 1). For AAA, all plans met a D2cc $< 110\%$ criteria while with AXB only 9 plans met this. Local dose differences between the algorithms of up to $\pm$ 2 Gy were observed within the PTV, but had little impact on overall plan quality. Mean dose to heart was also not statistically significantly different, however a pattern of decreased dose to the heart for left-sided treatments was observed.

Conclusion Minimal impact can be seen on PTV dose distribution for clinical breast plans when using the AXB dose calculation algorithm reporting dose to water. It does however, calculate D2cc to be an average of 1 Gy hotter than AAA, and higher for individual plans. This result should be considered before AXB is implemented for clinical breast planning.

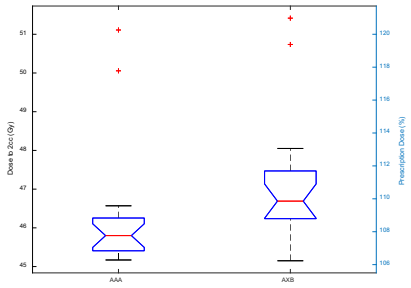

Figure 1. Box and whisker plot displaying the differences in D2cc between AAA and AXB dose calculations in breast plans. Notches indicated standard error on median

O71 Open source software to compare the reported MLC positions between Mosaiq and an Elekta linac

S. G. Biggs[a], M. J. Sobolewski[b]

RCCC. (me@simonbiggs.net [Presenting author]), (msobolewski@riverinacancercarecentre.com.au). [a]Registrar Medical Physicist. [b]Head of Physics

Introduction This project aims to create an open source, automated, independent verification tool for comparing MLC positions between the information system and linac that can be utilised to assess delivered dose accuracy for every treatment.

Method Recorded delivery parameters are extracted from the Elekta linac utilising high resolution logfiles and are correlated with the patient record in Mosaiq. The MLC, Jaw and delivered MU data is then collected from both the logfile and the Mosaiq SQL treatment record. This data is used to generate planned and delivered MU density maps so that meaningful comparisons can be made. A subset of plans for which MU density differences had been detected had their pre-treatment Delta4 QA measurement retrospectively analysed to determine if delivered MU density deviations correlated with delivered dose deviations.

Results In all, 14 months of logfile patient delivery data across three linacs were analysed. A given patient delivery highlighted by this procedure is shown in the figures. Figure 1 provides the logfile and Mosaiq MU density maps, as well as the MU density difference.

Figure 2 is the result of retrospectively investigating that plan as it was delivered on the Delta4 during the patient specific IMRT QA.

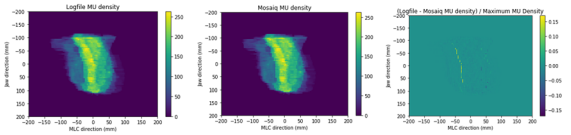

Figure 1: Logfile to Mosaiq comparison via MU density calculated from logfile record and OIS control points.

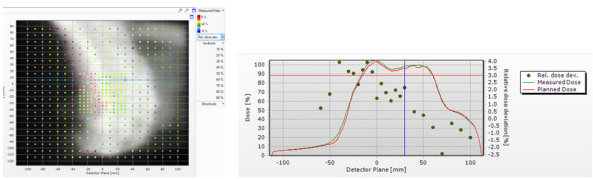

Figure 2: Delta4 relative dose deviation for the treatment plan compared in Figure 1.

Conclusion The initial work on this project indicates that discrepancies between planned and delivered doses are able to be predicted by comparing planned MU density maps to MU density maps generated from logfiles.

The underlying library code can be accessed from the pymedphys package (https://github.com/CCA-Physics/pymedphys). The application code can be accessed upon request by contacting the authors.

IS06 Deep learning in medical imaging, with applications in radiomics and diagnostics

L. Oakden-Rayner[1,2], MBBS FRANZCR[1,2]

[1]School of Public Health, University of Adelaide, Australia. [2]Jones and Partners Medical Imaging. (lukeoakdenrayner@gmail.com)

Artificial intelligence has seen a resurgence of interest in the field of medical image analysis due to the development of highly effective deep learning techniques. These techniques have allowed computers to "understand" the visual world for the first time, resulting in human level or even superhuman performance at visual medical tasks.

This talk will provide an overview of these methods, and cover recent advances in the field of medical image analysis. To highlight the potential scope of this technology, several pieces of local work will be discussed:

Predicting longevity using CT imaging [1]
Precision medicine approaches rely on obtaining precise knowledge of the true state of health of patients. We present experiments to demonstrate how CT imaging may be used to predict patient longevity as a proxy for overall health.

Detecting hip fractures from pelvic x-rays [2]
We developed a deep learning system to detect hip fractures from pelvic x-rays. We demonstrate diagnostic performance exceeding that of human radiologists.

Producing radiologist-quality reports [3]
We propose a simple extension to deep learning methods to produce report text directly from images, and show that the generated sentences are preferred by doctors compared to visualisations such as heatmaps.

References

1. Oakden-Rayner L, Carneiro G, Bessen T, Nascimento JC, Bradley AP, Palmer LJ. Precision radiology: predicting longevity using feature engineering and deep learning methods in a radiomics framework. *Scientific Reports.* 2017;7(1):1648.
2. Gale W, Oakden-Rayner L, Carneiro G, Bradley AP, Palmer LJ. Detecting hip fractures with radiologist-level performance using deep neural networks. *arXiv preprint* arXiv:171106504. 2017.
3. Gale W, Oakden-Rayner L, Carneiro G, Bradley AP, Palmer LJ. Producing radiologist-quality reports for interpretable artificial intelligence. *arXiv preprint* arXiv:180600340. 2018.

O72 Development of machine learning techniques to predict and grade prostate cancer in digital pathology data

O. Vandenberg[1], H. M. Reynolds[2], Y. Sun[3], A. Haworth[3]

[1]RMIT University, Melbourne, Australia. (owenvandenberg@gmail.com [Presenting author]). [2]Peter MacCallum Cancer Centre, Melbourne, Australia. (Hayley.Reynolds@petermac.org). [3]Institute of Medical Physics, University of Sydney, Australia. (yu.sun@sydney.edu.au), (annette.haworth@sydney.edu.au)

Introduction Staging of PCa includes assigning a Gleason score, determined by a pathologist based on small samples of tissue from biopsy or histology slides from pathological specimens. Machine learning (ML) techniques allow for digital pathology data to be assessed and graded automatically to assist with staging. This study presents an ML framework for the location and grading of PCa in digital pathology data.
Method A tile-based feature extraction method [1] was employed to create feature maps from high-resolution haemotoxylin and eosin (H&E) histology images, using expert pathologist annotations of small foci on 18 slides from a 45-patient cohort as training data. Random Forest (RF)-based feature selection techniques were applied, binary classification was performed on Cancer/Non-Cancer (CNC) classes, and Multiclass classification utilised multiple class labels for different categories of benign and cancerous tissues. Classification algorithms *k*-Nearest Neighbours (*k*-NN), RF, and Support Vector Machine (SVM) with linear and Gaussian kernels were compared using 10-fold cross-validation on the training dataset. Those with the highest accuracies were chosen to process a selection of 8 test slides independent of the training set, and predictive maps were generated.
Results Of the classification algorithms tested, the Gaussian SVM yielded the highest accuracy values of 96.4% for CNC classification, 93.3% for Multiclass classification, and AUC values on test slides ranged from 0.67 to 0.90. Sensitivity and specificity values ranged from 0.31 to 0.94 and 0.68 to 0.90 respectively. Predictive maps showed correlation with pathologist annotations for regions of tumour, but frequently predicted cancerous regions beyond the pathologist's annotations.

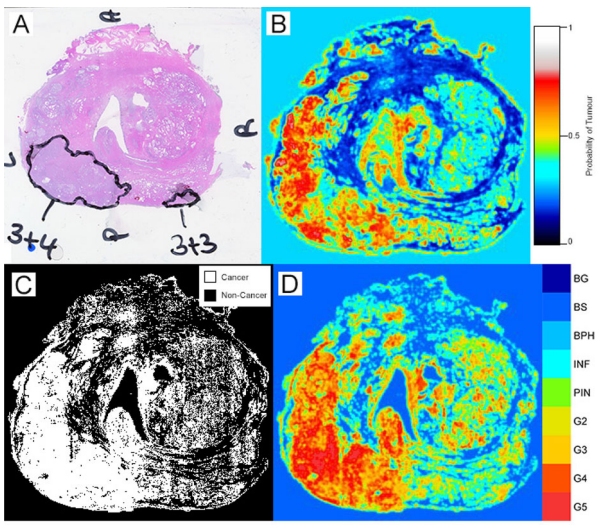

Figure 1: Example a) histology slide and (b-d) predictive maps for mrhist030_slide1.6.

Conclusion Results showed the Gaussian SVM classifier had the highest predictive accuracy, performing consistently above the *k*-NN and RF classifiers. The sensitivity and specificity values indicate a possible imbalance in the training data, which will be explored in future work.

References

1. Weingant, M., et al. *Ensemble Prostate Tumor Classification in H&E Whole Slide Imaging via Stain Normalization and Cell Density Estimation*. in *International Workshop on Machine Learning in Medical Imaging*. 2015. Springer.

Acknowledgements This work was supported by Movember through Prostate Cancer Foundation of Australia's Research Program and an NHMRC grant APP1126955. The authors would like to acknowledge the contribution of Dr Matthew DiFranco for providing early direction in this project, and Professor Rick Franich for peer review of this work.

O73 A non-small lung cancer decision support system model trained using distributed learning over a multicenter cohort

M. F. Field[1], L. C. Holloway[2,3,4], M. S. Barakat[1], S. Vinod[1,5], M. Carolan[3,6,7], M. Bailey[3,6,7,8], J. Sykes[9], E. Hau[9], J. Lehmann[10,11], A. Ghose[8,12], D. Stirling[12], A. Dekker[13], D. I. Thwaites[14]

[1]South West Sydney Clinical School, University of New South Wales, Australia. matthew.field@unsw.edu.au [Presenting author]). [2]Liverpool and Macarthur Cancer Therapy Centres and Ingham Institute, Australia. [3]Centre for Medical Radiation Physics, University of Wollongong, Australia. [4]Institute of Medical Physics, School of Physics, University of Sydney, Australia. [5]Cancer Therapy Centre, Liverpool Hospital, Australia. [6]Illawarra and Shoalhaven Cancer Care Centres. [7]Illawarra Health and Medical Research Institute, Wollongong, Australia. [8]Centre for Oncology Informatics, University of Wollongong, Australia. [9]Sydney West Radiation Oncology Network, NSW Australia. [10]Calvary Mater Hospital Newcastle, NSW Australia. [11]Institute of Medical Physics, University of Sydney, NSW, Australia. [12]Faculty of Engineering and Information Sciences, University of Wollongong, Australia. [13]Department of Radiation Oncology (MAASTRO), GROW School for Oncology and Developmental Biology, Maastricht University Medical Centre+, Maastricht, The Netherlands. [14]Institute of Medical Physics, School of Physics, University of Sydney, Australia. (david.thwaites@sydney.edu.au)

Introduction Clinical decision support systems (DSS) combine multiple variables in a statistical analysis to predict treatment outcomes. The selection of radiotherapy (RT) treatment of non-small cell lung cancer varies in practice, with different proportions of curative versus palliative RT use. We updated an overall survival DSS model for patients treated with curative RT by including data from additional institutes in the analysis. Data was stored in three institutions and the model was built using a distributed learning algorithm.
Method Clinical information and RT planning computed tomography (CT) data for 810 patients with inoperable, Stage I–III NSCLC treated with RT between 2003 and 2017 were compiled at three institutions. There were 511 patients at Institute 1, 96 at Institute 2 and 203 at Institute 3 for which all required variables were recorded. Of these patients 466 received curative RT(dose $\geq$ 48Gy). A support vector machine for predicting two-year survival was trained across the three institutions using distributed learning software on a randomly-selected half of the cohort. Assignment to one of three risk groups was adjusted towards providing treatment selection decision support between curative and palliative treatment based on the training cohort. The model was tested on the remaining half of the cohort. The attributes used were age, gender, performance status, tumour volume.
Results The model had a 0.65 AUC on the withheld data. Analysis for risk groups is displayed in Figure 1, including the patients who received palliative treatment. Here, 16% (n = 27) of patients treated with palliative RT resided in the predicted low risk group and observed significantly reduced survival($p < 0.01$) over curative treatment. Alternatively, 12% (n = 29) of curatively treated patients belonged to the predicted high-risk group and did not observe increased survival with curative RT($p = 0.075$).
Conclusion The distributed model exhibited competitive performance and is a novel approach to building models informing treatment selection.

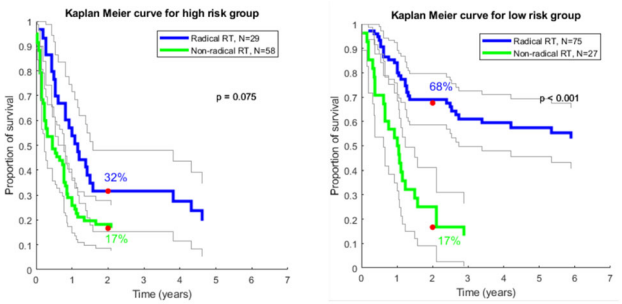

Figure 1: Survival of patients in test cohort grouped by high risk (left) and low risk (right) according to the DSS

O74 The impact of imaging variation on CT radiomics feature stability

L. C. Holloway[1,2,3,4,5], M. Field[2], C. Brink[5,6]

[1]Liverpool and Macarthur Cancer Therapy Centres and Ingham Institute, Australia. [2]South West Clinical School, University of New South Wales, Australia. [3]Centre for Medical Radiation Physics, University of Wollongong, Australia. [4]School of Physics, University of Sydney, Australia. [5]University of Southern Denmark, Denmark. (Lois.holloway@health.nsw.gov.au [Presenting author]). [6]Odense University Hospital, Odense, Denmark

Purpose Radiomics, mathematical features of images, is a rapidly expanding area of research. Radiomics features have shown to be useful in prognostic models predicting outcome for radiotherapy and other areas and also in predicting diagnosis. Radiomics features themselves however can vary with changes to the images used for the analysis. In this investigation we systematically considered the impact of changes to CT images and the associated radiomics analysis.

Methods CT data for 97 patients with non-small cell lung cancer from a single radiotherapy institution was utilised. The planning target volume region from these images was considered for radiomics analysis. Three variations to the image and analysis were considered. I) Increasing and decreasing voxel size by a factor of two ii) PTV contour expansion and contraction and iii) Hounsfield unit intensity binning (descretisation) was varied. Seventy-nine radiomics features as described in the paper by Aerts et al (Nature Communications 2014) were assessed for each of the datasets. A Pearson correlation test was used to assess correlation differences in radiomics features compared to baseline and Levene's test was considered to assess any changes in the distribution of the differencescompared to baseline. A principal component analysis was undertaken using radiomics features with all imaging variations and the variance per patient in the first and second principal components compared.

Results The majority of radiomics feature values were impacted by changes in voxel size, small variations in contour and Hounsfield unit intensity bin values. Only 3 features all related to distance measures showed no significant impact with all variations considered. Figure 1 demonstrates the variation in one feature with the variations considered.

Conclusion Variation in both imaging parameters and Hounsfield discretisation chosen for analysis can significantly impact radiomics feature calculation. Imaging and algorithm consistency should be carefully considered for radiomics analysis, particularly in multi-centre investigations.

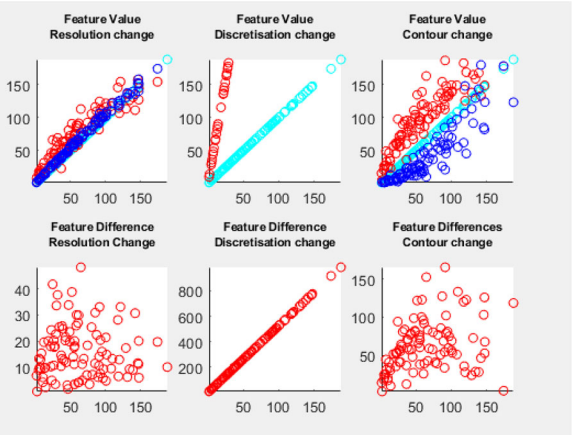

Figure 1: The variation of the radiomics feature 'Three dimensional gray level correlation matrix Variance'. The top rows demonstrate the variation in the values with the changes in images resolution, discretisation and contour expansion and contraction. The second row presents the differences in values, both are presented relative to the original value.

O75 Predicting Dice similarity coefficients for several automatically segmented pelvic CT structures using random forrest regression on intensity similarity and pyradiomics based quantitative image features

A. M. Kennedy[1], J. A. Dowling[2,3,4], P. B. Greer[3,6], L. Holloway[4,5,7,8], M. Jameson[4,7,8], D. Roach[4,8], M. Marcello[9], M. A. Ebert[1,5,9]

[1]Radiation Oncology, Sir Charles Gairdner Hospital, Nedlands, Australia. (Angel.Kennedy@health.wa.gov.au [Presenting author]), (Martin.Ebert@health.wa.gov.au). [2]Australian e-Health Research Centre, CSIRO, Royal Brisbane and Women's Hospital, Australia. ((Jason.Dowling@csiro.gov.au)). [3]School of Mathematical and Physical Sciences, University of Newcastle, Newcastle, Australia. [4]South Western Sydney Clinical School, University of new South Wales Sydney, Australia. (lois.holloway@health.nsw.gov.au), (michael.jameson@health.nsw.gov.au), (d.roach@student.unsw.edu.au). [5]Centre for Medical Radiation Physics, University of Wollongong, Wollongong, Australia. [6]Calvary Mater Newcastle Hospital, Newcastle, Australia. (peter.greer@newcastle.edu.au). [7]Ingham Institute for Applied Medical Research, Sydney, Australia. [8]Liverpool Cancer Therapy Centre, Liverpool Hospital, Sydney, Australia. [9]School of Physics and Astrophysics, University of Western Australia, Crawley, Australia. (20739859@student.uwa.edu.au)

Introduction When performing automatic segmentation it can be useful to automatically flag poor quality segmentations. These segmentations could be considered for closer inspection, exclusion from subsequent analyses or, during multi-atlas based segmentation (MABS), exclusion from contribution to a final segmentation potentially improving segmentation quality. Correlation coefficients between the Dice similarity coefficient (DSC; a popular measure of structure similarity) and intensity similarity (commonly used to rank atlases in MABS [1]) for low contrast pelvic CT organs are often only moderate (e.g. [1]). We combine intensity similarity metrics with quantitative image features to train a Random Forrest Regression (RFR) model to improve prediction of DSC.

Method Five atlas images were registered to a target set of 498 images with manually delineated structures and then used to propagate prostate, bladder and rectum structures to target images. Feature sets were constructed from general patient and image features, image

intensity similarity metrics and differences in quantitative features calculated using pyradiomics [2]. RFR was initially performed 20 times using all available features. The best features were retained for subsequent iterations. For each iteration 50% of the datasets, chosen randomly, were used for training and 50% for validation.

Results The best correlations between any single intensity similarity feature and DSC were 0.56, 0.77 and 0.59 for prostate, bladder and rectum respectively. In comparison correlations between predicted and actual DSC for the highest scoring models (scored on mean validation set r^2 and the out-of-bag error) were 0.75, 0.9 and 0.82 with and 0.66, 0.81 and 0.72 without using quantitative features.

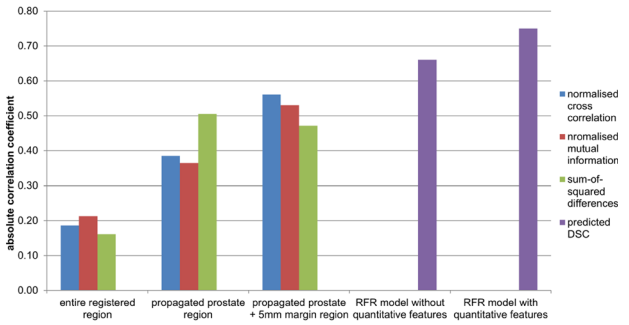

Figure 1: Correlations between sample DSC predictors and prostate DSC

Conclusion Quantitative features and intensity similarity can be used to create regression models that provide a level of DSC prediction that can increase confidence in atlas selection and evaluation of automatic segmentation success over intensity similarity alone.

Acknowledgements This work was supported by the National Health and Medical Research Council of Australia (NHMRC Project Grant 1077788).

References

1. Acosta O, Dowling J, Drean G, Simon A, de Crevoisier R, Haigron P (2014) Multi-Atlas-Based Segmentation of Pelvic Structures from CT Scans for Planning in Prostate Cancer Radiotherapy. In: El-Baz AS, Saba L, Suri J (eds) Abdomen and Thoracic Imaging: An Engineering & Clinical Perspective. Springer US, Boston, MA, pp 623–656. https://doi.org/10.1007/978-1-4614-8498-1_24
2. van Griethuysen JJM, Fedorov, A., Parmar, C., Hosny, A., Aucoin, N., Narayan, V., Beets-Tan, R. G. H., Fillon-Robin, J. C., Pieper, S., Aerts, H. J. W. L. (2017) Computational Radiomics System to Decode the Radiographic Phenotype. Cancer Research 77 (21):e104–e107. https://doi.org/10.1158/0008-5472.can-17-0339

O76 Automated atlas based quality assurance of clinical trial contouring using a random forest classifier: the radiotherapy Atlas contouring (TRAC) Tool

M. G. Jameson[1], J. A. Dowling[2], M. J. Faustino[1], K. Cloak[3], M. Sidhom[1], J. Martin[4], J. de Leon[5], M. Berry[1], D. Pryor[6], L. C. Holloway[1]

[1]Liverpool and Macarthur Cancer therapy Centres, Sydney, Australia. (michael.jameson@health.nsw.gov.au), (Maria.Faustino@health.nsw.gov.au), (mark.sidhom@health.nsw.gov.au), (megan.berry@health.nsw.gov.au), (lois.holloway@health.nsw.gov.au [Presenting author]). [2]Australian e-Health Research Centre, CSIRO, Royal Brisbane Hospital, Australia. (Jason.Dowling@csiro.au). [3]Ingham Institute for Applied Medical Research, Sydney, Australia. (k.cloak@unsw.edu.au). [4]Calvary Mater Newcastle Hospital, Radiation Oncology, Newcastle, Australia. (Jarad.Martin@calvarymater.org.au). [5]Illawara Cancer Care Centre, Wollongong, Australia. (Jeremiah.DeLeon@health.nsw.gov.au). [6]Princess Alexandra Hospital, Brisbane, Australia. (david.pryor@health.qld.gov.au)

Introduction It is acknowledged that contouring uncertainty is an obstacle to effective clinical trials in advanced radiotherapy treatment techniques. However, manual expert review of delineation for all patients enrolled prior to treatment is logistically arduous and expensive. We propose a scalable cloud based automated solution for trial specific review of delineation accuracy. This "TRAC" tool has the added benefit of enabling rapid clinical translation of study findings into regular practice.

Method Retrospective data from the prostate SBRT trial PROMETHEUS (ACTRN12615000223538) was utilised for this study. Multi-atlas generation consisted of MRI data from 10 patients, five observers, three anatomical structures and a rectal stabilisation device (SpaceOAR™ or Rectafix®). A random forest classifier was trained using a number of contour features (DSC, Components, Volume, Elongation, Perimeter, Roundness, SphericalRadius, EquivSphericalPerimeter, Flatness) to detect pass/fail on the treated and ground truth contours using ten-fold cross validation. Accuracy was calculated bases on how often the model correctly classified pass/fail contours.

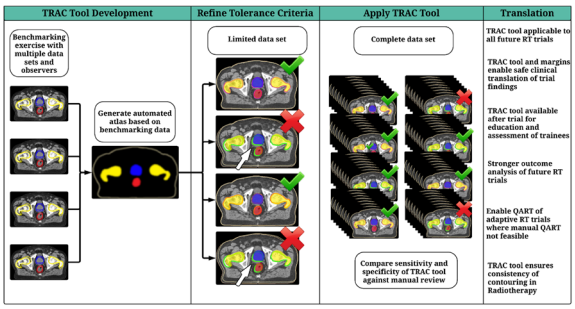

Figure 1 Workflow for applying the TRAC tool for QA of clinical trial contouring accuracy

Results

Results Analysis time was approx. 2 seconds per contour. The TRAC tool was tested on 93 individual trial patients, the number of cases for training varied from 38 to 80. For patients treated with the Rectafix™, the TRAC tool demonstrated accuracy (k = 6) results (mean ± SD) of 90.0 ± 0.6%, 57.4 ± 1.2% and 84.8 ± 0.4% for the bladder, rectum and prostate respectively. For patients treated with the SpaceOAR® the TRAC tool demonstrated accuracy results of 76.8 ± 0.9%, 72.9 ± 0.1% and 67.6 ± 0.1% for the bladder, rectum, and prostate respectively.

Conclusion The TRAC tool provides an automated and efficient means of conducting individual case review of delineation accuracy for the PROMETHEUS trial. Results reported here are for limited training data and could be improved with more data and refinement. Further testing is required for other treatment sites and imaging modalities.

Acknowledgements NHMRC program grant "*Reducing the greatest uncertainty in radiotherapy*" (APP1102198).

KS08 Bio-mathematical modelling for multi-modality clinical trial design

H. Paganetti

Massachusetts General Hospital

Radiation therapy physics is currently mainly focusing on advancing delivery and imaging technology to reduce planning and delivery uncertainties and on inverse treatment planning techniques to minimize dose to critical structures while ensuring the prescribed dose to the target. In recent years, there have been more and more efforts towards outcome imaging and outcome modeling based with the aim to better stratify treatment options for clinical trials. These efforts are expected to make an impact particularly in heavy charged particle therapy where it is important to identify those patients that will most likely benefit from these more expensive treatment options. Yet, the path to personalized patient selection and its impact on clinical trials is still long due to uncertainties in tumor control and normal tissue complication models.

While these efforts move towards personalized treatment planning in radiation therapy they do neglected a key aspect, i.e. that treatment optimization does focus mainly on the effects of radiation while other modalities are treated independently and empirically. Furthermore, both are typically standardized and not patient specific. With an increasing number of chemotherapy agents and the addition of targeted agents as well as immunotherapy, the doses and scheduling of combined therapies are largely based on clinical experience including clinical trials. Approaches are heuristically designed. There is no bio-mathematical modeling to optimize doses and schedules. This is in contrast to radiation treatments, where the optimization of delivery, fractionation and dose plays a major role. Bio-mathematical models are needed for the exploration of the trade-off between radiation and drug dose. Planning a schedule employing multiple drugs and radiation opens a wide spectrum of possibilities making modeling essential to guide clinical trial design.

This presentation will demonstrate how bio-mathematical modeling can impact clinical trial design in radiation oncology when administering radiation only as well as when prescribing multi-modality treatment approaches.

O77 Dose Quantification in carbon therapy using in-beam positron emission tomography

H. Rutherford[1], A. Chacon[1], D. Bolst[2], Y. Iwao[3], H. Tashima[3], E. Yoshida[3], F. Nishikido[3], A. Kitagawa[3], A. Mohammadi[3], T. Yamaya[3], K. Parodi[4], T. Hofmann[4], M. Pinto[4], M.-C. Gregoire[5], A. Rosenfeld[6], S. Guatelli[6], M. Safavi-Naeini[5]

[1]Centre for Medical Radiation Physics, University of Wollongong, Wollongong, NSW, Australia/Australian Nuclear Science and Technology Organisation (ANSTO), NSW, Australia. (hr962@uowmail.edu.au [Presenting author]), (ac917@uowmail.edu.au). [2]Centre for Medical Radiation Physics, University of Wollongong, Wollongong, NSW, Australia. (db001@uowmail.edu.au). [3]National Institute of Radiological Sciences (NIRS), National Institutes for Quantum and Radiological Science and Technology, 4-9-1 Anagawa, Inage-ku, Chiba, Japan. (iwao.yuma@qst.go.jp), (tashima.hideaki@qst.go.jp), (yoshida.eiji@qst.go.jp), (nishikido.fumihiko@qst.go.jp), (kitagawa.atsushi@qst.go.jp), (mohammadi.akram@qst.go.jp), (yamaya.taiga@qst.go.jp). [4]Department of Experimental Physics-Medical Physics, Ludwig-Maximilians-Universität München, Munich, Germany. (katia.parodi@lmu.de), (theresa.hofmann@physik.uni-muenchen.de), (marco.pinto@physik.uni-muenchen.de). [5]Australian Nuclear Science and Technology Organisation (ANSTO), NSW, Australia/Brain and Mind Centre, University of Sydney, Sydney, NSW, Australia. (mcg@ansto.gov.au), (mitras@ansto.gov.au). [6]Centre for Medical Radiation Physics, University of Wollongong, Wollongong, NSW, Australia/Illawarra Health and Medical Research Institute, University of Wollongong, Wollongong, NSW, Australia. (anatoly@uow.edu.au), (susanna@uow.edu.au)

Introduction During carbon therapy, nuclear inelastic collisions between primary ^{12}C ions and target nuclei produce a range of fragments along the beam path, some of which decay via positron emission after their creation [1]. Positron Emission Tomography (PET) can be used to obtain the spatio-temporal distribution of positron annihilations in the target. Direct quantification of the delivered dose from observation of the spatial distribution of positron-emitting fragments is difficult due to the complex physics of energy deposition and inelastic collisions [2]. In this study, a method for quantification of the dose distribution resulting from a poly-energetic ^{12}C beam is investigated in one dimension.

Method A relationship between observed positron annihilations and the delivered dose was developed based on the observation that the spatial distribution of each positron-emitting fragment species is unique for each primary beam energy and target material. Linear independence of generated fragment distribution profiles with respect to beam energy between each of three homogeneous phantoms, and with respect to the phantom type for each energy, were established for experimental and Monte Carlo simulation data using cross-correlation and singular value decomposition. Fragment profiles produced by a range of primary monoenergetic beam energies and target phantoms were used to perform factor analysis on activity profiles obtained following the delivery of randomly-weighted poly-energetic beams to estimate the proportional contribution of each energy.

Results The calculated set of weighting factors describing the proportional contribution of each energy to the beam were found to be within 6% of ground truth, and subsequently the dose was estimated in the entrance, spread-out Bragg peak and dose tail regions to within 4% of the ground truth value.

Conclusion The method for quantification of the dose distribution resulting from a poly-energetic ^{12}C beam investigated in this study was able to accurately estimate the dose profile in one dimension.

References

1. Pönisch F, Parodi K, Hasch B, Enghardt W (2004) The modelling of positron emitter production and PET imaging during carbon ion therapy. Phys Med Biol 49:5217–5232
2. Parodi K (2015) Vision 20/20: Positron emission tomography in radiation therapy planning, delivery, and monitoring. Med Phys 42:7153–7168

O78 Why carbon ions, as well as protons, in a national collaborative particle therapy network?

D. I. Thwaites[1], J. Sykes[2], V. Ahern[3]

[1]Institute of Medical Physics, School of Physics, University of Sydney, Australia. (David.thwaites@sydney.edu.au [Presenting author]). [2]Radiation Oncology, Blacktown Cancer Centre, Blacktown, NSW, Australia. (jonathan.sykes@health.nsw.gov.au). [3]Crown Princess Mary Cancer Centre, Westmead Hospital, Westmead, NSW, Australia. (verity.ahern@health.nsw.gov.au)

Introduction The first Australian particle therapy centre, the proton centre in Adelaide, has recently gained approval from state and federal government. There are other particle centre bids under development/discussion in other states. A national collaborative network is emerging with agreements in place between the SA, QLD and NSW bid groups and discussion ongoing with VIC. RANZCR and

ACPSEM have set up particle therapy working groups. One bid (NSW/ Westmead site) has included carbon (and other) ions, as well as protons, in its plans. The clinical, scientific and research rationale for this, within a wider national network is discussed.
Method The physics, radiobiology and clinical literature on carbon ions is summarised, in comparison to proton beams, to evaluate the case for carbon ions within a comprehensive Australia-wide approach to particle/hadron therapy. The current international situation for carbon ions is reviewed, including comparative costs and benefits for clinjcal use and for research potential.
Results There are 73 operating particle therapy beam facilities in the world (+ 42 under construction, + 25 others approved). 11, 5 and 1 respectively are carbon ion facilities. Of the 175k particle beam patient treatments, 10–15% have used carbon ions. Carbon ion facilities cost significantly more than for protons only, but the radiobiological/clinical considerations point to clinical sites where carbon has potential advantages and the use of low fraction numbers for carbon treatments begins to bring the costs per patient closer to protons. The research applications (radiobiology, clinical, medical physics and the potential use of these beams in many other areas of scientific research) present significant opportunities for Australia for a carbon ion centre within a collaborative network of proton centres, universities, ANSTO, etc.
Conclusion There is a clear rationale/role for a carbon ion centre in Australia within a comprehensive and collaborative nationally networked approach to particle therapy.

O79 Monte Carlo modelling of the Clatterbridge proton therapy beam line

J. S. L. Yap[1], M. Hentz[2], A. Kacperek[3], R. Schnuerer[1], S. Jolly[2], C. P. Welsch[4]

[1]University of Liverpool and Cockcroft Institute, UK. (Jacinta.yap@cockcroft.ac.uk [Presenting author]), (Roland.schnuerer@cockcroft.ac.uk). [2]University College London, London, UK. (m.hentz.13@ucl.ac.uk), (s.jolly@ucl.ac.uk). [3]The Clatterbridge Cancer Centre NHS Foundation Trust, Wirral, UK. (andrzej.kacperek@nhs.net). [4]University of Liverpool and Cockcroft Institute, UK. (carsten.welsch@cockcroft.ac.uk)

Introduction The Clatterbridge Cancer Centre (CCC) in the United Kingdom is the world's first hospital proton beam therapy facility, providing successful treatments for the past 30 years. A 60 MeV beam of protons is produced and transported through a passive delivery system enabling the precise delivery of uniform dose to ocular tumour sites. The QUASAR group is developing an online beam monitor based on LHCb VErtex LOcator (VELO) detector technology for implementation into the CCC clinical proton beamline. The design of the monitoring system allows real time measurements by correlation of the beam halo with the beam current. In order to investigate the capability of the system as a dose monitor, accurate and validated simulations are needed for the integration of the detector and also for the full characterisation of the beam.
Method A model of the beamline has been developed using the Monte Carlo simulation toolkit GEANT4 which describes the treatment line starting from the vacuum tube containing the double scattering foils, through to the nozzle. The geometry of the delivery system components are accurately defined, along with the VELO sensors positioned within a designated integration zone between the modulator box and treatment head. The simulation model has been validated against experimental data, including depth dose and transverse profiles.
Results The CCC beamline model is described in detail and experimental measurements are presented alongside simulated results achieved with the validated Geant4 model. The integration of the VELO detectors within the delivery system and recent progress to correlate halo measurements with delivered dose is also shown.
Conclusion An accurate and validated simulation model of the CCC beamline is essential to investigate the implementation of the VELO detector system and its viability as a candidate for online dose monitoring. This will also facilitate future work into radiobiological studies and facility upgrades.
Acknowledgements This project has received funding from the European Union's Horizon 2020 research and innovation programme under the Marie Skłodowska-Curie grant agreement No 675265, OMA – Optimization of Medical Accelerators and the Cockcroft Institute core Grant No. STGA00076-01.

O80 Dosimetric and modelled clinical effect of reduced range uncertainty in proton therapy for base of skull tumours

S. N. Penfold[1,2], R. Dalfsen[3], A. Austin[2], M. Douglass[1,2]

[1]Department of Medical Physics, Royal Adelaide Hospital, Australia. (scott.penfold@sa.gov.au [Presenting author]), (michael.douglass@adelaide.edu.au). [2]Department of Physics, University of Adelaide, Australia. (Annabelle.austin@adelaide.edu.au). [3]Department of Radiation Oncology, Royal Adelaide Hospital, Australia. (Raymond.dalfsen@sa.gov.au)

Introduction To ensure that the tumour is covered in proton therapy, proximal and distal margins are added to the clinical target volume (CTV) in addition to set-up margins to ensure target coverage. Proton CT (pCT) and dual-energy CT (DECT) are two technologies that have the capability of reducing the range uncertainty in proton therapy. In the current work we wish to examine the dosimetric and potential clinical outcome implications of utilizing these technologies for treatment planning of base of skull tumour locations.
Method Nine base of skull patients that had already received radiotherapy treatment were retrospectively replanned. For each patient, robustly optimized intensity modulated proton therapy (IMPT) treatment plans were created for a range uncertainty associated with conventional X-ray CT and also for a reduced range uncertainty associated with DECT or pCT. Dose volume histogram statistics and radiobiological model calculations were analysed for the plans. The brainstem is the dose limiting structure in this anatomical region and as such an equivalent normal tissue complication probability (NTCP) can be expected for the treatment plans. Therefore, radiobiological comparisons were made on the basis of tumour control probability (TCP) calculations.
Results On average, the D_{98} value of the CTV was increased when comparing plans generated with a 1.5% range uncertainty compared to plans with a 3% range uncertainty. This was achieved while maintaining a consistent or reduced brainstem maximum dose. In terms of TCP, values were on average greater for the 1.5% range uncertainty robust optimization, but differences were not statistically significant.
Conclusion Reducing proton range uncertainty to 1.5% with the use of DECT or pCT will improve dosimetric parameters of plans generated with robust optimization. The dosimetric improvements translated to an improvement in TCP on average with the model parameters used in the current work.

O81 Correlation between modulation complexity and plan robustness in intensity modulated proton therapy

S. N. Penfold[1,2], M. Douglass[1,2], R. Dalfsen[3], M. Jennings[1,2]

[1]Department of Medical Physics, Royal Adelaide Hospital, Australia. (scott.penfold@sa.gov.au [Presenting author]), (mdouglass@adelaide.edu.au), (Matthew.jennings@sa.gov.au).
[2]Department of Physics, University of Adelaide, Australia.
[3]Department of Radiation Oncology, Royal Adelaide Hospital, Australia. (Raymond.dalfsen@sa.gov.au)

Introduction Proton therapy dose distributions are sensitive to uncertainties in patient stopping power estimations and patient set-up variations. For this reason, the concept of robust optimization and robust plan analysis are becoming commonplace in proton therapy. We hypothesize that the greater the modulation complexity of a spot scanned intensity modulated proton therapy (IMPT) plan, the less robust the plan becomes. The purpose of this work was to investigate the correlation between plan robustness and modulation complexity using different metrics to quantify these concepts.
Method Nine base of skull patients that had already received radiotherapy treatment were retrospectively replanned. For each patient, two IMPT plans were generated; one with robust optimization and one without. For the robust optimization, range uncertainties of 3% and set-up uncertainties of 3 mm were included. Both plans were subject to robust plan analysis using the same values for range uncertainty and set-up uncertainties stated above. Plan robustness was quantified by assessing the spread in $D_{98\%}$ values of the clinical target volume (CTV) and $D_{0.3cc}$ of the brainstem dose volume histogram across all plan uncertainty scenarios. Modulation complexity was quantified using three metrics; the standard error in spot weights, the total variation in spot weights, and the entropy of spot weights.
Results The highest correlation between plan robustness and complexity of proton beams was observed when using the standard error to quantify beam complexity. Total variation displayed a similar level of correlation, while entropy did not display a strong correlation.
Conclusion The standard error in spot weights for each beam was found to correlate with plan robustness. This simple metric may be added to the cost function of inverse planning algorithms to further improve plan robustness to uncertainties in patient positioning and proton beam range.

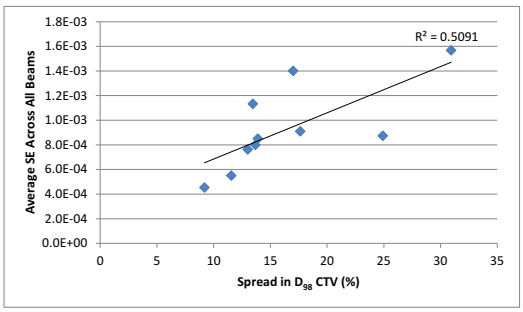

Figure 1: An example of the correlation between the standard error in spot weights and plan robustness as assessed by the spread in D_{98} values for all plan uncertainty scenarios.

O82 Using a high intensity LED worklight for annual testing of radiological personal protective equipment

L. E. Wilkinson

Department of Medical Engineering & Physics, St. Vincent's Hospital Melbourne. (luke.wilkinson@svha.org.au [Presenting author])

Introduction It has been recommended that radiological personal protective equipment (PPE) should be regularly tested for shielding integrity. For sites that do not have access to large field of view fluoroscopic equipment the process of testing PPE can be problematic. Alternative techniques for PPE testing include tactile testing and use of an infrared light source and camera. In this paper it is proposed that high brightness LED light sources can provide a low cost solution that operates at suitable level of detectability to be used in the clinical environment.
Method To test the limits of detectability several test phantoms with holes and slits of known size was developed and used with a 1800 lumen high brightness LED worklight as purchased from a national supermarket chain.
Results Limit of detectability was measured as being 1–2 mm diameter circular holes, 1 mm^2 for square holes and at least 10 mm for slits in the vinyl sub-layer. It is noted that successful application of this technique relies on (a) the ability of the operator to be able to effectively stretch the PPE material to ensure any cracks/slits open up and (b) the type of pattern on the outer covering of the PPE. Use of heavily patterned coverings can substantially reduce contrast detectability of defects/slits in the vinyl.
Conclusion The development of this innovative technique is a product of the cross-fertilisation of ideas between biomedical engineers and medical physicists. The outcome of this paper has determined that the use of a high intensity LED worklight allows for a practical cost-effective tool that can be used as an alternative method for regular testing of radiological PPE. It is considered that the best application of this technique is in low-risk areas where the gold-standard of fluoroscopic screening is not available.

O83 Occupational radiation doses in medical professions – a review of 30 years of data from the ARPANSA PRMS database

A. Hayton[1], M. Litwin[2]

[1]Primary Standards Dosimetry Laboratory, ARPANSA. (Anna.Hayton@arpansa.gov.au [Presenting author]). [2]Radiation Protection Services, ARPANSA. (Michael.Litwin@arpansa.gov.au)

Introduction The Personal Radiation Monitoring Service at the Australian Radiation Protection and Nuclear Safety Agency has been in operation for over 80 years and for the past 30 years all worker reported doses have been recorded in a digital database.
Methods The database was queried to calculate the average and 90th percentile annual radiation doses received by workers in various medical occupations over a range of years.
Results The occupations in which workers consistently receive the highest annual average doses are associated with Nuclear Medicine. In the most recent financial year Nuclear Medicine Technologists and Specialists received average annual doses of 0.90 mSv and 0.38 mSv respectively. Similarly, the occupations with the highest 90th percentile doses were also Nuclear Medicine Technologists with 2.21 mSv and Nuclear Medicine Specialists with 0.86 mSv. Medical Physicists in Radiation Oncology and Diagnostic Imaging both receive average annual doses of 0.12 mSv. Radiotherapists receive average annual doses of < 0.10 mSv. The largest group of workers, making up 33% of the total, was Radiographers who received an average annual dose of 0.10 mSv.
Of all workers in medical occupations 64% received average annual doses less than the minimum reportable limit for the system, which is 0.1 mSv. Of the workers who received doses higher than 0.1 mSv, 72% received doses < 0.25 mSv and 92% received doses less than 0.5 mSv.
Conclusion According to the ARPANSA PRMS database, the majority of radiation workers in medical occupations receive average annual doses of < 0.1 mSv, which is below the public exposure limit of 1 mSv and well below the occupational exposure limit of 20 mSv.

O84 Predictors of radiation dose in CT protocols from National Diagnostic Reference Level Service data

P. D. Thomas, M. Sanagou, T. E. Beveridge

Medical Imaging Section, ARPANSA.
(peter.thomas@arpansa.gov.au [Presenting author]),
(masoumeh.sanagou@arpansa.gov.au),
(toby.beveridge@arpansa.gov.au)

Introduction The Australian Radiation Protection and Nuclear Safety Agency (ARPANSA) has recorded CT scan parameter and dose index data from facilities utilising the National Diagnostic Reference Level Service (NDRLS) since 2011 [1]. Analysis of this data reveals trends in the relationships between scan parameters, patient characteristics and radiation dose. This information is potentially useful in guiding optimisation and informing comparisons of typical doses with DRLs.
Method Intra-class correlation (ICC) was used to measure the total variability in radiation dose metrics between and within surveys over the period 2011–2016. Linear regression models using generalized estimating equations (GEE) with an exchangeable working correlation structure were fitted to log(DLP) and log($CTDI_{vol}$) for each anatomical region in univariate and multivariate analyses. This yields estimated population-averaged relationships between the independent variables and patient-level outcomes, adjusting for any patient-level characteristics included in the model [2]. All analyses were performed using Stata/SE version 15.0 (StataCorp LP, College Station, TX) and statistical significance was assumed at $p < 0.05$.
Results After excluding surveys for young patients (< 20 years) and those with incomplete data, 3,844 surveys including 66,019 patients remained in the analysis. Example results for $CTDI_{vol}$ are shown in Table 1. Dose metrics showed a strong correlation with patient weight, increasing 20% per 10 kg for body scans, falling to only 2% for head scans. Doses also rose as a function of kV, around 10% per 10 kV step. As previously reported [3], doses were 15-30% lower with the use of iterative reconstruction. Doses for males tended to be lower than females for body scans but higher for the head and neck regions. Variations across scanner models covered ranges of 20–40%.

Table 1 – Effect of scan parameters on $CTDI_{vol}$

Parameter & change	Scan Region						
	Abdo-Pelvis	Head	Lumbar Spine	Chest	CAP (1Φ)	CAP (2Φ)	Neck
Weight /10 kg	+20%	+1.9%	+20%	+20%	+19%	+19%	+14%
Age /decade	+2.1%	N/S	+3.2%	N/S	N/S	N/S	N/S
Sex M vs F	-11%	+3.2%	-11%	+1.7%	-7.9%	-5%	+4.9%
Make (range)	20%	33%	23%	N/S	N/S	37%	42%
kVp /10 kV	+5.8%	+8.1%	+12%	+7.5%	+10%	N/S	+17%
Pitch /unit	-17%	N/S	N/S	-15%	N/S	N/S	-25%
Contrast Y vs N	N/S	N/S	N/S	N/S	N/S	N/S	-16%
Modulation Y vs N	N/S	-8.1%	-18%	N/S	N/S	N/S	N/S
Helical vs Axial	N/S	N/S	+25%	N/S	N/S	N/S	N/S
Iterative Y vs N	-24%	-15%	-19%	-30%	-33%	-31%	-26%
mAs /100 mAs	N/S	+8.8%	N/S	+3.7%	N/S	N/S	N/S

N/S – Not significant

Conclusion Analysis of NDRLS data quantifies trends in dose metrics as a function of scan parameters. These results may be used to inform comparisons of typical doses with DRLs, particularly for non-standard patient cohorts.

References

1. Hayton A, Wallace A, Marks P, Edmonds K, Tingey D, Johnston P (2013) Australian diagnostic reference levels for multi detector computed tomography. Australas Phys Eng Sci 36(1):19–26.
2. Zeger S, Liang K (1992) An overview of methods for the analysis of longitudinal data. Stat Med 11:1825–1839.
3. Thomas P, Hayton A, Beveridge T, Marks P, Wallace A (2015) Evidence of dose saving in routine CT practice using iterative reconstruction derived from a national diagnostic reference level survey. Br J Radiol. 88(1053):20150380. https://doi.org/10.1259/bjr.20150380.

O85 Revision of the Australian national diagnostic reference levels for adult CT

P. D. Thomas, T. E. Beveridge, P. A. Marks

Medical Imaging Section, ARPANSA.
(peter.thomas@arpansa.gov.au [Presenting author]),
(toby.beveridge@arpansa.gov.au), (paul.marks@arpansa.gov.au)

Introduction Australian National Diagnostic Reference Levels (DRLs) were first established for adult computed tomography (CT) procedures in 2012 [1]. Since that time, the ARPANSA National Diagnostic Reference Level Service (NDRLS) has continued to receive data submitted by facilities using the service to conduct comparisons of typical dose levels against the national DRLs. NDRLS data was reviewed in early 2018 to establish revised national DRLs for adult CT.
Method Dose metrics ($CTDI_{vol}$, DLP) and patient data are collected for a particular imaging protocol on a given imaging device at an imaging facility. Additional data describing the imaging protocol are also collected. Facility reference levels (FRLs) are computed for each such survey as the median values of the dose metrics. The distribution of FRLs for each imaging protocol is analysed to derive a DRL. A liaison panel comprising representatives from professional groups and industry bodies reviewed the data and recommended revisions to the DRLs.
Results The revised DRLs (Table 1) are based on the data submitted to the NDRLS in the 2017 calendar year. The liaison panel recommended that the neck region be split into separate cervical spine and soft-tissue neck categories. The existing neck data was assigned to the new categories using the implied scan length (DLP/$CTDI_{vol}$) and the additional protocol data. A new category for kidney-ureter-bladder has been created with DRLs based on the abdomen-pelvis data. The revised DRLs are 10–30% lower than the previous values.

Table 1. Revised Australian National DRLs for adult CT

Scan Region	$CTDI_{vol}$ (mGy)	DLP (mGy.cm)
Head	52	880
Cervical spine	23	470
Soft-tissue neck	17	450
Chest	10	390
Abdomen-pelvis	13	600
Kidney-ureter-bladder	13	600
Chest-abdomen-pelvis	11	940
Lumbar spine	26	670

Conclusion Revised national DRLs for adult CT have been adopted. The new DRLs are 10–30% lower.

References

1. Hayton A, Wallace A, Marks P, Edmonds K, Tingey D, Johnston P (2013) Australian diagnostic reference levels for multi detector computed tomography. Australas Phys Eng Sci Med 36:19–26

O86 Radiation protection- a new paradigm

M. Bhat

Adelaide Radiotherapy Centre, Genesis Care, The Adelaide University. (Madhava.Bhat@adradcentre.com.au [Presenting author])

Introduction There are facts, there are alternative facts (also called as opinions) and there are lies in any subject. The subject of ionising radiation protection is no exception to these diverging views. Activists, social media, political commentators have hijacked the domain of radiation protection and it appears scientists have fled the scene in desperation. This paper examines why such irrational media frenzy and social fear exists.
Method A vast amount of literature on radiation safety is available in public domain. While some literature has sound scientific foundation, much of the literature on radiation safety can be regarded as opinions of people and fails when tested with scientific scrutiny. When studying the history of x-rays for medical and industrial use one realises that dose limits for radiation protection have been progressively lowered. This paper examines the impact of the current radiation protection dose limits standards on the society.
Results While, the dose-response upon which these standards are based are accurate for high levels of acute radiation exposure they are not representative of the biological response of the human body at low levels of chronic radiation exposure [1]. Although exposure to low levels of radiation would cause some DNA damage, it would also trigger the defensive responses of the body by producing antioxidants and DNA repair enzymes [2]. With the boosted defences, there would be less endogenous DNA damage [3].
Conclusion The overt conservatism in radiation protection standards has led to large investments in protection infrastructure such as over engineered radiation protection mechanism, for no benefit to public health or safety. An open discussion based on sound scientific knowledge is needed to ensure evidence-based policies are implemented to deliver adequate levels of public health and safety and to remove unreasonable fear of radiation.

References

1. Doss, M. (2016). Changing the Paradigm of Cancer Screening, Prevention, and Treatment. Dose-Response, 14(4), 1559325816 680539.
2. Feinendegen, L. E., Pollycove, M. & Neumann, R. D. (2013). Hormesis by Low Dose Radiation Effects: Low-Dose Cancer Risk Modeling Must Recognize Up-Regulation of Protection. In: BAUM, R. P. (ed.) Therapeutic Nuclear Medicine. Springer.
3. Koana, T. & Tsujimura, H. (2010). A U-shaped dose-response relationship between x radiation and sex-linked recessive lethal mutation in male germ cells of Drosophila. Radiat Res, 174, 46–51.

O87 Do carers require lead aprons in general X-ray?

A. Perdomo, S. McMahon, T. Wilkie

Department of Medical Imaging, The Royal Children's Hospital, Melbourne, Victoria. (amanda.perdomo@rch.org.au [Presenting author]), (stacey.mcmahon@rch.org.au), (trent.wilkie@rch.org.au)

Introduction Radiation doses received by the public must be kept as low as reasonably achievable, economic and social factors being taken into account. One social factor to consider during paediatric examinations is anxiety for the carers. This anxiety can be magnified when the radiographers request that the carers don protective garments to restrain the child during a general X-ray examination, immediately after explaining the minimal radiation risks of the procedure to their child.
Method AirKERMA measurements were taken with a RaySafe X2 survey sensor (RaySafe, Sweden) using 10mAs exposures over a kV_p range from 40 to 100kV_p. Patient scatter was simulated with Perspex thicknesses between 2.5 and 22.5cm and measurements made at four different locations where a carer would likely be standing during an examination.
The measured AirKERMA was then matched to each general X-ray protocol at our clinic to estimate the potential radiation exposure to the carer.
Results Using the measured data, our protocol was revised to require that a protective garment be worn by carers when the expected radiation exposure is likely to be more than 2 uSv, or 12 h' worth of Australian natural background radiation. For ease of use by the Radiographers this translated to a work procedure stating that lead aprons must be worn by carers for "Patients above 60 kg for all general X-ray exposures except extremities and all spine X-rays in buckys". For all other examinations, a protective garment is not required but will not be refused.
Conclusion The introduction of this work procedure has allayed many concerns that parents may have while their child is undergoing a general X-ray examination and created an easier workflow for Radiographers as they do not have to ensure carers don lead for examinations resulting in negligible radiation exposure to the carer.

O88 Monte-carlo validation of the inverse broad beam geometry as a surrogate for the broad beam geometry when determining lead equivalence of protective garments

J. A. Laban[1], M. Wijesooriya[2], S. Marsh[2]

[1]Photon Physics Ltd, Christchurch, New Zealand. (johnny@photonphysics.co.nz [Presenting author]). [2]University of Canterbury, Christchurch, New Zealand. (manoj.wijesooriya@pg.canterbury.ac.nz), (steven.marsh@canterbury.ac.nz)

Introduction Ideally lead equivalence for protective garments should be determined using broad beam exposure conditions, but this is not practical, and unrealistic narrow beam geometries have been used in the past (in accordance with AS/NZS 4543-1 [1] for example). The second edition of IEC 61331-1 [2] provides an "inverse broad beam" geometry that is practical and apparently produces results equivalent to broad beam attenuation measurements.
Method This work uses monte-carlo simulation to compare the attenuation results of a conventional broad beam measurement set-up against an inverse broad beam geometry. The geometries as specified in IEC-61331 have been coded in EGSnrc, and transmission of typical diagnostic x-ray spectra with kVps in the range 50–120 kV through 0.3 mm of antimony have been modelled with kerma being scored in idealised ion chambers.
Results The inverse broad beam geometry produces a greater attenuation in all cases by amounts from 5 to 10 % for the beams from 50 to 120 kVp. The statistical uncertainty in the monte-carlo calculations is approximately 2 %, so the differences are significant.

Conclusion Whilst there is a difference in the attenuation ratios determined according to each geometry, this difference when expressed in terms of lead equivalence is relatively insignificant (0.20 mm Pb with broad beam geometry compared to 0.21 mm Pb for the inverse broad beam at 90 kV), and so the method prescribed in IEC-61331 can be considered valid according to the work reported here.

References

1. AS/NZS 4543.1 (1999). Protective devices against diagnostic medical X-radiation – Part 1: Determination of attenuation properties of materials.
2. IEC 61331-1 (2014) (2nd ed.). Protective devices against diagnostic medical X-radiation – Part 1: Determination of attenuation properties of materials.

O89 In vivo measurements of skin dose from total skin electron therapy treatments

T. Kairn[1,2], L. Yu[1,2], R. Wilks[1], C. Lancaster[1], S. B. Crowe[1,2]

[1]Royal Brisbane and Women's Hospital, Herston, Australia. (t.kairn@gmail.com [Presenting author]), (Nancy.Yu@health.qld.gov.au), (Rachael.Wilks@health.qld.gov.au), (Craig.Lancaster@health.qld.gov.au), (sb.crowe@gmail.com).
[2]Queensland University of Technology, Brisbane, Australia

Introduction Mycosis fungoides is a form of lymphoma that specifically affects the patient's skin, which can be effectively treated using total skin electron therapy (TSET, also known as TSEI and TESBT) [1]. During a TSET treatment the patient stands at a distance from the radiation source, so conventional computerised simulation and treatment planning methods cannot be used [2]. This study aimed to provide a preliminary analysis of an archive of in vivo dose measurement data obtained using optically stimulated luminescence dosimeters (OSLDs) and used to verify or modify monitor unit (MU) calculations for TSET patients treated over the last six years.
Method Records and OSLD measurement data were obtained for 10 TSET cases that were treated between 2013 and 2018, inclusive. All treatments were delivered using a local version of the Stanford technique [3, 4]. Measurement data were aggregated and analysed.
Results There was no recorded change in prescription for 5 cases. The remaining 5 cases required MU adjustments to compensate for dose differences of 3.5% to 16% that were detected using OSLDs on the front and back of each patient's thorax and abdomen. All large changes were attributed to "change in stance"; the patients were observed leaning closer to or further from the spoiler screen during treatment than they were during physical measurements for the initial dose calculation. OSLD measurements also indicated the necessity of adding or removing shielding of the hands and feet during each treatment course, to prevent localised over-dosing or under-dosing.
Conclusion The results of this preliminary investigation confirm the importance of obtaining in vivo measurements of skin dose at a range of points (from trunk to extremities) for patients treated using TSET or any other form of radiotherapy that requires the patient to stand with minimal support.

Acknowledgements The authors wish to thank the various physicists at the Royal Brisbane and Women's Hospital who performed, analysed and reported OSLD measurements for TSET treatments over the last six years.

References

1. Chowdhary M, Chhabra AM, Kharod S, Marwaha G. Total skin electron beam therapy in the treatment of mycosis fungoides: a review of conventional and low-dose regimens. *Clinical Lymphoma, Myeloma and Leukemia*. **16**(12): 662–671 (2016)
2. Kairn T. Patient rotation during linac-based photon and electron radiotherapy. *Journal of Medical Imaging and Radiation Oncology*, **in press** https://doi.org/10.1111/1754-9485.12757 (2018)
3. Fitchew RS, Nitschke KN, Christiansen PG. Total skin electron beam therapy using a Dynaray 18 linear accelerator. *Australasian Physical and Engineering Sciences in Medicine* **8**: 182–187 (1985)
4. Orth AG, Sylvander SR, Crowe SB. Comparative study of total skin electron therapy (TSET) treatments of Mycosis Fungoides. *Australasian Physical and Engineering Sciences in Medicine* **39**(4): 1168–1169 (2016)

O90 Clinical assessment of 3DBolus software including Electron Modulated Bolus

T. Ostwald, J. Wolf, S. Baddock, P. Simpson

Radiation Oncology Department, Calvary Mater Newcastle, Australia. (trish.ostwald@calvarymater.org.au [Presenting author]), (joshua.wolf@calvarymater.org.au), (shane.baddock@calvarymater.org.au), (paul.simpson@calvarymater.org.au)

Introduction 3DBolus by Adaptiiv is new software designed to produce 3D printed bolus for radiotherapy, including simple TPS generated bolus, modulated electron bolus and brachytherapy skin moulds. We assessed 3DBolus for designing 3D printed clinical bolus in-house, including modulation of electron bolus to more closely shape around the PTV, or reduce hotspots.
Method Previously treated clinical plans were anonymised and 3D bolus generated in the software. The plans included single thickness simple bolus for sites such as face, leg and vulva, a rectangular nose block, modulated bolus for nose, face, and chestwall, and brachytherapy moulds for scalp and lower leg. Test 3D prints were performed from the generated bolus. 3Dprinter filaments were tested for suitable clinical bolus material, and quality assurance procedures were developed.
Results Four Filaments (Polylactic Acid (PLA), Copolyester (CPE), Thermoplastic Polyurethane (TPU), Polycarbonate (PC) were tested for clinical bolus suitability, with TPU 95A identified as the preferred option due to its flexibility and durability. All four materials had relative electron densities of $\sim$ 1.09, physical densities of $\sim$ 1.2 g/cm^3 and $\sim$ 1% of dose enhancement compared to the same thickness of solid water.
3DBolus was found to be easy to use and provided a convenient software option for producing simple bolus. Brachytherapy bolus moulds allowed the catheter position to be changed and tested. The ease of generating modulated electron bolus was found to depend on the complexity of the PTV, surface anatomy and heterogeneity. Straightforward cases such as Figure 1 were easy to generate. Cases with very complex surface anatomy could produce over-modulated bolus, though simplifying the shape of the PTV reduces the over-modulation.

Figure 1 shows modulated bolus for treatment to the sternum while reducing dose to the heart.

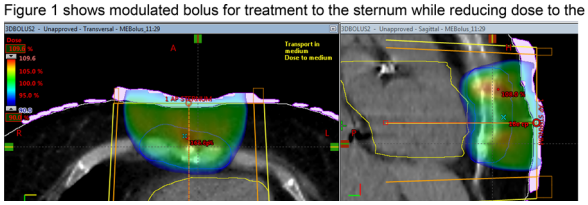

Conclusion 3DBolus was found to be a useful addition to our clinic.

References

http://www.nl-tec.com.au/Radiation-Therapy-Products/3D-Bolus-3

O91 A study of the radiological water equivalence of solid phantoms for very low energy x-ray beams

R. Hill

Department of Radiation Oncology, Chris O'Brien Lifehouse, Sydney, Australia and Institute of Medical Physics, School of Physics, The University of Sydney, Australia. (robin.hill@lh.org.au [Presenting author])

Introduction Kilovoltage x-ray beams are commonly used for the treatment of skin cancers. For the very low energy beams, the dosimetry can be challenging and many dosimeters are not waterproof. This project evaluated the radiological water equivalence of various solid phantoms for very low energy X-ray beams.

Method Percentage depth doses in eight different solid phantoms and surface doses to a small water volume were calculated using EGSnrc for four X-ray beams with peak potentials from 30 – 80 kVp (with HVLs from 0.3 to 1.2 mm Al). For the EGSnrc calculations, all the relevant calculation options were used as well as the XCOM photon cross section data option. The primary photon spectra was calculated using SpekCalc and the number of incident photons for the Monte Carlo calculations was chosen so that the calculated uncertainty was less than 1%. Reference doses were calculated in the water phantom only.

Results In general, the calculated PDDs and surface doses calculated in the solid phantom had increasing differences as the beam energy decreased. For the RMI457 Solid Water, Virtual Water and Plastic Water DT solid phantoms, the calculated depth doses were all within 1% as compared to those calculated in water for the 30 kVp X-ray beam. In comparison to the depth doses in water, the depth doses in Plastic Water had relative differences of up to − 19.8% and polystyrene had relative differences of up to 20.4% for the 30 kVp X-ray beam. The differences in doses generally decreased as the x-ray beam energy increased.

Conclusion This work has evaluated a number of solid phantoms for the dosimetry of very low energy x-ray beams. The RMI457, Virtual Water and Plastic Water DT solid phantoms have been shown to be suitable even at the very low energies without the need for any correction.

References

Hill – MP Solid Phantoms
SpekCalc

O92 Total skin electron therapy: the pitfalls, the peril and the ozone!

M. Douglass, S. Penfold, K. Quach, T. Rutten

Department of Medical Physics, Royal Adelaide Hospital, Adelaide, South Australia. (mdouglass@adelaide.edu.au [Presenting author])

Introduction Total skin electron therapy (also known as total body electron therapy) is used for the treatment of Mycosis fungoides, a common form of cutaneous T-cell lymphoma. Total skin electron therapy (TSET) employs a low energy electron beam from a clinical linear accelerator to deliver a whole body superficial radiation dose to the cutaneous lesions while sparing the underlying tissue and organs.

Method A commissioning workflow for the TSET technique on a Varian Truebeam linac using IAEA TRS-398 formalism [1] is presented in the current work. All dosimetric measurements were verified using Gafchromic EBT3 film and TLD chips. A number of unique phantoms were built and novel techniques employed during the process to enable an accurate and efficient commissioning work flow.

Results Verification of the TSET technique was performed using film and TLD in several end-to-end tests on the anthropomorphic phantom Rando. Average dose results from 40 pieces of radiochromic film and 13 TLDs attached to Rando were within 2.7% of the prescribed dose (12 Gy in 6 fractions) on all three occasions.

To date, three patients have been treated. Mean doses to the surface of the skin from TLD and film results for these patients were − 0.5%, + 9% and − 2.9% of the prescribed dose. Clinical follow-up of the first patient indicated excellent clinical response. The only remaining lesion after treatment was located in shielded left medial calf.

Conclusion TSET has been commissioned in the current work using IAEA TRS-398 formalism and a variety of custom phantoms designed to aid commissioning efficiency and accuracy. Patients treated to date have shown excellent clinical response.

Figure 1. Rendering of custom beam degrader used for commissioning and treatment in the current work.

Figure 2. End-to-end verification of treatment using the "Rando" anthropomorphic phantom.

Reference

P. Schiapparelli, D. Zefiro, F. Massone, and G. Taccini, Total skin electron therapy (TSET): A reimplementation using radiochromic films and IAEA TRS-398 code of practice, *Medical Physics* 37, 3510 (2010)

O93 Simplified input and reduced errors with mask factors for the WOmed T-200 kV treatment system

J. Lehmann[1,2,3], T. Ostwald[1]

[1]Department of Radiation Oncology, Calvary Mater Newcastle, Newcastle, Australia. (Joerg.Lehmann@calvarymater.org.au [Presenting author]), (Trish.Ostwald@calvarymater.org.au). [2]Institute of Medical Physics, The University of Sydney, Sydney, Australia. [3]School of Mathematical and Physical Sciences, The University of Newcastle, Australia

Introduction The WOmed T-200 kV therapy system includes PC-based "Radiation Control II" software (RC2) which operates the machine and features a database for scheduling and recording patient treatments. RC2 allows selection of beam, applicator, depth and an optional 'mask'. The treatment time is then calculated based on tables entered during commissioning. In addition, in our clinical practice standoff is often used and the prescription is sometimes changed following in vivo dosimetry. The goal was to operate the machine with real input parameters without the need to calculate factors separately as done elsewhere [1].

Method In our implementation the mask includes the impact of standoff and effective diameter (ED) of the field. RC2 allows 40 masks in total with mask values assigned to them for beam-applicator combinations. A set of depth doses can be defined for each mask.

The limit of 40 necessitated selection of combinations of standoff and ED. The EDs were selected based on the available applicators, and selected additional EDs to minimize dose error due to discretisation between EDs.

Since simple prescription changes were not easily performed, for each mask factor a three step depth dose was defined with 0.97, 0.95 and 0.9 relative doses, to allow prescription adjustments i.e. to the 97/95/90% isodose".

Results The masks were defined as in Table 1. Available standoffs were limited to 0, 0.5 cm and 1 cm. Mask factors were calculated using interpolated backscatter factors and effective SSDs and entered using .ini files. Each mask factor was manually verified.

Conclusion Using real input parameters for RC2 increases transparency of the process and thereby reduces the chances of errors. With a limited number of masks available, the necessary discretization of ED will lead to small, known systematic deviations. The discretization of standoff simplified the clinical process and might also reduce errors.

Table 1: Masks

Mask #	ED [cm]	Standoff [cm]	Comment
1	1	0	
2	2	0	Ø 2 cm applicator
3	2	0.5	Ø 2 cm applicator
4	2	1	Ø 2 cm applicator
5	2.5	0	
6	2.5	0.5	
7	2.5	1	
8	3	0	Ø 3 cm applicator
9	3	0.5	Ø 3 cm applicator
10	3	1	Ø 3 cm applicator
11	3.5	0	
12	3.5	0.5	
13	3.5	1	
14	4	0	Ø 4 cm applicator
15	4	0.5	Ø 4 cm applicator
16	4	1	Ø 4 cm applicator
17	5	0	Ø 5 cm applicator
18	5	0.5	Ø 5 cm applicator
19	5	1	Ø 5 cm applicator
20	6	0	
21	6	0.5	
22	6	1	
23	7	0	
24	7	0.5	
25	7	1	
26	7.7	0	(6 x 8 cm2 applicator)
27	7.7	0.5	(6 x 8 cm2 applicator)
28	7.7	1	(6 x 8 cm2 applicator)
29	9	0	
30	9	0.5	
31	9	1	
32	9.9	0	(8 x10 cm2 applicator)
33	9.9	0.5	(8 x10 cm2 applicator)
34	9.9	1	(8 x10 cm2 applicator)
35	13.3	0	(10 x15 cm2 applicator)
36	13.3	0.5	(10 x15 cm2 applicator)
37	13.3	1	(10 x15 cm2 applicator)
38	16	0	
39	16	1	
40	22.2	0	(20 x 20 cm2 applicator)

References

1. Aspradakis MM, Zucchetti P (2015) Acceptance, commissioning and clinical use of the WOmed T-200 kilovoltage X-ray therapy unit. Br J Radiol 88(1055):20150001

O94 Observations made while commissioning a WOmed T300 superficial unit using ACPSEM working group recommendations

S. B. Crowe[1,2], A. Dick[1], A. Livingstone[1], T. Kairn[1,2], S. R. Sylvander[1]

[1]Royal Brisbane & Women's Hospital, Herston, Australia. (sb.crowe@gmail.com [Presenting author]), (alastair.dick@health.qld.gov.au), (alexander.livingstone@health.qld.gov.au), (t.kairn@gmail.com), (steven.sylvander@health.qld.gov.au). [2]Queensland University of Technology, Brisbane, Australia.

Introduction The WOLF Medizintechnik (WOmed) T-300 system is a ceiling-suspended orthovoltage unit distributed with a timer calculator and record and verify system RadControl-II. The Royal Brisbane & Women's Hospital replaced a Gulmay D3300 with a T300 system in 2018.

Method Acceptance and commissioning was completed in accordance with recommendations of the customer acceptance test (CAT)

document [1], ACPSEM position paper [2], AAPM TG-61 [3] and CPQR guidelines [4]. Beam qualities, selected to nominally match existing D3300 values, are listed in Table 1.

Table 1. WOmed T-300 system beam qualities

	Filtration				V_{tube}	I_{gun}	HVL_{nom}
Filter	Be	Al	Cu	Sn	(kV)	(mA)	(mm Al)
1	3.0	0.9	-	-	70	30	1.11
2	3.0	2.1	-	-	100	30	2.67
3	3.0	3.7	-	-	100	30	3.89
4	3.0	0.8	0.2	-	100	30	5.97
	Filtration				V	I	HVL_{nom}
Filter	Be	Al	Cu	Sn	(kV)	(mA)	(mm Cu)
5	3.0	1.3	1.0	-	232	12	1.81
5	3.0	1.3	1.0	-	300	10	2.41
6	3.0	0.8	1.6	-	300	10	2.91
7	3.0	0.8	2.6	0.5	300	10	3.92

Results The treatment system satisfied conditions of the CAT document. Measured data was entered into the RadControl-II software for clinical timer calculations. Observations included: Half-value layer (HVL) calculations using absorber-specific Nk-corrected air-kerma values differed from HVLs calculated using raw ionisation measurements by 4.6% for 70 kV beam.

- The use of a single absorber measurement, as suggested in the CAT process resulted in a HVL that differed from corrected regression-derived HVL by 7.1%.
- The use of the Attix method for timer end effect calculation differed from extrapolation calculations by up to 9.6%.
- Plastic rubbish bin liners have an appropriate composition and thickness for removing contaminant electrons.

Conclusion The ACPSEM position paper, used in parallel with other international recommendations, provided valuable guidance that helped clarify the processes required for superficial system commissioning. Generally, established and widely-recommended test methods provided more accurate results than otherwise-attractive simplified techniques.

Acknowledgements The authors would like to acknowledge Hans Feitz, Julie-Anne Outhwaite, Jemma Blyth, Rachael Wilks, Craig Lancaster, Sylwia Zawlodzka-Bednarz, Alessandro Esposito, John Baines and Timothy Markwell for advice and assistance.

References

1. X-Ray therapy systems T-160/T-200/T-300 Customer Acceptance Test (v2018-02-22), Wolf-Medizintechnik GmbH, St. Gangloff, Germany
2. R. Hill, B. Healy, D. Butler, D. Odgers, S. Gill, J. Lye, T. Gorjiara, D. Pope, B. Hill, "ACPSEM kilovoltage dosimetry working group recommendations for quality assurance in kilovoltage radiation therapy", *Australas Phys Eng Sci Med* **in press** (2018)
3. C-M. Ma, C. W. Coffey, L. A. DeWerd, C. Liu, R. Nath, S. M. Seltzer, J. P. Seuntjens, "AAPM protocol for 40–300 kV x-ray beam dosimetry in radiotherapy and radiobiology", *Med Phys* **28**(6): 868–893 (2001).
4. C. Furstoss, "COMP report: CQPR technical quality control guidelines for kilovoltage X ray radiotherapy machines", *J Appl Clin Med Phys* **19**(2): 18–21 (2018)

O95 Dosimetric evaluation of small field electron beam for head and neck cases

S. Ulya[1], D. Ryangga[2], W. E. Wibowo[3], N. Nasution[3], S. A. Pawiro[1]

[1]Department of Physics, Faculty of Mathematics and Natural Sciences, Universitas Indonesia, Depok, West Java, 16424, Indonesia. (syariflia88@gmail.com), (supriyanto.p@sci.ui.ac.id). [2]Pasar Minggu Hospital, South Jakarta, 12550, Indonesia. (dea_ryangga@yahoo.com). [3]Department of Radiotherapy, National General Hospital Cipto Mangunkusumo, Jakarta, 10430, Indonesia. (wahyu.bovie@gmail.com), (didinn1412@gmail.com)

Introduction In regard to the increasing use of small field photon in clinical treatment, in this study, we investigate the use of small field electron beam in clinical treatment. The aim of this study was to evaluate small field electron beam dosimetry of the nasopharyngeal, thyroid and ethmoid sinus carcinoma cases.

Method Treatment planning was made using Precise plan and Eclipse TPS. Dose measurement was done using EBT3 film on Elekta Synergy Platform and Varian Trilogy LINAC using various field size from 5×5 cm^2 until 1×1 cm^2 with 6, 12, and 15 MeV. The evaluation was done to seek discrepancies of dose in the 100, 90, 80, 70 points of intersection between isodose and central axis, for each case.

Results In nasopharyngeal cases with a homogenous area and irregular surface, the dose discrepancies for 6 MeV energy was unpredictable except for 5×5 cm^2 field size. For all energies in 5×5 cm^2 field size, the dose discrepancies were less than 3%. In these cases, we found that smaller electron beam field will increase the percentage of the discrepancy. This is caused by the effect of the lateral scatter disequilibrium in small field electron beam that causes the decrease of the output factor. Otherwise, another analysis found in the increasing depth evaluation causes an increase of dose discrepancy. For ethmoid sinus cases, dose discrepancy depends on the field size and inhomogeneity of bone and tissue. From the result, inhomogeneity of the bone on small electron field does not significantly influence the dose discrepancies.

Conclusion Higher dose discrepancy correlates with smaller field size (lack of lateral scatter disequilibrium), smaller energy, greater depth and low homogeneity. From this research, we found that the effect of inhomogeneity caused by the air cavity (ethmoid sinus) contributes to higher dose discrepancy far more than the discrepancy caused by bone.

KS09 Advances and the role of Monte Carlo modelling in medical physics

M. Dingfelder

Department of Physics, East Carolina University, USA. (dingfelderm@ecu.edu [Presenting author])

Introduction Monte Carlo (MC) methods are widely used to solve complex physical and mathematical problems. This holds especially true for radiation transport simulations in complex and heterogeneous geometries. These specialized MC simulation codes rely on realistic transport models and interaction cross sections with the material under consideration. While full MC simulations are still not feasible for treatment planning, they can be used to study, benchmark, and improve treatment planning systems and to provide useful information on the interpretation of results in diagnostic imaging.

Method Basic principles of MC radiation transport simulations are reviewed for different radiation qualities and length scales. MC simulation codes range from specialized home-made codes (e.g., PARTRAC), to general purpose codes (e.g., Penelope, MCNP) to heavy ion codes and code systems (e.g., Fluka, Geant4, Gate, Topas).

Results Typical applications in the area of medical physics and diagnostic imaging as well as recent advances in the field are

discussed. Hot topics include heavy ion transport and *biological* dose and the modelling of nano-particles.

Conclusion Monte Carlo modelling and MC codes are an important tool in all aspects of medical physics. Codes and possibilities evolve with the evolution in computation.

Acknowledgements We thank the organizers for conference travel funding.

IS07 Partnering for success

K. J. Reynolds

Medical Device Research Institute, Flinders University, South Australia. (karen.reynolds@flinders.edu.au)

The Medical Device Partnering Program (MDPP) was established in 2008 by Flinders University as an "ideas incubator" connecting partners and de-risking product concepts. The Program supports the development of novel medical devices and assistive technologies by facilitating unique collaborations and partnerships between research institutions, companies, healthcare providers, and manufacturers. The MDPP provides a mechanism for prototype development, proof of concept studies, and clinical and market validation. It is tailored to deliver industry driven research outcomes with impact, providing a transparent, facilitated process of engagement, reduced risk in the innovation process, and access to relevant expertise.

Since its launch, more than 80 innovations have progressed towards market, including: a probe for determining cancer tumour margins during surgery; a hydration monitoring device; an arm-splint for first-aid; tools to enhance orthopaedic fixation; and light therapy glasses.

Due to the success in South Australia the MDPP is currently positioning itself for a national rollout of the program, with the aim of connecting research, healthcare and manufacturing capability across the nation and cementing Australia's position as a leader in the growing medical devices market.

In this presentation, Professor Karen Reynolds, Director of the MDPP, will provide insights into the Program and give examples of some of the companies and products it has supported.

O96 A year of volunteering in Cambodia

N. C. Shelton

Department of Radiation Oncology, ONJCRWC Austin Hospital, Australia. (Nikki.shelton@austin.org.au)

Introduction An update on the Australian Volunteers in International Development (AVID) Radiotherapy Physics Trainer assignment based in Phnom Penh, Cambodia. The objectives of AVID are to support the capacity of Host Organisations to deliver effective and sustainable development outcomes as well as to promote a positive perception of Australia in the Indo-Pacific region through the contribution of volunteers. The assignment titled "Radiotherapy Physics Trainer" is supported by the Australian Government Department of Foreign Affairs and Trade (DFAT), as part of Australia's Aid program, committed to promoting prosperity, reducing poverty and enhancing stability in the region.

The Partner Organisation in Australia is the Australasian College of Physical Scientists and Engineers in Medicine, which helps to support assignments like mine through The Better Healthcare Technology Foundation and the Asia Pacific Special Interest Group. The objectives of the assignment are to provide training to medical physicists and RTTs at National Cancer Centre (NCC) at Calmette Hospital in order to develop an international standard radiation oncology program. This involves the commissioning and development of QA for a Varian 21iX, Eclipse TPS, a Varian HDR with TPS and a GE RTCT Scanner.

The long-term plan for radiation oncology provision by the Calmette NCC is to establish themselves as the foremost cancer centre in Cambodia with the view to expand to 3 linacs in Phnom Penh as well as to set up regional centres for the provinces.

Conclusion This presentation will provide an overview of the work being done at Calmette Hospital, including an insight into the status of medical physics in Cambodia. I will discuss some of the challenges of teaching radiotherapy physics that presented themselves along the way as well as some of the highlights of being given the opportunity to lay a solid foundation for the future of radiotherapy treatment in Cambodia

Acknowledgements Department of Foreign Affairs and Trade, The Better Healthcare Foundation, APSIG, ACPSEM

O97 Diamond dosimetry on the Australian MRI-linac

N. Roberts[1,2], U. Jelen[2], B. Oborn[1,3], L. Holloway[1,2,4,5,6], G. Liney[2,4,7,8], M. Lerch[1], P. Metcalfe[1]

[1]Centre of Medical and Radiation Physics, University of Wollongong, NSW, Australia. (nr593@uowmail.edu.au [Presenting author]), (brad.oborn@gmail.com), (lois.holloway@sswahs.nsw.gov.au), (mlerch@uow.edu.au), (metcalfe@uow.edu.au). [2]Ingham Institute for Applied Medical Research, Sydney, NSW, Australia. (urszula.jelen@health.nsw.gov.au), (gary.liney@health.nsw.gov.au). [3]Illawarra Cancer Care Centre, Wollongong Hospital, NSW, Australia. [4]Department of Medical Physics, Liverpool and Macarthur Cancer Care Centres, Sydney, NSW, Australia. [5]SWS Clinical School, University of New South Wales, Liverpool, NSW, Australia. [6]Institute of Medical Physics, School of Physics, University of Sydney, Sydney, NSW, Australia. [7]South Western Sydney Clinical School, School of Medicine, University of New South Wales, Sydney, Australia. [8]Centre for Medical Radiation Physics, University of Wollongong, Australia

Introduction Dosimetry in MR-guided radiotherapy is challenging due to variation in response of detectors as a result of the magnetic field. These changes in response for microDiamond detectors have previously been explored through simulations [1], measurements in a perpendicular magnetic field [1–3] and measurements for a 0.21 T in-line magnetic field [4]. How the detector responds in a 1 T in-line magnetic field is of interest to the Australian MRI-linac (MRL) project.

Method The Australian MRL has the unique feature that the linac is mounted on rails allowing for measurements to be performed at different magnetic field strengths while maintaining a constant SSD. The microDiamond's response at 1 T has been assessed at the MRL isocentre, and the response at $\sim$ 0 T was achieved by retracting the linac so the phantom was within the fringe field of the magnet where the field drops off. PDDs were acquired for a range of field sizes for both setups. GAFchromic^{TM} film measurements at the surface of the phantom while inside the magnet were also obtained for different field sizes in order to characterise the size and intensity of the electron hot spot, caused by the fringe field of the Australian MRL system.

Results PDDs for a 6.1 $\times$ 5.8 cm^2 field are shown figure 1 (left) with a maximum difference of 0.7% between the PDDs. We can only compare depths 2 cm and beyond where the magnetically focused

contaminant electrons have been completely absorbed. Figure 1 (right) demonstrates the approximately linear increase in surface dose as a function of field size with 760% more dose at a depth of 1 mm relative to 51 mm for the largest field size, the size of the hot spot for this field can been seen in the 2D dose distribution.

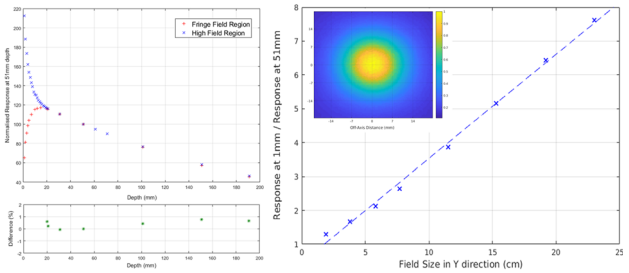

Figure 1: PDDs of 6.1x5.8 cm^2 field (left), surface dose as a function of field size, normalised 2D surface dose distribution of 23.5x23 cm^2 field overlaid (right)

Conclusion The microDiamond's relative response has no significant difference in the presence of a magnetic field. This detector has proven to be useful for characterising the surface dose for the Australian MRL.

References

1. Reynolds M et. al. (2014) Dose response of selected solid state detectors in applied homogeneous transverse and longitudinal magnetic fields. Med. Phys. 41 (9), 092103.
2. O'Brien D et. al. (2018) Relative dosimetry with an MR-linac - response of ion chambers, diamond and diode detectors for off-axis, depth dose and output factor measurements. Med. Phys. 45 (2), 884–897.
3. Woodings SJ et. al. (2017) Performance of a PTW 60019 microDiamond detector in a 1.5T MRI-linac. Phys. Med. Biol. https://doi.org/10.1088/1361-6560/aaa1c6.
4. Reynolds M et. al. (2015) Response measurement for select radiation detectors in magnetic fields. Med, Phys. 42 (6), 2837–2840.

IS08 Recent development of solid state microdosimetry and its applications in particle therapy

L. Tran

The University of Wollongong

Particle therapy has many advantages over conventional photon therapy, particularly for treating deep-seated solid tumours due to its greater conformal energy deposition achieved in the form of the Bragg peak (BP). Successful treatment with protons and heavy ions depends largely on knowledge of the relative biological effectiveness (RBE) of the radiation produced by primary and secondary charged particles. The RBE prediction based on microdosimetric approach using the tissue equivalent proportional counter (TEPC) measurements in ^{12}C therapy has been reported, however large size of commercial TEPC is averaging RBE which dramatically changes close to and in a distal part of the BP that may have clinical impact. Moreover, the TEPC cannot be used in current particle therapy technique using pencil beam scanning (PBS) delivery due to pile up problems associated with high dose rate in PBS.

Based on many years of experience in development of silicon-on-insulator (SOI) microdosimeter, the Centre for Medical Radiation Physics, University of Wollongong, has successfully developed a microdosimetric probe which is based on a SOI microdosimeter with 3D micron sized sensitive volumes (SVs) mimicking dimensions of cells, known as the "Bridge" and "Mushroom" microdosimeters, to address the shortcomings of the TEPC [1, 2]. The silicon microdosimeters provide extremely high spatial resolution and were used to evaluate the RBE of 290 MeV/u ^{12}C, 180 MeV/u ^{14}N and 400 MeV/u ^{16}O ions at Heavy Ion Medical Accelerator in Chiba (HIMAC), Japan [3] as well as to measure the microdosimetric distributions of a proton pencil-beam scanning (PBS) and passive scattering system at the Massachusetts General Hospital (MGH) Francis H. Burr Proton Beam Therapy Center, USA [4]. Preliminary cell survival experiments on proton therapy beam in conjunction with SOI microdosimetry demonstrated good correlation between cell survival based RBE and predicted RBE based on measured dose average lineal energy with developed probe and microdosimetric kinetic model (MKM).

References

1. Rosenfeld A. "Novel detectors for silicon based microdosimetry, their concepts and applications", Nucl. Instrum. Methods., Phys. Res. A 809, 156–170, February 2016
2. Linh T. Tran et. al., "Thin Silicon Microdosimeter utilizing 3D MEMS Technology: Charge Collection Study and its application in mixed radiation fields", IEEE Transactions on Nuclear Science, Volume: 65, Issue: 1, 467–472, Jan. 2018.
3. Linh T. Tran, et. al., "The relative biological effectiveness for carbon, nitrogen and oxygen ion beams using passive and scanning techniques evaluated with fully 3D silicon microdosimeters" Medical Physics, 2018, https://doi.org/10.1002/mp.12874.
4. Linh T. Tran, et. al., "Characterisation of proton pencil-beam scanning using a high spatial resolution solid state microdosimeter", Medical Physics, https://doi.org/10.1002/mp.12563, 2017.

O98 Investigation of lung tumour peripheral doses using normoxic polymer gel and film dosimetry techniques

A. J. Venning[1], M. M. Chandroth[1], B. J. Chick[1], B. L. Waller[1], C. Morgan[2]

[1]Mid North Coast Cancer Institute, Port Macquarie, Australia. (Tony.venning@ncahs.health.nsw.gov.au [Presenting author]), (Mahesh.chandroth@ncahs.health.nsw.gov.au), (Brendan.chick@ncahs.health.nsw.gov.au), (Brett.waller@ncahs.health.nsw.gov.au). [2]Mid North Coast Diagnostic Imaging, Port Macquarie, Australia. (Cian.morgan@healthcareimaging.com.au)

Introduction This study describes the investigation of lung tumour peripheral doses for a range of photon energies calculated in the Monaco® TPS and delivered using an Elekta Agility™.
Method To simulate a Lung tumour, a wet sponge of similar size to human lung with a 47 mm diameter hole holding gelatine filled polyethylene terephthalate (PET) vials was CT scanned. With a water retention weight of 640 grams the HU of the sponge was equivalent to that of lung tissue. Images were exported to the Monaco TPS.

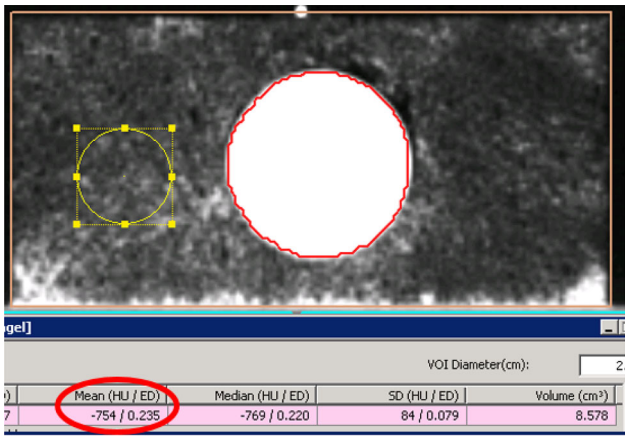

Figure 1 Sponge with gelatine filled vial.

To measure dose polymer gel dosimeters were manufactured using materials and methods described elsewhere (1), poured into vials and immersed within the sponge. A vial filled with 95% H_2O and 5% gelatine had a thin slit cut into its centre to hold a strip of EBT3 film and immersed within the sponge. Conformal arc treatment plans were generated with energies of 6MV, 6MV FFF, 10MV FFF and 15MV. Dose planes were exported for comparison with measurements. The sponge with dosimeters were then irradiated according to the treatment plan and the polymer gel dosimeters were imaged using a 1.5T MRI scanner with T_2 maps generated (2). The EBT3 films were scanned using an EPSON V850 scanner and profile comparisons between the TPS and dosimeters were performed using in-house Matlab™ code.

Results Measurements suggest that Monaco® over estimates dose in the build-up peripheral region of tumour equivalent tissue in lung for the photon energies investigated in this study.

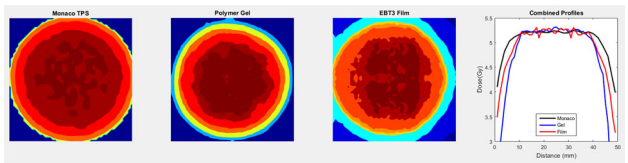

Figure 2 Profiles showing an overestimation of the Monaco TPS.

Conclusion Two independent dosimetry techniques indicate Monaco® is overestimating dose in the build-up peripheral region of tumour equivalent tissue in lung. Further investigations will be performed to fully characterise this finding including energy dependence.

References

1. Venning AJ, Hill B, Brindha S, Healy BJ, Baldock C (2005) Investigation of the PAGAT polymer gel dosimeter using magnetic resonance imaging Phys. Med. Biol. 50 3875–88
2. De Deene Y and Baldock C (2002) Optimization of multiple spin-echo sequences for 3D polymer gel dosimetry Phys. Med. Biol. 47 3117–41

O99 High resolution fibre-optic dosimetry in MRT

J. Archer, E. Li

Centre for Medical Radiation Physics, University of Wollongong, Australia. (jarcher@uow.edu.au [Presenting author]), (enbang@uow.edu.au)

Introduction Synchrotron microbeam radiation therapy (MRT) is a novel pre-clinical therapy that uses highly spatially fractionated low energy X-ray beams to target tumours, allowing doses much higher than conventional radiotherapies to be delivered. A dosimeter with a high spatial resolution is required to provide the appropriate quality assurance for MRT. We present the development of a plastic scintillator fibre optic dosimeter. The optimal one-dimensional spatial resolution of these dosimeters has been improved from 50 down to 10 μm.

Method The dosimetry probes have been tested on the Imaging and Medical Beam Line at the Australian Synchrotron. Multiple beam configurations have been tested with broadbeam X-rays with average energies between 60–90 keV, and dose rates between 200 and 2000 Gy/s. To test the probes, microbeam profiles were measured via continuous scanning, as well as broadbeam (no microbeam fractionation) depth dose profiles. These were compared with other dosimetry tools to assess accuracy.

Results The ability of these probes to resolve microbeams of width 50 mm has been demonstrated. The major limitations of these probes were identified, most notably the low-light signal resulting from the small sensitive volume, which made valley dose measurements very challenging. This was most significant with the 10 μm resolution probe, as expected. There is a dose discrepancy between the broadbeam depth dose measurements between the scintillator dosimeter and ionisation chamber at depths less than 20 mm, present for all field sizes and energies. Limitations in the data acquisition system are expected to be overcome as integration with a commercial dosimetry electrometer is in development.

Conclusion With improvements to the data acquisition, this probe design has the potential to provide a water-equivalent, inexpensive dosimetry tool for MRT.

O100 Investigating pulsed optically stimulated luminescence in beryllium oxide ceramics

A. M. C. Santos[1,2], R. Gowda[2], E. Bezak[1,3], S. Afshar V.[4]

[1]School of Physical Sciences, University of Adelaide, Adelaide, South Australia, Australia. (alexandre.santos@adelaide.edu.au [Presenting Author]), (Raghu.Gowda@sa.gov.au), (Eva.Bezak@unisa.edu.au). [2]Department of Radiation Oncology, Royal Adelaide Hospital, Adelaide, South Australia, Australia. [3]Sansom Institute for Health Research, Division of Health Sciences, University of South Australia, Adelaide, South Australia, Australia. [4]Laser Physics and Photonic Devices Laboratories, School of Engineering, University of South Australia, Australia. (Shahraam.AfsharVahid@unisa.edu.au)

Introduction One major issue with all fibre-coupled luminescence dosimetry systems is the stem effect. This is light generated by the optical fibre when it is exposed to ionising radiation. The purpose of this study is to investigate the pulsed optically stimulated luminescence (POSL) properties of a fibre-coupled beryllium oxide (BeO) dosimetry system.

Method Two fibres were used side by side, one to guide the luminescence from the BeO to a PMT, and the other used to guide the stimulation laser light to the BeO. By pulsing the laser during the irradiation, POSL readings are performed. By subtracting the count rate measured before the laser pulses from the that measured during the laser pulses, a POSL signal is obtained. The POSL is potentially independent of the stem effect. Measurements were taken with the use of a superficial x-ray unit with different detector distances to deliver varying dose-rates.

Results The POSL signal is observed to increase over time and hence the BeO is not bleached by each pulse. Therefore the POSL measured at any point in time is not only the OSL accumulated in the time between laser pulses, but also of the previous OSL with some decay due to laser stimulation. The decay is corrected using a constant decay value. The change in POSL was observed to have a linear dose-rate response, with a variation of ± 1.5% in the inverse square law corrected response. However the radioluminescence response is observed to increase as distance is increased. This is expected as more of the optical fibre is being exposed and hence the stem effect contribution is increasing.
Conclusion A POSL dosimetry system using BeO coupled to an optical fibre is investigated and the POSL from the BeO observed to have a linear dose-rate response and to be stem effect free.

O101 Characterisation of optical fibres for low energy proton beam scanning and dosimetry

J. Asp[1,2], A. Santos[3,4], S. Afshar[5,6], W. Zhang[5], E. Bezak[4,7,8]

[1]South Australian Health and Medical Research institute, Adelaide, Australia. [2]School of Engineering, University of South Australia, Australia. (johan.asp@sahmri.com [Presenting author]). [3]Department of Medical Physics, Royal Adelaide Hospital, Adelaide, Australia. (alexandre.santos@adelaide.edu.au). [4]Department of Physics, University of Adelaide, Adelaide, Australia. [5]Laser Physics and Photonic Devices, School of Engineering, University of South Australia, Australia. (Shahraam.Afshar@unisa.edu.au), (WenQi.Zhang@unisa.edu.au). [6]Institute for Photonics and Advanced Sensing, University of Adelaide, Australia. [7]Cancer Research Institute, University of South Australia, Adelaide, Australia. [8]School of Health Sciences, University of South Australia, Adelaide, Australia. (Eva.Bezak@unisa.edu.au)

Introduction The aim of this project is to develop a fibre optic based dosimetry system for proton beam monitoring. The system allows for small size dosimetry (approximately the diameter of a fibre) with a fast dose-rate measurement (0.1 s). These characteristics are ideal for the requirements necessary for real time, in-vivo dosimetry of proton beams in biological specimens or for proton beam therapy applications.
In these initial experiments, the radio luminescence (RL) generated in optical fibres exposed to proton irradiation were investigated as function of proton dose rate.
Methods Two fibres were compared: poly methyl methacrylate (PMMA) and silica. A photomultiplier tube (PMT) was used for photon counting and a spectrometer was used to analyse the optical spectrum emitted through the different types of optical fibre. Irradiations were performed with proton beam currents ranging from 0.1 to 120 nA.
Results Both fibres showed a linear response to dose rate. The PMMA fibre emitted 709 ± 31 count/s /nA and the Silica 1653 ± 31 counts/s /nA. The optical spectra differed significantly between the two fibre types. PMMA emitted light at a wavelength of 500 nm, while the silica spectrum showed two peaks; one peak at 460 nm and one peak at 650 nm. The 650 nm peak showed a linear response to proton dose rate while the 460 nm showed an over response to higher dose rates.
Conclusion These preliminary results suggest that the silica fibre could be used at lower beam currents but a band pass filter may have to be applied to isolate the linear response of the 650 nm emission. Further investigation into proton energy dependence of the fibres will be performed.

O102 Comparison of the performance of 3D automated random walks versus thresholding in the segmentation of static and gated PET images

T. Osman[1], B. McBride[2], T. Hennessy[2], S. Downes[2], A. Rosenfeld[1], A. Malaroda[1]

[1]Centre of Medical Radiation Physics, University of Wollongong, Australia. (to833@uowmail.edu.au [Presenting author]), (anatoly@uow.edu.au), (malaroda@uow.edu.au). [2]Prince of Wales Hospital, Australia. (bruce.mcbride@health.nsw.gov.au), (thomas.hennessy@health.nsw.gov.au), (simon.downes@health.nsw.gov.au)

Introduction In radiotherapy treatment planning, 4D-PET/CT allows the simultaneous visualisation of functional and anatomical information of moving lesions. Generally, radiotherapy GTVs and ITVs on PET images are delineated either manually or by setting a 40% threshold. Both these methods have shown inaccuracies. This study compared the performance of a 3D automated random walks algorithm against fixed value thresholding on static and gated PET images.
Method Static and gated 18F-FDG PET/CT images of a NEMA-IEC phantom (source-to-background ratios of 3:1, 6:1 and 9:1) were acquired on a Philips Ingenuity TF PET/CT scanner. Images were reconstructed using a clinical protocol and motion was simulated using a moving platform with 2.6cm displacement.
2D (2DARW) and 3D (3DARW) random walks algorithms, with automated seed selection inspired by [1], were developed in MATLAB-R2015a (3DARW). Their performance was compared using the Dice Coefficient (DC) against two threshold-based methods: a fixed 40% (T(40)) and an optimised (T_{opt}) threshold. T_{opt} was found as the threshold value that minimised the overall percentage difference of the lesion volumes. Gold standard volumes were defined on the CT images and comparison was carried out for the 4 largest sphere sizes (13–37 mm diameters).
Results DCs for each segmentation method, across sphere sizes and SBRs are summarised in Figure 1.

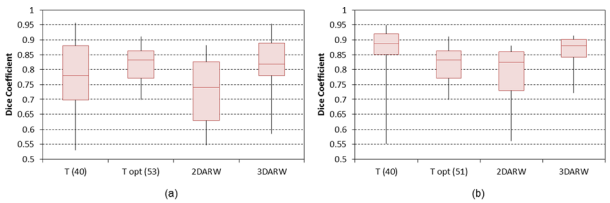

Figure 1: Dice coefficients indicating the concordance between the (a) static and (b) gated PET and CT segmentations for a fixed 40% threshold, a fixed optimum % threshold, 2DARW and 3DARW

In the static case, 3DARW and T(40) achieved the highest DC = ∼ 0.95, T_{opt}(50) had the smallest range and 75% of the 3DARW DCs were above 0.78 (Fig. 1a).

In the gated case, 3DARW DCs showed the smallest range with 75% of the values above 0.84 and T(40) had the highest DC = 0.95 (Fig. 1b).

For SBR = 3:1, static and gated cases, the T(40) was unable to segment multiple volumes, showing leakage.
Conclusion Preliminary results showed that 3DARW performs well in segmenting both static and gated PET images with DCs ranging between 0.59–0.95 (static) and 0.73–0.91 (gated). Further optimisation of the 3DARW is needed to improve performance for a wider range of lesion shape and sizes.

References

1. Stefano, A., Vitabile, S., Russo, G., Ippolito, M., Marletta, F., D'Arrigo, C., D'Urso, D., Gambino, O., Pirrone, R., Ardizzone, E., and Gilardi, M. C. A fully automatic method for biological target volume segmentation of brain metastases. International Journal of Imaging Systems and Technology, 26(1):29–37, 2016.

O103 The influence of computer-aided diagnostic software on the diagnosis of diffuse Lewy body disease using cerebral perfusion SPECT/CT imaging

A. Hull[1], K. Hickson[2], E. Bezak[1,3], M. Kitchener[2], N. Dhiantravan[2], R. Casse[2]

[1]School of Health Sciences, University of South Australia, Adelaide, Australia. (Hulaj001@mymail.unisa.edu.au [Presenting author]), (Eva.bezak@unisa.edu.au). [2]Department of Nuclear Medicine, The Queen Elizabeth Hospital, Adelaide, Australia. (Kevin.Hickson@sa.gov.au), (Rey.casse@gmail.com). [3]Department of Physics, University of Adelaide, Adelaide, Australia

Introduction Diffuse Lewy body disease (DLB) is a complex neurodegenerative disorder whose diagnosis may be assisted by cerebral perfusion single-photon emission computed tomography/computed tomography (SPECT/CT). However, the low specificity of cerebral perfusion SPECT/CT, and overlapping features of neurodegenerative disorders can impair image interpretation and diagnosis [1]. Computer-aided diagnostic software may improve image interpretation. In this study, we examined the effect of NEUROSTAT in the diagnosis of DLB by clinicians with varying years of experience. Additionally, we evaluated the cingulate island sign (CIS), a DLB biomarker, using Q-Brain.

Method Cerebral perfusion SPECT/CT data of 59 patients with suspected DLB were retrospectively retrieved from two sites and processed through NEUROSTAT. Three clinicians with varying years of experience individually interpreted the SPECT/CT data for each patient. The data was visually interpreted than re-interpreted with the addition of a NEUROSTAT-output. Following each analysis, clinicians assigned a diagnosis of not DLB, possible or probable DLB for all patients. The most senior clinician's responses determined the final clinical categorisation. The influence of NEUROSTAT was then evaluated against clinician experience. All SPECT/CT data was also processed through Q-Brain to quantify the CIS. This study received ethical approval from the SA Health and University of South Australia Human Research Ethics Committees.

Results Both the junior and middle clinician demonstrated weak correlation with the final categorisation. Compared to the NEUROSTAT-aided analysis, the junior clinician's visual analysis showed a stronger positive correlation with the final categorisation. Comparatively, the middle clinician's NEUROSTAT-aided analysis was more strongly correlated with the final categorisation compared to the visual analysis (Figure 1).

There was no clear relationship demonstrated between the CIS ratio and final clinical categorisation.

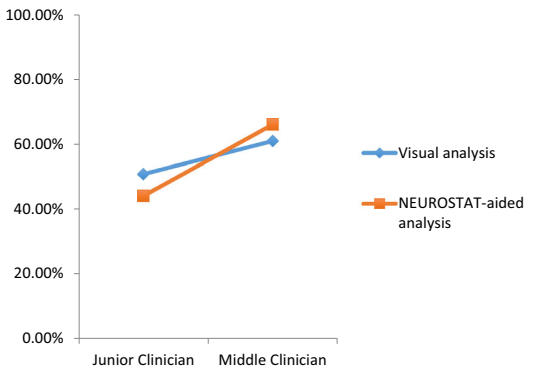

Figure 1: Comparison between the visual and NEUROSTAT-aided analyses on the percentage of agreement with the final clinical categorisation.

Conclusion NEUROSTAT may influence the diagnosis of DLB when assessing cerebral perfusion SPECT/CT studies. Larger prospective studies are required to further assess the effect of NEUROSTAT in SPECT/CT studies.

References

1. Imabayashi E, Yokoyama K, Tsukamoto T, Sone D, Sumida K, Kimura Y, Sato N, Murata M, Matsuda H (2016) The cingulate island sign within early Alzheimer's disease-specific hypoperfusion volumes of interest is useful for differentiating Alzheimer's disease from dementia with Lewy bodies. EJNMMI Res (2016) 6: 67. https://doi.org/10.1186/s13550-016-0224-5

O104 Monte Carlo simulation of the Compton camera for nuclear medical imaging

C. Z. Uche[1,2], M. Vyas[1], J. Thorogood[1], W. H. Round[3], M. Cree[3]

[1]Department of Healthcare, Unitec Institute of Technology, Auckland, New Zealand. (cuche@unitec.ac.nz [Presenting author]), (mvyas2@unitec.ac.nz), (jthorogood@unitec.ac.nz). [2]Oncology Department, Waikato District Health Board, Hamilton, New Zealand. [3]School of Engineering, University of Waikato, Hamilton, New Zealand. (howell.round@gmail.com), (michael.cree@waikato.ac.nz)

Introduction Single Photon Emission Computed Tomography (SPECT) has been used in nuclear medical imaging for several decades. The technique involves the use of a gamma camera which traditionally exhibits limitations arising from poor detection efficiency. In addition, gamma cameras do not foster the use of a wide range of radioisotope energies available. Consequently, the viability of the Compton camera to overcome these limitations has been investigated.

Method The GEANT4 simulation toolkit was used to study the behaviour of two Compton camera prototypes for SPECT imaging. Simulations were performed for silicon and cadmium zinc telluride based Compton cameras for breast and brain imaging. In order to study a challenging detection case, the volumes of two simulated breast tumours were chosen to be 0.65 mL, and embedded in the medial region of the breast. For the brain imaging, the multitracing capability of the camera was studied, with imaging performed parallel to the orbitomeatal line of the brain.

Results The results suggest that the Compton camera would visualize small breast lesions of about 0.65 mL volume, placed at the medial region of an average compressed human breast. Although brain imaging using the Compton camera also seemed promising, analyses suggest however that beyond a depth separation of 2 cm between two lesions in a brain phantom, there may be a need to rotate the camera around the human head for efficient brain imaging.

Conclusion It is the opinion of the authors that with further work, the Compton camera could compete favourably with the gamma camera in small lesions imaging where resolution is compromised due to the high septal penetrations.

O105 Monte Carlo modelling of HPGe detector efficiency for accurate activity measurement

C. D. Pain

Department of Molecular Imaging and Therapy, Austin Health, VIC. (cameron.pain@austin.org.au)

Introduction The following work aims to characterise the efficiency of an HPGe detector over a spectral range applicable to nuclear medicine isotopes for activity measurement of PET isotopes produced on site. Accurate measurement will allow for validation of dose calibrator gain settings of PET isotopes such as which have been reported to have significantly different gain settings than those specified by manufacturers [1]. Presented is a Geant4 model of an HPGe detector with calculated efficiency values compared to efficiency values measured using a standard source.
Method The efficiency of a Canberra^{TM} BE2020 HPGe was measured using a multi-isotope calibration source with activity uncertainties specified below 4% at 95% confidence interval (95% CI) aligned axially with the detector crystal at different source-detector separations. A Geant4 model of a generic HPGe detector was created using specifications provided by the manufacturer and information found in the literature [2,3]. The model was adjusted to maximise the conformance with measured efficiencies. The optimised model was ran with primaries for each photopeak in the calibration source.
Results Figure 1 shows the ratio of calculated efficiency and measured efficiency at each photopeak energy with error bars showing the 95% CI of the activity of the source. The 95% CI of the relative difference between modelled and measured efficiencies is 2.50%.

Figure1: Ratio of modelled to measured efficiencies for each photopeak. Error bars represent 95% CI of calibrated sources.

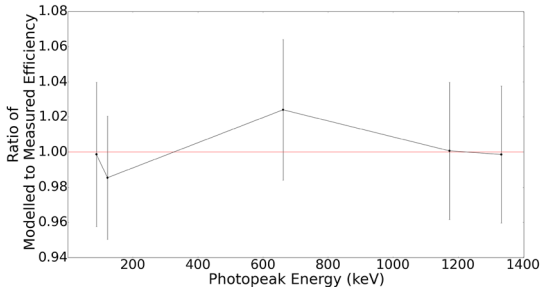

Conclusions The model produced efficiency values within 2.5% of the measured values at a 95% CI allowing for potential activity measurements under 5% at 95%CI. Future work will involve running the simulation for syringe geometries, more calibration photopeaks, testing the method with another independently calibrated NIST quality source and measuring the activity of different PET isotopes and looking at discrepancies in dose calibrator gain settings.

References

1. Beattie. B. J, Pentlow. K. S, O'Donoghue. J, Humm. J. L, 2014, A Recommendation for Revised Dose Calibrator Measurement Procedures for 89r and 124I, PLos One, e106868. https://doi.org/10.1371/journal.pone.0106868
2. Chuong. H. D, Thanh. T. T, Trang. L. T, Nguyen. V. H, Tao. C. V, 2016, Estimating Thickness of the inner dead-layer of n-type HPGe detector, Applied Radiation and Isotopes, Vol.116, pp. 174–177
3. Dryak. P, Kovar. P, 2006, Experimental and MC Determination of HPGe Detector Efficiency in the 40–2754 keV Energy Range for Measuring Point Source Geometry with the Source-to-Detector Distance of 25 cm, Applied Radiation and Isotopes, Vol.64, pp.1346–1349

O106 Optimisation of administered activities in PET

G. Rouvalis[1], J. Crocker[2], Z. Brady[2], R. Franich[1]

[1]RMIT University, Melbourne, Australia. (s3667823@student.rmit.edu.au [Presenting author]), (rick.franich@rmit.edu.au). [2]Alfred Health, Melbourne, Australia. (J.Crocker@alfred.org.au), (Z.Brady@alfred.org.au)

Introduction It has been common practice in PET imaging to deliver a fixed administered activity or employ a patient weight scaling, such as at The Alfred where weight scaling is used for full body ^{18}F-FDG PET scans. Opportunity exists for a more individualised dose administration protocol that will improve image quality and reduce dose.
Method Different methods for determining administered activity were reviewed (Figure 1). The current administered activities at The Alfred were compared to literature and the recently published Australia Diagnostic Reference Levels. To investigate the effects of reduced dose on patient scans, scans of lower administered activities were simulated through retrospective reconstruction of list-mode data. Various image quality metrics including the signal to noise ratio in the liver were used to compare images. The reconstructed image sets were also scored by Nuclear Medicine Physicians to assess diagnostic acceptability.
Results The current weight-based scaling of administered activity employed by Alfred Health does not adequately account for the changes in image quality with varying body habitus. It is seen (Figure 1) that The Alfred's weight-based model of 4 MBq/kg is below the Australian reference level of 2.5 kg $\times$ + 125 MBq for patients below 84 kg. Few locations appear to use a fixed activity for all patients, while most apply a weight-based scaling. Groot et al. noted that a quadratic relationship between administered activity and patient weight yielded lower doses required for imaging [5], while Wickham et al. has incorporated height and gender, as well weight in an optimised administering protocol [6].
Conclusion The current model of weight-based administered activity scaling in PET employed by The Alfred could be altered to incorporate greater patient factor specificity. Incorporating additional patient specific factors allows a more individualised dose to be determined.

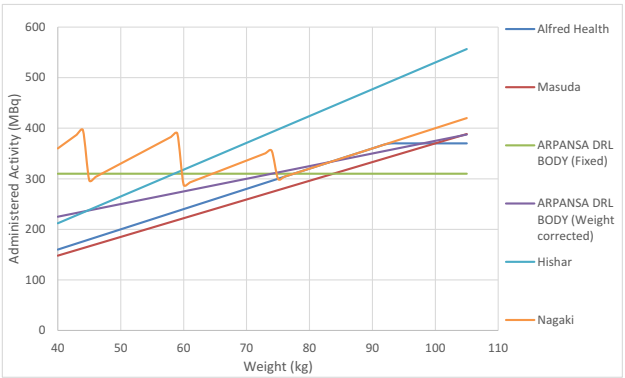

References

1. Hishar, H., Salasiah M., Fathinul Fikri A. S., & Nordin, A. J. (2015) Dose Optimisation of ^{18}F-Flurodeoxyglucose for Whole Body PET Oncology Examination in CDNI of UPM. Centre for Diagnostic Nuclear Imaging, University Putra Malaysia, 23(2), 187–192
2. Masuda, Y., Kondo C., Matsuo Y., Uetani, M., & Kusakabe, K. (2009). Comparison of Imaging Protocols for ^{18}F-FDG PET/CT in Overweight Patients: Optimizing Scan Duration Versus Administered Dose. The Journal of Nuclear Medicine, 50(6), 844–848

3. Nagaki, A., Onoguchi, M. and Matsutomo, N. (2011). Patient Weight-Based Acquisition Protocols to Optimize18F-FDG PET/CT Image Quality. Journal of Nuclear Medicine Technology, 39(2), pp.72–76.
4. ARPANSA. (2018). Nuclear medicine DRL tables. [online] Available at: https://www.arpansa.gov.au/research/surveys/national-diagnostic-reference-level-service-drls/nuclear-medicine-diagnostic [Accessed 22 Apr. 2018].
5. de Groot, E., Post, N., Boellaard, R., Wagenaar, N., Willemsen, A., & van Dalen, J. (2013). Optimized dose regimen for whole-body FDG-PET imaging. EJNMMI Research, 3(1), 63.
6. Wickham, F., McMeekin, H., Burniston, M., McCool, D., Pencharz, D., Skillen, A., & Wagner, T. (2017). Patient-specific optimisation of administered activity and acquisition times for 18F-FDG PET imaging. EJNMMI Research, 7(1).

KS10 Novel cancer biomarkers

L. Marcu

The University of Oradea

The latest leitmotif in oncology is personalised therapy and there is no doubt that the scientific community is working hard towards this aim. The main goal of radiotherapy is to optimise the therapeutic ratio by maximising tumour control and minimising normal tissue toxicity. Owing to the identification of various tumour markers and the possibility of their specific in vivo targeting the therapeutic ratio will increase even further. Tumour hypoxia, angiogenesis, proliferation, and the proportion of cancer stem cells are some of the culprits for treatment failure in oncology. Therefore, their identification and targeting plays a crucial role for optimum outcome. Furthermore, biomarkers are ideal candidates for the development of new radioconjugates and various drugs, to further progress the ever-expanding area of targeted therapies. Current research goes beyond generic study of these factors, investigating the arsenal of molecular markers that are specific for hypoxia, proliferation and cancer stem cells.

The aim of this talk is to discuss some of the novel cancer biomarkers and their corresponding imaging techniques. Biomarkers for generic tumour characteristics and molecular pathways (oxygenation status, stemness, growth factors, apoptosis, immune response) as well as tumour-specific marker developments will be presented. With the growing field of biomarker imaging, the need arises for image quantification and standardisation, key prerequisites for accurate treatment response assessment.

O107 Cancer stem cell diversity and response to radiation: the role of the human papillomavirus in head and neck cancers.

P. Reid[1,2], L. G. Marcu[1,3], I. Olver[2], A. Staudacher[4,5], L. Moghaddasi[6,7], E. Bezak[1,2,6]

[1]School of Health Sciences, University of South Australia, Adelaide, Australia. (Paul.reid@mymail.unisa.edu.au [Presenting author]), (loredana@marcunet.com), (Eva.Bezak@unisa.edu.au). [2]Cancer Research Institute, University of South Australia, Adelaide, Australia. ((Ian.Olver@unisa.edu.au)). [3]Faculty of Science, University of Oradea, Oradea 410087, Romania. [4]Translational Oncology Laboratory, Centre for Cancer Biology, SA Pathology and University of South Australia, Adelaide, Australia. [5]School of Medicine, University of Adelaide, Adelaide, Australia. (alex.staudacher@health.sa.gov.au). [6]Department of Physical Sciences, University of Adelaide, Adelaide, Australia. [7]Department of Medical Physics, Adelaide Radiotherapy Centre, Genesis Cancer Care, Adelaide, Australia. (Leyla.Moghaddasi@adradcentre.com.au)

Introduction The role played by cancer stem cells (CSCs) is fundamental to tumour progression, metastases and recurrence. These are the most treatment resistant of tumour cells and are irresponsive to therapy, accelerating their replication and tumour repopulation. The human papillomavirus (HPV) has emerged as a discrete aetiology in head and neck cancers (HNC). They demonstrate consistently better responses to radiotherapy initiating several clinical trials to de-escalate treatment. This study investigates in vitro differences in CSC responses to radiation in terms of their HPV aetiology.
Method A collection of 6 HNC cell lines were investigated. UM-SCC-47, UPCI-SCC-090 and UPCI-SCC-154 are HPV+ and UM-SCC-1, UM-SCC-17a and UM-SCC-22a are HPV-. Cells were irradiated in T75 flasks with 4 Gy using a RS2000 irradiator at 160 kVp and 25 mA. Flasks were encased in solid water (RW3) to achieve electronic equilibrium at the cell layer. Sham-irradiated flasks were used as controls. CSC proportions of cell populations were measured at 24, 48 and 72 h, and again at 14 days post irradiation. CSCs were identified by putative cellular markers CD44 and aldehyde dehydrogenase (ALDH), using flow cytometry.
Results Triplicate analysis of non-irradiated UM-SCC-47 cell cultures showed a mean population of CD44+/ALDH+ cells to be 2.87% ± 0.219, 5-fold that of the UM-SCC-1 population which was 0.57% ± 0.077. UM-SCC-47 and UM-SCC-1 showed increased ALDH+/CD44+ proportions of population following 4 Gy irradiation. The proportional increase for UM-SCC-47 was 3 to 4 times the control within 72 hrs post irradiation. After 10 days these cultures no longer presented significant differences in CSC population against the control. UM-SCC-1 showed the most significant increase in CSC proportion 24 hrs post irradiation and a persisting elevation in CSCs 10 days after irradiation.
Conclusion CSCs display significant heterogeneity between cell lines warranting investigation of the effect aetiology has on intrinsic population numbers and treatment responsiveness.

O108 Treatment response biomarker development: quantitative assessment of inter-scanner variability in multiparametric MRI

Y. F. Wang[1], G. Liney[2], R. Rai[3], L. Holloway[2], H. M. Reynolds[4], A. Haworth[1]

[1]Institute of Medical Physics, University of Sydney, Australia. (Ywan3672@uni.sydney.edu.au [Presenting author]), (Annette.Haworth@sydney.edu.au). [2]Ingham Institute for Applied Medical Research, Liverpool, Australia. (Gary.Liney@health.nsw.gov.au), (Lois.Holloway@health.nsw.gov.au). [3]Liverpool and Macarthur Cancer Therapy Centre, Liverpool Hospital, Sydney, Australia. (Robba.Rai@health.nsw.gov.au). [4]Department of Physical Sciences, Peter MacCallum Cancer Centre, Melbourne, Australia. (Hayley.Reynolds@petermac.org)

Introduction Biomarkers are used in the diagnosis, treatment decision making, and post-treatment monitoring of prostate cancer (PCa). Treatment response for PCa is typically measured by changes of prostate specific antigen (PSA) levels in the blood, with biochemical failure defined as either a number of consecutive rises in the PSA level, or rising above a certain threshold [1]. This method lacks sensitivity and specificity, and is unable to distinguish between benign rises of PSA, local recurrence and distant metastases. Quantitative

imaging using multiparametric MRI (mpMRI) has shown promise for providing potential biomarkers for PCa diagnosis and treatment response. However, inter-/intra-MRI scanner variability contribute to uncertainties in defining the parameters used for biomarker development. The goal of this study was to investigate inter-scanner variability in mpMRI parameters including apparent diffusion coefficient (ADC), T1, T2, and R2* using an in-house developed multi-compartment phantom.

Method The prototype multi-compartment phantom included regions of ethanol, gelatine, and gadolinium-doped (Gd) water to simulate a suitable range of in vivo tissue parameters. The phantom was scanned on three 3T MRI scanners (two Skyra and one Prisma, Siemens) to generate ADC, T1, T2, and R2* maps using standard clinical sequences. The parametric values for each sample were extracted from a region of interest and the coefficient of variance (CV) was calculated to evaluate the variability of the values across the scanners.

Results ADC values had CVs from 0.1–17.9%. T1 and T2 values had CVs from 2.2–25.4% and 0.3–16.8% respectively, with the largest CV in the ethanol compartment. R2* was the least reproducible, with CVs from 14.1–67.6%.

Conclusion Inter-scanner reproducibility of mpMRI parameters across three clinical scanners were assessed with an inhouse developed phantom. Results show that the highest variability was in R2* measurements and lowest variability in T2 measurements. Future work will focus on quantifying the longitudinal variability of mpMRI parameters between centres.

Reference

1. Roach M, Hanks G, Thames H, Schellhammer P, Shipley WU, Sokol GH, Sandler H (2006) Defining biochemical failure following radiotherapy with or without hormonal therapy in men with clinically localized prostate cancer: Recommendations of the RTOG-ASTRO Phoenix Consensus Conference. International Journal of Radiation Oncology*Biology*Physics 65 (4):965–974. https://doi.org/10.1016/j.ijrobp.2006.04.029

Acknowledgements This project was supported by NHMRC grant APP1126955.

O109 Correlations between utilisation of CT or MR for prostate contouring and recorded patient outcome, a retrospective analysis incorporating the RADAR dataset

D. Roach[1,2], J. Dowling[1,3,4,5], A. Kennedy[6], M. Jameson[1,2,3,7], P. Greer[5,8], M. Ebert[3,6,9], L. Holloway[1,2,7,10]

[1]Faculty of Medicine, University of New South Wales, Sydney, Australia. (d.roach@student.unsw.edu.au [Presenting author]), (Jason.Dowling@csiro.au), (Michael.Jameson@sswahs.nsw.gov.au), (Lois.Holloway@sswahs.nsw.gov.au). [2]Ingham Institute for Applied Medical Research, Sydney, Australia. [3]Centre for Medical Radiation Physics, University of Wollongong, Wollongong, Australia. (Martin.Ebert@health.wa.gov.au). [4]Australian e-Health Research Centre, CSIRO, Royal Brisbane Hospital, Australia. [5]School of Mathematical and Physical Sciences, University of Newcastle, Newcastle, Australia. (peter.greer@newcastle.edu.au). [6]Radiation Oncology, Sir Charles Gairdner Hospital, Nedlands, Australia. (Angel.Kennedy@health.ea.gov.au). [7]Department of Radiation Oncology, Liverpool and Macarthur Cancer Therapy Centres, NSW, Australia. [8]Calvary Mater Newcastle Hospital, Newcastle, Australia. [9]School of Physics and Astrophysics, Faculty of Science, University of Western Australia, Crawley, Australia. [10]Centre for Medical Radiation Physics, University of Wollongong, Wollongong, Australia

Introduction Prostate radiotherapy requires CTV contouring on CT for treatment planning, however MR scans are often incorporated to provide clearer soft-tissue definition [1, 2]. No study has shown utilisation of MR leads to an improvement in patient treatment outcome or reduction in toxicity. Retrospective analysis of the RADAR dataset provides an opportunity to investigate relationships between contouring modality and recorded patient outcome [3].

Method A prostate atlas consisting of five patients was constructed [4], with thirteen observers contouring CTV on both CT and co-registered T2-weighted MR scans. Atlas scans were non-rigidly registered to 750 RADAR patients, with contours propagated. CTV probability maps detailing inter-observer contouring variation were thresholded at multiple percentages, with similarity between these and original RADAR CTVs calculated using Dice Similarity Coefficient (DSC), 95th percentile Hausdorff Distance, and Volume Similarity. Correlations between differences in CT and MR contouring metrics, and recorded rectal toxicities were assessed using Wilcoxon signed-rank analysis ($p < 0.05$ significant).

Results Preliminary investigations of 50 RADAR patients have been completed. Volumes of CT (30.3 ± 10.0 cc) and MR (21.5 ± 7.2 cc) CTVs were significantly smaller than original RADAR CTVs (54.8 ± 28.5, Figure 1). This resulted in poor overlap (DSC = 0.67, 0.55 respectively). Significance levels for correlations are shown in figure 2, with no correlations initially found to be statistically significant.

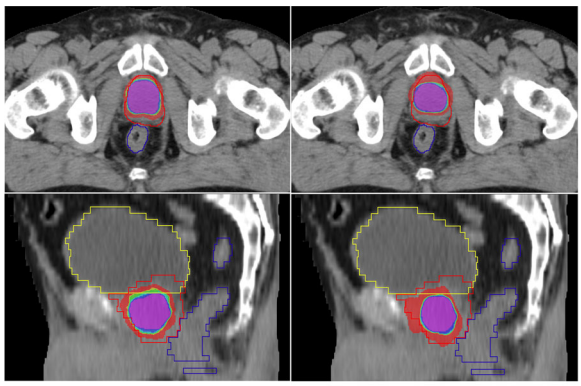

Figure 1: Sample RADAR patient with CT (left) and MR (right) CTV probability maps, along with original RADAR contours.

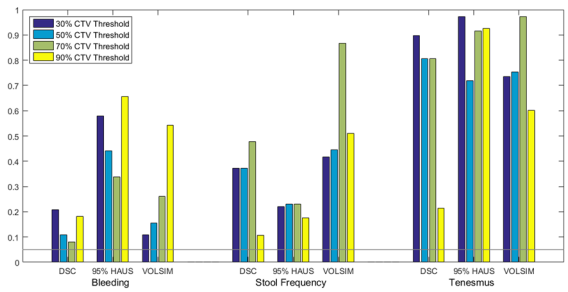

Figure 2: Significance of correlations between differences between CT and MR CTV contours and multiple rectal toxicities ≥ grade 2.

Conclusion CTV probability maps can be constructed to retrospectively analyse the RADAR dataset. Further investigation will include correlating CTV contouring variations with overall survival and

locoregional control, and dose to multiple pelvic structures additionally contoured within the atlas.

Acknowledgements Funding provided through NHMRC project grant (1077788).

References

1. Debois, M., et al., *The contribution of magnetic resonance imaging to the three-dimensional treatment planning of localized prostate cancer.* International Journal of Radiation Oncology* Biology* Physics, 1999. **45**(4): p. 857–865.
2. Rasch, C., et al., *Definition of the prostate in CT and MRI: a multi-observer study.* International Journal of Radiation Oncology* Biology* Physics, 1999. **43**(1): p. 57–66.
3. Trans-Tasman Radiation Oncology Group (TROG), *RADAR Trial - Randomised Androgen Deprivation and Radiotherapy*. 2005.
4. Kennedy, A.M., et al., *Cluster Based selection of CT exemplars from a clinical dataset for inter-patient registration and dose mapping*, in *International Conference on the use of Computers in Radiation Therapy*. 2016: London.

O110 Evaluating delivery of partial IMRT plans for free-breathing breast treatments

S. Alzaidi[1], S. Islam[2], R. Hill[1,2]

[1]Department of Radiation Oncology, Chris O'Brien Lifehouse, Sydney, Australia. (samara.alzaidi@gmail.com [Presenting author]). [2]Institute of Medical Physics, School of Physics, The University of Sydney, Australia

Introduction Breast cancer treatments at Chris O'Brien Lifehouse are planned using Hybrid IMRT technique, with 70% tangent fields and 30% IMRT fields. Deep inspiration breath hold (DIBH) technique is considered for the treatment of left-breast cancer patients to minimize dose to the heart. However, right-breast treatments are delivered with free- breathing. For IMRT portion of the treatment, planning target volume (PTV) dose may vary due to the movement during free-breathing. As IMRT delivers optimized high dose to the target volume, determination of the dose variation due to breathing movement during treatment is important to ensure the delivery of the correct dose to the desired volume.

Method In this study, a number of hybrid IMRT breast treatment plans treated with free- breathing were re-calculated incorporating a 3D shift for the IMRT fields portion. The 3D shifts were evaluated using 4DCT scans. The new plans were recalculated with two scenarios:

- full range of the 3D shifts, assuming that the 3DCT scan was captured at the most inhalation/exhalation points of the breathing
- half range of the 3D shifts, assuming that the 3DCT scan was captured in the middle of the breathing cycle

Results The Dose Volume Histogram (DVH) for the new plans were evaluated and compared to the original plans. The mean, maximum and minimum dose to CTV, PTV, boost PTV, and right lungs are considered. Initial results indicate that variations in dose delivery of IMRT fields in hybrid IMRT treatments is affected by the level of modulation complexity of the IMRT dose fluence.

Conclusion It is essential to understand the effect of patient breathing movement during delivery of breast IMRT fields. A range of IMRT fields with different levels of dose fleunce modulation complexities need to be investigated further.

O111 Supraclavicular junction dose for breast and chest-wall patients with and without deep inspiration breath hold (DIBH): an in-vivo dosimetry study

E. R. Claridge Mackonis[1], R. P. Estoesta[1], S Carroll[2]

[1]Department of Radiation Oncology, Chris O'Brien Lifehouse, NSW, Australia. (elizabeth.mackonis@lh.org.au [Presenting author]), (patrick.estoesta@lh.org.au). [2]Radiation Oncology Unit, Northern Sydney Cancer Centre, NSW, Australia. (susan.carroll@health.nsw.gov.au)

Introduction Aiming to reduce cardiac dose, and the associated major coronary events [1], deep inspiration depth-hold (DIBH) is becoming the standard of care for patients receiving radiotherapy for left-sided breast cancer. However, the technique is not universally adopted for patients receiving nodal irradiation, with most DIBH studies excluding these patients [2,3]. In this study, we use in-vivo dosimetry to assess the dose to the junction region of both DIBH and free-breathing patients.

Method GafChromic^{TM} EBT3 was used to measure the dose to the supraclavicular junction region over 3 treatment fractions for 19 patients. The mean doses for each patient and variability of the dose to the junction region were evaluated for both DIBH and free-breathing patients.

Results The results for each patient are shown in Figure 1. They show that the variation in dose is higher for the DIBH patients, however the average junction dose between the DIBH and free-breathing cohorts was not significantly different ($p > 0.05$).

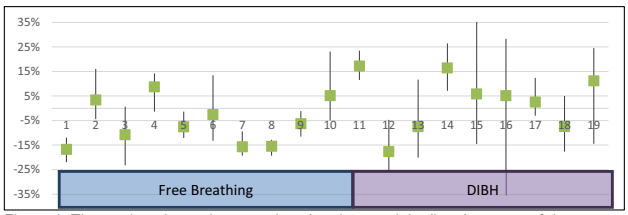

Figure 1: The marker shows the mean junction dose and the line the range of doses.

Conclusion This study shows that the mean junction dose is not compromised by the use of the DIBH technique. Concern about the additional variability should be weighed against the proven increased risks associated with cardiac dose. This in-vivo study could easily be replicated by centres implemented DIBH and wanting to verify the junction dosimetry.

References

1. Darby SC, McGale P, Taylor CW, Peto R (2005) Long-term mortality from heart disease and lung cancer after radiotherapy for early breast cancer: prospective cohort study of about 300,000 women in US SEER cancer registries. Lancet Oncol 6 (8):557–565. https://doi.org/10.1016/s1470-2045(05)70251-5
2. Smyth LM, Knight KA, Aarons YK, Wasiak J (2015) The cardiac dose-sparing benefits of deep inspiration breath-hold in left breast irradiation: a systematic review. J Med Radiat Sci 62 (1):66–73. https://doi.org/10.1002/jmrs.89
3. Latty D, Stuart KE, Wang W, Ahern V (2015) Review of deep inspiration breath-hold techniques for the treatment of breast cancer. J Med Radiat Sci 62 (1):74–81. https://doi.org/10.1002/jmrs.96

O112 Optimizing the use of EPIgray in-vivo dose verification for 3DCRT breast treatments

A. Rajasekar[1], A. Moggre[1], A. T. Cousins[1], S. Marsh[2]

[1]Medical Physics and Bioengineering Department, Canterbury District Health Board, NZ. (abinaya.rajasekar@cdhb.health.nz [Presenting author]), (alicia.moggre@cdhb.health.nz), (andrew.cousins@cdhb.health.nz). [2]Department of Physics and Astronomy, University of Canterbury, NZ. (steven.marsh@canterbury.ac.nz)

Introduction EPIgray is an in-vivo dosimetry system that uses linac-EPID acquired images to reconstruct in-vivo doses. EPIgray and TPS doses are compared for treatment verification. CDHB implements an investigation tolerance of % dose difference (DD) between EPIgray and TPS doses. Current tolerance results in false positives and false negatives. EPIgray implementation is improved with post-measurement processing of the EPIgray data, leading to more accurate treatment verification. In an ongoing retrospective study we have investigated the role of post-processing in EPIgray, and are in the process of verifying these results with a phantom study.

Method 249 treatment fields of breast patients treated using EPIgray were retrospectively analysed for impact of patient positioning offsets on DD. Additionally, a TPS-based study has considered the doses received by organs-at-risk and the target in response to offsets. The phantom study aims to validate these results with physical measurements. Breast phantoms incorporating lung inserts and the ability to include ion-chamber and film at various locations have been designed. Phantoms are setup at multiple treatment positions (intentional offsets of known magnitude) to allow comparisons between TPS-planned, EPIgray-calculated and measured doses.

Results Retrospective analysis of patient positioning offsets on treatment revealed that there are differences in EPIgray doses that arises from setup-error. Breast size appears to be a contributing factor. Initial DD for small, medium and large-breasts are 3.02.0%, 3.02.1% and 2.31.6% respectively. EPIgray correctional analysis on small-breasts improved the DD by an average of 1.0%. Corresponding offsets applied to treatment plans in TPS have found the impacts of positional errors on dose to target and organs-at-risk to be considerable. Initial results from the ongoing phantom study support these results.

Conclusion Results of this study will allow for the use of EPIgray to highlight instances where patient positioning errors on treatment are outside an acceptable tolerance for dosimetric accuracy of breast treatments.

O113 First implementation results of EPID-based in-vivo dosimetry using EPIGray®

R. A. Day, R. J. W. Louwe, D. B. Paterson, L. Greig

Wellington Blood and Cancer Centre, Wellington, New Zealand. (rebecca.day@ccdhb.org.nz [Presenting author]), (rob.louwe@ccdhb.org.nz), (dean.paterson@ccdhb.org.nz), (lynne.greig@ccdhb.org.nz)

Introduction The EPIgray® EPID dosimetry package (DOSIsoft, Paris, France) for EPID in-vivo dosimetry (IVD) has been commissioned at Wellington Hospital with the main aim to prevent major radiation incidents. This package enables reconstruction of the dose delivered to the patient at one or more points of interest.

Method A three month clinical pilot study was used to develop the IVD workflow, assess limitations of the system, acquire a dataset of results to establish tolerance levels, and develop a procedure for out-of-tolerance results before full clinical implementation. IVD results were collected for the first three treatment fractions of: Low complexity single and parallel opposed field treatments, VMAT and SRT brain, and lung SBRT.

Results The average IVD deviation at the TPS reference point was $0.2 \pm 3.4\%$ (1 S.D.) and $-0.3 \pm 1.4\%$ (1 S.D.) for low complexity treatments and VMAT Brain, respectively, which compares well with literature [1–4]. Out-of-tolerance results were traced to various causes including patient positioning issues, moving gas and limitations of the EPIGray dose reconstruction model for both small fields and inhomogeneous media. These limitations resulted in systematic IVD deviations of approximately + 5% for SRT Brain, and larger than + 10% for lung SBRT

Table 1 Average percentage IVD deviation (± 1 SD) observed during the clinical pilot study. Reference points are the points created during treatment planning while auto-points are the 50 points automatically generated by EPIGray in the high dose region for each treatment plan.

Patient group		Number of plans measured	Average deviation per beam and per fraction (%) for reference points	Average deviation per fraction (%) for auto-points
Low complexity		109	+0.2 ± 3.4	+1.1 ± 2.8
Brain	VMAT	6	-0.3 ± 1.4	-0.5 ± 0.7
	SRT	4	+3.1 ± 1.3	+6.2 ± 0.6
Lung SBRT		3	+9.7 ± 3.2	+14.5 ± 3.6

Figure 1 Histogram of observed IVD deviations for at the TPS reference points during low complexity treatments

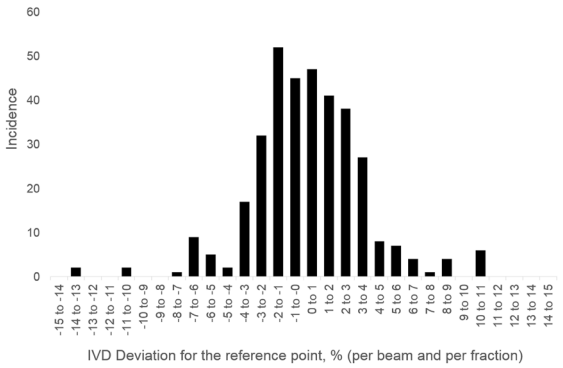

Conclusions EPIgray IVD was found to be suitable for use with low complexity and brain treatments and it is now routinely applied during the first treatment fraction for these indications. Two tolerances are employed: a lower site-dependent action level (5–10%) triggering further IVD measurements and an investigation to be completed before fraction 4; and a 10% action level triggering immediate investigation prior to fraction 2. A comprehensive set of guidelines to streamline investigation of out-of-tolerance results was formulated. Limitations of the current EPIgray dose reconstruction model prevented implementation of IVD for lung SBRT. Further implementation for other treatment indications using subsequent clinical pilot studies is now being conducted.

References

1. Celi S, Costa E, Wessels C, Mazal A, Fourquet A, Francois P (2016) EPID based in vivo dosimetry system: clinical experience and results. Journal of Applied Clinical Medical Physics, 17: 3
2. Francois P, Boissard P, Berger L, Mazal A (2011) In vivo dose verification from back projection of a transit dose measurement on the central axis of photon beams. Physica Medica, 27:1–10
3. Camilleri J, Mazurier J, Franck D, Dudouet P, Latorzeff I, Franceries X (2014) Clinical results of an EPID-based in-vivo dosimetry method for pelvic cancers treated by intensity-modulated radiation therapy. Physica Medica. 30:690–695

4. Ricketts K, Navarro C, Lane K, Moran M, Blowfield C, Kaur U, Cotton G, Tomala D, Lord C, Jones J, Adeyemi A (2016) Implementation and evaluation of a transit dosimetry system for treatment verification. Physica Medica, 32:671–680

O114 Development of an 'in-house' Varian log file analysis tool for IMRT/VMAT patient specific QA

M. Douglass, M Jennings

Department of Medical Physics, Royal Adelaide Hospital, Adelaide, South Australia. (mdouglass@adelaide.edu.au [Presenting author]), (Matthew.jennings2@sa.gov.au)

Introduction It is a requirement in Australia that the accuracy of each modulated radiotherapy patient plan be verified. This traditionally involves measurements of planar or reconstructed 3D dose distributions using a variety of commercial detectors. The quality assurance requirements for the increasing numbers of intensity modulated patient treatments makes such labour-intensive procedures time prohibitive.
Method An efficient patient specific QA workflow has been implemented at the Royal Adelaide Hospital. The workflow is a two-step process. Firstly, a secondary 3-D, dosimetric calculation of the plan on the patient's dataset is performed using an independently commissioned treatment planning system. Secondly, an analysis of the machine log files created during the delivery of the patient plan on a Varian (Varian Medical Systems, Palo Alto, CA) Linac is performed. An 'in-house' software written in python and utilising the python toolkit PyLinac [1] has been developed to batch analyse the log files from the treatment plan delivery and compare against the expected DICOM plan parameters. This is the focus of the current work.
Results By comparing the results in the machine log files with the expected plan parameters from DICOM plan files, subtle differences in plan delivery have been identified between Trilogy and TrueBeam model linear accelerators. This is partially due to the well documented "Overshoot" effect of Varian Trilogy and Clinac linear accelerators MLC controllers.
The customisable nature of the software allows the user to collect and analyse long term statistics of linac performance. This software could potentially be made open source to allow interdepartmental collaboration to further expand its capabilities.
Conclusion An efficient departmental workflow for patient specific QA has been developed, tested and implemented in the current work.

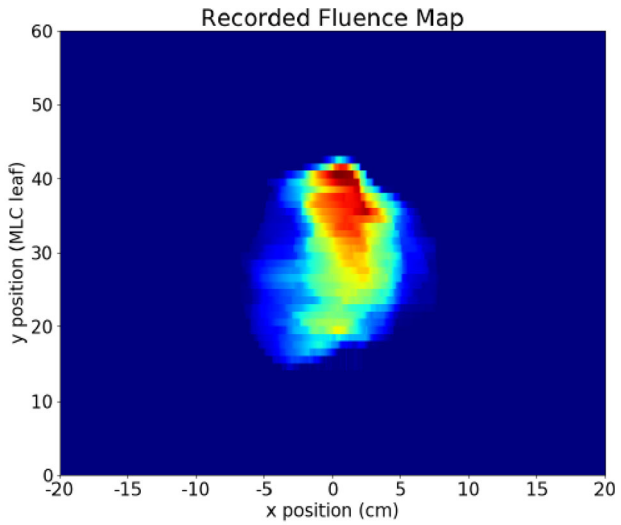

Figure 1. The predicted fluence map from a VMAT treatment delivery

Reference

1. James Kerns: Toolkit repository: //github.com/jrkerns/pylinac

O115 Verification of a 4D transperineal ultrasound target localisation system for intrafraction prostate motion monitoring in external beam radiotherapy

S. J. Gibson[1,2], S. Penfold[1,3], L. Fourie[1,2]

[1]Department of Physics, University of Adelaide, SA. (stephen.gibson@health.qld.gov.au [Presenting author]), (scott.penfold@adelaide.edu.au), (louis.fourie@health.qld.gov.au).
[2]Medical Physics Department, The Townsville Hospital, QLD.
[3]Department of Medical Physics, Royal Adelaide Hospital, SA

Introduction Lachaine and Falco introduced the Clarity Autoscan 4D prostate motion management system in 2013 [1]. A 1D ultrasound array is mechanically swept in the pseudo-sagittal plane. The resulting volume is reconstructed multiple times per second allowing for frequent updating of the target position relative to a pre-fraction reference scan.
The purpose of this work was to verify the target positions reported by the Clarity Autoscan system compared to known target positions.
Method A prostate analogue was mounted to the scanning mechanism of a PTW MP3-XS scanning water tank. The Clarity probe was positioned externally against the wall of the scanning tank in the treatment orientation. The scanning mechanism was programmed to make in-plane, cross-plane and diagonal 'profiles' ranging approximately ± 30 mm from the isocentre. Seven sets of four 'profiles' were acquired between ± 30 mm in the vertical direction.
A bi-layer 3D refraction correction algorithm was derived to account for refraction caused by differences between the speed of sound in both PMMA and water from the speed of sound in soft tissue assumed by the system.
Results Without refraction correction the reported positions differed from the programmed positions by up to 9.3 ± 0.1 mm. Refraction correction reduced this to a maximum of 3.4 ± 0.1 mm, and generally well within ± 2 mm. The worst results were at the peripheries and near to the PMMA where the effect of the refraction is exaggerated. Here the prostate analogue images were visibly distorted which likely will have affected the accuracy of the Clarity centroid position calculation.
Conclusion The target positions reported by the Elekta Clarity Autoscan system can potentially be validated using a programmable scanning water tank by employing a refraction correction. Further improvement might be achieved by using a smaller target phantom to reduce the effect of the refraction-induced distortion on the Clarity centroid calculation.

References

1. Lachaine M, Falco T (2013) Intrafractional prostate motion management with the clarity autoscan system. Medical Physics International 1:72–80.

O116 The first real-time implementation of markerless lung tumour tracking on a standard linear accelerator

Reza Zolfaghari[1], Adam Briggs[2], Hugo Furtado[3], Jeremy Booth[2,4], Paul Keall[1], Chun-Chien Shieh[1]

[1]ACRF Image X institute, The University of Sydney, Australia. (reza.zolfaghari@sydney.edu.au [Presenting author]), (paul.keall@sydney.edu.au), (andy.shieh@sydney.edu.au). [2]Royal North Shore Hospital, Sydney, Australia. (adam.briggs@health.nsw.gov.au), (jeremy.booth@health.nsw.gov.au). [3]Department of Radiation Oncology & Christian Doppler Laboratory for Medical Radiation Research for Radiation Oncology, Medical University of Vienna, Austria. (hugo.furtado@meduniwien.ac.at). [4]School of Physics, University of Sydney, Sydney, Australia

Introduction The ability to track lung tumours without implanted markers on a standard linear accelerator enables broad access to motion-adaptive radiotherapy for cancer patients globally. Previously, we developed and tested our algorithm offline with clinically acquired patient images from a single kilo-voltage imager on a standard linear accelerator. At present to prepare for future clinical trials, we prospectively implement the technology on a standard linear accelerator and characterize its live performance.

Method Our algorithm tracks tumours with low and variable visibility by removing the contribution of anatomic structures from kV images. First, an anatomical and tumour model are built using the 4D-CT and GTV contour. Next, the anatomical and tumour models are forward-projected onto live streamed kV projections utilizing a graphical processing unit. Tumour motion is computed by aligning the forward-projection and kV image using fast template matching in OpenCV. Sinusoidal and patient breathing traces were used to program the superior-inferior motion of a dynamic CIRS lung phantom containing a spherical 1 cm tumour. kV images were captured in real-time on a Varian Truebeam for tracking while a VMAT plan was delivered. Tracking error and algorithm latency were investigated.

Results The mean±std error along the LR, SI and AP direction was 0.26 ± 0.05, 0.30 ± 1.2, and -0.12 ± 0.05 mm, respectively. The percentage of frames with > 2 mm error in any direction was 4%. The average latency in processing the kV images was 68 ± 22 ms. Figure 1 and Table 1 show the performance of the algorithm with respect to ground truth.

Conclusion Markerless lung tumour tracking has been implemented on a standard linear accelerator for the first time and submillimetre accuracy was demonstrated on a lung phantom. This work supports further clinical implementation of markerless tumour tracking, which if successful will enable the use of the technology with almost all cancer radiotherapy systems.

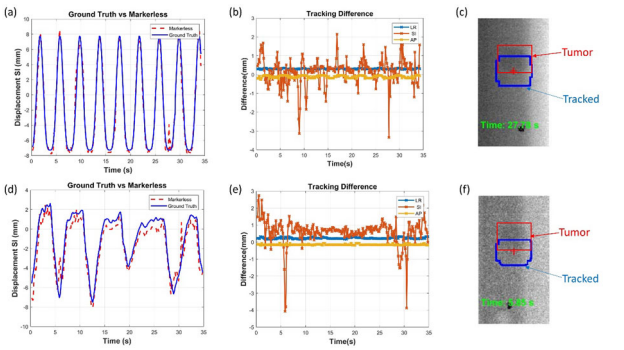

Figure1: Tracking analysis for sinusoidal (top) and patient traces(bottom). (a, d) Ground truth versus markerless tracking. (b, e) Tracking error versus time (c, f) Tumor position versus tracked position when tracking was poor. Blue contour is markerless tracking and red contour is the ground truth (c) t = 27.8 s (f) t = 5.8 s

	LR	*SI*	*AP*
Mean Error Sinusoid	0.30±0.02	0.18±0.79	-0.10±0.06
Mean Absolute Error Sinusoid	0.30(0.02)	0.58(0.56)	0.10(0.06)
Mean Error Patient	0.22±0.04	0.43±1.5	-0.14±0.02
Mean Absolute Error Patient	0.22(0.04)	0.90(1.2)	0.14(0.02)

Table 1: The mean error and mean absolute error in tracking accuracy is shown in the format mean±std for mean error and mean(std) for mean absolute error. Errors are reported across principal directions LR, SI and AP. All units are in millimeter.

O117 Extending the use of Mobius: a useful tool for verifying a treatment planning system beam model

S. Lydiard, C. Thompson, N. Campbell

Radiation Oncology, Auckland City Hospital, NZ. (SLydiard@adhb.govt.nz [Presenting author]), (CThompson@adhb.govt.nz), (NCampbell@adhb.govt.nz)

Introduction Mobius3D is a second-check dosimetric verification system that calculates 3D dose on the patient's CT. It uses treatment parameters exported from the treatment planning system (TPS) and a collapsed cone convolution-superposition algorithm.

The TPS used for Head and Neck VMAT planning in our clinic was switched from Pinnacle to Raystation. Treatment QA measurements were mostly in good agreement with Raystation, but large mean PTV dose differences were seen between Raystation and Mobius3D (up to 5.6%). To investigate, the beam models of Mobius3D and our TPS's were examined and compared to measured doses.

Method Four clinical Head and Neck VMAT plans were measured with a diode array dosimeter. Point dose measurements were also acquired in the dosimeter using a 0.4cc cylindrical ion chamber.

(1) To investigate the modelling of collimator scatter, point doses were measured for a 10cmx2cm field at various depths in solid water; once where the jaws matched the MLC aperture and again with 20x20cm^2 jaw positioning.
(2) Differences between measured and calculated doses were assessed by percentage dose differences and gamma analysis.

Results The average percentage difference between measured and calculated point doses was smaller for Mobius ($0.6 \pm 0.8\%$) than Raystation ($-1.3 \pm 0.8\%$). The average 3%, 2 mm gamma was better for Mobius ($98.1 \pm 0.6\%$) compared to Raystation ($96.8 \pm 2.2\%$). Measured and calculated point doses for the elongated field were in good agreement for all TPS when jaws were matched to the MLC aperture, but Raystation showed dose differences of $> 4\%$ when jaws were 20x20cm^2. This suggested incorrect modelling of collimator scatter in the Raystation beam model and consequent amendments were made beyond the scope of the user manual. This achieved better agreement with measured data.

Conclusion Mobius proved to be a useful tool for identifying limitations in our clinical TPS beam model even when QA measurements were not showing concerning discrepancies.

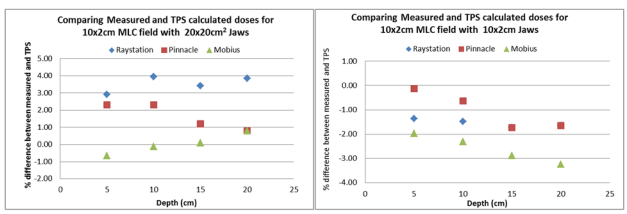

Figure 1 Point dose differences between measured and TPS for an elongated field measured in solid water where the jaws were set to (A) 20x20cm^2 or (B) match the MLC aperture.

O118 ACDS mail-out and onsite reference dosimetry audits of kilovoltage radiotherapy photon beams

F. Kadeer[1], A. Alves[1], D. Butler[2], C. Davey[1], J. Kenny[1], M. Shaw[1], J. Supple[1], S. Keehan[1,3], J. Lye[1]

[1]Australian Clinical Dosimetry Service (ACDS), ARPANSA. (Fayz.Kadeer@arpansa.gov.au [Presenting Author]), (Andrew.Alves@arpansa.gov.au), (Cate.Davey@arpansa.gov.au), (John.Kenny@arpansa.gov.au), (Maddison.Shaw@arpansa.gov.au), (Jeremy.Supple@arpansa.gov.au), (Stephanie.Keehan@petermac.org), (Jessica.Lye@arpansa.gov.au).
[2]Radiotherapy, ARPANSA. (Duncan.Butler@arpansa.gov.au).
[3]Physical Sciences, Peter MacCallum Cancer Centre

Introduction The ACDS provides a nation-wide mail-out dosimetry auditing service using OSLDs enclosed in Perspex phantoms, and an onsite reference dosimetry service for electrons and MV photons using ionisation chambers. The ACDS is extending the scope of these audits to kilovoltage (40–300 kV) radiotherapy photon beams.

Method The onsite kV reference-dosimetry audit has been built upon AAPM's TG-61 Protocol (2001) [1] using the in-air method of obtaining dose to water at the surface, from air kerma measurements. Al_2O_3 OSLD energy responses at kV energies were modelled using EGSnrc Monte Carlo, and validated by irradiating with known doses of 1 Gy from ARPANSA Primary Standard kV beams. Field trials at 4 existing facilities have been conducted.

Results The on-site field trial measurement results are given below in *Fig 1*. The average ACDS-Facility dose variation with a Farmer-type chamber was found to be − 0.5% (0.6% standard deviation), and the plane-parallel thin-window chamber average variation was − 0.5% (0.9% standard deviation). The existing MV onsite reference-dosimetry audit has a k = 1 uncertainty of 0.7% for MV photons. A preliminary kV ACDS-Facility correlation-exclusive uncertainty budget has been derived, with Optimal-scoring on variations up to 2.1% (k = 2).

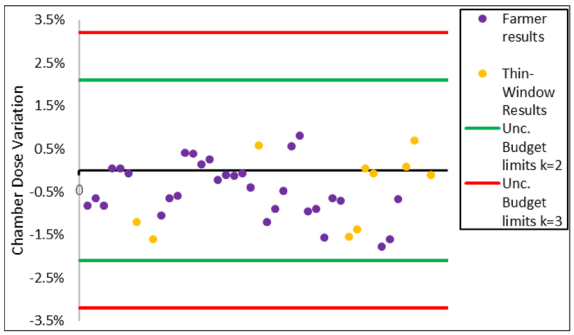

Figure 1: Dose measurement variations between the facility and the ACDS.

The OSLD audit results are shown below in *Fig 2*. The average dose variation between the facility and the OSLD is − 0.1% (2.7% standard deviation). An empirical uncertainty budget suggests ~ 5% (k = 2) may be appropriate for OSLD kV measurements, due to uncertainties associated with Al_2O_3 overresponding at kV energies.

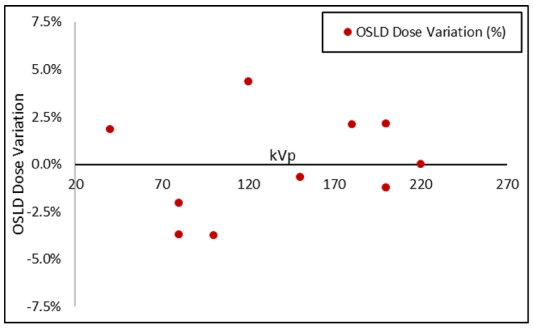

Figure 2: OSLD measurement variations between the facility and the ACDS.

Conclusion 41 on-site kV measurements were performed. Applying a derived uncertainty budget of 2.1% (k=2) yields Optimal-scoring results on all measurements.
The empirical OSLD measurement standard deviation of 2.7% suggests that a higher uncertainty budget of ~ 5% (k = 2) may be required.

Reference

1. Chair CMM, Coffey CW, DeWard LA, Liu C, Nath R, Seltzer SM, Seuntjens (2001) AAPM's TG61 protocol for kilovoltage x-ray beam dosimetry. Med. Phys. 28:868–893

O119 Can dosimetry audits inform clinical IMRT/VMAT treatment planning decisions and review of patient specific quality assurance results?

J. Kenny[1,2], A. Alves[1], C. Davey[1], F. Kadeer[1], M. Shaw[1], J. Supple[1], J. Lye[1]

[1]Australian Clinical Dosimetry Service, ARPANSA, Melbourne VIC Australia. (john.kenny@arpansa.gov.au [Presenting author]), (Andrew.Alves@arpansa.gov.au), (Cate.Davey@arpansa.gov.au), (Fayz.Kadeer@arpansa.gov.au), (Maddison.Shaw@arpansa.gov.au), (Jeremy.Supple@arpansa.gov.au), (Jessica.Lye@arpansa.gov.au).
[2]Health STEM Solutions, Melbourne VIC Australia

Introduction Following the introduction of IMRT/VMAT into the ACDS national dosimetry audit program [1, 2], outcomes were reviewed to determine if IMRT/VMAT treatment planning choices may predict audit outcome.

Method The "National Data Set" is a substantial body of audit dosimetry and associated data acquired since 2011. The audits compare treatment planning beam models to measured doses. Aggregate data for Level II and III audits was reviewed to determine if sub-optimal outcomes were due to IMRT/VMAT specific factors. An optimal audit outcome was defined as agreement between measurement and plan of $\leq$ 3.3% (point doses) and $\gamma < 1$ at 3%/3 mm for $\geq$ 97.5% points (2D array). The review included outcomes from initial and follow-up audits, treatment plan properties and all recommendations made.

Results The distribution of audit types is shown in Table 9. Of the 112 recommendations made, only two were definitively IMRT/VMAT beam modelling related. Potential errors were sometimes not identified by patient specific QA or considered permissible under Facility protocols.

Table 1: Dosimetry Audits Reviewed

Audit Level	Measurement Configuration	Audit Type	Audits	IMRT/VMAT Cases
Level III	1. end-to-end • thorax phantom • nine ionisation chambers	3DCRT	73	-
		3DCRT + IMRT/VMAT	11	246
Level II	• planning-to-delivery • slab phantom • 2D array	3DCRT	50	-
		3DCRT + IMRT/VMAT	37	145

In three specific cases, the facility re-planned out-of-tolerance IMRT cases, typically resulting in less beam modulation and an improved audit outcome. Cases with low planned OAR doses, used as a surrogate for plan complexity, correlated with higher variability in the point dose differences in the target volume.

Conclusion IMRT treatment planning constraints could have a greater impact on dosimetry than small deficiencies in beam modelling. This raises the clinical consideration of whether an ideal treatment plan that optimises dose constraints with a higher degree of uncertainty is preferable to a satisfactory but less ideal treatment plan that can be delivered with a high degree of dosimetric accuracy.

References

1. Lehmann J, Alves A, Dunn L, Shaw M, Kenny J, Keehan S, Supple J, Gibbons F, Manktelow S, Oliver O, Kron T, Williams I, Lye J (2018) Physics and Imaging in Radiation Oncology 6:5–11. https://doi.org/10.1016/j.phro.2018.03.006
2. Lye J, Kenny J, Lehmann J, Dunn L, Kron T, Alves A, Cole A, Williams I (2016) A 2D ion chamber array audit of wedged and asymmetric fields in an inhomogeneous lung phantom. Medical Physics 41:101712. https://doi.org/10.1118/1.4896097

O120 Monte Carlo k_Q values for the revision of IAEA TRS-398: experience of the ARPANSA PSDL

M. D. Hanlon[1], C. P. Oliver[1], T. Bailey[1], J. Lye[2], D. J. Butler[1]

[1]Primary Standards Dosimetry Laboratory, Medical Radiation Services Branch, ARPANSA, Melbourne, Australia. (Max.Hanlon@arpansa.gov.au [Presenting author]), (Chris.Oliver@arpansa.gov.au), (Tracy.Bailey@arpansa.gov.au), (Duncan.Butler@arpansa.gov.au). [2]Australian Clinical Dosimetry Service, Medical Radiation Services Branch, ARPANSA, Melbourne, Australia. (Jessica.Lye@arpansa.gov.au)

Introduction The Primary Standards Dosimetry Laboratories (PSDL) at ARPANSA has been invited by the IAEA to participate in the update of TRS-398 [1], by determining Monte-Carlo values for k_Q, the beam quality conversion factor. Values calculated by ARPANSA are being collected alongside other results from invited groups to form consensus values.

Method The EGSnrc user code egs_chamber was used to simulate various ionisation chambers, including the classic Farmer chamber. Both the ARPANSA ^{60}Co teletherapy source and Elekta Synergy linac were modelled in BEAMnrc. Two methods were used; phase-space files and BEAM shared libraries.

k_Q values were calculated from the ratio of scored doses in the air cavity of the chamber and dose to water. Figure 1 gives an illustration of interactions occurring in the chamber.

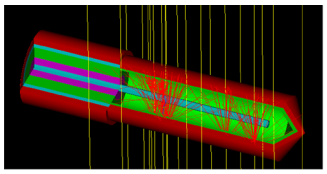

Figure 1 : Visualisation of interactions inside a NE2571 ionisation chamber with photon source incident from the top. The yellow marks represent photons, and the red marks electrons. Cross section enhancement is used to increase the production of electrons.

Results For the NE2571 Farmer chamber, simulated k_Q values were similar to both TRS-398 and published Monte-Carlo values [2], and agreed with other invited groups. Both the phase-space and BEAM shared library sources produce similar results, agreeing within 1σ. Figure 2 shows the two calculated results compared to TRS-398 and reference data. Other chambers, including the PTW 30013, IBA FC65-G and CC13, have been successfully modelled and associated results will be shown.

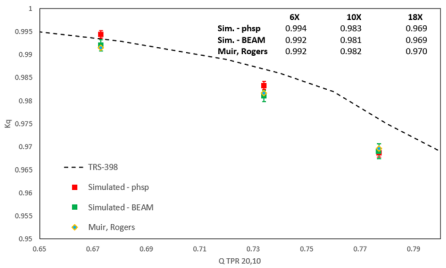

Figure 2 : ARPANSA simulated values for the NE 2571 with two calculation pathways, BEAMnrc shared library (BEAM) and phase space input (phsp) compared to TRS-398 and published Monte Carlo[2] values. The table insert gives numerical values.

Conclusion We have successfully calculated k_Q values for various ionisation chambers, with the results for the NE2571 shown here. Our initial results compare well to other international groups.

References

1. Andreo P, et al. (2000) Absorbed dose determination in external beam radiotherapy: an international code of practice for dosimetry based on standards of absorbed dose to water. *IAEA TRS* 398 (2000)
2. Muir B R, and Rogers D W O (2010) Monte Carlo calculations of kQ, the beam quality conversion factor. *Medical physics* 37.11 (2010): 5939–5950

O121 Improvement in Australian reference dosimetry measured by the Australian clinical dosimetry service

A. Alves[1], C. Davey[1], F. Kadeer[1], J. Kenny[1], M. Shaw[1,2], J. Supple[1], D. Butler[3], I. Williams[4], J. Lye[1]

[1]Australian Clinical Dosimetry Service, ARPANSA, Melbourne VIC Australia. (Andrew.Alves@arpansa.gov.au [Presenting author]), (Cate.Davey@arpansa.gov.au), (Fayz.Kadeer@arpansa.gov.au), (John.Kenny@arpansa.gov.au), (Maddison.Shaw@arpansa.gov.au), (Jeremy.Supple@arpansa.gov.au), (Jessica.Lye@arpansa.gov.au). [2]Genesis Cancer Care, Melbourne VIC Australia. [3]Primary Standards Dosimetry Laboratory, ARPANSA, Melbourne VIC Australia. (Ducan.Butler@arpansa.gov.au). [4]Medical Radiation Services Branch, ARPANSA, Melbourne VIC Australia. (Ivan.Williams@arpansa.gov.au)

Introduction The Australian Clinical Dosimetry Service (ACDS) has audited reference dosimetry since its inception in 2011. Auditing is envisioned as a driver for improved performance, so for regular (flattened) photon beams we assess the impact on audit results from the program over 7 years. We also assess the impact on Australian dosimetry arising from ionisation chamber specific energy correction factors, k_Q, which have been partially adopted over the last 2 years.
Method The ACDS follows the TRS-398 protocol[1] for onsite level Ib reference dosimetry audits with a PTW-30013 ionisation chamber. In this study the method used by the facility to obtain k_Q (either from the published values or via direct measurement) was also adopted by the ACDS prior to the calculation of dose variation.
Results Fig. 1 shows the audit dose variations from approximately 200 photon beams. For audits using published k_Qs the standard deviation (SD) was calculated (sample size of 50) over the audit period and the trend in SD has been plotted. A reduction in audit SD from 0.60% to 0.44% is observed. For recent audits using measured k_Qs SD was calculated once (sample size of 23) and returns a value of 0.24%.

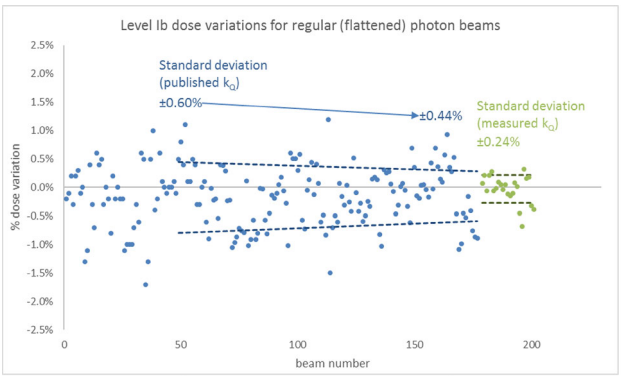

Figure 1. The dose variation for each audit beam has been calculated after matching the k_Q method (either published or measured) adopted by the facility.

Conclusion While anecdotal evidence of improved dosimetry following auditing has been observed in the past (through practices such as equipment modernisation), we also observe a gradual decrease in the overall SD of audit results, suggesting that auditing is a driver of improvement. Also observed is the benefit of the technological advance of directly measuring chamber k_Qs during calibration.

Reference

1. INTERNATIONAL ATOMIC ENERGY AGENCY, Implementation of the International Code of Practice on Dosimetry in Radiotherapy (TRS 398): Review of Test Results, IAEA-TECDOC-1455, IAEA, Vienna (2005).

O122 ARPANSA's radiotherapy calibration services: update on the overseas equivalence of the ^{60}Co and linac beams calibration services

P. D. Harty, D. J. Butler, C. P. Oliver, V. Takau, M. Hanlon, C. Smith, A. Hayton

Primary Standards Dosimetry Laboratory, Medical Radiation Services Branch, ARPANSA. Peter.Harty@arpansa.gov.au [Presenting author])

Introduction In recent years, Australian radiotherapy centres have used the ARPANSA ^{60}Co absorbed dose to water calibration of their ionisation chamber as the basis of their dose determination in the clinic, applying a calculated k_Q factor from TRS-398 to correct to the linac beam quality they use in treatments. More accurate dosimetry can be achieved if calibration of the ionisation chamber is performed as well at the three ARPANSA linac beam qualities available and the appropriate calibration factor for the particular beam quality of the clinic determined by interpolation.
Method ARPANSA now calibrate all reference-class ionisation chambers submitted for calibration for linac beams as well as ^{60}Co. The linac calibration is a cross calibration against two ARPANSA reference chambers of the same type, which have been calibrated against the graphite calorimeter primary standard. This allows determination of the absorbed dose to water calibration factor at the beam quality of the radiotherapy centre by interpolation, using $TPR_{20,10}$ to define the beam quality.
Results ARPANSA's radiotherapy calibrations are traceable to the Australian primary standard of absorbed dose, the ARPANSA graphite calorimeter. This is true both for ^{60}Co and direct calibrations using the ARPANSA medical linear accelerator. ARPANSA's graphite calorimeter has been compared internationally through the BIPM Key Comparisons Program and in bi-lateral comparisons such as with NMIJ[1] in Japan. These comparisons have shown that ARPANSA's graphite calorimeter agrees well with other international primary standards. Fig. 1 below shows the latest K6 comparison data.

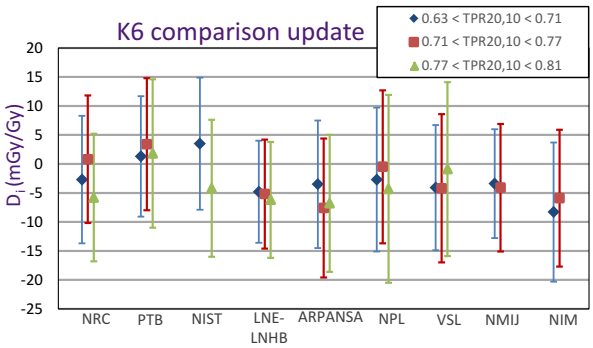

Figure 1: Latest K6 comparison data from 9 Primary Standards laboratories

There has also been a recent comparison in May 2018 between NMIJ and ARPANSA, with results which will be soon be available.
Conclusion The calibration service offered by ARPANSA, combining ^{60}Co and linac beam qualities will potentially lead to better dosimetry accuracy for Australian radiotherapy clinical treatments.

Reference

1. Shimizu M et al (2014) Comparison of the NMIJ and the ARPANSA standards for absorbed dose to water in high-energy photon beams. Radiat Prot Dosim 164:181–186.

O123 The ARPANSA PSDL measured and calculated MV photon k_Q values for the revision of IAEA TRS-398

C. P. Oliver[1], V. Takau[1], M. D. Hanlon[1], T. Bailey[1], J. Lye[2], D. J. Butler[1]

[1]Primary Standards Dosimetry Laboratory, Medical Radiation Services Branch, ARPANSA, Melbourne, Australia. (Chris.Oliver@arpansa.gov.au [Presenting author]), (Viliami.Takau@arpansa.gov.au), (Max.Hanlon@arpansa.gov.au), (Tracy.Bailey@arpansa.gov.au), (Duncan.Butler@arpansa.gov.au).
[2]Australian Clinical Dosimetry Service, Medical Radiation Services

Branch, ARPANSA, Melbourne, Australia.
(Jessica.Lye@arpansa.gov.au)

Introduction The ARPANSA Primary Standard Dosimetry Laboratory (PSDL) was invited by the IAEA to contribute to the update of IAEA TRS-398 for high energy photons. A range of independent groups were asked to provide new k_Q factors for the revision of the high-energy photon section. The ARPANSA PSDL has committed to providing both experimental and Monte Carlo calculated k_Q factors.
Method The ARPANSA PSDL has been measuring k_Q values of ionisation chambers since 2014 by measuring absorbed dose to water calibration factors in Co-60 gamma radiation, and 6X, 10X and 18X photon beams from an Elekta Synergy linear accelerator. These measurements are traceable to the graphite calorimeter which is the Australian primary standard for absorbed dose. k_Q have also been calculated with Monte Carlo simulations. The EGSnrc used code egs_chamber has been used to construct realistic models of a number of reference class ionisation chambers. BEAMnrc models of the Co-60 source and the linear accelerator photons beams were then used to calculate the doses to the sensitive volumes of the chambers and the dose to water to realise the theoretical k_Q value.
Results k_Q values have been measured for eight different types of ionisation chambers. The differences between IAEA TRS-398 k_Q values and those measured will be presented along with comparison to those given in the updated AAPM TG-51 protocol.

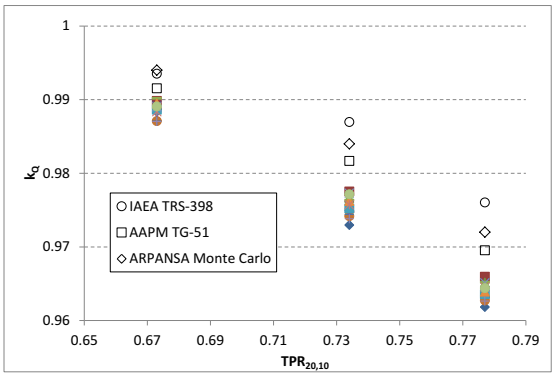

Figure 1: Experimental k_Q measured for twenty 2571 chambers (coloured) compared to two current protocols and Monte Carlo calculated values.

The initial results of the Monte Carlo k_Q calculations for three Farmer chamber types will also be presented comparing with our experimental results and other Monte Carlo calculations.
Conclusion The ARPANSA PSDL has measured and calculated k_Q values for a range of reference ionisation chambers. These will contribute to the revision of the high-energy photon dosimetry update of IAEA TRS-398.

References

1. Andreo, Pedro, et al. (2000) Absorbed dose determination in external beam radiotherapy: an international code of practice for dosimetry based on standards of absorbed dose to water. *IAEA TRS-398*.
2. McEwen, Malcolm, et al. (2014) Addendum to the AAPM's TG-51 protocol for clinical reference dosimetry of high-energy photon beams. Med Phys 41(4):041501-1-20

O124 Future directions of ACDS audits

J. Lye[1], A. Alves[1], C. Davey[1], F. Kadeer[1], J. Kenny[1], M. Shaw[1,2], J. Supple[1]

[1]Australian Clinical Dosimetry Service, ARPANSA, Melbourne VIC Australia. (Jessica.Lye@arpansa.gov.au [Presenting author]), (Andrew.Alves@arpansa.gov.au), (Cate.Davey@arpansa.gov.au), (Fayz.Kadeer@arpansa.gov.au), (John.Kenny@arpansa.gov.au), (Maddison.Shaw@arpansa.gov.au), (Jeremy.Supple@arpansa.gov.au), [2]Genesis Cancer Care, Melbourne VIC Australia

Introduction The evolution of the Australian Clinical Dosimetry Service (ACDS) audits to keep pace with the changing aspects of radiotherapy technology is important for a clinically relevant national dosimetry service. The audit coverage now standardly includes conformal, IMRT, VMAT and FFF treatments. This year has seen a focus on small field and SABR and both are in active field trial around the country. New challenges for the ACDS is not only coverage of clinical practice of standard machines, but also how we can adapt our audits for non-standard technology, both existing and soon-to-be deployed.
Method Tomotherapy, Cyberknife, Gammaknife, and Halycon linacs are all in clinical use around Australia. Field trials on Tomotherapy and Halcyon demonstrated the ACDS audits can be effectively used with only minor modifications of audit procedures required. The inclusion of SABR capability allows measurements on Cyberknife and proposed addition of an SRS cranial phantom opens the possibility of Gammaknife measurements. The inclusion of a cranial phantom also supports clinical trial credentialing and moves the ACDS in line with equivalent international auditing bodies.
MRI Linacs are expected to be in clinical use in Australia in 2019 and magnetic field dosimetry has been an animated discussion point. The ACDS is collaborating with the National Physical laboratory (NPL) in the UK for traceable reference dosimetry in a magnetic field, and to perform intercomparison between ion chamber and alanine based end-to-end measurements on modulated fields with a MRI Linac.

Proton auditing and a harmonised approach for clinical trial credentialing is a focus of international auditing and trial groups. ARPANSA is considering proton dosimetry all the way from primary standard calorimetry through to end-to-end Level III audit testing.

Results

Table of audit modality status and planning for 2018-2019 (Live, *Field trial*, *Planned*)

Level	Modality	Applicable technology
I	Reference	Linac
	FFF Reference	Linac
	kV	*kV*
Ib	Reference	Linac
	FFF Reference	Linac, *Tomo, Halcyon*
	Small field	Linac
	FFF small field	Linac
	MRI Reference	*MRI Linac*
	kV	*kV*
II	3DCRT	Linac
	IMRT	Linac,
	IMRT FFF	Linac, *Halcyon*
	VMAT	Linac,
	VMAT FFF	Linac, *Halcyon*
	SABR/SRS	*Linac*
III	3DCRT	Linac, *Tomo*
	IMRT	Linac,
	IMRT FFF	*Linac, Halcyon, Tomo*
	VMAT	Linac,
	VMAT FFF	*Linac, Halcyon, Tomo*
	SABR	Linac, Cyberknife
	SRS (cranial)	*Linac, gammaknife, cyberkinfe*
	MR RT	*MRI Linac*
	4D IGRT	*Linac*

Conclusion The ACDS is developing a comprehensive suite of audit modalities aimed at ensuring patient safety across a range of clinical practice and radiotherapy technologies.

IS09 Developing a clinically approved nanoparticle for detecting and diagnosing metastases with simultaneous PET-MRI

Y. H. Gholami

The University of Sydney

Metastases, the leading cause of death from all types of cancer, first appears in tumour draining lymph nodes. Due to their small size and low vascularisation, metastases are very difficult to detect. To address this, we have developed a radiolabeled nanoparticle platform for simultaneous Positron Emission Tomography (PET) and Magnetic Resonance Imaging (MRI) that not only provides contrast-enhanced diagnostic imaging, but also provides significant image quality gain from integrating the high spatial resolution of MRI with the high sensitivity of PET. A commercially available, FDA-approved magnetic nanoparticle, Feraheme® (FH), was developed for this application. FH is increasingly being used off-label as an MRI contrast agent for diagnostic lymph node imaging. Following intravenous injection, FH extravasates from vascular space to interstitial space, from where it is taken up by immune cells (monocytes/macrophages) and delivered via lymphatic vessels to lymph nodes. The FH nanoparticles remain in normal nodal tissue and thus provide MRI contrast against any metastatic lesions in the nodes.

FH was radiolabeled with the PET radioisotope ^{89}Zr using a novel chelate-free radiolabeling technique, heat induced radiolabeling (HIR). Radiochemical analysis demonstrated a high radiochemical yield (92%) and purity (98%) of the ^{89}Zr-FH product. Pre-clinical simultaneous PET-MRI scans confirmed the capability of ^{89}Zr-FH for this multi-modal imaging technique. Furthermore, the relative contrast image analysis showed that ^{89}Zr-FH can combine PET and MR images in a complementary manner to achieve high quality imaging using a minimal dose of radioisotope and Fe.

O125 An in-house automated quality assurance (QA) tool for quantitative patient specific evaluation of deformable image registration

S. Deshpande[1,2,3], P. Chlap[2], M. Jameson[1,2,3], L. Holloway[2,3,4,5,6]

[1]Department of Medical Physics, Liverpool and Macarthur Cancer Therapy Centre, Australia. (Shrikant.deshpande@health.nsw.gov.au [Presenting author]), (Michael.Jameson@health.nsw.gov.au). [2]Ingham Institute for Applied Medical Research, Sydney, NSW 2170, Australia. (phillip.chlap@unsw.edu.au), (Lois.Holloway@health.nsw.gov.au). [3]South Western Sydney Clinical School, University of New South Wales, Sydney, NSW 2052, Australia. [4]Department of Medical Physics, Liverpool and Macarthur Cancer Therapy Centre, Sydney NSW 2170, Australia. [5]Centre for Medical Radiation Physics, University of Wollongong, Wollongong NSW 2170, Australia. [6]Institute of Medical Physics, School of Physics, University of Sydney, Sydney, NSW 2006, Australia

Introduction Deformation image registration(DIR) supports a clinical decision which required quantification of DIR error per patient[1]. The aim of this work is to present an in-house automated QA tool for quantitative evaluation of DIR performance.

Method An in-house QA tool was developed as an extension within MiM software®(MIM Software Inc., Cleveland, OH). The QA tool uses a DICOM registration as an input. It processes the deformation vector field (DVF) at each voxel inside user defined regions of interests (ROIs) and on the entire dataset. Further, the QA tool calculates various metrics such as total registration error (TRE), DVF statistics, Jacobean determinant (JD), harmonic energy (HE) and a result summary report and database is automatically populated. A comprehensive validation of this QA tool was performed including masking the defined ROI and reporting the metrics using pseudo dataset with known ground truth. Also, the calculated TRE was compared with MIM reported values using POPI dataset[2] having predefined anatomical landmarks. Finally, the sensitivity of QA tool was assessed by changing the smoothness factor and analysing the resultant DVF for each change made.

Results Figure 1(a) shows an overlay of defined a ROI and the masked region by the QA tool demonstrating the accuracy of the masking functionality. The TRE calculated from QA tool and MiM software agreed within 0.3 mm. Figure 1(b and c) shows DVF statistics and DVF overlay of ROI. Figure 2 shows changes in JD and HE map with change in smoothness factor suggesting the sensitivity of metrics to detect the non-physical deformation.

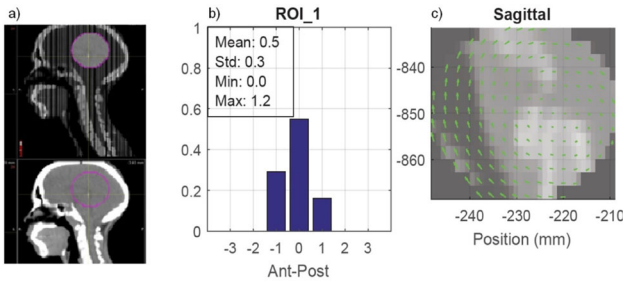

Figure 1: a) Overlay of defined ROI and mask region to validate the mask function of QA tool. b) DVF statistics within the region of interest and c) overlay of DVF on the masked ROI

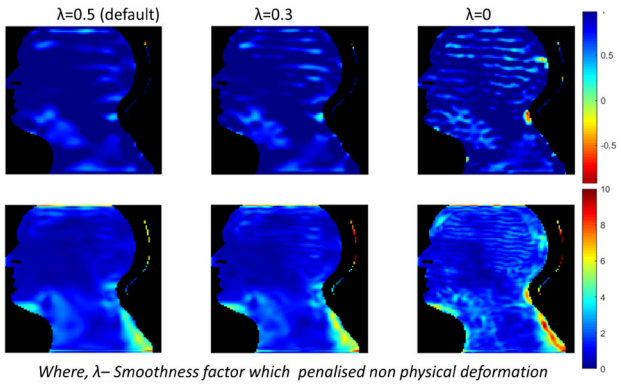

Where, λ– Smoothness factor which penalised non physical deformation

Figure 2: Illustration of metrics sensitivity with change in smoothness factor.(λ). Top row is Jacobean determinant maps (increase in negative) and bottom row is harmonic energy map (increase HE value) changes with smoothness factor from left to right with 0.5 (default), 0.3 and 0 respectively.

Conclusion An automated in-house automated quality assurance (QA) tool for quantitative patient specific evaluation of DIR was developed and implemented clinically. Future work is underway by datamining the QA results to understand the sensitivity each of the metrics under an individual clinical situation and also develop realistic QA tolerances.

References

1. AAPM Task Group No. 132 Med Phys 44(7) 2017:e43–e76
2. Castillo et al Phys Med Biol. 2013 May 7; 58(9): 2861–2877

O126 Rigid and deformable image registration practice pattern: Australasian results

J. Yuen[1], A. Ralston[1], A. Gray[2,3,4], A. Walker[2,3,4,5], M. Jameson[2,3,4,5], N. Hardcastle[6], L. Schmidt[1], K. Harrison[7], J. Poder[1], J. Sykes[8], J. Barber[8,9]

[1]St George Hospital Cancer Care Centre, Kogarah, NSW, Australia, 2217. (Johnson.Yuen@health.nsw.gov.au), (Anna.Ralston@health.nsw.gov.au), (Laurel.Foessel@health.nsw.gov.au), (Joel.Poder@health.nsw.gov.au [Presenting author]). [2]Liverpool and Macarthur Cancer Therapy Centres, NSW Australia. (Alison.Gray@health.nsw.gov.au), (Amy.Walker@health.nsw.gov.au), (Michael.Jameson@health.nsw.gov.au). [3]South Western Clinical School, University of New South Wales, Sydney, Australia. [4]Ingham Institute for Applied Medical Research, Sydney, Australia. [5]Centre for Medical Radiation Physics, University of Wollongong, NSW, Australia. [6]Physical Sciences, Peter MacCallum Cancer Centre, Melbourne, Australia. (Nick.Hardcastle@petermac.org). [7]Genesis Cancer Care, Newcastle, NSW, Australia. (Kristie.Harrison@cancer.com.au). [8]Blacktown Cancer & Hematology Centre, Sydney West Cancer Network, Sydney, Australia. (Jonathan.Sykes@health.nsw.gov.au), (Jeffrey.Barber@health.nsw.gov.au). [9]School of Physics, University of Sydney, Sydney, Australia

Introduction Interest in the potential clinical benefits of rigid and deformable image registration has increased since the release of the AAPM TG132 report on this topic. Data on departmental practice patterns in image registration was acquired to facilitate further implementation.

Method The AAPM TG132 report was analysed on a process level to generate a survey to assess potential variations in resources, implementation, and criteria for clinical image registration. Radiotherapy sites from Australia-New-Zealand (ANZ) and internationally (INTL) were surveyed.

Results 67% of the 12 ANZ responses were from NSW. 19 INTL responses were from Americas (47%), Europe (32%), and Asia (21%). Sites tended to use DIR with dedicated software (ANZ 42%, INTL 63%) vs. treatment planning system (ANZ 33%, INTL 32%). DIR was most common for CT-CT registration (ANZ 17%, INTL 63%), followed by CT-PET (ANZ 16%, INTL 53%).

Centres have implemented or are implementing DIR clinically for atlas-based segmentation (ANZ 67%, INTL 42%), multi-modality treatment planning (ANZ 50%, INTL 68%), and dose deformation (ANZ 50%, INTL 68%). Our data suggests that most sites will use DIR clinically by 2019–2023.

While sites were aware of TG132 request/report forms (ANZ 100%, INTL 74%), adoption was limited as of 2018 (ANZ 33%, INTL 11%) but was expected to increase (ANZ 58%, INTL 27%).

ANZ physicists had limited involvement with registration processes (ANZ 40%, INTL 80%). The key challenge (Figure 1) was insufficient trained staff (ANZ 50%, INTL 32%) but internationally, it was determining whether registrations were satisfactory (ANZ 33%, INTL 52%), and actions when registrations were not (ANZ 33%, INTL 47%).

Conclusion Australasian-specific practice pattern shows who, what, when, and how tasks are performed for image registration, enabling adaptation for local challenges. Institutional or state consensus on best practice for image registration in Radiation Oncology could be facilitated by practice pattern data.

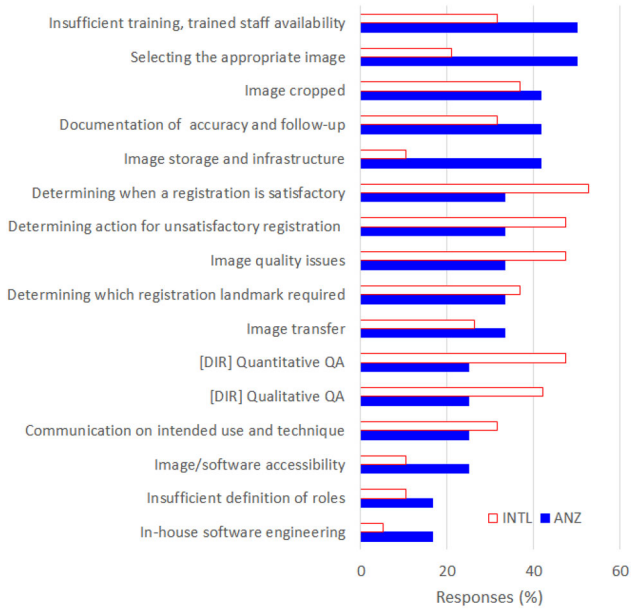

Figure 1: Key challenges in image registration

O127 Evaluation of deformable image registration for MIRADA

S. Behin-Ain[1], B. Chick[2], A. Kovendy[3]

[1]Northern NSW Cancer Institute, Lismore, NSW. (Setayesh.BehinAin@ncahs.health.nsw.gov.au [Presenting author]). [2]Mid North Coast Cancer Institute, Port Macquarie, NSW. (Brendan.Chick@ncahs.health.nsw.gov.au). [3]Mid North Coast Cancer Institute, Coffs Harbour, NSW. (Andrew.Kovendy@ncahs.health.nsw.gov.au)

Introduction MIRADA is a commercial software package that allows image registration, rigid and deformable, of different imaging modalities (multi-modality). It also allows automatic anatomical segmentation based on atlas databases (provided or user defined). NCCI is the first centre in Australia to implement MIRADA. This work involves evaluation of deformable registration and using in-house Matlab software to both introduce known mathematical deformation and evaluation of multi-modality registration.

Method Multi-modal image datasets (CT, MRI, PET, CBCT) are imported into in-house Matlab software. Known deformations are applied to alter the studyset. Mirada was then used to register the deformed studyset to the original studyset. The quality and extent of the registration was then assessed using the deformation vector field within Mirada, 2D correlation method and mutual information developed in Matlab. Both phantom and clinical patient datasets for various anatomical sites were used.

Results Results show the correlation for deformable registration is generally above 0.98. This depends on initial rigid correlation as an optimisation problem initial point can largely influence the final quality of the result. High degree and complexity of deformation when mathematical deformation is introduced, or presence of random and extended variation in signal (e.g., gas in abdomen) degrade the correlation.

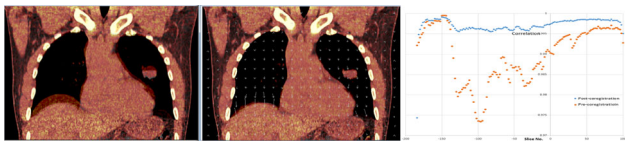

Conclusion This evaluation indicates MIRADA as a useful quality tool to enable better image registration and identification of tumour/anatomy. A characterization of the correlation as a global metric to quantify reregistration is likely necessary and will need to be augmented by a human observer.

References

1. K K Brock *et al*, Use of image registration and fusion algorithms and techniques in radiotherapy: Report of the AAPM Radiation Therapy Committee Task Group No. 132
2. Manual Mirada Medical, 2016 and personal communications.

Acknowledegements The authors acknowledge the input and support of the Mirada WG at NCCI.

O128 Challenges in Atlas-based cardiac segmentation

R. N. Finnegan[1,2], C. Brink[3,4], E. L. Lorenzen[4], J. A. Dowling[1,5,6,7,8], D. I. Thwaites[1], L. C. Holloway[1,2,6,7,9]

[1]Institute of Medical Physics, School of Physics, University of Sydney, Sydney, Australia. (robert.finnegan@sydney.edu.au [Presenting author]). [2]Ingham Institute for Applied Medical Research, Liverpool, Australia. [3]Institute of Clinical Research, University of Southern Denmark, Odense, Denmark. [4]Laboratory of Radiation Physics, Odense University Hospital, Odense, Denmark. [5]The Australian e-Health and Research Centre, CSIRO Health and Biosecurity, Herston, Australia. [6]School of Mathematical and Physical Sciences, University of Newcastle, Newcastle, Australia. [7]South Western Sydney Clinical School, University of New South Wales, Sydney, Australia. [8]Centre for Medical Radiation Physics, University of Wollongong, Wollongong, Australia. [9]Liverpool Cancer Therapy Centre, Liverpool Hospital, Sydney, Australia

Introduction Adjuvant radiotherapy for thoracic malignancies involves radiation dose to the heart and coronary arteries, which is associated with an increase in the risk of cardiovascular complications. The relationship between the specific dose and radiation-induced cardiac disease is complex and poorly understood. Retrospective analysis of the dose to cardiac substructures involves segmentation of these volumes in planning computed tomography (CT) images. An automated method for cardiac segmentation is required, and a multi-atlas approach can provide the accuracy, consistency and performance required. We present the challenges and solutions in the implementation of atlas-based cardiac substructure segmentation.
Method We develop an end-to-end automatic atlas-based segmentation framework, which includes image preprocessing, rigid and deformable registration, label fusion, threshold optimisation and automatic vessel segmentation. During the validation of this framework we implement one Danish and one Australian CT atlas dataset. We examine these datasets in terms of inter- and intra-atlas consistency.
Results Incremental improvements lead to a robust and flexible segmentation framework. The development of an automatic vessel fitting algorithm for coronary arteries provides a solution to vessel segmentation and offers a major improvement to previous methods. Overall analysis of the segmentation framework demonstrates excellent overall performance, as well as necessary efficiency for planned future studies. The mean symmetric surface distance for whole heart segmentation is 1.91±0.60mm and for the left anterior descending coronary artery is 5.78 ± 3.53mm; these values are similar to estimates of inter-observer variability. Using automated reporting we are able to identify inconsistently contoured images in an atlas set, and use this information to improve atlas consistency.
Conclusion This study presents solutions to challenges encountered in automatic segmentation of cardiac and coronary structures, with a focus on the application in large-cohort retrospective studies in radiation oncology.

O129 Dosimetric validation of automatic segmentation of the left anterior descending coronary artery in radiotherapy of the left anterior descending coronary artery in radiotherapy

R. N. Finnegan[1,2], C. Brink[3,4], E. L. Lorenzen[4], J. A. Dowling[1,5,6,7,8], D. I. Thwaites[1], L. C. Holloway[1,2,6,7,9]

[1]Institute of Medical Physics, School of Physics, University of Sydney, Sydney, Australia. (robert.finnegan@sydney.edu.au [Presenting author]). [2]Ingham Institute for Applied Medical Research, Liverpool, Australia. [3]Institute of Clinical Research, University of Southern Denmark, Odense, Denmark. [4]Laboratory of Radiation Physics, Odense University Hospital, Odense, Denmark. [5]The Australian e-Health and Research Centre, CSIRO Health and Biosecurity, Herston, Australia. [6]School of Mathematical and Physical Sciences, University of Newcastle, Newcastle, Australia. [7]South Western Sydney Clinical School, University of New South Wales, Sydney, Australia. [8]Centre for Medical Radiation Physics, University of Wollongong, Wollongong, Australia. [9]Liverpool Cancer Therapy Centre, Liverpool Hospital, Sydney, Australia

Introduction During thoracic radiotherapy the heart and left anterior descending coronary artery (LADCA) are subject to radiation dose. The correlation between this radiation dose and an increase in the risk of coronary events later in the patient's life is not particularly well understood, in part due to the variability in contouring practices. In order to better understand this relationship a consistent method of generating segmentations of these volumes is necessary.
Method We generate automatic segmentations of the whole heart and LADCA with a multi-atlas based approach. A dataset consisting of 15 left-sided breast cancer patients was contoured by 9 experienced observers, both before and after adherence to common guidelines. The effect of atlas selection on dose is evaluated by automatically segmenting the images with a Danish atlas set and an Australian atlas set. The dosimetric consequences of the use of automatic segmentations are evaluated with respect to the inter-observer variability.dosimetric consequences of the use of automatic segmentations are evaluated with respect to the inter-observer variability.
Results After following guidelines the automatic and manual whole heart segmentations have excellent agreement and little difference in dosimetric measures. For the LADCA, adherence to guidelines often improves the agreement to the automatic segmentation, however it does not necessarily reduce the interobserver variability, as can be seen in Figure 1. measures. For the LADCA, adherence to guidelines often improves the agreement to the automatic segmentation, however it does not necessarily reduce the interobserver variability, as can be seen in Figure 1.
Conclusion This study presents a validation of automatic segmentation of the whole heart and LADCA in terms of dosimetry during left-sided breast cancer.

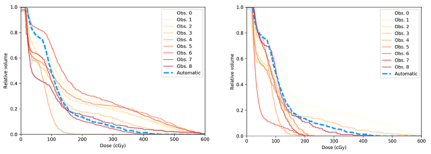

Figure 1. Dose volume histograms for the LADCA before (left) and after (right) guideline adherence.

IS10 No research time, no research staff, and a hundred published papers: the horrors and the fun of sharing clinical medical physics work via the scientific literature

T. Kairn

Royal Brisbane and Women's Hospital

The clinical responsibilities of the radiation oncology medical physicist usually include investigating and commissioning radiotherapy techniques and technologies that are new to the local radiotherapy department. That work may involve using standard equipment and methods to perform tests against internationally-recommended tolerances. Often, however, medical physics tasks involve the design and use of completely new equipment, software and methods, or the development of techniques for using of existing systems for purposes other than those for which they were designed, or simply the development of methods for improving the accuracy or efficiency of existing processes. All such novel investigations should be recognised and shared, as research.

Sharing the methods and results of medical physics investigations allows physicists, radiation oncology staff and ultimately patients at other institutions to benefit from work completed locally. Using the scientific literature to share this information has the advantages of giving authors access to (usually free and unbiased) peer review by experts in the field, as well as international distribution and promotion of the work by commercial publishers.

Based on years of maintaining a high research output despite a full-time clinical workload, this presentation provides hints and tips for turning clinical medical physics work into publishable research, as well as anecdotes and horror stories of problems that can be encountered and how they can be handled.

KS11 Publishing in 2018: is it harder than 15 years ago?

L. Marcu

The University of Oradea

Is it harder to publish in 2018 than 15 years ago? If the number of scientists roughly doubled in the last 15 years and the number of scientific journals also doubled in that period, why is the general feeling in scientific circles that is has become harder to publish? The publishing effort probably depends on the quality standard of the targeted journals. Considering the growing importance of a scientist's publication record quality, are there significantly more well-respected scientific journals than there were 15 years ago or are we all competing for the same, limited publishing space? Papers often get rejected up-front, without any peer review, owing to the large number of manuscripts submitted. A common complaint from authors is that nowadays peer reviewers ask for more or even different experiments to prove the results, leading to a prolonged reviewing/publishing process. If a paper goes through several journals before eventual acceptance, did the multiple reviewing process improve the quality of the manuscript or just increased its time to publication?

On the other side of the equation, did the editorial process change significantly over the years to keep up with the exponential increase in submitted manuscripts? An emerging aspect that increases the burden on editors is the growing interest in interdisciplinary research, which often turns the review of an interdisciplinary paper into a saga due to incongruities between authors and referees. The broad range seen in publication times among journals is greatly influenced by the diligence of the editors and the scientific maturity of the referees.

Are we, as experienced scientists who one day seek to publish and another day are requested to review, treat this responsibility with its due importance? How could we improve both the editorial and reviewing processes to cut down the time to return a decision to the authors?

O130 Radiation therapy for patients with palliative care needs in the modern era: why medical physicists should care

W. A. Beckham[1], M. Chan[2], P. Hawley[3], M. McKenzie[3], R. Olson[4], I. Serrano[2], C. Tayler[5], S. Thomas[3], S. Tyldesley[3], K. Yue[5]

[1]BC Cancer – Victoria & University of Victoria, BC, Canada. (wbeckham@bccancer.bc.ca [Presenting author]). [2]BC Cancer – Vancouver, BC, Canada. (Matthew.Chan02@bccancer.bc.ca), (isabel.serranomartinez@bccancer.bc.ca). [3]BC Cancer – Vancouver, University of British Columbia, Vancouver, BC, Canada. (phawley@bccancer.bc.ca), (mmckenzi@bccancer.bc.ca), (sthomas-02@bccancer.bc.ca), (styldesl@bccancer.bc.ca). [4]BC Cancer – Prince George, University of British Columbia, Vancouver, BC, Canada. (rolson2@bccancer.bc.ca). [5]BC Centre for Palliative Care, New Westminster, BC, Canada. (CTayler@bc-cpc.ca), (kyue@bc-cpc.ca)

Introduction It is estimated in British Columbia (population 4.5 million) that only 15% of the 27,000 that die each year with palliative care needs actually access specialist palliative care services. 12,000 patients are treated annually at BC Cancer with radiation therapy (RT) about 6,000 are palliative intent. We assume that many in this latter group have unmet palliative care needs.

Cancer patients who are deemed palliative depend on appropriate RT to improve their health/quality of life. RT interventions can range from single field/fraction to complex stereotactic techniques[1,2]. Matching RT intervention with the patient's needs on a timely basis is key to effective palliative treatment.

Method On April 10, 2018 BC Cancer held a 1 day workshop in Vancouver to consider the development of an Interprofessional Provincial Palliative Care Radiation Oncology Site Group. There were about 50 participants from across the province including representatives from all disciplines and patient representatives. "World Café[3]" methodology was used to consider how the group could work together to improve quality of care and experience of patients and their families referred for palliative RT.

Results Several important concepts emerged from the workshop that medical physicists would generally be unaware of. Major impact on patient outcomes from palliative RT and treatment urgency reduction can be realised if the appropriate intervention is timed around symptom onset.

Regular stress screening of patients with palliative care needs is critical. Infrastructure is required to support stress screening in ways that maximise patient compliance. Existing patient reported outcomes processes[4] could be developed and allow measurable impact of optimised use of palliative RT.

Conclusion A major opportunity exists to improve quality of life for a large group of patients receiving RT that have palliative care needs.

Medical physicists are integral to developing efficient workflow processes for appropriate RT techniques.

References

1. Conway JL, Yurkowski E, Glazier J, Gentles Q, Walter A, Bowering G, Curtis S, Schellenberg D, Halperin R, Lapointe V, Beckham WA, Olivotto IA, Olson RA (2016) Comparison of patient-reported outcomes with single versus multiple fraction palliative radiotherapy for bone metastasis in a population-based cohort. Radiotherapy and Oncology 119:202–207.
2. Pfeffer MR & Blumenfeld P (2017) The Changing Paradigm of Radiotherapy in the Elderly Population. The Cancer Journal 23:223–230
3. The World Café Website. http://www.theworldcafe.com/. Accessed 29 May 2018.
4. Olson RA, Howard F, Lapointe V, Schellenberg D, Nichol A, Bowering G, Curtis S, Walter A, Brown S, Thompson C, Bergin J, Lomas S, French J, Halperin R, Tyldesley S, Beckham WA (2018) Provincial development of a patient-reported outcome initiative to guide patient care, quality improvement, and research. Healthcare Management Forum 31:13–17

O131 PAROT: a patient rotation study for MR-guided radiotherapy

J. Buckley[1], G. Liney[2], J. Dowling[3], R. Rai[4], B. Whelan[5], L. Holloway[4], P. Metcalfe[1], P. Keall[5]

[1]CMRP, University of Wollongong, NSW, Australia. (jgb552@uowmail.edu.au [Presenting author]), (metcalfe@uow.edu.au). [2]Ingham Institute for Applied Medical Research, Liverpool, NSW, Australia. (gary.liney@health.nsw.gov.au). [3]CSIRO Australian eHealth Research Centre, Herston, QLD, Australia. (jason.dowling@csiro.au). [4]Liverpool Hospital Cancer Therapy Centre, SWSLHD, Liverpool, NSW, Australia. (robba.rai@health.nsw.gov.au), (lois.holloway@health.nsw.gov.au). [5]ACRF Image-X Institute, Central Clinical School, University of sydney, NSW, Australia. (Brendan.whelan@sydney.edu.au), (paul.keall@sydney.edu.au)

Introduction The Australian MRI-Linac [1] combines a bespoke split bore 1.0 T MRI magnet with a fixed 6MV linear accelerator. Since the magnet and linac are both fixed, patient rotation will be required to achieve multiple beam angles.

One of the challenges with patient rotation is understanding and adapting for induced anatomical deformations. Limited literature exists in this space [2] and this knowledge gap forms the basis of this study.

Method A HREC approved pilot study has been initiated (PAROT) which will recruit 10 healthy volunteers to be followed by 30 radiotherapy cancer patients. Volunteers are imaged on a dedicated 3 Tesla radiotherapy MR scanner in a patient rotation system [2] (figure 1) at angles 0, 45 and 180-degrees. Angled scans were acquired using a fast (~50s) 2D T2w turbo spin echo (TSE) sequence. The images are rigidly aligned to a high resolution 0-degree image (3D isotropic T2w TSE 'SPACE' ~6min acquisition) followed by a non-rigid registration [3] to obtain a deformation field. The deformation field was exported to MATLAB to obtain mean, maximum and minimum deformations with standard deviation. This work describes initial imaging results.

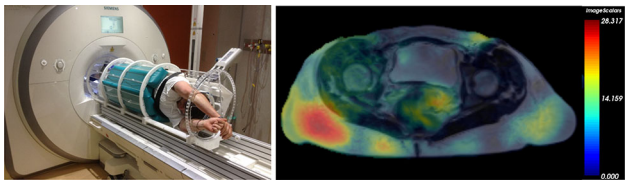

Results Maximum deformation was slightly worse at 45-degrees, measured as 32.00 mm compared with 28.00 mm for 180°. Maximum deformations occurred around the external surface due to changes in adipose tissue (figure 2). The lack of deformation around the bladder, rectum and cervix suggests deformations could be accounted for using rigid registration.

Conclusion A healthy volunteer was imaged on a patient rotation system at 0, 45 and 180-degrees. Mean deformations relative to the 0-degree of 3.40 ± 4.10 mm were observed, with the largest deformations at the external surface. Understanding the impact of anatomical deformation with rotation will be integral in the development of adaption methods for fixed beam patient rotation systems including the Australian MRI-Linac.

References

1. Keall PJ, Barton M, Crozier S (2014). Australian Mri-Linac Program. *Semin Radiat Oncol.* 24:203–206. http://dx.doi.org/10.1016/j.semradonc.2014.02.015
2. Whelan B, Liney GP, Dowling JA, et. al. (2017) An MRI-compatible patient rotation system—design, construction, and first organ deformation results. *Medical physics.* 44:581–588. https://doi.org/10.1002/mp.12065
3. Vercauteren T, Pennec X, Perchant A, Ayache N. (2009) Diffeomorphic demons: Efficient non-parametric image registration. *NeuroImage.* 45:S61–S72. https://doi.org/10.1016/j.neuroimage.2008.10.040

O132 Dosimetric optimisation and commissioning status of the Australian MRI-linac

U. Jelen[1], J. Begg[1,2,3], B. Dong[1], B. Whelan[4], N. Roberts[5], K. Zhang[1], A. George[2], L. Holloway[1,2,3,4,5], P. Keall[1,4], G. Liney[1,2,3,5]

[1]Ingham Institute for Applied Medical Research, Liverpool, Australia. (Urszula.Jelen@health.nsw.gov.au [Presenting author]), (Jarrad.Begg@health.nsw.gov.au), (KevinKun.Zhang@health.nsw.gov.au), (Bin.Dong@health.nsw.gov.au), (Lois.Holloway@health.nsw.gov.au), (paul.keall@sydney.edu.au), (Gary.Liney@health.nsw.gov.au). [2]Liverpool and Macarthur Cancer Therapy Centre, Liverpool, Australia. (Armia.George@health.nsw.gov.au). [3]University of New South Wales, Sydney, Australia. [4]University of Sydney, Sydney, Australia. (brendan.whelan@sydney.edu.au). [5]University of Wollongong, Wollongong, Australia. (nr593@uowmail.edu.au)

Introduction One challenge in MRI-linac technology is the magnetic field effect on radiation beam generation and dose deposition. The Australian MRI-linac prototype explores an inline configuration, which potentially allows to minimise or even to exploit these effects. This work describes dosimetric optimisation of the system and reports on its commissioning status.

Method The system consists of a 1 T split-bore magnet (Agilent) and an on-rail 6 MV linear accelerator (Varex) allowing SID variation. To utilise the shortest SIDs, alignment of the radiation beam to the magnetic field and magnetic shielding of the radiation head were

optimised. These steps were guided by investigative measurements: an MR test object (LTO), cross-hair phantoms and an EPID (Perkin Elmer) were used to refine the alignment and a Starcheck $^{maxi\ MR}$ (PTW) ionisation chamber array was used to assess the beam output loss and asymmetry resulting from undesired deflection of electrons in the linac.

Subsequently, machine performance was tested according to IEC60976/77 tailoring the methods to the unique aspects of our system. Absolute dose, beam quality and output factors were measured in a 1D water tank using a Farmer-type ionisation chamber FC-65G (Scanditronix Wellhöfer). The profile symmetry was assessed using Starcheck and depth and lateral dose profiles were acquired using EBT3 films (Ashland) in solid water.

Results Congruence of the radiation beam axis and the imaging isocentre within 2 mm was obtained. The dose monitoring system met IEC criteria. Symmetry was $< 103\%$ for fields up to 25x25 cm^2. Penumbra width was: 10.3 mm parallel and 8.7 mm perpendicular to the leaf direction and did not show asymmetry inherent to perpendicular configurations.

Conclusion The inline MRI-linac has been dosimetrically optimised and characterised constituting a key step towards its clinical application.

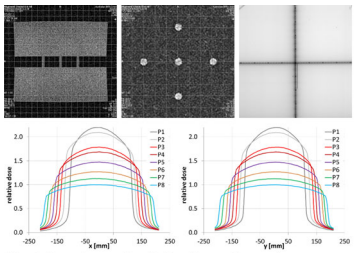

Fig. 1. Imaging and radiation beam isocentre congruence and beam profiles at various SIDs (P1-P8).

O133 Commissioning of an Elekta Leksell Gamma Knife (LGK) Icon^{TM} cone beam computer tomography (CBCT) and high definition motion management (HDMM) system

C. E. Jones[1], V. Seshadri[1], T. Markwell[2], B. Perrett[1]

[1]Radiation Oncology, Princess Alexandra Hospital, Brisbane. (catherine.jones3@health.qld.gov.au), (venkatakrishnan.seshadri@health.qld.gov.au [Presenting author]), (ben.perrett@health.qld.gov.au). [2]Radiation Oncology PA Raymond Terrace, Brisbane. (tim.markwell@health.qld.gov.au)

Introduction The GammaKnife Icon^{TM} enables frameless radiosurgery via a CBCT unit that both defines the stereotactic coordinate system and corrects for inter-fraction motion. The frameless co-ordinate system is determined from a high-dose preset CBCT to which the planning dataset is co-registered. Prior to each treatment fraction, a low-dose CBCT is registered to the initial high-dose acquisition. In addition, its HDMM system monitors intra-fraction motion with infrared reflectors and pauses treatment when patient motion exceeds a pre-defined limit. In this study we evaluate the performance of the ICON^{TM}'s frameless radiosurgery system.

Method Image quality was evaluated from CBCT acquisition of the Catphan 503 phantom which was docked to the treatment couch. Dosimetric parameters (CTDI, beam quality, mAs) were measured with a head CTDI phantom and Unfors detector.

Coincidence of the CBCT-based with the frame-based coordinate system was tested using a spherical solid water phantom to which the (frame-based) localizer box could be attached, and which could be docked to a CT-scanner and the treatment couch. Hence its coordinate system could be defined by fiducial markers (used in frame-based radiosurgery) and via CBCT. The coordinates of landmarks in each system were compared.

CBCT-to-CBCT registration was evaluated by translating and rotating a phantom on the treatment head support. Between movements, a CBCT was acquired, registered, and the location of landmarks recorded in each dataset.

The HDMM calibration was evaluated by moving an infra-red reflector a known distance in all three directions using Vernier dials, then observing the motion recorded by the HDMM system. HDMM functionality during treatment was observed by moving an infra-red marker with a motion platform operated from the control room.

Results Image quality and dosimetry were within Elekta specifications [1]. No error in image registration beyond the estimated experimental uncertainty was measured.

Conclusion The ICON's CBCT system has been successfully commissioned and is now being used for frameless and fractionated radiosurgery.

Reference

1. Design and performance characteristics of a Cone Beam CT system for Leksell Gamma Knife® Icon^{TM} (Elekta white paper). Downloaded 31/03/2018. www.careforthebrain.com/pdfs/Design_and_performance_1509394-03.pdf

O134 A data mining approach to monitor IGRT uncertainties to validate margins for stereotactic ablative body radiotherapy (SABR)

J. Luo

Nepean Cancer Care Centre, NSW. (jianjie.luo@health.nsw.gov.au mailto:a.n.author@gmail.com [Presenting author])

Introduction In order to insure uncertainties in the SABR treatment process are compatible with the clinical CTV to PTV margin, it is necessary to monitor a range of variables. This can be found in multiple clinical and physics databases. In this work, a tool for aggregating and analysing data is reported.

Method Data extraction was performed using web application utilising PHP and SQL from the Mosaiq OIS, Elekta's XVI imaging database and an in-house physics QA database. This data was analysed to determine trends in treatment sites, machine used and various setup changes.

The following patient specific data was assessed:

1. Patient Setup errors
    a) Intra-fraction motion

Quality assurance parameters may also influence calculated margins:

a) kV/MV deviation
b) Linear accelerator Iso-sphere

This uncertainty data was used to calculate a margin expansion, which was compared with clinical margin.

Results Margins for varies techniques are shown in table below. The margin for lung SABR, Spine SABR and Brain SRS were approx. 3.6 mm, 6.2 mm and 3.5 mm respectively. A difference of 0.7mm was noticed for Spine SABR between LA1 and LA2. However, this was not statistically significant. For Brain SRS, additional 1.3 mm margin for non-coplanar was required.

	mm	Brain SRS	Lung SABR	Spine SABR
LA1	X	3.6	6.4	3.8
	Y	3.5	6.3	3.8
	Z	3.6	6.6	3.8
LA2	X		6.0	3.5
	Y		5.8	3.1
	Z		6.2	3.3

Conclusion A tool was developed that could determine a margin to be utilised to determine patient specific margins for various treatment techniques. This program can be used to quickly and efficiently provide an up to date evaluation of the uncertainties based on current machine and patient performance. In future, the additional factors will be extracted from the databases and machine learning use for quality control.

KS13 Medical physics education in the USA

M. Dingfelder

Department of Physics, East Carolina University, USA. (dingfelderm@ecu.edu [Presenting author])

Introduction Medical physics education in the United States is strongly regulated to ensure a consistent quality and qualification of medical physicists entering the board certification process and the profession. In order to be eligible for board certification by the American Board of Radiology (ABR) [1], candidates must graduate from a CAMPEP (Commission on Accreditation of Medical Physics Education Programs) [2] accredited graduate program and complete a CAMPEP accredited residency program.
Method CAMPEP is a non-profit and sponsor-independent organization. On recommendation and in collaboration with the American Association of Physicists in Medicine (AAPM) [3] and the ABR, CAMPEP developed minimum standards every medical physics graduate program and residency has to meet. Individual institutions can develop and design program specific curricula by complementing the minimal standards with institutional or programmatic content. CAMPEP reviews and accredits educational programs. The Society of Directors of Academic Medical Physics Programs (SDAMPP) [4] which promotes the advancement of medical physics education worldwide also provides recommendations to the AAPM and CAMPEP.
Results This communication introduces first CAMPEP standards for graduate programs and residencies and illustrates how they are implemented in existing programs. East Carolina University [5] serves as an example, housing a Master's in Physics, a PhD in Biomedical Physics, and a residency program in therapy.
Conclusion This study provides information on medical physics education programs in the United States of America.
Acknowledgements We thank the organizers for conference travel funding.

References

1. The American Board of Radiology (ABR), www.theabr.org.
2. Commission on Accreditation of Medical Physics Education Programs (CAMPEP), www.campep.org.
3. American Association of Physicists in Medicine (AAPM), www.aapm.org.
4. The Society of Directors of Academic Medical Physics Programs (SDAMPP), www.sdampp.org.
5. Department of Physics, East Carolina University (ECU), www.ecu.edu/physics; Department of Radiation Oncology, Brody School of Medicine, ECU, www.ecu.edu/radiationoncology

O135 Australian postgraduate medical physics and the university of the future

Andrew L. Fielding

Science and Engineering Faculty, Queensland University of Technology, Brisbane, Australia. (a.fielding@qut.edu.au)

Introduction The Australian higher education sector is undergoing rapid changes. These changes will have an impact on the way teaching and research is conducted in Australian Universities. Additionally, the Medical Physics profession, through the MedPhys3.0 initiative is recognising that it is going to have to adapt to maintain relevance in the technology driven health care system of the future. The traditional role of being the scientific expert for the safe and effective use of ionising radiation for imaging and radiotherapy will need to be complemented by knowledge and skills in new areas such as robotics, big data, and artificial intelligence.
Method Ernst and Young [1] recently published a report outlining four possible models for the Australian University of the Future: (1) the Champion University, (2) the Commercial University, (3) the Disruptor University, and (4) the Virtual University. The consequences of what each of these models could mean for the highly specialised medical physics postgraduate course is considered.
Results The current scenario resembles the Champion University model with six campus based highly specialised Medical Physics postgraduate courses run largely independently. This would almost certainly not be sustainable in the Commercial University model. The Disruptor and Virtual University models will favour short unbundled courses where students study to gain new knowledge and skills at the appropriate point in their training and throughout their careers. This could lead to a more integrated, but modularised, medical physics education and training that could include traditional ionising radiation roles as well as new areas such as robotics, big data and artificial intelligence.
Conclusion The changes in the higher education sector in Australia could have profound implications on the way we deliver medical physics education and training and it is important that as a profession we are prepared.

Reference

1. Can the universities of today lead learning for tomorrow? The University of the Future, Ernst and Young. (2018)

IS12 Updates on TEAP from the ACPSEM

P. H. Charles[1,2]

[1]Radiation Oncology, Princess Alexandra Hospital, Brisbane, Australia. [2]Science & Engineering Faculty, Queensland University of Technology, Brisbane, Australia. (Paul.Charles@health.qld.gov.au)

A number of new initiatives to improve RO TEAP have recently begun. This talk will highlight some of these projects including: more robust examination assessment, improvements to the best works concepts, COMET and greater use of online resources (e.g. for level 1

sign offs and APR assessments), improvements to the points progress system, changes to the federal funding models (there are good changes!), and the impending TEAP review. Plus probably more, there's always more.

IS13 EPSM 2018 abstract: point of care ultrasound (POCUS) training in Papua New Guinea (PNG)

N .Parange

The University of South Australia

Papua New Guinea has one of the world's highest maternal mortality rates (MMR) with approximately 215 women dying per 100,000 live births. The comparable statistic for Australia is 7.1 deaths per 100,000 live births in non-indigenous population.

Infant mortality rate is 42.4 deaths per 1000 live births. In recent years, there have been increased efforts to reduce the high maternal mortality ratio (MMR) in Papua New Guinea, yet the lifetime risk of dying in pregnancy for a PNG mother is one in 20.

The World Health Organization's (WHO) Sustainable Development Goals aim to reduce the global MMR from 220 in 2013 to 70 by 2030 [1].

Common causes of maternal death in PNG include sepsis, low lying placenta leading to postpartum haemorrhage, ectopic pregnancies leading to catastrophic bleeds. Fetal and neonatal deaths here are common because of growth restriction and prematurity. A clear majority of these problems can be recognised on ultrasound, and most often, interventions can be applied to prevent mortality and morbidity, but there is a shortage of skilled personnel to diagnose these problems to be able to manage them effectively. POCUS training can be an efficient way of upskilling health professionals in a short period of time to enable them to learn life-saving skills.

This presentation will present the author's experiences and discuss advantages, challenges and benefits of POCUS training in PNG.

Reference

1. Sustainable Development Goals 2015. Transforming Our World; The 2030 Agenda for Sustainable Development A/RES/70/1. 2015. Geneva, Switzerland: World Health Organization; Available at: https://sustainabledevelopment.un.org/content/documents/21252030%20Agenda%20for%20Sustainable%20Development%20web.pdf. Accessed October 16th, 2017.

O136 Considerations for a dedicated MRI-simulator in a clinical radiation oncology setting

J. B. Simpson

Department of Radiation Oncology, Calvary Mater Newcastle, NSW. (john.simpson@calvarymater.org.au [Presenting author])

Introduction The increasing demands for tumour and soft tissue visualisation for improved radiotherapy targeting and normal tissue sparing has led to the increasing use of MRI in treatment planning. However utilising radiology based MRI in the simulation process produces compromises resulting from access constraints and temporal and physical remoteness from the radiation oncology department. Furthermore, recent developments in MRI-only treatment planning means that it is becoming possible to avoid CT-simulation altogether. Hence we are entering an era where CT-simulators can be replaced by MRI-simulators. The Calvary Mater Newcastle has just replaced one of its two CT scanners with an MRI scanner, in what is perhaps the first truly dedicated clinical MRI-simulator to enter service in Australia.

Method Drawing partly upon the recent Newcastle experience, this presentation will provide the author's personal insights into the subject. In particular he will be discussing the pros and cons for acquiring and/or replacing a CT-simulator with an MRI-simulator, the current technology, the clinical indications and future directions for MRI-simulation as well as the threats and opportunities that an MRI-simulator provides for the medical physics profession.

Results and conclusion In addition to improving the solutions for MRI-simulation including couch tops, coil bridges and acquisition protocols; commercial solutions are appearing for MRI-only planning and treatment response monitoring. However MRI-simulation is a developing field and many issues remain unresolved. Geometric distortion is a significant consideration for the selection of MRI-field strength and optimal scan technique. CT replacement requires an assurance of MRI-simulation workload which requires workable solutions for MRI-only treatment planning and efficient adaptive workflows which in turn requires solutions for quantitative MRI. An MRI facility produces unique challenges for site planning, safety and staff training. Finally, as a profession, the role and opportunities for the clinical medical physicist in the field of MRI-simulation, need to be appreciated.

O137 "Dose to Medium" a step in the wrong direction with regard to clinical radiotherapy

N. Bennie

North Coast Cancer Institute, Lismore, NSW, Australia. (Nick.Bennie@ncahs.health.nsw.gov.au [Presenting author])

Introduction This paper presents the case that Absorbed dose to water [1], which is the energy absorbed by a small volume of water, is a better indicator of the biological effect of ionising radiation than "Dose to Medium", a term used by several commercial, computer based TPS, that represents an estimate of the energy absorbed by a voxel, a defined unit of a patient which has a real size and in which the material properties are represented by a bulk average of all the individual parts that constitute a clinical tissue.

In modern clinical radiotherapy it is now recognised that damage to DNA is the principle mechanism of cell death [2], however it has always been recognised that it is only the effect of radiation on tissues that are actually alive that is important.

Previous generation TPS did not account for Mass Stopping Power, generally assuming all material had the same properties as water but did account for photon attenuation by allowing for Relative Electron Density, generally derived from CT data. Assuming a phantom with RED=1.0, then MSP accounts for the mass of a voxel and the energy absorbed by that voxel being different from water equivalent. That is, the Dose to parts composed of different materials is different.

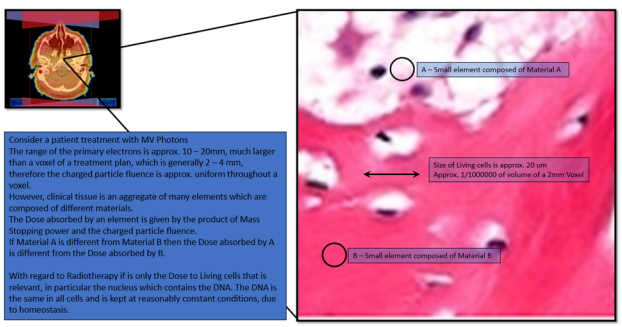

Fig. 1. Expanded representation of a patient at a scale comparable to Living cells

For a small "water like" cell within a voxel of "non-water like" material, Absorbed Dose to water is representative of the effect of the radiation on that living cell.

Method and materials Representative data was calculated using the Elekta Monaco and the Elekta XiO planning systems and compared against measurements in "non-water like" phantoms. Measurements were made with both ion chambers and film.

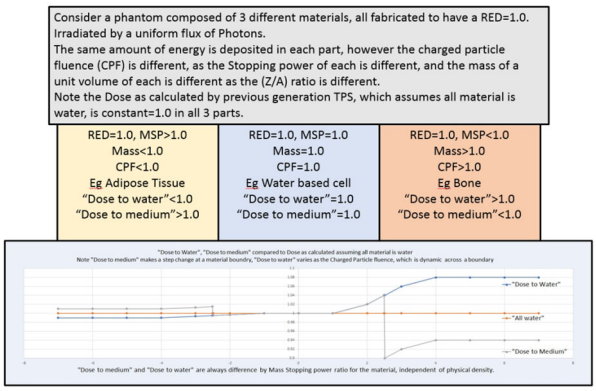

Fig. 2. Graph demonstrating Dose in different materials

Conclusion "Dose to Medium" is always a worse approximation to Absorbed dose to water than dose as calculated by previous generation TPS. That is, "Dose to Medium" is a step in the wrong direction with regard to predicting clinical effect in Radiotherapy.

References

1. Khan, F. M. (1994). The Physics of Radiation Therapy. 2nd Edition. Lippincott Williams & Wilkins. (ISBN 0-683-04502-4)
2. Hall, E. J. and Giaccia, A. J. (2012). Radiobiology for the Radiologist. 7th Edition. Lippincott Williams & Wilkins. (ISBN 978-1-60831-193-4)
3. Mayles, P., Nahum, A. and Rosenwald, J. C. (2007). Handbook of Radiotherapy Physics. Taylor & Francis. (ISBN 978-0-7503-0860-1)
4. Chetty, I. J. et Al (2007). Report of the AAPM Task Group No. 105: Issues associated with clinical implementation of Monte Carlo-based photon and electron external beam treatment planning. Medical physics, 34(12).
5. Andreo, P., Burns, D. T., Hohlfeld, K., Huq, M. S., Kanai, T., Laitano, F., … & Vynckier, S. (2000). IAEA TRS-398–Absorbed Dose Determination in External Beam Radiotherapy: An International Code of Practice for Dosimetry based on Standards of Absorbed Dose to Water. IAEA.
6. Elekta (Elekta AB, Stockholm, Sweden.) documents including: Monaco Dose Calculation Technical Reference and letter titled "SUMMARY OF DOSE TO WATER CALCULATIONS IN MONACO (V3.1 and later)" dist. Feb 2013.
7. ICRU 2011 Fundamental quantities and units for ionizing radiation ICRU Report 85a (Bethesda, MD)

O138 On the use of Eclipse's beam angle optimizer (BAO) for conformal planning: a feasibility study

Y. Yousif, J. Zifodya, W. Hsieh, S. McKinnon, A. Judge

North West Cancer Centre, Tamworth, Australia.
(yousif.yousif@hnehealth.nsw.gov.au),
(jackson.zifodya@hnehealth.nsw.gov.au [Presenting author]),
(wen-Long.hsieh@hnehealth.nsw.gov.au), (sally.mckinnon@hnehealth.nsw.gov.au), (Ali.Douglas@hnehealth.nsw.gov.au)

Introduction Current planning of 3DCRT is heavily dependent on the planner's experience, preferences and treatment facility expectations. Historical beam arrangements are often utilized. The objectives of this study were to employ Eclipse's Beam Angle Optimizer (BAO) to see if using the BAO for 3DCRT planning would: (1) produce better plans as compared to conventional methods, (2) reduce the planning time, and (3) partially reduce the dependence of plan quality on planner experience.

Method Eleven 3D conformal lung plans, with tumour volumes ranging from 32-3008 cc, were retrospectively studied. For each clinical plan (non-BAO plan), a separate plan (BAO plan) was produced using alternative beam angle arrangements generated using the BAO. The BAO plans were then optimized by an experienced planner. Plan quality was assessed using ICRU-83 and RTOG recommended dose reporting metrics for dose volume prescribing and reporting.

Results The difference in the DVHs for both the BAO and non-BAO plans showed no clinical significance. The PTV maximum doses for both plans were comparable and within the ICRU guidelines1. The reported maximum doses to the spinal cord as well as the doses to 33% and 67% volume of the heart were within the RTOG recommended limits. The mean lung V20 values for BAO and Non-BAO plans were 20% and 16% respectively. The average MUs for the BAO plans were about 11% lower than the non-BAO plans. The scored values of the conformity and homogeneity indices were within the acceptable range for both cases. On average, it took 23 min to plan using the BAO compared to 68 min for the non-BAO plans.

Conclusion The Eclipse BAO method shows the potential of reducing the time required to produce an acceptable conformal plan. The BAO tool can be utilized to produce good quality conformal plans and reduce planning time. It would be very helpful if the BAO could incorporate inserting MLCs as well as optimal collimator angles as these had to be inserted manually.

References

1. ICRU. International Commission on Radiation Units and Measurements Prescribing, recording and reporting photon beam therapy. ICRU Report 50. Oxford, United Kingdom: Oxford University Press; 1993.
2. Moore KL, Brame RS, Low DA, Mutic S. Quantitative metrics for assessing plan quality. Semin Radiat Oncol 2012; 22(1): 62–69
3. Crowe SB, Kairn T, Middlebrook N, Hill B, Christies DRH, Knight RT et al. Retrospective evaluation of dosimetric quality for prostate carcinomas treated with 3D conformal, intensity modulated and volumetric modulated arc radiotherapy. J Med Rad Sci 2013;60;131–138

O139 Commissioning and verifying doses from an automatic planning software for treating multiple brain metastases with single isocentre multiple dynamic conformal arcs

C. R. Moulton[1], R. Gajewski[1], T. Moodie[1], R. Stensmyr[1], S. Yau[1,2]

[1]Crown Princess Mary Cancer Centre, Westmead Hospital, Australia.
(calyn.moulton@health.nsw.gov.au [Presenting author]),
(romuald.gajewski@health.nsw.gov.au),
(trevor.moodie@health.nsw.gov.au),
(rachel.stensmyr@health.nsw.gov.au),

(shan.yau@health.nsw.gov.au). [2]Nepean Cancer Care Centre, Nepean Hospital, Australia.

Introduction Multiple brain metastases (mets) can be treated with stereotactic radiosurgery using automatic treatment planning software (TPS) such as Brainlab Elements which plans multiple dynamic conformal arcs with a single isocentre [1, 2]. This study covers the recent clinical implementation of the new technique including the aspects unique to the commissioning and the methods developed to verify doses.

Method The data and parameters for pencil beam modelling were verified by repeated measurements according to protocols from Brainlab [3]. To check the dose calculation, a dose was planned and measured for three mets centred over diodes in a ScandiDos 3D Delta [4] diode array phantom with multiple couch angles. The plan was mapped to a cylinder phantom with a CC04 chamber insert, the dose at the centre of each met was re-calculated and the plan was measured with the cylinder phantom. Additionally, a plan more representative of expected patient treatments was included as part of an end-to-end test by planning three mets on an anthropomorphic phantom with multiple couch angles. The plan was then delivered using ExacTrac positioning and measured by slices of radiochromic film within the phantom. The planned dose at centre of each met for the anthropomorphic (Rando) phantom plan was also verified by CC04 chamber measurements of mapped plan on the cylinder phantom. Additionally, the cylinder phantom was used for dose verification for five patients. Differences between the measured and TPS values were calculated.

Results The tables below summarise the results for commissioning and dose verification.

Test	Difference (Measured versus TPS)
Nominal linac output (beam parameter)	0.17%
Small field scatter factors (beam data)	-0.61% (MLCs 25 mm^2 and Jaws 64 mm^2)
Static leaf shift (beam parameter)	0.04 mm
Dynamic leaf shift (beam parameter)	-0.03 mm
MLC leakage (beam parameter)	-0.02%
Jaw+MLC leakage (beam parameter)	0.01%

Test	Max. Difference (Measured versus TPS)
Delta 4 measurements (commissioning)	-2.28%
Cylinder measurements for the Delta 4 plan (commissioning)	-0.19%
Film measurements for the Rando phantom plan (commissioning)	1.90%
Cylinder measurements for the Rando phantom plan (commissioning)	1.66%
Cylinder measurements for patient plans (dose verification)	1.57% (4 mets/plan) -2.01% (5 mets/plan) -2.47% (6 mets/plan) -1.87% (7 mets/plan) 2.23% (15 mets/plan)

Conclusion The Delta [4], cylinder and film were useful for commissioning the technique. A perturbation factor due to the CC04 chamber within the cylinder phantom was determined and applied for dose verification. Patient specific quality assurance includes comparing doses from Elements with re-calculations in the Varian Eclipse TPS using the anisotropic analytical algorithm [4].

References

1. Brainlab AG (2016) Software user guide revision 1.0: Elements physics administration version 5.0. Brainlab AG, Munich.
2. Brainlab AG (2017) Software user guide revision 1.0: Multiple brain mets SRS version 1.5.0. Brainlab AG, Munich.
3. Brainlab AG (2016) Technical reference guide revision 2.0: Brainlab physics. Brainlab AG, Munich.
4. Varian Medical Systems, Inc. (2015) Eclipse photon and electron algorithms reference guide. Varian Medical Systems, Inc., Palo Alto.

O140 MRI-only treatment planning for lung cancer using a single MRI sequence

T. Young[1,2], J. Dowling[3,4,5,6], D. Thwaites[2], S. Kumar[7], R. Rai[1,8], S. Vinod[8], G. Liney[7,10], A. Stemmer[12], S. Josan[12], L. Holloway[1,10,11,13]

[1]Liverpool and Macarthur Cancer Therapy Centres and Ingham Institute, Sydney, Australia. (Tony.Young@health.nsw.gov.au [Presenting author]), (Robba.Rai@health.nsw.gov.au), (lois.holloway@health.nsw.gov.au). [2]Institute of Medical Physics, School of Physics, University of Sydney, Sydney, Australia. (david.thwaites@sydney.edu.au). [3]CSIRO Health and Biosecurity, The Australian e-Health & Research Centre, Australia. (Jason.Dowling@csiro.au). [4]South Western Sydney Clinical School, University of New South Wales, Australia. [5]Institute of Medical Physics, University of Sydney, Australia. [6]School of Mathematical and Physical Sciences, University of Newcastle, Australia. [7]Liverpool and Macarthur Cancer Therapy Centres and Ingham Institute, Sydney, Australia. (Shivani.Kumar@health.nsw.gov.au), (Gary.Liney@health.nsw.gov.au). [8]University of New South Wales, Sydney, New South Wales, Australia. (Shalini.Vinod@health.nsw.gov.au). [9]Liverpool and Macarthur Cancer Therapy Centres, Sydney, Australia. [10]University of New South Wales, Sydney, New South Wales, Australia. [11]Centre for Medical Radiation Physics, University of Wollongong, Wollongong, New South Wales, Australia. [12]Siemens Healthcare, Erlangen, Germany. (alto.stemmer@siemens-healthineers.com), (sonal.josan@siemens-healthineers.com). [13]Institute of Medical Physics, School of Physics, University of Sydney, Australia.

Introduction The need for an MRI-only workflow which provides electron density information for hybrid Magnetic Resonance Imaging guided Linear Accelerators (MRIg-linacs) in radiotherapy has increased. Investigations into segmented bulk density corrections to tissue, bone and lung have reported results for point dose calculations in lung within 2% [1]. However, a more recent study investigating the effect on dose volume parameters concluded that this approach may not be appropriate for lung MRI only planning [2]. Other correction methods including atlas and voxel based methods have been used in sites such as brain and prostate for MRI only treatment planning with success [3]. In this study the accuracy of an atlas based auto segmentation method to generate substitute CT (sCT) for lung patients from a single MRI sequence was investigated.

Method Simulation CT and MRI scans were completed on 11 lung cancer patients. 3D ultrashort-echo-time (UTE) images were acquired on a Siemens MAGNETOM Skyra 3T MRI under free breathing using a prototype spoiled gradient echo sequence utilizing a variable TE stack of spirals trajectory (SpiralVIBE) [5, 6]. The SpiralVIBE MRI scans were converted to sCT using an existing methodology validated for the male pelvis [4]. All generated sCT were compared against the original CT dataset for Hounsfeld Unit (HU) differences, and 10 sCT datasets were evaluated for dosimetric differences against the clinical treatment plan.

Results The mean error for the 11 generated sCT datasets was 17.2HU (SD 71.3HU), and the mean absolute error was 162HU (SD 66.7HU). For dose calculations, 9/10 datasets met a 3% point dose tolerance.

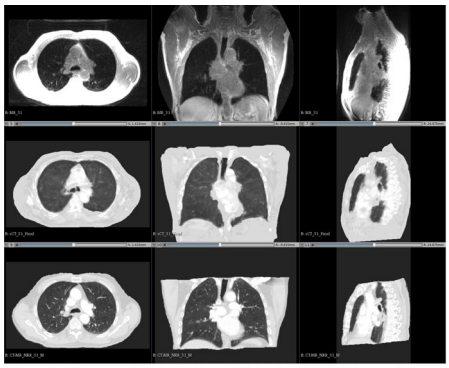

Figure 1 – An example of a patient MRI (top), clinical CT scan (bottom) and generated sCT (middle)

Conclusion Lung MRI datasets were converted to sCTs for treatment planning with reasonable agreement with the original CT datasets, and treatment plans.

References

1. Jonsson J, Karlsson M, Karlsson M, Nyholm T (2010) Treatment planning using MRI data: an analysis of the dose calculation accuracy for different treatment regions. Radiation Oncology 5 (1):62
2. Phil P, Xinfeng C, Elizabeth G, Candice J, Allen LX (2017) Technical Note: Is bulk electron density assignment appropriate for MRI-only based treatment planning for lung cancer? Medical Physics 44 (7):3437–3443. https://doi.org/10.1002/mp.12267
3. Johnstone E, Wyatt JJ, Henry AM, Short SC, Sebag-Montefiore D, Murray L, Kelly CG, McCallum HM, Speight R (2018) Systematic Review of Synthetic Computed Tomography Generation Methodologies for Use in Magnetic Resonance Imaging–Only Radiation Therapy. International Journal of Radiation Oncology Biology Physics 100 (1):199–217
4. Dowling JA, Sun J, Pichler P, Rivest-Hénault D, Ghose S, Richardson H, Wratten C, Martin J, Arm J, Best L (2015) Automatic substitute computed tomography generation and contouring for magnetic resonance imaging (MRI)-Alone external beam radiation therapy from standard MRI sequences. International Journal of Radiation Oncology* Biology* Physics 93 (5):1144–1153
5. John P. Mugler, III, Samuel W. Fielden, Craig H. Meyer, Talissa A. Altes, G. Wilson Miller, Alto Stemmer, Josef Pfeuffer, and Berthold Kiefer. Breath-hold UTE Lung Imaging using a Stack-of-Spirals Acquisition. Proc. Intl. Soc. Mag. Reson. Med. 23 (2015) #1476.
6. Samuel Fielden, John Mugler, Wilson Miller, Alto Stemmer, Josef Pfeuffer, Berthold Kiefer, and Craig Meyer. A Variable-TE Stack-of-Spirals Sequence for 3D UTE Imaging. Proc. Intl. Soc. Mag. Reson. Med. 24 (2016) #1062

O141 PlanEval: a dose volume metric reporting tool for multivendor treatment planning system environment

P. Narayanan[1], C. Ochoa[1], G. Dinsdale[1], J. Veneran[1], S. Arumugam[2,3,4]

[1]Macarthur and Liverpool Cancer Therapy Centres, SWSLHD, Sydney Australia. (Pradush.Peethambaran@health.nsw.gov.au [Presenting Author]), (Cesar.Ochoa@health.nsw.gov.au), (Glen.Dinsdale@health.nsw.gov.au), (Joanne.Veneran@health.nsw.gov.au). [2]Liverpool and Macarthur Cancer Therapy Centres, Liverpool, NSW, Australia. (Sankar.Arumugam@health.nsw.gov.au). [3]Ingham Institute for Applied Medical Research, Sydney, NSW, Australia. [4]South Western Sydney Clinical School, University of New South Wales, Sydney, NSW, Australia.

Introduction Modern radiotherapy plan evaluation requires Dose Volume Metrics (DVMs) of number of target volumes (TVs), organs at risk (OARs) to be quantified for its compliance with the planning guidelines. The purpose of this study is to present the development and validation of an in-house tool that generates a formatted report of DVMs for plan evaluation, reporting and documentation in a multi-vendor Treatment Planning System (TPS) environment.
Method An in-house software system, PlanEval, was developed to analyse the dose volume histograms (DVHs) exported from Pinnacle and Tomotherapy TPSs in ASCII file format. The system allows the configuration of site specific treatment protocols. Within each protocol, the TVs and OARs structure names and the required DVMs for each structure can also be configured. In clinical sites where multi-level target dose and different dose combinations being used, the system allows the user to enter the dose values. From this, the system automatically identifies the TVs for the entered dose and computes the relevant DVMs. Additionally, the system automatically populates the computed DVM data in a structured format and reports its compliance with department planning guidelines. The performance of PlanEval was verified by analysing the DVH data of head and neck, lung, prostate and cervix modulated treatment plans from Pinnacle and Tomotherapy TPSs. The accuracy of PlanEval reported DVMs were verified against the same metrics calculated in the TPS.
Results The PlanEval system successfully analysed the DVH data exported from both Pinnacle and Tomotherapy TPSs. PlanEval has generated the formatted report for above mentioned clinical protocols with multilevel dose prescription. A maximum difference of 0.6 and 1% was observed between PlanEval reported and TPS calculated absolute and relative DVMs respectively.
Conclusion PlanEval has shown to successfully generate the formatted DVM reports which can improve the efficiency of plan evaluation and dose reporting.

O142 Daily dose accumulation for individual patients to assess the validity of reduced PTV margin plans in head and neck radiation oncology

N. Lowther[1], K. Peick[1], S. Marsh[2], R. Louwe[1]

[1]Wellington Blood and Cancer Centre, Wellington, New Zealand. (nick.lowther@ccdhb.org.nz [Presenting author]), (karsten.peick@ccdhb.org.nz), (rob.louwe@ccdhb.org.nz). [2]University of Canterbury, Department of Physics and Astronomy, Christchurch, New Zealand. (steven.marsh@canterbury.ac.nz)

Introduction Reduced treatment toxicity while maintaining equivalent local-regional control rates have been reported after reducing planning target volume (PTV) margins from 5 to 3 mm for Head and Neck radiation oncology [1, 2]. This retrospective study investigates the feasibility of a 3 mm PTV margin plan in combination with a 5 mm backup plan to account for clinically relevant anatomical changes. Specifically, the robustness of treatment plans using a 3 or 5 mm PTV margin for anatomical changes will be investigated as well as strategies for timely intervention.
Method Volumetrically modulated arc therapy (VMAT) plans for 12 patients using 3 or 5 mm PTV margins were created. Deformable image registration (DIR) of the planning CT-to-cone beam CTs was performed to reconstruct the daily delivered dose to target and organ-

at-risk (OAR) structures. The cumulative DVH was calculated for clinical target volumes (CTVs), PTVs and OARs as input data to develop different strategies for treatment adaptation.

Results Preliminary results for the 3 patients (7 CTVs and 7 PTVs total) demonstrating the largest anatomical changes during treatment showed an average salivary gland sparing of 2.6 Gy (D_{mean}) for 3 mm PTV margin plans. Overall, the increase in reconstructed OAR delivered dose from the start to end of treatment was small. The maximum OAR increase was 2.2 and 2.8 Gy for 3 mm and 5 mm plans for the parotid glands, respectively. For a 3 mm PTV margin, the cumulative D_{98} was less than 95% for 1 CTV (Figure 1) and 6 PTVs. For a 5 mm expansion, this was observed for 6 PTVs but not for the CTVs.

Conclusion PTV margin reduction resulted in increased OAR sparing. Timely detection of inadequate target coverage due to anatomical changes is feasible and enables timely intervention by using a 5 mm PTV margin plan for the remaining treatment fractions.

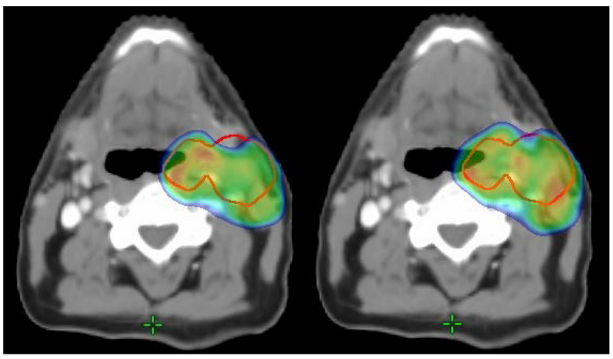

Figure 1: Deformed high-dose CTV (red contour) and the dose ≥ 95% $D_{prescribed}$ shown as colourwash for patient 1, treatment fraction 20. The CTV coverage (V95%) is less than 98% for the 3 mm PTV margin plan (left) but fully preserved for the 5 mm PTV margin plan (right).

References

1. Chen AM, Farwell DG, Luu Q, Donald PJ, Perks J, Purdy JA. Evaluation of the planning target volume in the treatment of head and neck cancer with intensity-modulated radiotherapy: What is the appropriate expansion margin in the setting of daily image guidance? Int J Radiat Oncol Biol Phys 2011;81:943–9. https://doi.org/10.1016/j.ijrobp.2010.07.017.
2. Chen AM, Yu Y, Daly ME, Farwell DG, Benedict SH, Purdy JA. Long term experience with reduced planning target volume margins and intensity modulated radiotherapy with daily image guidance for head and neck cancer. Head Neck 2014;36:1766–72. https://doi.org/10.1002/hed.

O143 Radiation oncology medical physics in Bangladesh: origin and future directions

M. Akhtaruzzaman[1], H. A. Azhari[2], G. A. Zakaria[3]

[1]Clinical Oncology Department, Ahsania Mission Cancer and General Hospital, Dhaka, Bangladesh. (akhzam@gmail.com [Presenting author]). [2]Department of Medical Physics & Biomedical Engineering, Gono Bishwabidyalay, Dhaka, Bangladesh. (ahasinanupama@gmail.com). [3]Department of Medical Radiation Physics, Gummersbach Hospital, Academic TeachingHospital of the University of Cologne, Gummersbach, Germany. (golam.zakaria@hs-anhalt.de)

Introduction Activities of medical physics in Bangladesh were started in the nineties mainly through several international seminars. As a result, a two-year M.Sc (2000) and a four-year B.Sc course (2005) have been started at Gono Bishwabidyalay (GB), Dhaka.According to WHO, 640 radiation oncology medical physicists (ROMPs) and 320 radiotherapy centers are required for about 160 million people of Bangladesh. However, there are only 20 centers equipped with 13 Co-60, 18 linacs, 10 CT-Simulators, 10 Brachytherapy and the total number of ROMPs is 40.

Methods From the beginning, the establishment of medical physics course in GB starts under a collaboration between Heidelberg University, Germany and GB. During 2003–2006 and 2014–2017, a total of 70 manpower has been trained in different aspects such as MSc degree, PhD experimental part, academic and clinical training for medical physicists under the financial support of German Academic Exchange Programme (DAAD). This collaboration is extended further for 2018–2021 for fostering the educational and professional development in Bangladesh as well as South Asia. However, a majority of students completes their B.Sc and M.Sc with a six-month clinical attachment under a collaboration between the university and the local radiotherapy centers.

Results ROMPs having MSc in Medical Physics are working in almost all radiotherapy centers in Bangladesh. Bangladesh Medical Physics Society (BMPS) has already been taken initiatives creating more medical physicist positions in the public hospitals. Establishment of a national certification board and a clinical residency programme with the support of International Medical Physics Certification Board (IMPCB) is on the process. Recently, IMPCB exam held in Dhaka on 13–14 March 2018.

Conclusion The ROMP situation in all aspects is improving remarkably. In future,national and international cooperation will augment the development process and a certain number of qualified medical physicists will be developed to establish the accreditation programme nationally.

O144 The influence of inhomogeneity correction factors on beam quality variations performed with the AAA correction method implemented in the Eclipse treatment planning system

M. Akhtaruzzaman[1,2], P. Kukolowicz[2]

[1]Clinical Oncology Department, Ahsania Mission Cancer and General Hospital, Dhaka, Bangladesh. (akhzam@gmail.com [Presenting author]). [2]Medical Physics Department, Maria Sklodowska-Curie Memorial Cancer Centre and Institute of Oncology, Warsaw, Poland. (pawel.kukolowicz@gmail.com)

Introduction The purpose of the study was to investigate the dependence of tissue inhomogeneity correction factors (ICFs) for a range of photon beam quality.

Methods Heterogeneous lung (0.26 g/cm^3), adipose tissue (0.92 g/cm^3) and bone (1.85 g/cm^3) phantoms were constructed in Eclipse treatment planning system. The calculations were performed with Anisotropic Analytical Algorithm (AAA) for a range of beam quality for 6MV ($TPR_{20,10} = 0.670 \pm k*0.01$) and 15MV ($TPR_{20,10} = 0.670 \pm k*0.01$), $k = -3, -2, -1, 0, 1, 2, 3$. This range of energy spectrum was obtained based on the data collected for the 42 accelerators installed in Poland. The ICFs were calculated for several beam sizes and for points lying at several depths inside and below of different thicknesses of heterogeneous tissues.

Results Experiments showed that ICFs increase for lung and fat with increasing the beam quality, while decrease for bone tissue. Calculations with AAA predicted that the 6% variations in energy lead to changes of ICFs 5.7% (6MV) and 8.7% (15MV) for points inside lung tissue. For points just below the water-lung interface, ICFs differed

the maximum of 9.2% and 13.8% for 6MV and 15MV respectively. In case of fat, less than 1% differences were obtained for both 6 MV and 15 MV, when calculated inside and below fat tissues. For bone, 1% (6 MV) and 1.5% (15 MV) variations were observed for points inside, while 2% (6 MV) and 2.4% (15 MV) differences were found for points lying just below the bone slab. These differences of ICFs decreased with increased radiation fields and the calculation depths below heterogeneous slabs where charged particle equilibrium (CPE) exists.
Conclusion Variations of beam quality lead to considerable changes in ICFs for points inside and below the inhomogeneity. Much smaller differences were obtained for larger fields and for points lying below inhomogeneous tissues where CPE exists.

P01 A dosimetric study on the dose to normal lung for lung cancer patients undergoing intensity modulated radiation therapy (IMRT) and volumetric modulated radiation therapy (VMAT)

H. Albarakati, P. Ramachandran, M. Geso

Peter MacCallum Cancer Centre, VIC.
(Hassan.Albarakati@petermac.org Presenting Author]),
(Ramachandran.Prabhakar@petermac.org),
(Moshi.Geso@rmit.edu.au)

Introduction Radiotherapy has been shown to be effective in improving the longevity of most lung cancer patients. Dose to normal lung poses a limit on the dose delivered to lung tumor volume and the dose to healthy lung volume is also impacted by the type of radiotherapy treatment techniques. In this study, we compared V5, V20, V30 volumes received by normal lung for patients undergoing intensity modulated radiatio therapy (IMRT) and volumetric modulated radiation therapy (VMAT) to large centralised tumor volumes.
Methods Ten patient undergoing lung cancer radiotherapy were selected for this study. IMRT Plans were generated for all patients with six to seven coplanar beam angles and two arcs VMAT plans were generated with collimator angles at 30° and 330° for arc 1 and arc 2. Two normal lung volumes that excludes the clinical target volume and the gross target volume were computed volumes receiving V5, V20 and V30. In addition to this we also computed the dose to heart, lung, Oesophagus and the various dosimetric indices for PTV. The mean GTV, CTV and PTV volumes included in this study were 204.29 cc, 430.1 cc and 648.96 cc respectively. We also computed the normal tissue complication probability for both treatment techniques.
Results The mean dose to normal lung receiving 5 Gy (Bilateral lung–GTV) was 56.72 ± 11.68% for IMRT as compared to 64.62 ± 17.32% for VMAT. The mean dose to bilateral lung–GTV was 14.43 ± 3.39 Gy for IMRT as opposed to 16.28 ± 3.96 Gy for VMAT plans. The results of our study shows that dose to normal lung with VMAT was higher than the dose with IMRT for large centralised lung volume.
Conclusion Our study shows that IMRT results in relatively less dose to normal lung as compared to VMAT for centralised tumors. However, VMAT exhibited improved dosimetry as compared to IMRT.

P02 A Monte Carlo study of the effects of monochromatic synchrotron-generated x-rays on mammalian cell lines

C. Allen, L. J Day, J. C. Crosbie

School of Science, RMIT University, Australia.
(cjlallen93@gmail.com [Presenting author]),
(liam.day@rmit.edu.au), (jeffrey.crosbie@rmit.edu.au)

Introduction Cell irradiation studies are an important technique for determining the fundamental mechanisms behind the cellular response to radiation [1–3]. These studies are an important method for understanding novel radiotherapy techniques to eventually predict and improve patient outcomes. However, as radiation effects are generally dose dependent, it is of little value to observe a given radiation response with limited knowledge of the dose used to obtain it. Therefore, we aim to use Monte Carlo methods to simulate the dose deposition in mammalian cells, as a result of an x-ray microbeam probe and an x-ray broad beam.
Method Monte Carlo simulations were performed using the Geant4 toolkit [4]. The 12 keV x-ray microbeam source is based on the X-ray Fluorescence Microbeam (XFM) beamline at the Australian Synchrotron [5]. Cellular irradiation geometries used range from a simple x-ray microbeam incident on a single cell, to an x-ray broad beam incident on a monolayer cell culture, based on cellular irradiations currently being performed at the Australian Synchrotron.
Results Preliminary results show a difference of approximately 6% between the dose deposited in a single cell model consisting of soft tissue, and a cell model consisting of water. An initial calculation for the absorbed dose to a cell comprised of soft tissue, was 276 nGy/photon ± 1%. A plot of energy deposited per photon, based on our preliminary results, is given in Figure 1.

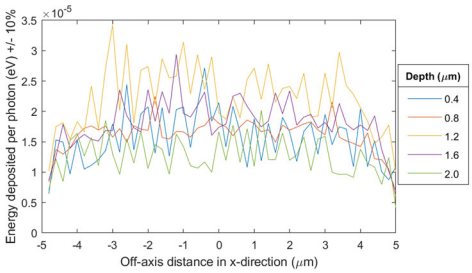

Figure 1. Energy deposited per photon at varying depths for a cell comprised of soft tissue.

Conclusion Estimating the dose deposition on the scale of micrometres is exceedingly difficult. Monte Carlo methods provide a more accurate method of estimating the dose to cells in cellular irradiation studies.

References

1. Prise KM, Schettino G (2011) Microbeams in radiation biology: review and critical comparison. Radiat Prot Dosimetry 143:335–339. https://doi.org/10.1093/rpd/ncq388
2. Kobayashi Y, Funayama T, Hamada N, et al (2009) Microbeam Irradiation Facilities for Radiobiology in Japan and China. J Radiat Res 50:A29–A47 . https://doi.org/10.1269/jrr.09009s
3. Sprung CN, Cholewa M, Usami N, et al (2011) DNA damage and repair kinetics after microbeam radiation therapy emulation in living cells using monoenergetic synchrotron X-ray microbeams. J Synchrotron Rad, J Synchrotron Radiat 18:630–636 . https://doi.org/10.1107/s0909049511011836
4. Agostinelli S, Allison J, Amako K, et al (2003) Geant4—a simulation toolkit. Nuclear Instruments and Methods in Physics Research Section A: Accelerators, Spectrometers, Detectors and Associated Equipment 506:250–303 . https://doi.org/10.1016/s0168-9002(03)01368-8
5. Paterson D, Jonge MD de, Howard DL, et al (2011) The X-ray Fluorescence Microscopy Beamline at the Australian Synchrotron. In: AIP Conference Proceedings. AIP Publishing, pp 219–222

P03 Study of radiation dose from computed tomography technique in Aljouf Region (Saudi Arabia)

Z. A. Alrowaili, M. Ashari

Physics Department, Faculty of Science, Jouf University, KSA. (zalrowaili@ju.edu.sa. [Presenting author]), (mashari@ju.edu.sa)

Introduction The goal of this work is to survey radiation absorbed doses from CT examinations of patients in Aljouf region in northern Saudi Arabia and to compare the results with the reference dose values.
Method The required data was collected using a questionnaire form in ten hospitals for a sample of 750 patients. Information about the patient, scanner, procedure, and technique for routine CT examinations has been collected. For each examination, the absorbed dose has been observed on a CT dose phantom measuring 16 cm (head) and 32 cm (body) in diameter. The normalized computed tomography dose index was calculated by using the collected data. Volume computed tomography index (CTDIVOL) and computed tomography dose-length product (DLP) value was calculated using the observed normalized CT index and questionnaire information. The effective dose was determined using the measurements and suitable normalized coefficients.
Results The sample size ensured a good representation of CT practice patterns in Aljouf. The results are as follows: the mean CTDIVOL and DLP values were comparable or below the reference doses: 58mGy and 753mGycm, respectively at head CT; 10.9mGy and 259mGycm, respectively at pelvis CT; 11.1mGy and 428mGycm, respectively at abdominal CT; and 10.9mGy and 319mGycm, respectively at chest CT. The corresponding effective doses were 1.5, 3.9, 6.4 and 4.6 mSv, respectively.
Conclusion The study is offering a first national dose survey in Aljouf region and establishes basis for quality control.

References

1. International Atomic Energy Agency. Dosimetry in diagnostic radiology: an international code of practice. IAEA TRS. No 457. Vienna: IAEA; 2007.
2. Muhogora WE, Ahmed NA, Almosabihi A, et al. Patient doses in radiographic examinations in 12 countries in Asia, Africa, and Eastern Europe: initial results from IAEA projects. AJR Am J Roentgenol 2008; 190:1453–61.
3. Muhogora WE, Ahmed NA, Beganovic A, et al. Patient doses in CT examinations in eighteen countries: Initial results from International Atomic Energy Agency Project. Rad Prot Dosim 2009;136(2):118–26.
4. International Commission on Radiation Measurements and Units. Patient dosimetry for X-rays used in medical imaging, ICRU report no. 74. ICRU, Bethesda, MD; 2006.
5. I.I. Suliman, S.E. Abdalla, et al. Survey of computed tomography technique and radiation dose in Sudanese hospitals, EURR 2011; 5116: 544–551.
6. European Communities. European guidelines on quality criteria for computed tomography. EUR 16262. Luxembourg; 1999.
7. International Electrotecnical Commission. Medical electrical equipment – part 2–44: particular requirements for the safety of X-ray equipment for computed tomography. IEC-60601-2-44. Geneva: IEC; 2002.
8. Kalender WA,Wolf H, Suess C, et al. Dose reduction in CT by on-line tube cur- rent control: Principles and validation on phantoms and cadavers. Eur Radiol 1999;9:323–8.

P04 Initial results from an inter-departmental comparison of VMAT patient QA using the ArcCheck device

S. Alzaidi[1], D. Truant[2], E Claridge Mackonis[1], J Sykes[2,3], R Hill[1,3]

[1]Department of Radiation Oncology, Chris O'Brien Lifehouse, Sydney, Australia. (samara.alzaidi@gmail.com [Presenting author]). [2]Radiation Oncology Medical Physics, Blacktown Cancer & Haematology Centre, Sydney West Cancer Network. [3]Institute of Medical Physics, School of Physics, The University of Sydney, Australia

Introduction 3D detector arrays are commonly used for pre-treatment verification of IMRT/VMAT patient treatment plans. The commissioning of these devices is involved, which could lead to variation in performance of the 3D dose verification system. The purpose of this project was two inter-compare the implementation of two independent SunNuclear ArcCheck devices used for the verification of VMAT plans at two institutions.
Method A range of VMAT patient treatment plans, both passing and failing local tolerance criteria were selected at both sites for comparison. The verification DICOM plan files were exported from Eclipse TPS at Centre 1 and re- imported and recalculated at Centre 2 using their Eclipse and beam model. Plan verification was performed at Centre 2 Truebeam linear accelerator with Centre 2 ArcCheck device. This was repeated in reverse with Centre 2 plans verified at Centre 1. Measured vs. TPS doses were analysed using both centres' tolerances being either Gamma calculations at 3%/3 mm (Tol1) or DTA at 3%/2 mm(Tol2) with a 10% threshold.
Results Centre 1 plans when measured at centre 2 had a significantly higher percent agreement in measured points compared to measurement at centre 1 with both Tol1 and Tol2 ($P < 0.001$). However, there was no significant difference between Centre 2 plans measured at the two centres with the range of differences between the paired measurements much greater than with Centre 1 plans.
These initial results suggest either beam modelling was closer to delivered beam or ArcCheck performance was superior at Centre 1. The lower percent agreement and increased range of differences between measurements at Centre 1 and 2 indicate that Centre 1's plans were more difficult to verify.
Conclusion Initial results point to differences in verification performance between the centres. These will be investigated further by also swapping the ArcCheck and widening the audit to include more centres.

P05 Real-time abdominal tumour tracking in a general purpose accelerator using an in-house developed position monitoring system

S Arumugam[1,2,3], A. Xing[1,2,3], L. Holloway[1,2,3,4,5]

[1]Liverpool and Macarthur Cancer Therapy Centres, Liverpool, NSW, Australia. (Sankar.Arumugam@health.nsw.gov.au [Presenting author]), (Aitang.Xing@health.nsw.gov.au), (Lois.Holloway@health.nsw.gov.au). [2]Ingham Institute for Applied Medical Research, Sydney, NSW, Australia. [3]South Western Sydney Clinical School, University of New South Wales, Sydney, NSW, Australia. [4]Institute of Medical Physics, School of Physics, The University of Sydney, Sydney, New South Wales, Australia. [5]Centre for Medical Radiation Physics, University of Wollongong, Wollongong, NSW, Australia.

Introduction Purpose: To develop and validate a real-time position monitoring system that enables abdominal tumour tracking in a general purpose linear accelerator.
Methods A software tool, SeedTracker, was developed in-house to enable online position verification of abdominal tumours by monitoring the position of implanted low contracst markers. The developed system estimates the 3D position of the tumour using monoscopic x-ray images acquired using the Elekta XVI system by following two main steps.

1. Calculate the amplitude binned 3D positions of markers and plan isocentre using Cone Beam Computed Tomographic (CBCT) projection images acquired for patient positioning.
2. Estimate the 3D position of isocentre based on the marker positions in the projection image acquired during treatment and learned 3D position information.

The performance of SeedTracker was evaluated using retrospective analysis of two sets of CBCT projection images, acquired in the same treatment session, of five liver and pancreas SBRT patients. The first set of projection images were used for learning the 3D position. The 3D position of markers and isocentre during the acquisition of second set of monoscopic images was estimated using the binned data and markers position in the images.. The accuracy of estimated 3D positions were compared with the XVI reconstructed 4D-CBCT data of the second image set.
Results The SeedTracker system successfully segmented the low contrast markers in the projection images acquired at gantry angles ranging from 0° to 360° and showed a True Positive Rate of 94%. The 3D position of markers and plan isocentre estimated by SeedTracker agreed with the XVI reconstructed data with a mean (σ) difference of 0.3 (1.6) mm.
Conclusion The developed software has been shown to estimate the 3D position of the markers and planned isocentre using the monoscopic x-ray images. This system has the potential application of monitoring tumor position during abdominal hypofractionated radiotherapy.

P06 Implementation of VMAT for craniospinal irradiation (CSI): overcoming treatment couch design

V. Beenstock[1], J. P. Ronaldson[1], C. Pyle[2], B Hindson[2]

[1]ROMP, Medical Physics and Bioengineering, Christchurch Hospital, New Zealand. (victoria.beenstock@cdhb.health.nz [Presenting author]), (paul.ronaldson@cdhb.health.nz). [2]CRCBS, Christchurch Hospital, New Zealand. (cassey.pyle@cdhb.health.nz), (benjamin.hindson@cdhb.health.nz)

Introduction In 2017 we implemented VMAT for craniospinal irradiation previously treated with 3D conformal radiation therapy to improve dose homogeneity, conformity and reduce treatment times. Set-up was changed from prone to supine to improve GA access and patient stability. Treatment through the end of the couch was required to treat the whole volume with only longitudinal couch shifts. We developed a model of the iBeam evo couch-top in the treatment planning system to ensure accurate dose calculation and delivery.
Method Patient immobilisation was developed by the radiation therapists establishing a fixed position for the end of the couch against the immobilisation. The magnitude of the couch attenuation was assessed using the ArcCHEK diode array to create a model in Monaco and validated using GafChromic Film with solid water. Parts of this model and immobilisation were used for treatment set up verification.
Results The end of the couch is not uniform in shape or density resulting in attenuation between 5–40%. Six structures requiring relative electron densities between 0.05–1.35 were made.

The fluence measurements with ArcCHECK and GafChromic film agreed with Monaco with a 100% pass rate for a 2%/2 mm absolute dose gamma analysis

Monaco IMRT optimises delivery to account for the couch to maintain a homogenous dose distribution. The position of the couch is fixed relative to the S-frame immobilisation device so the high density edges and S-frame locking pins were required to ensure couch position reproducibility in patient set-up.
Conclusion We have shown that a couch model in Monaco can be created using physical and dose attenuation properties. The impact of couch design and position during treatment is significant for both planning and treatment delivery and must be considered with this technique. Not accounting for this will impact delivered doses by up to 40 % in places.
Acknowledgements J Mulligan and D Ly, Elekta Ltd Support, North Sydney NSW 2060, Australia. B Sarkar, Physicist, Radiation oncology, Fortis Memorial Research Institute, 122002 Gurgaon, Haryana, India

P07 Experimentally derived ion chamber magnetic field correction factors (k_B)

J. Begg[1,2,3], Urszula Jelen[1,2], Brendan Whelan[2], Bin Dong[1,2], Natalia Roberts[5], Gary Liney[1,2,3,5], Lois Holloway[1,2,3,4,5,6]

[1]Department of Medical Physics, Liverpool and Macarthur Cancer Therapy Centre, Sydney, Australia. (jarrad.begg@health.nsw.gov.au [Presenting author]), (bin.dong@health.nsw.gov.au), (urszula.jelen@health.nsw.gov.au), (gary.liney@health.nsw.gov.au), (lois.holloway@health.nsw.gov.au). [2]Ingham Institute for Applied Medical Research, Sydney, Australia. [3]South Western Sydney Clinical School, School of Medicine, University of New South Wales, Sydney, Australia. [4]Radiation Physics Lab, University of Sydney, Sydney, Australia. (brendan.whelan@sydney.edu.au). [5]Centre for Medical Radiation Physics, University of Wollongong, Wollongong, Australia. (nr593@uowmail.edu.au). [6]Institute of Medical Physics, School of Physics, University of Sydney, Sydney, Australia

Introduction Reference dosimetry is a requirement for any clinical machine. Ion chamber response changes in magnetic fields, which must be corrected for on MRI-Linacs [1]. Magnetic field correction factors (k_B) have previously been derived from Monte-Carlo simulations [2] or chemical dosimeters [3]. This work presents a methodology for experimentally deriving k_B for an in-line MR-linac.
Method The Australian MR-Linac utilises a unique rail system, allowing movement of chambers into different magnetic field strengths whilst maintaining a constant source to chamber distance [4] and consistent scattering conditions. k_B can be calculated from the ratio of absorbed dose to water at the magnetic field strength relative to absorbed dose at 0 T [5]. Dose deposition to water at depth and beam quality has previously been shown to be independent of the magnetic field [6], therefore k_B can be calculated from the ratio of the output at 0 T relative to the output in the magnetic field. Output for a Farmer chamber was measured at various magnetic field strengths along the MR bore. Output at 0 T was linearly extrapolated and used to calculate k_B. Constancy of the linac's output was measured via two

methods; a second chamber between the source and MLC and a diamond detector behind the chamber being investigated.

Results Figure 1 shows k_B at various magnetic field strengths, with the farmer chamber as reference. k_B at 1 T was 0.987 ± 0.002. A k_B of 0.993 ± 0.002 at 1 T was measured using the diamond detector as a reference. The presented methodology was able to determine k_B similar to Monte-Carlo simulations [2].

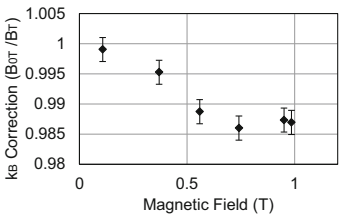

Figure 1: Magnetic field correction factors at various magnetic field strengths. Error bars represent measurement range at the maximum and minimum source to isocentre

Conclusion Ion chamber magnetic field correction factors (k_B) were derived using a variable magnetic field, demonstrating an approach for determining these factors without Monte-Carlo simulations or chemical dosimeters.

References

1. Meijsing, I., et al., *Dosimetry for the MRI accelerator: the impact of a magnetic field on the response of a Farmer NE2571 ionization chamber.* Physics in medicine and biology, 2009. **54**(10): p. 2993.
2. Reynolds, M., B.G. Fallone, and S. Rathee, *Dose response of selected ion chambers in applied homogeneous transverse and longitudinal magnetic fields.* Medical Physics, 2013. **40**(4):
3. Billas, I., et al. *Reference dosimetry measurements in the Australian MRI-linac*. in *World Congress on Medical Physics and Biomedical Engineering*. 2018. Prague, Czech Republic.
4. Liney, G.P., et al., *Experimental results from a prototype high-field inline MRI-linac.* Medical Physics, 2016. **43**(9): p. 5188–5194.
5. O'Brien D, et al. Reference dosimetry in magnetic fields: formalism and ionization chamber correction factors. *Medical Physics.* 2016;43(8):4915–4927.
6. Oborn B, Metcalfe PE, Butson M, Rosenfeld AB, Keall P. Electron contamination modeling and skin dose in 6 MV longitudinal field MRIgRT: Impact of the MRI and MRI fringe field. *Medical Physics.* 2012;39(2):874–890.

P08 Radiochromic film dosimetry process used at the North Coast Cancer Institute

N. Bennie

North Coast Cancer Institute, Lismore, NSW, Australia.
(Nick.Bennie@ncahs.health.nsw.gov.au [Presenting author])

Introduction This technical note outlines the method used at the North Coast Cancer Institute to process radiochromic film for Patient QA dosimetry, in transverse and sagittal planes. It will form part of a study guide for TEAP registrars, as documentation of an actual clinical implementation. It is an implementation of [1] published 2016 and it should be noted that due to the evolving usage of film, certain aspects are now optimised for use with SABR/SBRT type treatments, which are now the main clinical group at NCCI that makes use of film dosimetry. These treatments generally have a target dose in the range 5–20 Gy per fraction. The process is validated to 50 Gy to allow for the transfer of the clinical plan to QA phantom.

Method and materials The film product used was Ashland Gafchromic EBT3®, standard film 254 × 203 mm. The scanner was an Epson V800. The phantom was an IBA ImRT. Software products included EpsonScan, ImageJ and SNC Patient.

The sheet of film to be exposed, was marked to allow consistent orientation. It was then scanned prior to exposure and the file saved, to be used as a reference. The sheet was then inserted into the IBA ImRT phantom and exposed to the Patient radiation treatment. After 1 h, the exposed film was scanned and the file saved.

The initial processing of the data files was done using ImageJ. The Green channel data was separated for both the pre and post exposures and processed using the following formula:

The resultant data was exported and converted to a format suitable for SNC Patient. SNC Patient was then used to compare this data with the dose plane from the treatment planning system.

Conclusion The method was demonstrated to be both effective and efficient.

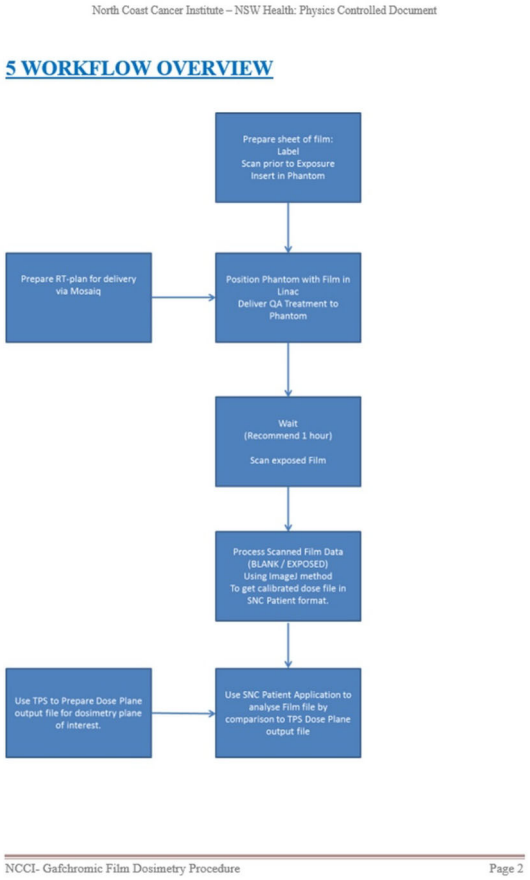

References

1. Bennie, N., & Metcalfe, P. (2016). Practical IMRT QA dosimetry using Gafchromic film: a quick start guide. Australasian Physical & Engineering Sciences in Medicine, 39:533–545

P09 Comparison between Silver Halide and Radiochromic film for dosimetry

N. Bennie[1], P. Metcalfe[2]

[1]North Coast Cancer Institute, Lismore, NSW, Australia. (Nick.Bennie@ncahs.health.nsw.gov.au [Presenting author]). [2]Centre for Medical Radiation Physics, University of Wollongong, NSW, Australia. (metcalfe@uow.edu.au)

Introduction This paper compares aspects of silver halide film used for dosimetry with radiochromic film. It will form part of a study guide for TEAP registrars, as a summary reference. The intention is to aid in the understanding of radiochromic film by comparison with the well-established process of SH film. However, some clarification of the SH process for dosimetry is also required as it is often confounded with the use of SH film for diagnostic use. For example, the emphasis on optical properties, which was a requirement for diagnostic where radiographs were assessed by eye, however for modern dosimetry where the data is stored in digital format it is no longer relevant what method is used to determine the amount of medium converted, only the characteristics relevant to accuracy.

Both products can be considered chemical dosimeters, where radiation initiates a chemical reaction, the resulting product having different optical properties, such that the change can be measured using an optical device, such as a densitometer or a scanner. However, the two chemicals and the types of reactions are completely different. Further, their optical absorption properties are significantly different, such that they have to be taken into account in characterizing the sensiometric curve, which relates the optical absorption to absorbed dose.

A key difference is in the dose range at which the film saturates. Saturation is when effectively all the active medium has been converted. That is, the film cannot get any darker. The SH films that are still available were designed to saturate at a little more than the common RT fraction of 2 Gy, usually approx. 5 Gy. However, $< 1\%$ of the active medium of EBT3® film is converted at 5 Gy.

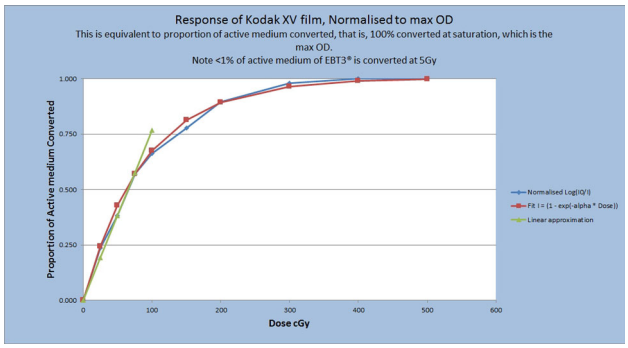

Conclusion Both methods are valid for use as film dosimeters, however a clear understanding of their characteristics is required to optimise use in a clinical radiotherapy department.

P10 Using a standard office MFU scanner for film dosimetry

N. Bennie[1], P. Metcalfe[2]

[1]North Coast Cancer Institute, Lismore, NSW, Australia. (Nick.Bennie@ncahs.health.nsw.gov.au [Presenting author]). [2]Centre for Medical Radiation Physics, University of Wollongong, NSW, Australia. (metcalfe@uow.edu.au)

Introduction: This technical note outlines a method to use a standard office Multi-Function Unit (MFU) scanner for film dosimetry. It has been validated for Patient QA dosimetry, in transverse and sagittal planes. It will form part of a study guide for TEAP registrars, as a method that can be used without need for a specialist scanner. It is noted that most general purpose scanners have 8-bit amplitude resolution, which is considered a major limitation with regard to dosimetry. This paper explains how the signal processing concepts of Dithering and Anti-aliasing can be used to convert high spatial resolution to amplitude resolution.

Fig. 1 Canon C5240 Multi-function Unit scanner

Method and materials The film product used was Ashland Gafchromic EBT3® and EBT XD®, standard film 254 × 203 mm. The scanner was a Canon C5240 MFU. The phantom was an IBA ImRT. Software products included ImageJ and SNC Patient.

The method of preparing film and exposing was as per [1], apart from process used to convert spatial to amplitude resolution.

The scans of the film were done at the maximum spatial resolution available on the scanner, which was 600 dpi for the Canon 5240. ImageJ was then used to extract the Green channel for both the pre and post image. The data type was then set to 32-bit, which is Single floating point, to preserve numeric resolution. The spatial resolution was reduced to 1 point per mm using the average of the approx. 558 values from the 600dpi square pixel. This effectively increased the amplitude resolution by 2 orders of magnitude.

The process as per [1] was again followed and the data exported and converted to a format suitable for SNC Patient and comparison to the planned data.

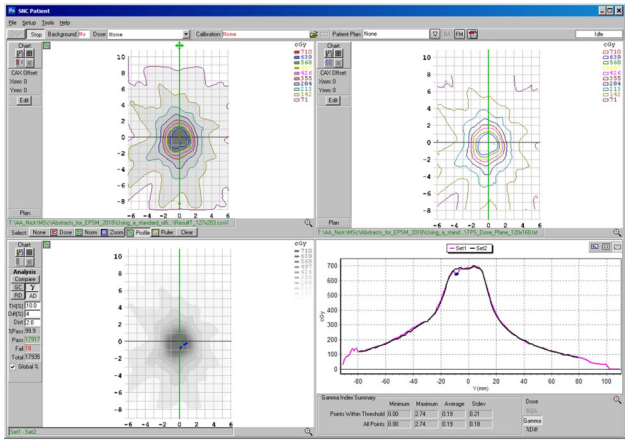

Fig. 2 IMRT QA analysis using film data acquired on MFU scanner

Conclusion: The resultant data was demonstrated to have an amplitude resolution that was suitable for comparison and analysis of exposures of approx. 7 Gy for EBT3 and 20 Gy for EBT XD.

References

1. Bennie, N., & Metcalfe, P. (2016). Practical IMRT QA dosimetry using Gafchromic film: a quick start guide. Australasian Physical & Engineering Sciences in Medicine, 39:533–545

P11 Intrafraction imaging: the effect of MV field size on image quality

G. P. Brown, P. O'Connor

Radiation Oncology, Princess Alexandra Hospital, Brisbane, Australia. (Georgia.brown@health.qld.gov.au [Presenting author]), (Patrick.Oconnor2@health.qld.gov.au)

Introduction Intrafraction imaging (IFI) is an emerging technology in the field of radiation therapy. It involves concurrent kV CBCT imaging and MV treatment delivery and allows tracking of anatomical motion during treatment [1].
IFI provides information on tumour and organ at risk (OAR) motion during treatment and allows the healthcare team to adjust the patient position as required. However, IFI has a disadvantage over traditional CBCT in that IFI image quality can degrade due to MV scatter from the treatment beam. This project explored the effect of MV field size and patient size on kV CBCT image quality.
Method Square 6 MV photon fields with side lengths ranging from 1 cm to 25 cm were delivered over full arcs to a number of phantoms; simultaneously an IFI CBCT was acquired. The phantoms irradiated included a chest, pelvis, CatPhan and a small and large Plastic Water phantom. The CBCT images were analysed and the effect of MV field size and phantom size on image quality was found. The homogeneity and standard deviation of voxel greyscale values were used to quantify the quality of the images.
Results Image quality was found to decrease as MV field size increased (see figure 1). It was found that by decreasing the MV beam repetition rate, the image quality increased as kV data was acquired at more points. Small and large phantom were affected differently by an increase in MV field size.
Conclusion The quality of IFI was reduced as increasingly large MV field sizes were used. Images of were also better quality when smaller phantoms were used. This information is useful for the radiation therapy healthcare team and can aid the decision making of when IFI should be used, and guide the optimization of IFI kV settings for larger patients and large treatment field sizes.

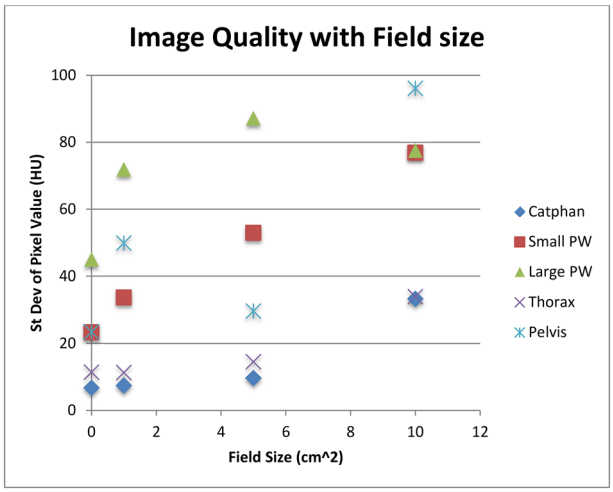

Figure 1: Standard deviation of voxel value with MV field size

References

1. Purdie, T.G., et al., *Cone-beam computed tomography for on-line image guidance of lung stereotactic radiotherapy: localization, verification, and intrafraction tumor position.* Int J Radiat Oncol Biol Phys, 2007. **68**(1): p. 243–52.

P12 B1 Shimming of dielectric artefacts on a 3T radiation therapy scanner

J. Buckley[1], R. Rai[2], G. Liney[3]

[1]CMRP, University of Wollongong, NSW, Australia. (jgb552@uowmail.edu.au [Presenting author]). [2]Liverpool Hospital Cancer Therapy Centre, SWSLHD, Liverpool, NSW, Australia. (robba.rai@health.nsw.gov.au). [3]Ingham Institute for Applied Medical Research, Liverpool, NSW, Australia. (gary.liney@health.nsw.gov.au)

Introduction 3T clinical MR scanners have become popular primarily due to their improved signal to noise ratio. However the increased field strength can also produce dielectric artefact when the RF wavelength is comparable to the size of the object being imaged[1]. A volunteer imaging study currently being undertaken at our institution[2] may be influenced by dielectric artefact at certain patient positions. A study was undertaken to investigate variation in the dielectric artefact for different positions of the imaging volume and assess the impact of various B1 shim techniques.
Method Two 20 L containers, one filled with oil and the other with water, were imaged on a 3T clinical MR scanner. The containers were imaged lying down, to simulate a prone/supine volunteer, and upright to simulate a volunteer on their side (figure 1). Three B1 shim settings available on the MR scanner were applied and compared—A site specific shim (TrueForm), a volume-specific shim, which optimised on a selected ROI within the phantom, and a patient-specific shim which required a 30 s B1 map prior to acquiring the image.
Oil and water were deliberately used to evaluate any subtle angle differences and then observe control of the various methods respectively.

Results No artefact was observed in the oil phantom in either horizontal or vertical positions, nor was any change observed by modifying the B1 shim settings. Significant dielectric artefact was present within the water filled phantom (figure 2). The artefact did vary when the B1 shim was adjusted, however the artefact was not significantly reduced.

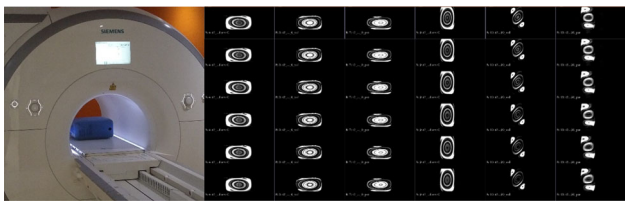

Conclusion Changing the B1 shim settings gave no significant improvement to water or oil phantom images in either phantom orientation. The default B1 shim (Trueform) is appropriate for all angles for the volunteer imaging study, though a volume specific shim may be applied in some instances.

References

1. Whelan B, Liney GP, Dowling JA, et al. An MRI-compatible patient rotation system—design, construction, and first organ deformation results. *Medical physics.* 2017;44(2):581–588.
2. Bernstein MA, Huston J, Ward HA. Imaging artifacts at 3.0 T. *Journal of magnetic resonance imaging.* 2006;24(4):735–746.

P13 Investigation into the required source geometry when using Eu-155 as a source for dual-energy cone beam computed tomography

G. M. Caporaso[1] S. N. Penfold[1,2], A. M. C. Santos[1,2]

[1]Department of Physics, University of Adelaide, Adelaide. (a1668975@adelaide.edu.au [Presenting Author]), (scott.penfold@adelaide.edu.au), (alex.santos@adelaide.edu.au). [2]Department of Medical Physics, Royal Adelaide Hospital, Adelaide

Introduction Proton therapy is a highly conformable radiation treatment modality which provides superior dose distributions in comparison to photons. To maximise the potential of proton therapy, patient specific data in the form of three-dimensional anatomical geometry and tissue stopping power ratios (SPR) must be known immediately prior to treatment and to high accuracy. We propose the use of dual-energy cone beam computed tomography (DECBCT), utilizing Eu-155 as a source of photons with two discrete energies to reduce proton range uncertainty [1]. An investigation into the required source characteristics was performed in the current work.
Method Geant4 Monte Carlo simulations were performed to determine the effect of source self-attenuation on different source geometries for Eu-155 based DECBCT. The Geant4 Eu-155 radioactive decay spectrum was modified to agree with photon intensity values in the literature [2]. Specifically, the effect of source self-attenuation on photon yield and energy spectrum was assessed. This was achieved by performing simulations with a spherical source of 4 mm diameter, and cylinders of 1 mm, 2 mm and 6 mm diameter, but with equivalent volume as the 4 mm sphere. The volume corresponds to an activity of 85 Ci at 100% Eu-155 purity. Simulations were run with and without Eu-155 material occupying the volume of the source. This was possible because Geant4 separates the physical geometry from the generation of primary particles.
Results Source self-attenuation was successfully quantified. It was found that the 4 mm spherical source reduced the emission of 86.5 keV photons from 0.3 to 0.05 photons per decay and from 0.2 to 0.05 photons per decay at 105.3 keV. The spherical source was found to provide a good compromise between photon yield and source size as seen by the detector.
Conclusion A spherical source of approximately 4 mm diameter appears to be the appropriate source geometry for radioactive Eu-155 as a source for DECBCT.

References

1. Zhu, J. and Penfold, S. N. (2017), Europium-155 as a source for dual energy cone beam computed tomography in adaptive proton therapy: A simulation study. Med. Phys., 44: 5143–5152.
2. Chechev, V. P. and Sergeev, V. O. (2004) Table de Radionucleides, Laboratiore National Henri Becquerel, http://www.lnhb.fr/nuclear-data/nuclear-data-table/, accessed 08/06/2018

P14 Investigation into the inclusion of XVI kV isocentre QA in the daily stereotactic imaging QA

P. Hanlon[1], P. Charles[1,2]

[1]Radiation Oncology, Princess Alexandra Hospital, Brisbane, Australia. (Peta.Hanlon@health.qld.gov.au), (Paul.Charles@health.qld.gov.au [Presenting author]). [2]Science & Engineering Faculty, Queensland University of Technology, Brisbane, Australia

Introduction AAPM TG 142 specifies the tolerance for the imaging and treatment coordinate coincidence to be $\leq$ 1 mm, for both planar (e.g. ExacTrac) and CBCT imaging. Due to the large inter-physicist variation found in a manual CBCT match of a BB phantom against a reference data set, a new phantom was designed to enable automatic registration.
The phantom has two end frames which are connected by 5 rods, the central rod containing a Ball Bearing (BB). The frames have CT marker dots to allow automated matching in the IGRT systems.
Method The phantom was CT scanned and the isocentre located at the central BB in the TPS. This dataset was imported into the IGRT systems (BrainLab ExacTrac and Elekta XVI), and auto-registration options were investigated for accuracy and reproducibility.
Results The use of the ExacTrac system in conjunction with the HexaPOD couch can align the phantom at the isocentre within 0.5 mm. The use of the consistent setup point, with a set clipbox location has proven that the auto-registration of the CBCT using the CT marker dots provides far more reproducible results than a manual match.
Conclusion A new phantom and methodology has been developed to include a user independent test of the XVI kV isocentre against the treatment isocentre, capable of achieving a tolerance of $<$ 1 mm as required.

P15 MV Radiation isocentre localization software QA image

P. Hanlon[1], J. Boyd[1], J. Shakeshaft[2], P. H. Charles[3]

[1]Radiation Oncology, Princess Alexandra Hospital, Brisbane, Australia. (Peta.Hanlon@health.qld.gov.au), (Joshua.Boyd@health.qld.gov.au). [2]Radiation Oncology Centres,

Gold Coast University Hospital, Australia. [3]Radiation Oncology, Princess Alexandra Hospital, Brisbane, [4]Science & Engineering Faculty, Queensland University of Technology, Brisbane, Australia. (Paul.Charles@health.qld.gov.au [Presenting author])

Introduction Accurate localisation of the MV isocentre with a Ball Bearing (BB) is required for the spatial calibration of Image Guidance Systems (e.g. ExacTrac, CBCT Systems). There are several independent software programs available to determine the distance between a BB and the radiation field isocentre, along with those provided by the linear accelerator manufacturers.
Discrepancies in detected shifts have been noted between manufacturer software and in-house developed software programs. To determine the source of the discrepancies, and provide confidence in the software analysis program used, an artificial QA image has been developed.
Method An artificial ideal image has been created in Matlab, with the location of the BB and field centre controlled to coincide with each other and the image centre. The image is symmetrical, and only contains a centrally located BB generated using a Gaussian distribution, within a uniform field; the field edges defined using a scaled section of a sinusoidal curve. This removes any uncertainty caused by non-uniformity of the EPID panel response, and also any impact of a stem that most BB phantoms incorporate. This image was run through various third party software and the offset calculated, with the expectation that the result would be perfectly 0.0 mm.
Results The artificial image was successfully imported into the available third-party software, and they all correctly identified the BB as coincident with the field centre with 0 shift required. However, when imported 8 times into the Elekta XVI software v4.5 as required for shift determination, an offset in the direction of the gantry rotation axis was observed, as noted in the literature. The discrepancy seen in the literature was proven to be due to the steepest gradient method used for field edge detection in the Elekta software algorithm.
Conclusion The use of artificial QA images with known geometry provides a quick simple check of the functional accuracy of isocentre localisation software, independent of phantom design and image acquisition effects.

Reference

Riis H L et al (2016) *Investigation of the accuracy of MV radiation isocentre calculations in the Elekta cone-beam CT software XVI*, Phys. Med. Biol 61 N249–N256

P16 Portal dosimetry configuration for a TrueBeam with an MLC-120 and DMI: do we need a beam profile correction algorithm?

S. L. Elliott

AHRO, Melbourne, Australia. (sarah.elliott@wbrc.org.au [Presenting Author])

Introduction The EPID is a diversely used tool in radiotherapy. Configuration of Portal Dosimetry (Varian) includes the Portal Dose Image Prediction algorithm and Dosimetry Calibration. Pre-treatment verification for IMRT plans is improved on an aS1000 EPID when a beam profile algorithm is applied during the Dosimetry Calibration[1,2,3,4].
In-house configuration of Portal Dosimetry is required for a TrueBeam with an MLC-120 and Digital Megavoltage Imager; the aim of this work is to evaluate the need for a correction algorithm with this combination of equipment.
Method The PDIP model was created for a 6MV beam and Dosimetry Calibration performed with a measured d_{max} diagonal profile[4].
A dynamic 40 × 40cm^2 open field was delivered (MLCs moving behind jaws), a simple 1D correction algorithm calculated from the ratios of predicted and measured dose at various distances from central axis[1] and applied to the beam profile.

Dynamic open fields and five large field IMRT plans were delivered after performing the Dosimetry Calibration with the uncorrected and corrected beam profiles. Fields were analysed using absolute gamma evaluation.
Results Gamma pass rates were similar for small open fields (< 20cm^2) using the uncorrected and corrected beam profiles. For larger open fields, the pass rates were improved with the corrected beam profile (Figure 1); for a 30cm^2 field size the (2%, 2 mm) gamma pass rate increased from 80.5 to 97.5%.

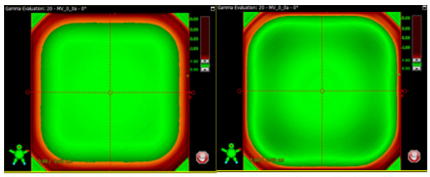

Figure 1: Portal Dosimetry Gamma Evaluation for a 40x40cm^2 open field using an uncorrected (left) and corrected (right) beam profile.

While some clinical plans showed improvement in gamma pass rates with the corrected beam profile, results were not consistent for all patients and fields.
Conclusion Initial results demonstrate that an uncorrected measured diagonal profile can be used for Portal Dosimetry configuration for our TrueBeam with DMI. Improvements in pass rates for IMRT verification plans using a corrected beam profile are not significant for analysis of fields using gamma criteria of 3%, 3mm.

References

1. Bailey DW, Kumaraswamy L, Podgorsak MB (2009) An effective correction algorithm for off-axis portal dosimetry errors. Med. Phys. 36(9):4089–4094
2. Bailey DW, Kumaraswamy L, Bakhtiari M, Podgorsak MB (2013) A two-dimensional matrix correction for off-axis portal dose prediction errors. Med. Phys. 40(5):051704-1-051704-7
3. Taylor RJ (2015) A dosimetric correction algorithm for intensity modulated radiation therapy pre-treatment verification using an amorphous silicon electronic portal imaging device, MSc thesis, RMIT University
4. Eclipse Photon and Electron Algorithms Reference Guide, Varian Medical Systems (2015) Chapter 12: 258–284

P17 Implementation of 4D brachytherapy at St George Cancer Care Centre

K. F. Enari[1], L. Taylor[2], D Malouf[1], D. L. Cutajar[3], J. A. Bucci[1]

[1]St George Cancer Care Centre, The St George Hospital, Kogarah, Australia. (Ese.Enari@health.nsw.gov.au [Presenting author]), (david@drdavidmalouf.co.au), (Joseph.Bucci@health.nsw.gov.au). [2]North Coast Cancer Institute, Coffs Harbour Health Campus, Coffs Harbour, Australia. (Lee.Taylor@ncahs.health.nsw.gov.au). [3]Centre for Medical Radiation Physics, University of Wollongong, Australia. (Dean_Cutajar@uow.edu.au)

Introduction Low dose rate prostate brachytherapy has been used at the St George Cancer care Centre for the treatment of prostate cancer routinely since 2003. To optimise the delivery of the treatment technique for improving of both the workflow and patient experience, a real-time procedure has been implemented based on a technique utilised by Langley and Laing [1]. This procedure uses a nomogram, from over 1800 previously performed procedures, to pre-calculate the required seed loading pattern based on a volume study (MRI or ultrasound images) obtained 3 weeks prior to the treatment. As intraoperative seed loading is no longer a necessity, the in-theatre time is greatly reduced, providing a streamlined procedure.
Method Variations to the procedure outlined by Langley and Laing were performed to suit the implantation environment at the St George Cancer Care centre. This included the adoption of the IsoLoader (Theragenics inc) for loose seed deployment and the Variseed V8.02 treatment planning system (Varian). The adapted protocol was commissioned in the clinical environment through a total of 22 tests, from individual equipment verification to an end to end test via the implantation of a CIRS prostate phantom.
Results 4D brachytherapy provided a reduction in real-time LDR brachytherapy implantation time by up to 50%. Post implant dose metrics also showed 4D brachytherapy to provide equivalent coverage to traditional LDR brachytherapy procedures.
Conclusion The implementation of 4D brachytherapy was successfully achieved at St George Cancer Care Centre, with patients to be treated with this procedure from January 2019. It is estimated that the provided optimisation in workflow will allow 50% more patients to be treated within the same allotment of theatre time.

Reference

1. Langley SE and Laing RW (2012) 4D Bachytherapy, a novel real-time prostate technique using stranded and loose seeds. BJU Int 109 Suppl 1:1–6.

P18 Verification of intensity modulated radiosurgery treatment fields using portal dosimetry

A. Espinoza[1], T Moodie[2], G Trompp[2], J Barber[1], J Sykes[1], S Yau[2,3,4]

[1]Blacktown Cancer and Haematology Centre, Blacktown, Australia. (Anthony.Espinoza@health.nsw.gov.au [Presenting author]), (Jeffrey.Barber@health.nsw.gov.au), (Jonathan.Sykes@health.nsw.gov.au). [2]Crown Princess Mary Cancer Centre, Westmead, Australia. (Trevor.Moodie@health.nsw.gov.au), (Gavin.Trompp@health.nsw.gov.au), (Shan.Yau@health.nsw.gov.au). [3]Nepean Cancer Care Centre, Nepean, Australia. [4]Blacktown Cancer & Haematology Centre, Blacktown Hospital

Introduction Intensity modulated radiosurgery (IMRS) for single and multiple intracranial metastases normally involves multiple small fields per lesion to deliver the treatment. IMRS uses highly conformal doses to target each lesion, sparing surrounding tissue. Quality assurance (QA) of these treatments may result in a large workload for the physicist due to the number of fields to be verified and there are few suitable QA solutions to assess each dose distribution. A potential QA method is to verify the fluence distribution of each field using the high resolution electronic portal imaging device (EPID) and compare it to a predicted response using Varian Portal Dosimetry.
Method The Crown Princess Mary Cancer Centre, Westmead, use a Varian TrueBeam STx linac for stereotactic treatments. It features the amorphous silicon aS1200 electronic portal imaging device (EPID) which was used to commission the portal dosimetry image prediction model (v13.7.16) for the 6MV beam. Five retrospective patient plans created in BrainLab iPlan RT 4.5 were transferred to a test patient in Varian Eclipse TPS and the portal dose image was predicted based on the iPlan calculated fluence and monitor units, and subsequently measured. Analysis of each field was performed using the gamma pass rate for multiple dose and distance criteria.
Results For the 5 measured plans, 26 small fields were measured with the EPID and compared to the predicted dose. From the range of gamma criteria, it was found that using a 2%/1 mm with global normalisation was suitable, with a pass rate for all measured fields of 98.9 $\pm$ 2.0% (1 S.D).
Conclusion Portal dosimetry for the verification of IMRS fields has been found to reduce workload and verification time and can provide a good indication of plan deliverability. The use of this system alongside point-dose measurements will improve confidence in future treatments and potentially reduce risk to the patient.

P19 Optimising cone beam CT of obese patients

L. Garrett[1], N. Hardcastle[2], P. Lonski[2], T. Kron[2], R. D. Franich[1]

[1]School of Science, RMIT University, Melbourne, Australia. (lachlan.garrett@rmit.edu.au [Presenting Author]), (rick.franich@rmit.edu.au). [2]Peter MacCallum Cancer Centre, Melbourne, Australia. (nick.hardcastle@petermac.org), (peta.lonski@petermac.org), (tomas.kron@petermac.org)

Introduction Cone Beam Computed Tomography (CBCT), as used in linac On Board Imaging systems in radiotherapy, suffers lower image quality than fan-beam diagnostic CT, predominantly due to increased scatter. Patient positioning could be compromised by the reduced tissue contrast and spatial resolution, and this image quality deterioration is exacerbated for obese patients. We propose to optimise the imaging parameters, kVp and mAs, for patients of different body size, by using a unique phantom that can be enlarged to represent overweight and obese patients.
Method A female anthropomorphic phantom (CIRS, Norfolk, USA) was enlarged with custom-made layers made from solid water to represent normal, overweight, and obese patients. CBCT images were taken with various kVp and mAs settings. Images were analysed for contrast resolution by recording CT numbers in 5 regions of interest (ROI) in 3 different tissues: lung, muscle and bone. Spatial resolution was assessed utilising line-pair structures near the centre and the periphery of each of the phantom configurations.
Results CT number differentiation was greatest with the lowest kVp and mAs on the largest phantom, and had the smallest variation with the highest kVp and mAs with the smallest phantom. The ROI in the obese patient without lung in the path length showed a decrease in average CT number when compared to the same ROI in the overweight patient. This is likely due to a transition from scattering to beam hardening at a longer path lengths.
The spatial resolution results showed that with increase phantom size and lower imaging parameters, the comparative spatial resolution was lower than with a smaller phantom and higher imaging parameters.
Conclusions With the increased kVp and mAs, the contrast and spatial resolution improved which is a step toward improving OBI protocols for obese patients. However with the increase in image quality there is an increased dose to the patient, which is undesirable.

P20 Clinical applications of a dynamic anthropomorphic phantom for radiotherapy

Chuan-Dong Wen[1,3], Trevor Ackerly[2,3], Moshi Geso[3]

[1]INWENTECH, Melbourne, VIC 3150 Australia. [2]Alfred Radiation Oncology, Alfred Health, VIC 3004 Australia. [3]School of Biomed. & Health Sciences, RMIT University, VIC 3083 Australia. (moshi.geso@rmit.edu.au)

Introduction A novel and inventive dynamic anthropomorphic breathing phantom, ChestPhan[4D] has been designed and built in Australia to assist the clinical implementations of advanced radiotherapy techniques since 2015. It is available for clinical research and training purposes, has wide applications due to its unique capabilities of expandable chest and deformable and movable organs included. This paper describes the phantom's readily available and potential clinical applications in 4D treatment and imaging of tumours in the thorax.

Method The published studies on tumour movements due to respiratory and cardiac motions were reviewed. The direct applications on thorax tumour tracking and targeting using current technologies were analysed from both temporal and spatial aspects. Possible applications in deformable imaging registration (DIR) and proton therapy QA process are also primarily investigated. The potential application of this phantom as "dosimetry discrepancy identifier" is explored with 4DCT data sets.

Results It has demonstrated that the phantom has the required features of organ motion and deformity of chest, lung, heart and skin during a breathing cycle. It has direct applications in SBRT, DIBH, DIR planning verification processes. With some modifications, it can be applied in proton therapy QA and to be used for verification of DIR software programs.

Conclusion A list of clinical applications with this dedicated, diseases-focused phantom has been preliminarily explored and its clinical application value has been confirmed.

References

1. Keall et al. (2006) The management of respiratory motion in radiation oncology report of AAPM Task Group 76 Med. Phys. 33 10, 3874–900
2. Seppenwoolde et al. (2002) Precise and real-time measurement of 3D tumor motion in lung due to breathing and heartbeat, measured during radiotherapy Int. J. Radiat. Oncol. Biol. Phys. 53 822–34
3. Hayden et al. (2012) Deep inspiration breath hold technique reduces heart dose from radiotherapy for left-sided breast cancer J of Med Imag and RadOnc 56 464–472
4. P Steidl et al. (2012) A breathing thorax phantom with independently programmable 6D tumour motion for dosimetric measurements in radiation therapy Phys. Med. Biol. 57 2235–2250
5. The Italian paper Moshi referred to Wen
6. The Austrian paper Wen has referenced

P21 Dosimetric comparison of electrons and photons treatment plans in craniospinal irradiation

M. U. Ghani[1], A. Razzaq[2], N. Amjad[2], M. I. Karamat[2], M. Shamshad[2], A. Farooq[3], A. Shahid[4]

[1]Medical Physicist, BINOR Bannu, Pakistan. (mug1771@gmail.com [Presenting Author]). [2]Medical Physicist, INMOL Lahore Pakistan. (asiarazzaq_pk@hotmail.com), (quarkssu3@yahoo.com), (Irfankaramat@msn.com), (mshamshad859@hotmail.com). [3]Consultant Radiation Oncologist, INMOL Lahore Pakistan. (aahmadfarooq@gmail.com). [4]Chief Consultant Radiation Oncologist, INMOL Lahore Pakistan. (drabubaker@hotmail.com)

Introduction The treatment of medulloblastoma involves surgery, radiotherapy and adjuvant chemotherapy. In radiotherapy, craniospinal irradiation (CSI) is prescribed, where two lateral cranial fields and one or two spinal beams are applied in CSI [1–6]. Different multi-field techniques (coplanar and/or non-coplanar) are used to register the prescribed dose. The purpose of this study was to assess plan quality in terms of dose coverage of spine with both photon and electron beam therapy and sparing of organ at risks.

Method Ten paediatric patients (age 6–10 years) were immobilized in the prone position for simulation. The CTV, PTV and OARs were contoured. Prowess Panther (v4.71) was used for dose computations. Two lateral parallel-opposed 6 MV photon cranial fields with the spinal beam(s) (either 6 MV photons or 21 MeV electrons) were used in planning. Electron beams were added posteriorly on the spine with parallel-opposed cranial fields. The electron and photon dose distribution in one of the treatment plan is given in Figure 1. The treatment plans were computed for 3600 cGy in 21 fractions.

Results For comparable conformity number of electron versus photons beam plans (0.68 ± 0.41 versus 0.66 ± 0.47, not significantly different at $p < 0.05$) and homogeneity index (1.22 ± 0.03 versus 1.25 ± 0.04, significantly different at $p < 0.05$), the photon doses were higher for underlying OARs (heart, liver and thyroid) and were lower for partially in-field organs (lungs and kidneys) compared to electrons as shown in Figure 2.

Conclusion The underlying organs i.e. thyroid, heart and liver receive lesser dose in case of electrons while partially in-field organs are exposed more compared to photons mainly due to ballooning effect in electrons. The study shows that both electrons and photons can be used for CSI, however electron may be preferred due to better sparing of underlying structures.

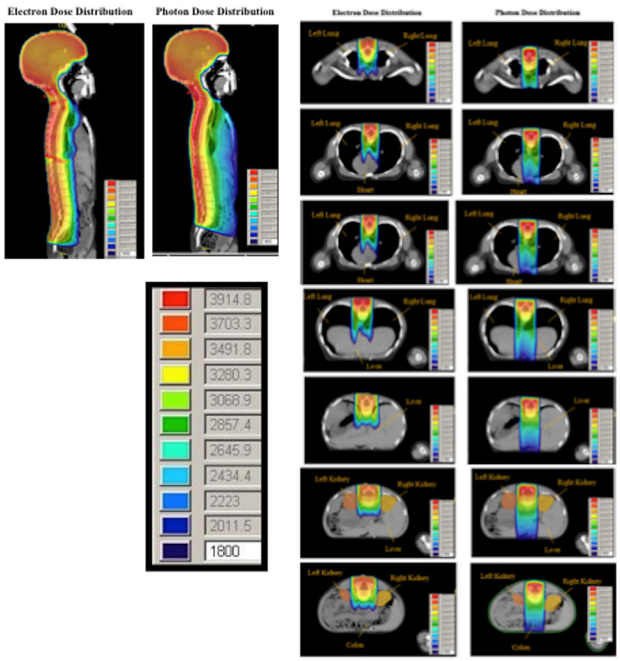

Figure 1: Isodose distribution of electron and photon beam plan.

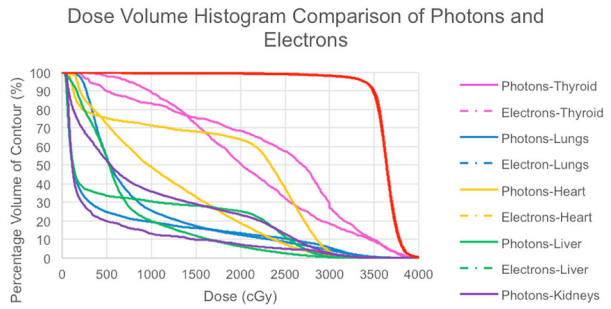

Figure 2 : Comparison of dose volume histograms (DVHs) of photons against electrons

References

1. M. Chojnacka, A. Skowronska-Gardasa, M. Morawska-Kaczynska, A. Zygmuntowicz-Pietka, K. Pedziwiatr and A. Semaniak, "Craniospinal radiotherapy in children: Electron- or photon-based technique of spinal irradiation.," Rep Pract Oncol Radiother. 2010 Feb 18;15(1):21–4.
2. L. Dewit, J. V. Dam, A. Rijnders, G. V. D. Velde, K. K. Ang and E. V. D. Schueren, "A modified radiotherapy technique in the treatment of medulloblastoma," Int. J. Radiat. Oncol. Biol. Phys, vol. 10, no. 2, pp. 231–241, 1984.
3. M. H. Maor, R. S. Fields, K. R. Hogstrom and J. V. Eys, "Improving the therapeutic ratio of craniospinal irradiation in medulloblastoma Int. J. Radiat. Oncol. Biol. Phys, vol. 11, no. 4, pp. 687–697, 1985.
4. L. Feuvret, G. Noel, J.-J. Mazeron and P. Bey, "Conformity index: a review," Int. J. Radiat. Oncol. Biol. Phys, vol. 64, pp. 333–342, 2006. https://doi.org/10.1016/j.ijrobp.2005.09.028
5. P. Myers, S. Stathakis, A. N. Gutiérrez, C. Esquivel, P. Mavroidis and N. Papanikolaou, "Dosimetric Comparison of Craniospinal Axis Irradiation (CSI) Treatments Using Helical Tomotherapy, Smartarc, and 3D Conventional Radiation Therapy," International Journal of Medical Physics, Clinical Engineering and Radiation Oncology, vol. 2, pp. 30–38, 2013. DOI: https://doi.org/10.4236/ijmpcero.2013.21005
6. C. H. Stokkevåg, G.-M. Engeseth, K. S. Ytre-Hauge, D. Röhrich, O. H. Odland, L. P. Muren, M. Brydøy, L. B. Hysing, A. Szostak, M. B. Palmer and J. B. B. Petersen, "Estimated risk of radiation-induced cancer following paediatric cranio-spinal irradiation with electron, photon and proton therapy," Acta Oncol, pp. 1048–1057, 2014. https://doi.org/10.3109/0284186x.2014.928420

P22 Computationl approach for determining the complex double strand breaks of DNA damage using Monte Carlo

K. Haneda

Department of Clinical Radiology, Hiroshima International University, Japan. k-haneda@hs.hiroskoku-u.ac.jp (Presenting author)

Introduction The aim of this study is to present the spectrum of initial radiation-induced cellular DNA damage [with particular focus on complex-double-strand break (DSB) damage] generated by computer simulations.
Method The radiation types modeled in this study were monoenergetic electrons (10–300 keV), protons (1–100 MeV), and carbon-ions (5–300 MeV/u). Monte Carlo track structure methods were used to simulate damage induction by these radiation types in a cell-mimetic condition from a single-track action. The simulations took into account the action of direct energy deposition events and the reaction of hydroxyl radicals on atomistic linear B-DNA segments of a few helical turns including the water of hydration.
Results Our results permitted the following conclusions: The absolute levels of different types of damage [SSBs and simple- or complex-DSBs] vary depending on the radiation type; Within each damage class, the relative proportions of simple and complex damage vary with radiation type, the latter being higher with high-LET radiations; The simple-DSB/SSB ratio is about 3–6%, and the complex-DSB/SSB ratio is about 1–2% for both low-LET radiations. The simple-DSB/SSB ratio is about 3–14%, and the complex-DSB/SSB ratio is about 1–6% for both low-LET radiation; which is about 3 times higher than that for high-LET radiations.
Conclusion The hypothesis that clustered DNA damage is more difficult for cells to repair has gained currency among radiobiologists. However, as yet, there is no direct in vivo experimental method to validate the dependence of kinetics of DNA repair on DNA damage complexity. The data on the detailed spectrum of DNA damage presented here, in particular the complex-DSB type, provide a good basis for testing mechanistic models of DNA repair kinetics.

P23 Review of a cranial stereotactic radiosurgery service

K. M. Harrison, R. Moylan, M. Fay

Genesis Care, Newcastle, NSW, Australia.
(Kristie.harrison@cancer.com.au [Presenting author]),
(Rebecca.moylan@genesiscare.com.au),
(Mike.fay@genesiscare.com.au)

Introduction Stereotactic radiosurgery consists of delivering a high dose on a small target with minimal margins to spare the surrounding healthy tissue. Consequently, this treatment requires rigorous precision in all aspects of planning, QA and delivery. Following a careful commissioning process, Genesis Care Newcastle has offered cranial stereotactic radiosurgery for 1 year and presents the review of the program.
Method During the QA processes undertaken for each patient, data was collected to ensure acceptable trending of results and appropriate tolerances had been established. This data has been collectively analysed to better understand the patient cohort and to look for opportunities for improvements or investigation.
Results A total of 14 patients have received treatment from 18 treatment plans. Ten patients were irradiated for a single lesion, and four patients with dual lesions. The patients received VMAT, DCAT or both modalities depending on PTV volume and proximity of organs at risk. QA results using film were within tolerances and the average gamma score (criteria 5% and 1.5mm) was 99.5% and an overall lowest result of 97.3%.
Conclusion Trending review of the SRS protocol in context with the results from QA, indicate good protocol adherence and acceptable tolerances to control the quality of SRS plans.
Acknowledgements Thanks to Alissa Baker and Matt Kemp

P24 CT reconstruction variables and their effects on the CT to electron density calibration for radiotherapy treatment planning

H. M. Deloar, J. Mathew[1], L. Marsh[1], T. Kron

Department of Physical Sciences, Peter MacCallum Cancer Centre, Bendigo, Australia. (Deloar.Hossain@petermac.org. [Presenting author]), (Joby.Mathew@petermac.org.), (Linda.Marsh@petermac.org.), (Tomas.Kron@petermac.org.)

Introduction Treatment planning systems require CT-to-RED (Relative-Electron-Density) data for radiotherapy treatment planning. CT imaging can be done with different slice thickness, field of view (FOV), reconstruction filters, reconstruction algorithms, option to correct metal artifacts (O-MAR), etc. In this study, effects of these variables on CT images were investigated.

Method A CT-to-ED phantom (CIRS-phantom, model-062M) with deferent material inserts was scanned using 120kVp and 140kVp of a Philips CT 16-bit scanner and images were reconstructed for FBP (filtered-back-projections), iDose, O-MAR (Orthopedic-Metal-Artifact-Reduction-Algorithm). The iDose reconstructions were performed for different reconstruction filters such as Standard-B, Smooth-B, Y-Sharp, and Y-detail. The iDose with standard-B filter as per the clinical practice was used to verify CT numbers for different slice thickness (1mm, 2mm, 3mm and 6mm). All of the above scans were performed without high density inserts. Additional scans with iDose and O-MAR were performed by placing the high density inserts (titanium-core and SS-alloy-20) into the middle hole to obtain their CT numbers.

Inserts Name	120kVp	140kVp
Air	-1000.0	-1000.0
LUNG (INHALE)	-777.3	-769.3
LUNG (EXHALE)	-508.4	-507.2
ADIPOSE	-65.5	-62.5
BREAST 50/50	-30.4	-28.0
Water	0.0	0.0
MUSCLE	37.8	36.2
LIVER	50.3	52.2
BONE 200 mg/cc	199.7	181.3
BONE 800 mg/cc	830.4	747
BONE 1250 mg/cc	1291.3	1153.9
TITANUM CORE	8003	6788.5
SS Alloy 20		15387

Figure1: CT numbers of different inserts for 120kVp and 140kVp

Results CT numbers of different inserts for 120kVp and 140kVp from CIRS phantom in iDose reconstructions is shown in figure1. For lower density materials the HU between the 120 and 140 kVp were very similar but those numbers increased for 120 kVp with increasing density.

The CT numbers with different slice thicknesses, reconstruction filters and algorithms were very similar to the results shown in figure1. The impacts of artifacts on the HU of other inserts were negligible. For extended field of view the CT numbers changes significantly. CT numbers of the high density materials changes with the size of region-of-interest (ROI).

Conclusion Differences in CT numbers for various slice thickness, reconstruction filters and algorithms are insignificant. Any appropriate reconstruction filters in conjunction with reconstructions algorithm can be used to calibrate the CT. Appropriate ROI should be used to get the CT number of high density inserts.

References

3. Constantinou C, Harrington JC, DeWerd LA (1992) An electron density calibration phantom for CT-based treatment planning computers. Med Phys 19:325–37.
4. Cozzi L, Fogliata A, Buffa F, Bieri S. (1998) Dosimetric impact of computed tomography calibration on a commercial treatment planning system for external radiation therapy. Radiother Oncol 48:335–8.
5. Seco J, Evans PM. (2006) Assessing the effect of electron density in photon dose calculations. Med Phys 33:540–52.

P25 Dosimetric effects of build-up thickness on OMAR CT reconstruction: a phantom study

Hossain M. Deloar[1], Joby Mathew[1], Linda Marsh[1], Tomas Kron[2]

[1]Department of Physical Sciences, Peter MacCallum Cancer Centre, Bendigo, Australia. (Deloar.Hossain@petermac.org. [Presenting author]), (Joby.Mathew@petermac.org.), (Linda.Marsh@petermac.org.). [2]Department of Physical Sciences, Peter MacCallum Cancer Centre, Australia. (Tomas.Kron@petermac.org.)

Introduction Philips CT scanner provides the option of O-MAR reconstruction, an algorithm to reduce artifacts in CT images. The aim of this study is to evaluate the effects of build-up thickness on O-MAR CT and hence, the prosthesis volumes, HU, artifacts and dosimetry.

Method Metal hips prosthesis were placed in a plastic container filled with wax. Build-up thicknesses; 1 cm, 2 cm and 5 cm were placed on top of the prosthesis container. CT scans were performed using 140 kVp for each of the thicknesses and images were reconstructed using normal-iDose and O-MAR methods. All images were exported to Eclipse planning system. Patient body, artifacts and prosthesis were contoured. For both CT reconstructions and the different build-up thicknesses, volume of the contours, HU, artifacts and dosimetry were evaluated. To evaluate dosimetry, treatment plans were generated on each CT data using 6×, 10× and 18× open beams. The dose files were evaluated using 3D gamma analysis software to compare normal-iDose and O-MAR methods.

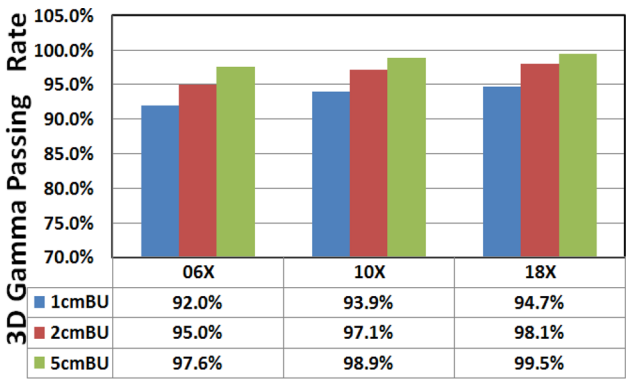

	06X	10X	18X
1cmBU	92.0%	93.9%	94.7%
2cmBU	95.0%	97.1%	98.1%
5cmBU	97.6%	98.9%	99.5%

Figure 1: 3D-Gamma between normal (iDose) and O-MAR reconstructions with 2% (global)/2mm and 10% thereshold.

Results The volume and the artifacts of the prosthesis were larger by around 13% and 11%, respectively, in normal-iDose than the O-MAR reconstruction. The HU of the patient contour excluding prosthesis for different buildup thickness were very similar in both iDose and O-MAR reconstruction but standard deviation of the HU improved by about 17%, 18% and 25% for 1cm, 2cm and 5cm, respectively in O-MAR. In dosimetry, the passing percentage of the 3D gamma (with 2%, 2mm and 10% threshold) between normal and O-MAR reconstructions were more than 92% (figure1).

Conclusion The O-MAR reconstruction can improve the image quality and HU value accuracy of the CT data with the prosthesis. Although the image quality is improved in O-MAR the dosimetry between iDose and O-MAR are clinically acceptable and a little improvement can be seen with higher buildup thickness.

References

1. Glover G. and Pelc N. (1981) "An algorithm for the reduction of metal clip artifacts in CT reconstructions." Medical Physics 4, 799–807.
2. Hu Y, Pan S, Zhao X, Guo W, He M, Guo Q, et al. (2017) Value and clinical application of orthopedic metal artifact reduction algorithm in CT scans after orthopedic metal implantation. Korean J Radiol. 18:526–35.
3. Rinkel J, Dillon WP, Funk T, Gould R, Prevrhal S. (2008) Computed tomographic metal artifact reduction for the detection and quantitation of small features near large metallic implants: A comparison of published methods. J Comput Assist Tomogr 32:621–9.

P26 Retrospective review of brain dose from stereotactic radiosurgery treatments of brain oligometastases

T. Kairn[1], Y. Ikeda[3], D. Schlect[3], S. B. Crowe[1,2]

[1]Royal Brisbane and Women's Hospital, Herston, Australia. (t.kairn@gmail.com [Presenting author]), (sb.crowe@gmail.com). [3]Genesis Cancer Care Queensland, Genesis Care, Auchenflower, Australia. (Yurissa.Ikeda@genesiscare.com.au), (David.Schlect@genesiscare.com.au). [2]Queensland University of Technology, Brisbane, Australia

Introduction The use of stereotactic radiosurgery to treat brain metastases requires consideration of the radiation doses delivered to the surrounding healthy brain [1]. For linac-based treatments the expected relationship between brain dose and total target volume can be complicated by geometric limitations resulting from the treatment of multiple metastases [2]. This study aimed to clarify the effects of target volume on brain dose from linac-based stereotactic radiosurgery treatments, by examining treatments planned for single oligometastasis cases only.

Method In-house treatment and dose assessor (TADA) code [2] was used to evaluate 60 single-fraction stereotactic radiosurgery treatment plans, 14 of which were identified as involving isolated brain metastases and selected for further analysis. The TADA code was modified so that the planning target volumes (PTV) was excised from the brain volume, without the additional dose falloff margin used in previous work [3]. The PTV dose, the healthy brain dose and the PTV volume were identified and compared. TADA was also used to calculate fractionation-insensitive generalised equivalent uniform doses (gEUDs) [4, 5], to consolidate brain dose volume histogram (DVH) data.

Results The PTV coverage dose reflected the treatment prescription dose, significantly trending downward with increasing metastasis volume, conforming with the established local practise of optimising the prescription for maximal treatment effectiveness with minimal healthy brain dose [3]. Healthy brain dose was substantially lower for the cases with very small metastases (PTVs less than 4 cc in volume) but was nonetheless controlled in the treatments of larger targets.

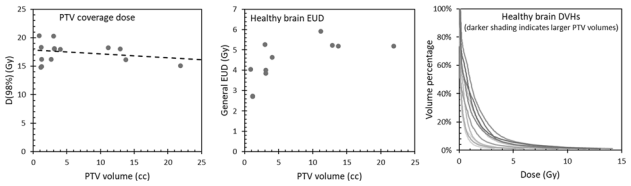

Conclusion By investigating the simple situation where the number of metastases stays constant while the volume of metastases varies, this retrospective analysis of stereotactic radiosurgery treatments showed that the dose to the healthy brain may increase as expected, but can also be controlled by carefully limiting the prescription dose in cases where such limits are clinically acceptable.

Acknowledgements The authors wish to thank the radiation oncologists and radiation therapists specialising in stereotactic radiosurgery at Genesis Cancer Care Queensland, who prescribed and planned the treatments evaluated in this study.

References

6. Lawrence,Y.R., Li, X.A., el Naqa, I., et al. Radiation Dose-Volume effects in the brain. *Int. J. Radiat. Oncol. Biol. Phys.* **76**(3), S20–S27 (2010).
7. Crowe, S.B., Kairn, T., Middlebrook, N., et al. Retrospective evaluation of dosimetric quality for prostate carcinomas treated with 3D conformal, intensity-modulated and volumetric-modulated arc radiotherapy. *J. Med. Radiat. Sci*. **60**(4): 131–138 (2013)
8. Kairn, T., Zolfaghari, S., Papworth, D., et al. Stereotactic radiosurgery for multiple brain metastases: A dose-volume study. *IFMBE Proc.* **68**(3): 443–445 (2018)
9. Niemierko A. Reporting and analyzing dose distributions: a concept of equivalent uniform dose. *Med. Phys*. **24**(1): 103–110 (1997)
10. Allen Li, X., Alber, M., Deasy, J.O., et al. The use and QA of biologically related models for treatment planning: Short report of the TG-166 of the therapy physics committee of the AAPM. *Med. Phys*. **39**(3): 1386–1409 (2012)

P27 Producing inserts for a commercial motion phantom using 3D printing

T. Kairn[1,2], S. B. Crowe[1,2]

[1]Royal Brisbane and Women's Hospital, Herston, Australia. [2]Queensland University of Technology, Brisbane, Australia. (t.kairn@gmail.com [Presenting author]), (sb.crowe@gmail.com)

Introduction Despite the wide range of contemporary commercial radiotherapy phantoms, changing clinical and research needs can result in demands for bespoke inserts for particular purposes. This study exemplifies the use of consumer-grade 3D printing to produce in-house inserts for a complex commercial phantom.

Method Inserts were designed to be substituted for an ionisation chamber insert in a CIRS dynamic thorax phantom, model 008A. Two workable phantom inserts were created. One insert was created in four pieces, so that a tissue-equivalent sphere with 2 cm diameter could be fitted into a void in a lung-equivalent insert, with a central division to allow film to be placed inside the phantom. The other insert was an abdominal-tissue-equivalent cylinder, containing a spherical void with 2 cm diameter.

Results After a process of trial-and-error (see Figure 1), a wood-PLA mixture was used to print the lung-equivalent phantom inserts, with a density of 0.4 g/cm^3 and a wall thickness of 0.3 mm, to minimise the effect of high-density phantom edges on any subsequent film measurements. The tissue-equivalent sphere that was used to model the lung tumour was printed using 90% PLA with a density of approximately 1 g/cm^3 and the tissue-equivalent cylinder that was used to model abdominal tissue with an air pocket was printed using 80% PLA with a density of approximately 0.9 c/cm^3. All densities were verified using CT imaging.

Figure 1 (left to right): Abdominal tissue insert during printing, collection of test prints, final lung insert with tumour, lung insert shown within CIRS phantom insert.

Conclusion The two phantom inserts were found to be suitable for their intended purposes and the process of creating them provided useful institutional experience in 3D print design techniques. In-house creation of bespoke inserts can be an educational and economical means to produce phantoms for specific clinical or research purposes.

P28 Level III audit of two stereotactic radiosurgery treatment planning and delivery systems

N. Cassim[1], K. Biggerstaff[2], Y. Ikeda[2], C. Skidmore[3], R. Wilks[4], S. B. Crowe[1,4], T. Kairn[1,4]

[1]Queensland University of Technology, Brisbane, Australia. (naasiha.cassim@connect.qut.edu.au), (sb.crowe@gmail.com), (t.kairn@gmail.com [Presenting author]). [2]Genesis Cancer Care Queensland, Genesis Care, Auchenflower, Australia. (Katrina.Biggerstaff@genesiscare.com.au), (Yurissa.Ikeda@genesiscare.com.au). [3]Genesis Cancer Care Queensland, Genesis Care, Southport, Australia. (Charlotte.Skidmore@genesiscare.com.au). [4]Royal Brisbane and Women's Hospital, Herston, Australia. (Rachael.Wilks@health.qld.gov.au)

Introduction The purpose of this study was to create and perform a level III audit of two cranial stereotactic radiosurgery systems. The systems evaluated were the Brainlab iPlan RTDose treatment planning system (TPS), used with a Brainlab m3 microMLC, and the Brainlab Elements Multiple Brain Mets SRS TPS, used with a Varian Trubeam STx (Novalis) linac with HD-MLC.
Method For each TPS, a treatment plan for 6 brain metastases was created using the CIRS 605 head phantom. Both plans used a nominal 6 MV photon beam, with reference to beam data measured using established small field dosimetry techniques [1]. The iPlan/m3 treatment plan used 22 non-coplanar static conformal arcs delivered using a multiple-isocentre technique. The Elements/HD-MLC treatment plan used 9 non-coplanar dynamic conformal arcs delivered using a single isocentre technique. Both treatment plans were copied onto a homogenous phantom, to evaluate the audited centre's proposed quality assurance (QA) process. EBT3 radiochromic film was used to verify dose delivery in both phantoms.
Results The geometric measurements obtained from the CT interface and the two TPSs were consistent with the physical measurement of the head phantom within ± 0.5 mm and all HU values from the CT and the two TPSs agreed within uncertainties. The relative electron densities produced by the two TPSs also agreed with vendor reported values within uncertainties. Agreement between the planned and measured PTV doses in the head phantom was within 3% for both TPSs, though the Elements TPS system showed some larger dose differences in MLC-shielded brain regions. The QA measurements showed better agreement (less sensitivity) than the head phantom measurements for the iPlan/m3 plans and poorer agreement (more sensitivity) than the head phantom measurements for the Elements plans.
Conclusion This comprehensive end-to-end testing produced results indicating that both TPSs produced dose calculations that were in acceptable agreement with measurements, although ongoing patient specific quality assurance, including testing with humanoid phantoms and evaluation of out-of-field dose, remains advisable.
Acknowledgements The authors wish to thank Alexander Livingstone, Holly Stephens, Emma Spelleken and Joanne Mitchell for additional oversight and assistance during the audit process.

Reference

1. Kairn, T., Charles, P.H., Cranmer-Sargison, G., Crowe, S.B., Langton, C.M., Thwaites, D.I., Trapp, J.V. Clinical use of diodes and micro-chambers to obtain accurate small field output factor measurements. *Australas. Phys. Eng. Sci. Med.* **38**(2): 357–367 (2015)

P29 Use of slow gantry rotations to reduce motion artefacts in cone-beam computed tomography images of radiotherapy patients

P. Fogg[1], M. West[2], T. Kairn[3,4]

[1]Genesis Cancer Care Queensland, Genesis Care, Nambour, Australia. (Penny.Fogg@genesiscare.com.au). [2]Genesis Cancer Care Queensland, Genesis Care, Auchenflower, Australia. (Mark.West@genesiscare.com.au). [3]Royal Brisbane and Women's Hospital, Herston, Australia. [4]Queensland University of Technology, Brisbane, Australia. (t.kairn@gmail.com [Presenting author])

Introduction Three-dimensional cone-beam computed tomography (3D CBCT) imaging is often used for localisation and verification imaging, before radiotherapy treatments are delivered. When an anatomical region containing steep density gradients (eg. tissue-air interfaces) undergoes respiratory motion, the resulting artefacts can increase the difficulty of accurately identifying the treatment target and nearby organs at risk. This study investigated a method of potentially reducing motion artefacts, using slow gantry rotations during 3D CBCT image acquisition.
Method 3D CBCT images of a motion phantom containing a simulated tissue-air interface were acquired using an on-board imaging system on a Varian Truebeam linear accelerator. Gantry speeds during image acquisition were reduced from the default 6°/s, to 3°/s and 1°/s. Imaging dose was limited by setting the tube current for all scans to equal the default value, 1080 mAs. Variation of the frame acquisition rate was also investigated, to keep the imaging beam-on time as low as possible.
Results The standard deviation from the mean Hounsfield units (HU sd) in a low-density stationary region of the motion phantom are presented in table 1, to provide a quantitative indication of the extent to which each image was affected by motion artefacts (the more similar the HU sd are to the "no motion" values, the less motion artefacts were present). Clearly, the slowest scans resulted in the least motion artefact. There were no significant changes in the noise level between scans obtained with the same tube current and the different total number of frames.

Table 1: HU sd in moving phantom imaged with constant mAs..

Phantom motion	Gantry speed (°/second)	Frames for "Pelvis" protocol	HU sd for "Pelvis" protocol	Frames for "Spotlight" protocol	HU sd for "Spotlight" protocol
No motion	6	900	8	500	11
Regular breathing	6	900	58	500	44
Regular breathing	3	1800	49	1000	43
Regular breathing	1	5400	17	3000	17

Conclusion The results of this study indicate that slow 3D CBCT imaging is a promising solution to the problem of motion artefacts in reconstructed images of moving tissue, especially in the abdominal region where tissue-air interfaces are often present, due to intestinal gas pockets. This method may be particularly useful during stereotactic body radiotherapy treatments, where treatment delivery precision is usually a higher priority than imaging speed.

P30 Characterisation of multi-leaf collimators designed for stereotactic and small field applications

E. Spelleken[1], J. Rijken[2], T. Kairn[3,4]

Genesis Cancer Care Queensland, Genesis Care, Rockhampton, Australia. (Emma.Spelleken@genesiscare.com.au). [2]Adelaide Radiotherapy Centre, Genesis Care, Adelaide, Australia. (James.Rijken@adradcentre.com.au). [3]Royal Brisbane and Women's Hospital, Brisbane, Australia. [4]Queensland University of Technology, Brisbane, Australia. (t.kairn@gmail.com [Presenting author])

Introduction This study aimed to provide a comparison of the physical and dosimetric properties of two specialised multi-leaf collimators (MLCs), the Vairan HD-MLC and the Brainlab m3 μMLC. The HD-MLC is an internal linear accelerator component that consists of 60 pairs of leaves: the 32 inner leaf pairs, 26 outer leaf pairs, and 2 outermost pairs of leaves that respectively project 2.5, 5.0 and 7.0 mm at the isocentre [1]. The m3 MLC is an external device that attaches to the accessory mount of the linear accelerator [2] that contains 26 pairs of leaves with varying thicknesses: 14 inner leaf pairs, 6 intermediate leaf pairs and 6 outer leaf pairs that respectively project to 3.0, 4.5 and 5.5 mm at the isocentre [3]. Both of these MLCs are used routinely for small field radiation therapy where high accuracy and precision are required.
Method The penumbra of square fields, slit fields and small fields, abutting leaf leakage, inter and intra-leaf leakage and the tongue and groove effect of the two MLCs were compared and analysed. The fields were exposed on EBT3 film and analysed using the red colour channel with ImageJ using an established film dosimetry method [4]. All pieces of film were analysed separately, and the same tests and number of fields were exposed using both MLCs.
Results A sample of the results obtained in this study are shown in table 1. After performing analyses on numerous fields, the m3 μMLC was found to have slightly narrower penumbrae, less abutting leaf leakage and a much smaller tongue-and-groove effect than the HD-MLC. The HD-MLC was found to produce less inter-leaf leakage and transmission than the m3 μMLC. Both systems showed leaf positioning reproducibility that was accurate to within 0.1 mm.

Table1: Comparison of dosimetric features of the two MLC systems.

Parameter	HD-MLC	m3 μMLC
Tongue and groove effect	26.1%, inner leaves	3.5%, all leaves
	19.1%, outer leaves	
Average penumbra width	3.7 mm	2.1 mm
Abutting leaf leakage	33.5%	12.4%
Inter-leaf leakage	1.3%	2.0%
Intra-leaf transmission	1.1%	1.7%

Conclusion Although the two MLC systems were physically and dosimetrically different from each other, they may both be considered suitable for use in high-precision treatments such as stereotactic radiosurgery and extra-cranial stereotactic ablative body radiotherapy, provided that their dosimetric features are accurately modelled in the chosen treatment planning system.

References

11. Sharma DS, Dongre PM, Mhatre V, Heigrujam M. Physical and dosimetric characteristic of high-definition multileaf collimator (HDMLC) for SRS and IMRT. *Journal of Applied Clinical Medical Physics* **12**(3): 142–160 (2011)
12. Xia P, Geis P, Xing L, et al. Physical characteristics of a miniature multileaf collimator. *Medical Physics* **26**(1): 65–70 (1999)
13. Cosgrove VP, Jahn U, Pfaender M, et al. Commissioning of a micro multi-leaf collimator and planning system for stereotactic radiosurgery. *Radiotherapy and Oncology* **50**(3): 325–335 (1999)
14. Aland T, Kairn T, Kenny J, Evaluation of a Gafchromic EBT2 film dosimetry system for radiotherapy quality assurance, *Australasian Physical and Engineering Sciences in Medicine* **34**(2): 251–260 (2011)

P31 Development of an experience-based end-to-end test

T. Kairn[1,2], S. B. Crowe[1,2]

[1]Royal Brisbane and Women's Hospital, Herston, Australia. [2]Queensland University of Technology, Brisbane, Australia. (t.kairn@gmail.com [Presenting author]), (sb.crowe@gmail.com)

Introduction End-to-end testing is an important quality assurance tool, allowing all steps in the radiotherapy treatment chain, from simulation to treatment delivery, to be assessed and verified. This study exemplifies the process of retrospectively analysing local treatment planning data, to obtain a quality assurance plan that directly evaluates current local practise.
Method The treatment modality chosen for investigation was stereotactic radiosurgery for brain metastases, due to the difficulty of designing a suitable end-to-end test based on individual recall of the range and complexity of treatment geometries involved. In-house treatment and dose assessor (TADA) code [1] was used to evaluate multiple-isocentre treatment plans from 60 patient treatments, to identify common features.
Results
Plan data analysis showed that 68% of cases involved more than one metastasis, 15% of cases had more than 6 metastases and the median number of metastases was 3. There was a general increase in the number of monitor units (MU) per beam as the field size decreased (see figure), due to both the increasing number of MU needed to deliver a given prescription dose and the increasing prescription doses that are clinically achievable for small volumes [2]. 64% of cases used either 5 or 6 beams to treat each metastasis, though this number decreased for cases with 6 or more metastases. 65% of plans included static conformal arcs. Few arcs had an initial gantry angle near zero (see figure). Collimator and couch positions were limited by linac geometry but were otherwise dominated by cardinal angles.

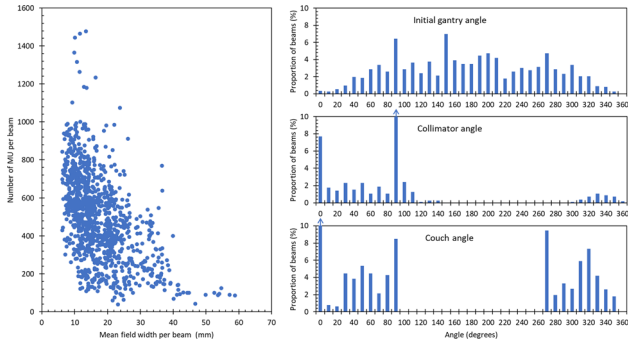

Conclusion For the specific stereotactic radiosurgery treatment planning process used for this work, a suitable end-to-end test plan should include at least 3 metastases, 5 or 6 beams per metastases (mostly arcs), a large proportion of small and very small fields and a range of gantry, collimator and couch angles. This method of evaluating local treatment planning data to produce quality assurance guidance may be adapted for other radiotherapy techniques.

Acknowledgements The authors wish to thank the radiation oncologists and radiation therapists specialising in stereotactic radiosurgery at Genesis Cancer Care Queensland, who prescribed and planned the treatments evaluated in this study. Thanks also go to the Genesis Cancer Care Queensland stereotactic radiosurgery physics team, especially Mark West, for providing assistance with the exporting and anonymisation of patient treatment plans.

References

15. Crowe, S.B., Kairn, T., Middlebrook, N., et al. Retrospective evaluation of dosimetric quality for prostate carcinomas treated with 3D conformal, intensity-modulated and volumetric-modulated arc radiotherapy. *J. Med. Radiat. Sci.* **60**(4): 131–138 (2013)
16. Kairn, T., Zolfaghari, S., Papworth, D., et al. Stereotactic radiosurgery for multiple brain metastases: A dose-volume study. *IFMBE Proc.* **68**(3): 443–445 (2018)

P32 Validation of the MRtrix tractography software for clinical use

O. Lannan, D. McRobbie, A. Santos

The University of Adelaide. (olivia.lannan@adelaide.edu.au [Presenting author])

Introduction Multi-directional diffusion-weighted magnetic resonance imaging (MDDW-MRI) harnesses the principles of diffusion to non-invasively probe white matter fibres of the brain. White matter maps or 'tractograms' can reveal critical microstructural details inaccessible to other imaging modalities that have proven instrumental in the diagnosis, intervention and management of neurological conditions such as acute ischemic stroke. However, many tractography models, such as the diffusion tensor model, are fraught with limitations. One method with reported superior performance is Constrained Spherical Deconvolution (CSD). In this study, qualitative and quantitative means were devised to evaluate whether CSD implemented in the program MRtrix can reliably delineate white matter tracts and is thus viable for clinical use.

Method MDDW-MRI data were acquired from 13 patients exhibiting various neurological conditions. Increments of artificial white Gaussian noise (WGN) and motion were added to the raw data. Tractograms were generated in MRtrix and tracts extracted for analysis.

Noise was quantified by SNR and intensity-based automatic image registration was used to measure slice-wise translation and rotation in the MDDW-MRI scans. Changes in tract lengths and orientations were visualised with polar plots and histograms. The resemblance of modified tracts to their original counterparts was quantified by Chi-squared tests and distance measures. False positive and negative rates were approximated by a nearest point search method.

Results The results indicate that tracts reconstructed by MRtrix retain some anatomic accuracy irrespective of noise level, despite terminating prematurely beyond 20dBW added WGN. An increased rate of false positives and false negatives is observed for added translations/rotations of the order of a few pixels/degrees.

Conclusion The software's robustness to noise and patient movement has been examined using a range of qualitative and quantitative techniques. With further refinement, these metrics may provide a tool to determine whether MRtrix will produce a reliable tractogram from a given dMRI scan on a per-patient basis.

P33 Investigation of applicator leakage radiation for a WOmed T-200 kilovoltage unit

B. Beeksma[1], J. Lehmann[1,2,3]

[1]Department of Radiation Oncology, Calvary Mater Newcastle, Newcastle, Australia. (Bradley.beeksma@calvarymater.org.au [Presenting author]), (Joerg.Lehmann@calvarymater.org.au). [2]Institute of Medical Physics, The University of Sydney, Sydney, Australia. [3]School of Mathematical and Physical Sciences, The University of Newcastle, Australia

Introduction Radiation leakage measurements are often performed during commissioning and generally not checked again for the lifetime of the machine. Australian standards [1] establish safety requirements for the maximum permissible leakage radiation outside the radiation field. This work aims to assess the leakage of a new applicator for the WOmed-T-200 kilovoltage system relative to the standards and provide recommendations based on these findings.

Method Radiochromic (RTQA2) film was wrapped around the length of a 3cm diameter, 24cm long applicator and also affixed to its base plate. Radiation was delivered with the highest energy available (200kV) for 15 mins to identify hot spots. A Farmer type chamber was then used to measure dose at various locations on the anode side of the applicator. The dose at each location was expressed as a percentage relative to the dose at the end of the applicator. The energy dependence of the leakage radiation was also assessed.

Results A hotspot was identified on the film attached to the base plate of dimensions equivalent to that of the unit's primary collimator (figure 1). For a 200kV beam, the dose at the location nearest to the applicator and base plate was 11.3% of central axis dose. In the patient plane, the maximum dose was 1.5% at a distance of 40mm from the applicator. This exceeds the Australian standards [1] tolerance of 0.5%. Transmission was reduced by 85% at 150kV and negligible for 100kV.

Conclusion The leakage radiation was caused by the size of the primary collimator exceeding the outer dimension of the applicator (figure 2) while the thickness of the baseplate in that area was insufficient to attenuate the radiation beam adequately. Appropriately increasing this thickness will reduce the leakage radiation to within

acceptable limits. The manufacturer agreed to retrofit a shielding disk to the applicator.

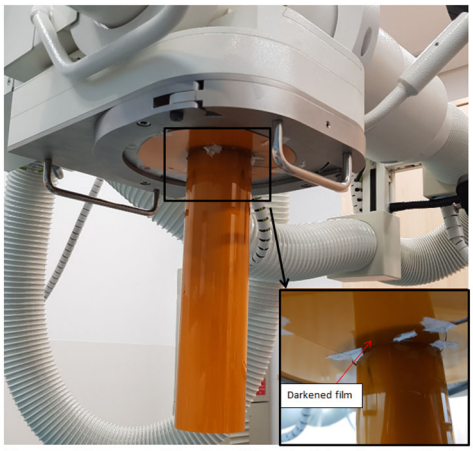

Figure 1: Film wrap of the 3cm Diameter 24cm long applicator showing hotspot of dimensions of that of the primary collimator.

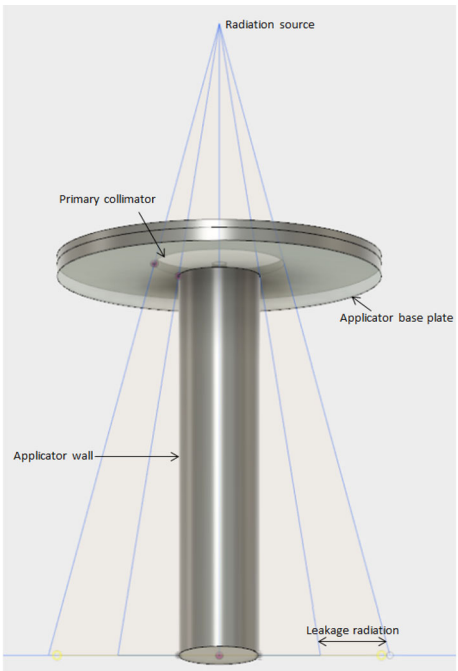

Figure 2: Schematic of the cause of the leakage radiation

Reference

17. Australian/New Zealand Standard IEC 60601.2.1.2015, Medical electrical equipment – Part 2.8: Particular requirements for the basic safety and essential performance of therapeutic X-ray equipment operating in the range 10kV to 1MV.

P34 Lessons learnt from the commissioning of a WOmed T-200 kV treatment system

J. Lehmann[1,2,3], A. Wilfert[1], R. Blackmore[1], M. Doebrich[1,3], T. Ostwald[1]

[1]Department of Radiation Oncology, Calvary Mater Newcastle, Newcastle, Australia. (Joerg.Lehmann@calvarymater.org.au [Presenting author]), (Alex.Wilfert@calvarymater.org.au), (Renee.Blackmore@calvarymater.org.au), (Marcus.Doebrich@calvarymater.org.au), (Trish.Ostwald@calvarymater.org.au). [2]Institute of Medical Physics, The University of Sydney, Sydney, Australia. [3]School of Mathematical and Physical Sciences, The University of Newcastle, Australia

Introduction Introduction of a new type of treatment machine adds to the complexity of the commissioning. The WOmed T-200 is a new generation kV therapy machine with control software and a database for scheduling and recording patient treatments. Mechanical advances include internal beam filters, which automatically move into the beam path when a beam has been selected, and motorised movement of the x-ray tube assembly.

Method Commissioning was organised as a multidisciplinary effort. Experience from Lucerne [1] helped in several, but not all aspects. For dosimetry, the TG61 protocol [2] was followed using the in air method. Backscatter calculation proved challenging as the applicator endplate thickness (1 mm) was different than that in the protocol's data. Also interpolations between SSDs, beam quality and field sizes were necessary.

Depth doses needed to be measured, as published data did not cover the beam qualities and SSDs required and literature indicated differences between existing published data and measurements for this machine [1]. Combinations of measurements in water and in solid water were employed.

Results Five beams were commissioned (Table 1), with four closed applicators useable for all beams (Table 2). The four open applicators have been limited to energies 100 kV and below, as the surface doses from high energy beams proved problematic. Additional closed applicators were ordered to meet clinical demands for higher energy with small apertures. To better match desired depth dose profiles, the 40 cm SSD option was chosen for the additional applicators, which will only be employed for the 150 and 200 kV beams.

Conclusion The system was commissioned fully and on schedule in 7 weeks, while allowing for brachytherapy treatments to continue in the room 2–3 times per week. More detailed initial discussion about beam energies and applicators would have been useful.

Table 1: Beams and beam parameters

Nominal settings kV	mA	Added filtration	Nominal HVL
60	20	2.6 mm Al	2.3 mm Al
80	20	4.5 mm Al	3.9 mm Al
100	20	4.5 mm Al	4.8 mm Al
150	20	0.4 mm Cu + 1 mm Al	0.68 mm Cu
200	13	1.3 mm Cu + 1 mm Al	1.8 mm Cu

Table 2: Applicators

Size	Nominal SSD [cm]	End	Equivalent diameter [cm]
Ø 2 cm	30	open	2
Ø 3 cm	30	open	3
Ø 4 cm	30	open	4
Ø 5 cm	30	open	5
6 x 8 cm^2	30	closed	7.7
8 x 10 cm^2	40	closed	9.9
10 x 15 cm^2	40	closed	13.3
20 x 20 cm^2	50	closed	22.2

References

1. Aspradakis MM, Zucchetti P (2015) Acceptance, commissioning and clinical use of the WOmed T-200 kilovoltage X-ray therapy unit. Br J Radiol 88(1055):20150001
2. Ma C-M et al (2001) AAPM protocol for 40–300 kV x-ray beam dosimetry in radiotherapy and radiobiology. Med Phys 28(6)

P35 Towards proactive maintenance of medical linear accelerator (LINAC): Big-data analysis using statistical methods

K. W. Li, K. H. Lee

Medical Physics Unit, Tuen Mun Hospital, HK. (lkw823@ha.org.hk [Presenting author])

Introduction Big-data analysis is the process of examining large amounts of data in an effort to expose hidden patterns or unknown correlations. This type of analysis can be applied on medical LINAC, in which plenty of digital data are readily available. The aim of this study is to predict the time of gun filament replacement and explore ways to extend its lifetime by exploiting these not yet fully utilized data.

Method During the period of January 2014 to September 2017, three LINACs were being monitored, Elekta Synergy Platform (TM1), Elekta Versa HD (TM3) and Elekta Infinity (TM4). Machine parameters, including but not limited to gun filament voltage (Gun V) and current (Gun I), vacuum level at gun side and target side and ambient temperature, were routinely captured during morning quality assurance. Gun filament resistances were calculated by Gun V divided by Gun I and categorized into two groups according to the ambient temperature at that period of time: (1) below 20 °C and (2) at or above 20 °C.

Results The TM4 gun filament current was shown in Fig. 1 after each gun filament replacement. The rate of change of gun filament resistances of TM4 at different periods of time was represented by the slope calculated by linear regression as shown in Fig. 2. Results show that the rate of change of gun filament resistance of group 2 was greater than that of group 1.

Conclusion This work preliminarily demonstrates the feasibility of using the system data already stored in our database to predict the downtime before actuation of interlocks. The findings will be further verified in the coming experiments by decreasing the ambient temperature and comparing the frequency of gun filament replacement with the previous service records. More beam control parameters will be included in the future to make the analysis more comprehensive.

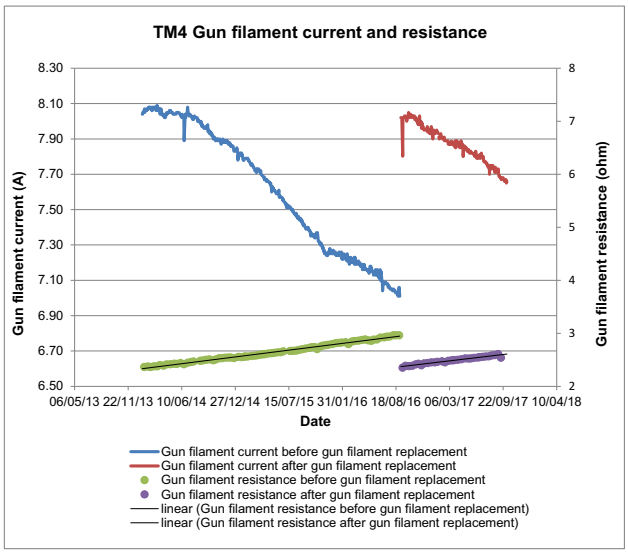

Fig. 1: Gun filament current and resistance of TM4 recorded from January 2014 to September 2017

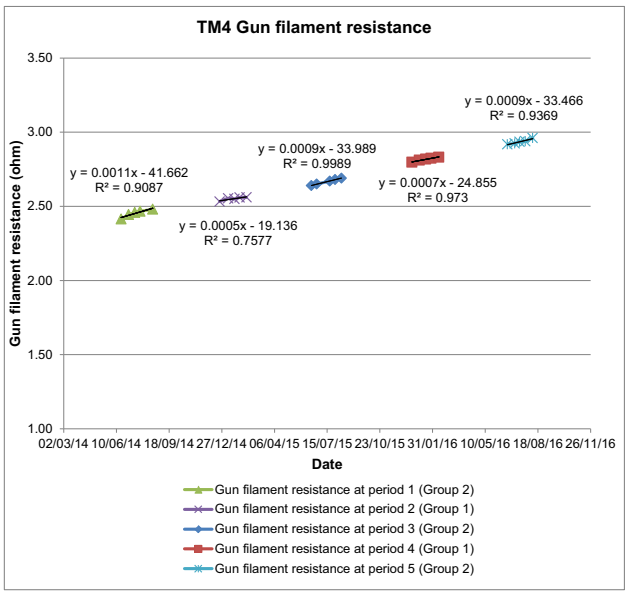

Fig. 2: The rate of change of TM4 gun filament resistance from June 2014 to August 2016

Reference

Able CM, Baydush AH, Nguyen C, Gersh J, Ndlovu A, Rebo I, Booth J, Perez M, Sintay, Munley MT (2016) A model for preemptive maintenance of medical linear accelerators – predictive maintenance. Radiat Oncol. 11:36. https://doi.org/10.1186/s13014-016-0602-1

P36 In-house quality assurance (QA) of dual-energy computed tomography (DECT) and its post-processing software

K. W. Li

Medical Physics Unit, Tuen Mun Hospital, HK. (lkw823@ha.org.hk [Presenting author])

Introduction Quantitative imaging has become more common in diagnostic radiology. Yet, there are just a few QA protocols on this subject. DECT has many clinical applications for its strong ability in material differentiation. In this work, an in-house QA of DECT is developed which can be easily applied in routine practice.

Method The anthropomorphic abdomen phantom (QRM-Abdomen) fitted with the dual-energy cylinder (QRM-DEP-002) was used in this QA program. The phantom was scanned on Siemens Somatom Definition Flash dual-source CT system at 80 kVp, 140 kVp and 80 kVp/Sn 140 kVp using helical scan with a pitch value of 0.6. The images were reconstructed at a slice thickness of 1 mm with an increment of 1 mm, using filtered back projection with B30f medium smooth convolution kernel and 512 × 512 matrix. A circular region of interest was used to measure the CT number of each iodine and calcium insert in each of the image set: (1) 80 kVp, (2) 140 kVp and (3) 80 kVp/Sn 140 kVp mixed image with weighting factor of 0.5. The image sets were transferred to syngo.via and CT Dual Energy Liver VNC application profile was used for quantifying iodine concentration.

Results Mean CT numbers with standard deviations of the calcium and iodine inserts in different layers of the phantom scanned at single energy and dual energy were summarized in Table 1. The mean CT numbers in the mixed image agreed with the linear weighting of the two spectra. Iodine concentration measurements in syngo.via were shown in Fig. 1. Differentiation between calcium and iodine could be seen on the overlaying color-coded iodine map.

Conclusion The above measurements can be done during acceptance testing for characterization of DECT performance and baseline establishment. Deviations from baseline are recorded in subsequent QAs to ensure the consistency and reproducibility of the DECT.

Table 1: Mean CT number (CT no.) with standard deviation (SD) of each calcium (Ca) and iodine (I) insert in different layers of the phantom scanned at single energy and dual energy

Energy	80 kVp			140 kVp			80 kVp/ Sn 140 kVp		
Layer A Ca no.	1st	2nd	3rd	1st	2nd	3rd	1st	2nd	3rd
Mean CT no. (HU)	302	602	832	189	370	525	236	461	671
SD CT no. (HU)	18	19	11	8	11	5	18	13	11
Layer A I no.	1st	2nd	3rd	1st	2nd	3rd	1st	2nd	3rd
Mean CT no. (HU)	328	626	924	177	316	456	247	448	656
SD CT no. (HU)	17	19	34	8	9	16	7	18	23
Layer B Ca (half) no.	1st	2nd	3rd	1st	2nd	3rd	1st	2nd	3rd
Mean CT no. (HU)	287	554	776	185	365	500	227	461	627
SD CT no. (HU)	16	11	21	7	13	8	10	18	10
Layer B I (half) no.	1st	2nd	3rd	1st	2nd	3rd	1st	2nd	3rd
Mean CT no. (HU)	315	614	894	168	309	459	218	451	660
SD CT no. (HU)	19	14	26	6	6	6	10	15	17
Layer B I (full) no.	1st	2nd	3rd	1st	2nd	3rd	1st	2nd	3rd
Mean CT no. (HU)	54	91	164	30	52	90	33	65	123
SD CT no. (HU)	23	25	18	6	12	8	13	15	17
Layer C Ca no.	1st	2nd		1st	2nd		1st	2nd	
Mean CT no. (HU)	-131	-120		-132	-134		-144	-154	
SD CT no. (HU)	16	11		10	6		12	12	
Layer C Ca + I no.	1st	2nd		1st	2nd		1st	2nd	
Mean CT no. (HU)	71	82		-7	-22		16	14	
SD CT no. (HU)	9	24		14	12		12	16	

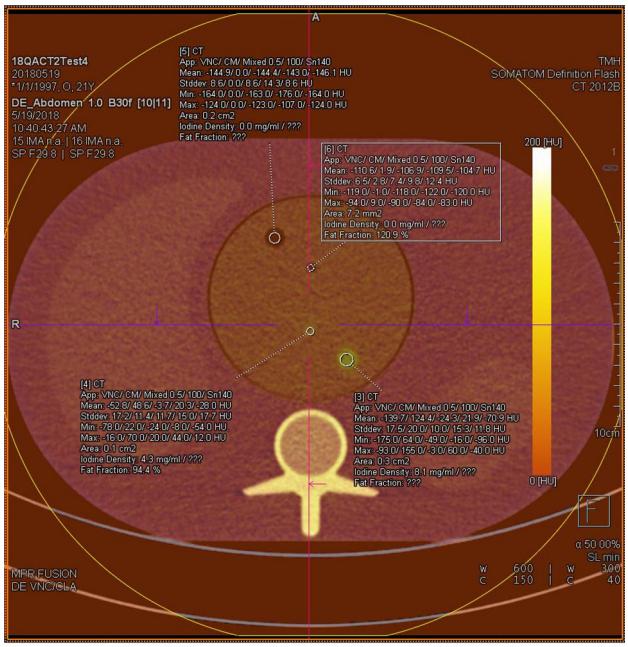

Fig. 1: Iodine concentration measurements in syngo.via

Reference

Schmidt B, Sedlmair MU, Krauss B, Tyan J, Flohr TG (2008) Assessment of a quality assurance phantom for dual energy CT. Radiological Society of North America 2008 Scientific Assembly and Annual Meeting. http://archive.rsna.org/2008/6018424.html.

P37 Comparison of performance of three commercially available automatic PET contouring tools

C. Marciniak

Department of Nuclear Medicine, St George Hospital, NSW. (casper.marciniak@health.nsw.gov.au [Presenting author])

Introduction PET imaging is used routinely for screening and staging of cancer and there is interest in using it for tumour delineation during radiotherapy treatment planning. Many medical imaging packages offer automatic segmentation tools for PET images. These require validation before introduction into the clinical workflow.

Aim To evaluate and compare the tumour delineation performance of three software packages; MIM, Varian VelocityAI and GE PET VCAR.

Method A NEMA IEC body phantom was filled with aqueous Ga-68 such that the target to background ratio was 4:1. A single 30min PET-CT was acquired and retrospectively divided into four frames simulating 5-min acquisitions with 100MBq initial activity. A digital phantom representing the ground truth (GT) geometry was created using in-house software.

Reconstructed images were segmented using each package and the results saved as RTSS. One image was segmented multiple times to test for reproducibility. The GT RTSS was segmented using Velocity. All RTSS were loaded into MIM and analysed to obtain mean distance to agreement (MDA), Dice similarity, and compare measured volume and centroid positions to GT.

Results For repeat measurements VCAR yielded identical results whilst Velocity and MIM showed comparable low-level variability (MDA ≈ 0.25mm, Dice ≈ 0.95). Compared to GT, Velocity generally placed first when ranked for individual spheres but performed poorly for small spheres and placed last on overall combined averages (MDA 1.01mm, 1.24mm, 1.37mm & Dice 0.80, 0.78, 0.76 for VCAR, MIM, Velocity). The centroid shifts from GT were 1.0mm 1.1mm & 1.3mm (MIM, Velocity & VCAR) and the mean measured/GT volume ratio was 1.09, 1.38 & 2.02 (MIM, VCAR & Velocity).

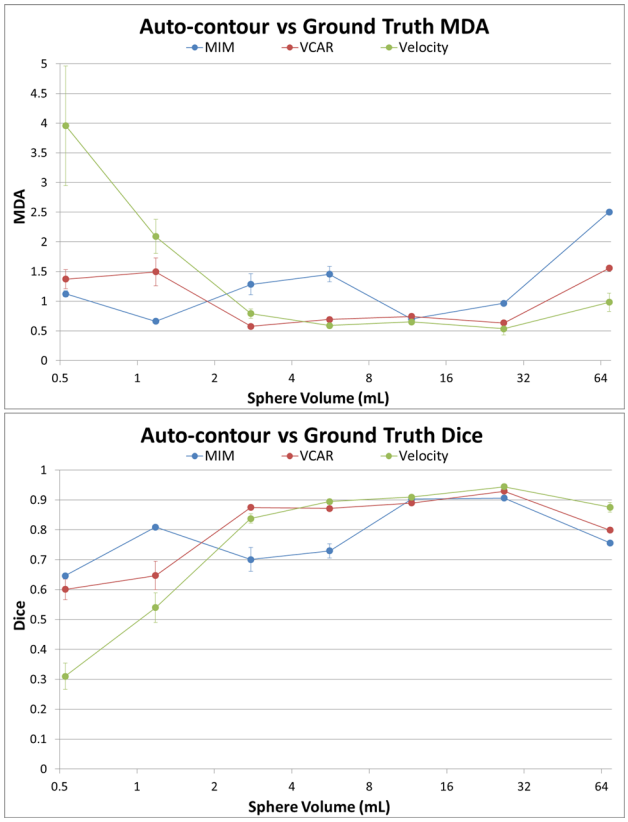

Conclusion The performance of all three packages was comparable. Velocity performed marginally better for large spheres >2mL but significantly worse for small. VCAR produced consistent results for any given dataset; this was not the case for the other two.

P38 Correlations of treatment plan parameters and quality metrics

L. Marsh[1], J. Mathew[1], H. M. Deloar[1]

[1]Department of Physical Sciences, Peter MacCallum Cancer Institute, Bendigo, Victoria. (Linda.Marsh@petermac.org [Presenting author]), (Joby.Mathew@petermac.org), (Deloar.Hossain@petermac.org)

Introduction 106 Volumetric Modulated Arc Therapy (VMAT) and Intensity Modulated Radiation Therapy (IMRT) plans were calculated using Eclipse V13.6 AAA algorithm. Patient specific quality assurance (QA) was performed including, phantom measurement with ArcCheck (non-prostate only), independent calculation with Mobius3D (M3D) and log file analysis with MobiusFX (MFX). Correlation coefficients for basic plan parameters and quality metrics were used to explore potential relationships.

Method M3D collapsed cone convolution (CCC) used independent beam data to perform 3D calculation on the patient dataset. M3D calculated global gamma (3%,3mm), local gamma for contoured volumes, mean dose (Dmean) and other volume doses. From the plan, number of segments, monitor units per fraction (MU), number of

Arcs/Fields and an X-jaw opening metric (Xtravel) were extracted. ArcCheck Gamma (2%, 2mm) was for composite fields and total points were the number of diodes in the irradiated volume. Treatment site was considered, eg prostate, head and neck (HnNk) or other. Treatment delivery, either IMRT or VMAT was also used to categorize the plans.

Results Figure 1 illustrates the significant (alpha = 0.05) correlation coefficients, relating to the PTV volume. Many relationships although significant were weak. Figure 2 plots M3D Global and ArcCheck composite parameters. ArcCheck gamma was correlated to PTV volume (R = 0.33) and MU per fraction, however it was not correlated to either M3D Global or M3D local gamma. M3D Global gamma was correlated with M3D local gamma (R = 0.31) and to Xtravel (R = − 0.19). When split into the treatment site and treatment delivery many of the above relationships changed.

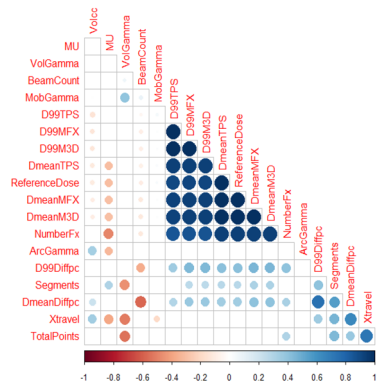

Figure 1 : Correlation matrix for PTV parameters, the size and colour indicate pearson correlation coefficient. Blank means not signifcant with alpha=0.05.

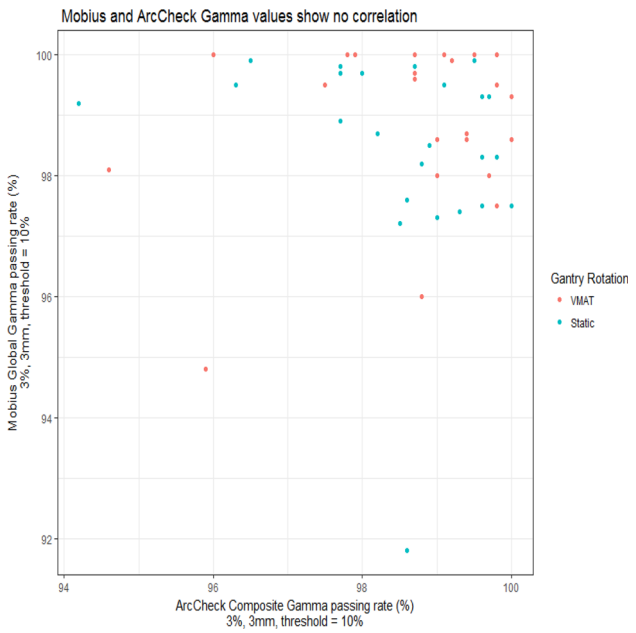

Conclusion Correlations between quality metrics and plan parameters do exist, however the relationships are influenced by each other and by patient geometry.

References

1. Mohammad Hussein and Pejman Rowshanfarzad and Martin A. Ebert and Andrew Nisbet and Catharine H. Clark (2013) A comparison of the gamma index analysis in various commercial IMRT/VMAT QA systems.Radiotherapy and Oncology109:370 – 376. https://doi.org/10.1016/j.radonc.2013.08.048
2. Bekelman, J. E., Deye, J. A., Vikram, B., Bentzen, S. M., Bruner, D., Curran, W. J., … Purdy, J.(2012)Redesigning Radiotherapy Quality Assurance: Opportunities to Develop an Efficient, Evidence-Based System to Support Clinical Trials: Report of the National Cancer Institute Work Group on Radiotherapy Quality Assurance. International Journal of Radiation Oncology, Biology, Physics 83:782–790. https://doi.org/10.1118/1.4899177
3. McKenzie Elizabeth M. and Balter Peter A. and Stingo Francesco C. and Jones Jimmy and Followill David S. and Kry Stephen F.Toward optimizing patient-specific IMRT QA techniques in the accurate detection of dosimetrically acceptable and unacceptable patient plans.Medical Physics 41:121702
4. Stephen F. Kry, PhD, Andrea Molineu, MS, James R. Kerns, MS, Austin M. Faught, PhD, Jessie Y. Huang, BS, Kiley B. Pulliam, MS, Jackie Tonigan, MS, Paola Alvarez, MS, Francesco Stingo, PhD, David S. Followill, PhD. (2014) Institutional Patient-specific IMRT QA Does Not Predict Unacceptable Plan Delivery.International Journal of Radiation Oncology, Biology, Physics 90:1195–1201.
5. M. Hussein, C.H. Clarke, A. Nisbet (2017) Challenges in calculation of the gamma index in radiotherapy – Towards good practice.Physica Medica 36:1–11

P39 Nanoparticle dose enhancement for Cu-67 internal radionuclide therapy: a Monte Carlo study

R. T. Maschmeyer[1], Y. H. Gholami[1], D. L. Bailey[2,3], Z. Kuncic[1]

[1]Institute of Medical Physics, School of Physics, University of Sydney, NSW 2006, Australia. (richard.maschmeyer@sydney.edu.au [Presenting author]), (yaser.gholami@sydney.edu.au), (zdenka.kuncic@sydney.edu.au).[2]Department of Nuclear Medicine, Royal North Shore Hospital, St Leonards NSW 2065. [3]Faculty of Health Sciences, University of Sydney, NSW 2141, Australia. (dale.bailey@sydney.edu.au).

Introduction Nanoparticles are being increasingly investigated for their potential to enhance radiation dose on the nanoscale. To date, however, these investigations have only focussed on the use of nanoparticles to enhance *external* beam radiotherapy; little attention has been paid to potential enhancements to *internal* radionuclide therapy.[1]

We performed a nanoscale simulation study using Monte Carlo radiation transport methods to investigate the potential for iron-oxide nanoparticles to enhance the dose due to copper-67 (a β^--emitting radioisotope) when labelled to the nanoparticles' surface.

Method Monte Carlo simulations using GATE 8.0[2] were performed to investigate the radio-enhancement effects of iron-oxide nanoparticles with 5 nm and 25 nm diameters. 1500 nanoparticles were individually labelled with β^- particles (with energies corresponding to the β^- spectrum of Cu-67) and placed in nanoscale cubic volumes of water (ranging from 10^6 to 10^{10} nm^3). Nanoparticle concentrations corresponding to iron/water concentrations ranging from 0.02 to 35

g/kg were simulated using 5×10^6 primary β^- particles (figure 1). Energy deposition and number of radiation hits was recorded. This was contrasted against an identical scenario, except with the iron-oxide content being dispersed homogeneously.

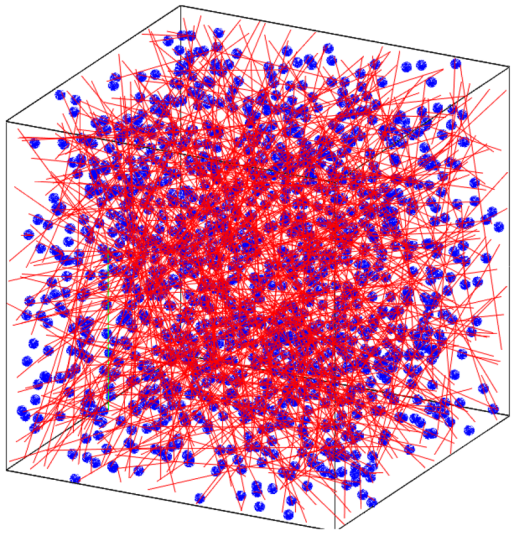

Figure 1: Visualisation of simulation. Blue spheres represent nanoparticles, red lines represent β^- trajectories

Results Enhancements to energy deposition and the number of radiation hits was found for most concentrations studied, with the 5 nm nanoparticle producing the largest enhancement. Specifically, an increase in total energy deposition in the water medium *between* the nanoparticles was observed, as well as an increase in the number of radiation hits (figure 2). This trend also holds when the nanoparticle suspension is contrasted against water.

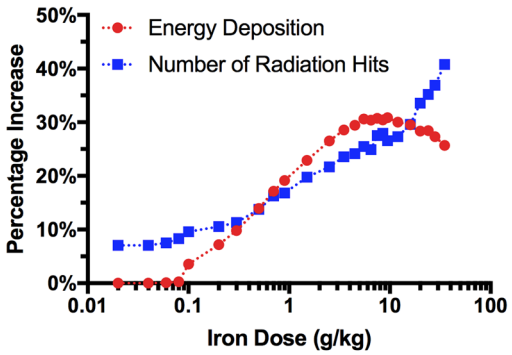

Figure 2: Relative enhancements to water medium containing 5 nm diameter iron-oxide nanoparticles when compared to homogeneously distributed iron-oxide in water.

Conclusion Monte Carlo simulations demonstrated the potential for iron-oxide nanoparticles to enhance the dose during copper-67 based internal radionuclide therapy.

References

1. Jan S, et al. (2004) GATE: a simulation toolkit for PET and SPECT, Phys. Med. Biol., vol. 49, no. 19, p. 4543.
2. Kuncic Z and Lacombe S (2018) Nanoparticle radio-enhancement: principles, progress and application to cancer treatment, Phys. Med. Biol., vol. 63, no. 2, p. 02TR01.

P40 Study of fluoroscopic system dose rate dependence on additional beam collimation

Y. V. Matyagin[1], J. Wong[1], C. Boyd[1], K. Hickson[2]

[1]South Australian Medical Imaging, Royal Adelaide Hospital, Australia. , (Yuri.Matyagin@sa.gov.au [Presenting author]), (Juji.Wong@sa.gov.au), (Chris.Boyd2@sa.gov.au). [2]South Australian Medical Imaging, Queen Elizabeth Hospital, Australia. (Kevin.Hickson@sa.gov.au)

Introduction On image-intensifier-equipped fluoroscopic systems, additional collimation of X-ray beam with adjustable collimator blades allowed to reduce radiation exposure to patients and staff [1, 2]. There were reports from vascular surgeons and radiographers of the Royal Adelaide Hospital (RAH) that modern Automatic-Exposure-Control (AEC)-guided fluoroscopic systems may significantly increase dose rate when the beam is additionally collimated. There is a concern that additional collimation of the beam may in fact lead to the radiation exposure increase for the patient. The aims of this phantom study were to investigate, for a digital fluoroscopic (DF) system under AEC, the effect of additional X-ray beam collimation on the entrance air kerma rate and dose-area product (DAP) rate.
Method Siemens Artis-Q Floor DF system was tested at several field-of-view (FOV) settings with collimations kept close to a square shape. Measurements were conducted with/without water phantom (20-cm-deep, 26-cm-diameter). A 3-mm-thick copper plate was positioned at the collimator during tests without the phantom. Air kerma rates were measured either at the phantom entrance surface or at image receptor (IR).
Results Air kerma rates measurement results normalised to an output from a fully open collimator are illustrated on figures below for exposures with and without phantom.
Conclusion Beam collimation to a size larger than a specific minimal size allowed a significant reduction in the DAP rate, despite some increase in entrance air kerma rate. In patient fluoroscopic procedures, a moderate collimation of the X-ray beam should be used, if required, for reduction of the effective dose from the procedure to the patient and staff. Beam collimation down to a smaller size is not recommended as this may result in a substantial increase in both the entrance air kerma and DAP rates. The specific minimal size is related to the size and location pattern of AEC dose rate sensors.

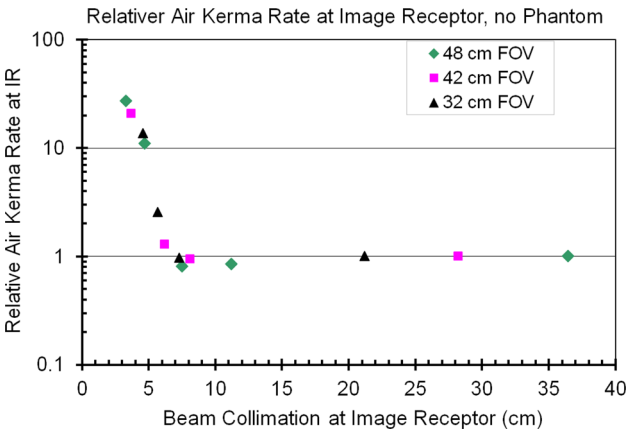

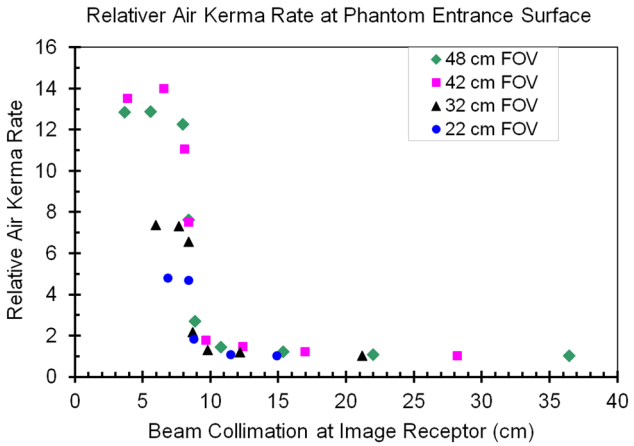

References

1. Baek SW, Ryu JS, Jung CH, Lee JH, Kwon WK, Woo NS et al (2013) A randomized controlled trial about the levels of radiation exposure depends on the use of collimation C-arm fluoroscopic-guided medial branch block. Korean J Pain 26(2):148–153. https://doi.org/10.3344/kjp.2013.26.2.148
2. State University of New York, Upstate Medical University. Radiology. Academics. Collimation effects. http://www.upstate.edu/radiology/education/rsna/fluoro/collimation.php. Accessed 30 April 2018

P41 OpenDose: an extensible, open-source internal dosimetry calculator

E. McKay[1], A. Malaroda[2]

[1]Department of Nuclear Medicine, St. George Hospital, Sydney, Australia. (erin.mckay@health.nsw.gov.au [Presenting author]).
[2]Centre for Medical Radiation Physics, University of Wollongong, Australia. (malaroda@uow.edu.au)

Introduction The MIRDose [1] and OLINDA/EXM [2] software tools have long been accepted as de-facto standards for internal radionuclide dosimetry. Both packages facilitate calculations of absorbed and effective dose for several anthropomorphic geometries and a large range of decay spectra. However, neither package allows the user to define new geometries or spectra, restricting their applicability to the built-in models.
Aim To develop an open-source software implementation of the MIRD internal dosimetry procedure which supports extension with user-defined geometry models, decay spectra, residence time calculations and effective dose calculations.
Method The OpenDose software package was developed using the Java 1.8 platform. It provides both a graphical user interface and a command line interface, the latter intended both for automated software testing and for batch processing.
The package includes algorithms for constructing dose factor arrays from user-defined decay spectra and specific absorbed fraction data, calculating a remainder-of-body dose factor from user-specified dose factors, production of residence time data using ICRP bladder and gut models, and calculation of effective dose using the methods of ICRP publications 60 and 103. It also includes packaging tools to facilitate construction of user-defined geometries and emission spectra, which are stored in JSON structured text files.

The software is presently being validated against the output of the OLINDA/EXM software, using decay spectra (H-3, P-32, I-125 and I-131) and specific absorbed fractions (for Adult & Pregnant Female models) obtained via the RADAR web-site [3].
Results Dose factors are reproduced to within 2% of OLINDA/EXM results for better than 98% of evaluated source/target pairs. Significant discrepancies are noted in the dose to bone marrow and osteogenic cells from bone sources; these arise from a presently incomplete representation of some source material [4,5] in data files.
Conclusion An extensible, open-source software for internal dosimetry calculations using the MIRD method has been developed and is presently undergoing validation.

References

1. M.G. Stabin. *MIRDOSE: Personal Computer Software for Internal Dose Assessment in Nuclear Medicine*. J Nucl Med 1996; 37:538–546.
2. M.G. Stabin, R.B. Sparks, E. Crowe. *OLINDA/EXM: The Second-Generation Personal Computer Software for Internal Dose Assessment in Nuclear Medicine*. J Nucl Med 2005; 46:1023–1027.
3. RADAR web site: http://www.doseinfo-radar.com/.
4. L.G. Bouchet, D.W Jokisch, W.E. Bolch. *A Three-Dimensional Transport Model for Determining Absorbed Fractions of Energy for Electrons Within Trabecular Bone*. J Nucl Med 1999; 40:1947–1966.
5. L.G. Bouchet, W.E. Bolch. *A Three-Dimensional Transport Model for Determining Absorbed Fractions of Energy for Electrons Within Cortical Bone*. J Nucl Med 1999; 40:2115–2124.

P42 A comparison between automatic planning and customisable volumetric modulated arc therapy planning for single isocentre treatment of multiple brain metastases

C. R. Moulton[1], R. Gajewski[1], C. Owen[1], R. Stensmyr[1], D. Mason[1], S. Yau[1,2]

[1]Crown Princess Mary Cancer Centre, Westmead Hospital, Australia. , (calyn.moulton@health.nsw.gov.au [Presenting author]), (romuald.gajewski@health.nsw.gov.au), (catherine.owen@health.nsw.gov.au), (rachel.stensmyr@health.nsw.gov.au), (daniel.mason@health.nsw.gov.au), (shan.yau@health.nsw.gov.au).
[2]Nepean Cancer Care Centre, Nepean Hospital, Australia.

Introduction It is efficient to treat multiple brain metastases (mets) using single isocentre stereotactic radiosurgery. Two possible planning methods are: volumetric modulated arc therapy (VMAT) delivering multiple dynamic arcs, via a treatment planning system (TPS) such as Varian Eclipse [1]; or multiple dynamic conformal arcs via an automatic TPS such as Brainlab Elements [2]. This study explores whether plan quality is similar between Elements and VMAT.
Method Four patients (5–15 mets/plan) were planned in Elements (pencil beam model, version 1.5.0), then exported and re-calculated in Eclipse (anisotropic analytical algorithm, version 13.7.16) [1–3]. VMAT plans were created in Eclipse to meet objectives set by the oncologists. Doses to mets were compared using D100% and maximum dose. Doses to organs at risk (OARs) were compared using mean dose and maximum dose. V5Gy/V10Gy were used to compare

dose wash in the brain. The modulation was assessed via monitor units.

Results VMAT achieved similar target coverage as Elements which demonstrated more met-to-met inconsistency in under-dosage/over-dosage. VMAT gave some higher maximum doses to mets. Dose wash was in most cases very similar or slightly larger (smaller) for VMAT with a smaller (larger) number of mets. In most cases, VMAT achieved marginally worse OAR sparing for orbits and lenses, but marginally better sparing of optic nerves and tracks. The comparison of OAR sparing for the brainstem was dependent on the number/location of mets. VMAT generally achieved less modulation.

Conclusion VMAT achieved similar plan quality to Elements. The inferior OAR sparing for the orbits/lenses from VMAT makes it a candidate for further optimisation as it was a low priority. The issue with applying VMAT was that it required considerable planning experience and planning time to fine tune the optimal collimator and couch angles. In comparison, the automatic Elements planning was efficient with reduced workload for the planner.

References

1. Varian Medical Systems, Inc. (2015) Eclipse photon and electron algorithms reference guide. Varian Medical Systems, Inc., Palo Alto.
2. Brainlab AG (2017) Software user guide revision 1.0: Multiple brain mets SRS version 1.5.0. Brainlab AG, Munich.
3. Brainlab AG (2016) Technical reference guide revision 2.0: Brainlab physics. Brainlab AG, Munich.

P43 The potential for elevated neutron dose rates at the entrances of radiotherapy bunkers when linear accelerators are upgraded from 6 MV to 10 MV

C. R. Moulton[1], R. Gajewski[1], R. Stensmyr[1], S. Yau[1,2]

[1]Crown Princess Mary Cancer Centre, Westmead Hospital, Australia. (calyn.moulton@health.nsw.gov.au [Presenting author]), (romuald.gajewski@health.nsw.gov.au), (rachel.stensmyr@health.nsw.gov.au), (shan.yau@health.nsw.gov.au). [2]Nepean Cancer Care Centre, Nepean Hospital, Australia.

Introduction A Varian TrueBeam STx (6/10 MV) linear accelerator was installed in an existing bunker (previously 6 MV) after renovation. A post-installation radiation survey identified radiation protection concerns. The subsequent investigations and resolutions will be discussed with a consideration of neutron production given the bunker entrance design.

Method A full radiation survey for 6 and 10 MV was performed according to NCRP Report 151 [1]. Instantaneous dose rates (IDRs) for photons and neutrons were measured with a Fluke 451P-DE pressurised ion chamber survey meter and a Nuclear Enterprises NM2B BF_3 proportional counter respectively. IDRs were converted to expected weekly doses for the primary workload (600 Gy/week) and machine output rate (600 MU/min) [1]. For neutrons, leakage workload was calculated as it increases primary workload by a modulation factor ($\geq$ 3) [1]. Weekly doses for occupancies were compared with local design goals (25% of legislated dose limits).

Results The figure below indicates high IDR areas. Steel was added to primary barriers because new excessive laser recesses resulted in high photon IDRs at points A/B. The new sub-wait (point D) was replaced with a cupboard due to high photon/neutron IDRs around point C. 10 MV was disabled due to high photon IDRs and expected violations of local design goals at the edge of primary barriers (points E/F). Local design goals were achieved for 6 MV at points E/F with complications for 10 MV arising from the combined impact of an isocentre shift and increased beam penetration.

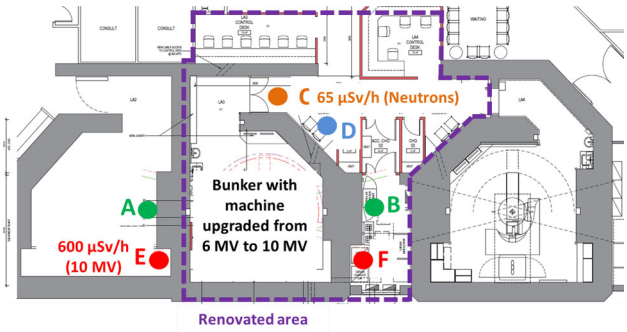

Conclusion 10 MV provided elevated neutron IDRs at the bunker entrance. Hence, full shielding calculations and surveys which include neutrons are important if the beam spectrum contains $\geq$ 10 MV. Elevated neutron IDRs could be avoided for bunkers with neutron shielded doors or longer inner/outer maze entrance. A comparison of neutron measurements and shielding calculations will be presented.

References

1. National Council on Radiation Protection and Measurements (2005) NCRP 151: Structural shielding design and evaluation for megavoltage X- and gamma-ray radiotherapy facilities. National Council on Radiation Protection and Measurements, Bethesda.

P44 Dose size really matter?: Comparison of contour volumes treatment planning systems and MIM

Z. Moutrie[1], V. Moutrie[2]

[1]Department of Radiation Oncology, The Mater Hospital, GenesisCare, Crows Nest, NSW 2065 (zoe.moutrie@cancer.com.au [Presenting author]). [2]Department of Radiation Oncology, Macquarie University Hospital, GenesisCare, North Ryde, NSW

Introduction In radiation therapy Dose Volume Historgram metrics are used to assess how well a radiation therapy plan meets clinical planning objectives. It is also commonplace to use these to compare planning techniques between departments or in benchmarking a new treatment technique. This relies on a DVH equivalency which requires firstly that the dosimetric accuracy in each department and treatment planning system is equivalent and secondly that the volumetric precision and/or accuracy in each treatment planning system is the same. The first requirement has been the basis of previous research [1–10], however has been done to investigate creating a VOI in one software and its representation or equivalent delineation in other software. This work investigates how a number of treatment planning systems and one contouring software create volumes and how they are translated when imported from each other.

Method An artificial CT was created with very high resolution voxels and a standard CT was acquired with clinically relevant slice thickness. Several simple contours were created manually on both CT datasets, using the best available tools in Oncentra, Eclipse, Pinnacle, iPlan and Mim Maestro.

For each set of contour and CT dataset the volumes were exported and imported into each of the other available software(s) where the reported volumes were compared to the theoretical volume.

Results Transferring volumes from one software to another provided varying levels of agreement depending upon the settings of the software. While some software recreated the volumes upon import such that when volumes created in TPS1 were transferred to TPS2 and reimported into TPS1 again, TPS1 reported a new volume.
Conclusion For small volumes or complex geometries the differences between the software investigated does not yield equivalent results and could (and would) lead to deviations in DVH analysis for treatment plan evaluation.
Acknowledgements The authors wish to acknowledge the assistance of Nathan Hu (work completed while employed at GenssisCare).

References

1. Knöös T, Wieslander E, Cozzi L, Brink C, Fogliata A, Albers D, Nystrom H, Lassen S (2006) Comparison of dose calculation algorithms for treatment planning in external photon beam therapy for clinical situations. Physics in Medicine and Biology 51 (22):5785–5807
2. Knöös T, Ceberg C, Weber L, Nilsson P (1994) The dosimetric verification of a pencil beam based treatment planning system. Physics in Medicine and Biology 39 (10):1609–1628
3. Irvine C, Morgan A, Crellin A, Nisbet A, Beange I (2004) The Clinical Implications of the Collapsed Cone Planning Algorithm. Clinical Oncology 16 (2):148–154
4. Hogstrom KR, Mills MD, Almond PR (1981) Electron beam dose calculations. Physics in Medicine and Biology 26 (3):445–459
5. Hasenbalg F, Neuenschwander H, Mini R, Born EJ (2007) Collapsed cone convolution and analytical anisotropic algorithm dose calculations compared to VMC++ Monte Carlo simulations in clinical cases. Physics in Medicine and Biology 52 (13):3679–3691
6. Edimo P, Clermont C, Kwato MG, Vynckier S (2009) Evaluation of a commercial VMC++ Monte Carlo based treatment planning system for electron beams using EGSnrc/BEAMnrc simulations and measurements. Physica Medica 25 (3):111–121
7. Carrasco P, Jornet N, Duch MA, Weber L, Ginjaume M, Eudaldo T, Jurado D, Ruiz A, Ribas M (2004) Comparison of dose calculation algorithms in phantoms with lung equivalent heterogeneities under conditions of lateral electronic disequilibrium. Medical Physics 31 (10):2899–2911
8. Aspradakis MM, Morrison RH, Richmond ND, Steele A (2003) Experimental verification of convolution/superposition photon dose calculations for radiotherapy treatment planning. Physics in Medicine and Biology 48 (17):2873–2893
9. Rana S (2014) Clinical dosimetric impact of Acuros XB and analytical anisotropic algorithm (AAA) on real lung cancer treatment plans : review, vol 2. 2014, vol 1.
10. Fotina I, Winkler P, Künzler T, Reiterer J, Simmat I, Georg D (2009) Advanced kernel methods vs. Monte Carlo-based dose calculation for high energy photon beams. Radiotherapy and Oncology 93 (3):645–653

P45 Does the Dose of SIB VMAT smell sweater?: Commissioning of a VMAT technique

Z. Moutrie, A. Hollands

Department of Radiation Oncology, The Mater Hospital, GenesisCare, Crows Nest, NSW 2065. (zoe.moutrie@cancer.com.au [Presenting author])

Introduction Historically the treatment of lesions located in- or around- the Nose would have been delivered with simple electron fields or parallel opposed photons to a single dose level. With the implementation of inverse planned VMAT treatments it is now possible to treat targets having complex geometries and collocated organs at risk with doses to different values.
Validation of an optimisation and dose calculation algorithms are be made to ensure accurate deliverability of a plan for a variety of treatment volumes, however certain anatomical regions and dosimetric levels can push these algorithms to their limits. For the case of simultaneous integrated boost nose treatment our department saw a need to confirm dosimetric accuracy and deliverability before its clinical implementation.
Method An anthropomorphic phantom was simulated and clinically relevant OARs were contoured with two sets of targets: A single PTV and three boost GTVs. One set of GTvs were located < 8 mm apart and < 1 cc each, the second were 8 mm apart and > 1cc. For both sets of targets a treatment plan was created using Eclipse (v11).
Each plan was delivered to the ArcCheck to assess the deliverability of the optimised plan (DVO algorithm) and delivered to the anthropomorphic phantom with EBT invivo dosimeters placed at key locations on the phantom surface and within the transverse plane to assess the dosimetric accuracy of the dose calculation (AAA algorithm).
Results All ArcCheck measurements passed the criteria of $> 97\%$ point using 3%, 3mm DTA.
EBT film exhibited regions of high and low dose, but otherwise indicated within 5% of the TPS calculated dose.
Conclusion The delivery of an SIB Nose treatment using a VMAT technique is well handled using Eclipse TPS and Truebeam linear accelerator. The treatment of SIB Nose VMAT was successfully implemented clinically.
Acknowledgements The authors wish to acknowledge the assistance of Neal Molloy and Kim Buman.

P46 Micro-slit beam radiation therapy for multiple lung-metastatic tumor

N. Mukumoto[1], M. Nakayama[2], H. Akasaka[1], Y. Shimizu[3], K. Umetani[4], D. Miyawaki[1], R. Sasaki[5]

[1]Division of Radiation Oncology, Kobe University Hospital, Kobe, Japan. (nmukumot@med.kobe-u.ac.jp [Presenting author]), (akasaka@harbor.kobe-u.ac.jp), (miyawaki@med.kobe-u.ac.jp). [2]Discipline of Medical Radiations, School of Biomedical & Health Sciences, RMIT University, Australia. (masao.nakayama@rmit.edu.au). [3]Division of Radiation Oncology, Graduate School of Medicine, Kobe University, Kobe, Japan. (innocell@live.jp). [4]Japan Synchrotron Radiation Research Institute, Mikazuki, Sayo, Hyogo, Japan. (umetani@spring8.or.jp). [5]Division of Radiation Oncology, Kobe University Hospital, Kobe, Japan. (rsasaki@med.kobe-u.ac.jp)

Introduction Synchrotron X-ray beams permit the delivery of very high radiation doses to tumors in short period of time with a single fraction using arrays of micro-slit beam radiation therapy. In this study, we have challenged to treat multiple metastatic lung tumors by applying MRT to mouse tumor-bearing right lung with comparing to the broad beam treatment from the same radiation source.
Method Synchrotron X-ray beam radiation was performed using BL28B2 beam-line at the SPring-8 facility, Hyogo, Japan. The animals used were male DBA/2 mice aged 13–15 weeks old, inoculated KLN205 2.5 x 10^6 cells/mouse 4 weeks before the exposure of the beam. As for radiation techniques, anterior-posterior 12 x 30 mm

windows were set, and either a conventional unidirectional broad beam or unidirectional array of MRT (25 μm width, 200 μm center-to-center spacing) was used. Delivered dose of the broad beam was 36 Gy while that of the MRT were 36–120 Gy. The observation period was 27 days after the irradiation. Histopathological evaluation of the irradiated lung tissues was performed with hematoxylin and eosin staining.

Results According to microscopic observations, the areas of tumor on the slides were reduced to one-third compared to the unirradiated region in the slides of 120 Gy MRT while the total lung area was not collapsed and maintained its original size

Conclusion Such high doses of MRT can diminish the tumor volumes without breaching of lung tissue scaffoldings. There is a good possibility that MRT would control the growth of metastatic lung tumors.

References

1. Mukumoto N, Nakayama M, Akasaka H, Shimizu Y, Osuga S, Miyawaki D, Yoshida K, Ejima Y, Miura Y, Umetani K, Kondoh T, Sasaki R (2017) Sparing of tissue by using micro-slit-beam radiation therapy reduces neurotoxicity compared with broad-beam radiation therapy. J Radiat Res. Jan;58(1):17–23 https://doi.org/10.1093/jrr/rrw065
2. Saito A, Morishita N, Mitsuoka C, Kitajima S, Hamada K, Lee KM, Kawabata M, Fujisawa M, Shirakawa T (2011) Intravenous injection of irradiated tumor cell vaccine carrying oncolytic adenovirus suppressed the growth of multiple lung tumors in a mouse squamous cell carcinoma model. J Gene Med. Jun;13(6):353–61. https://doi.org/10.1002/jgm.1578
3. Nariyama N (2012) Macroscopic and microscopic X-ray dose mappings with CCD-based GafChromic film dosimeters. Appl Radiat Isot. Jul;70(7):1214–8 https://doi.org/10.1016/j.apradiso.2011.12.009

P47 Reactive oxygen species generated by titanium peroxide nanoparticles as a radiosensitizer compared to gold nanoparticles

M. Nakayama[1], H. Akasaka[2], C. Ogino[3], M. Geso[1], R. Sasaki[4]

[1]Discipline of Medical Radiations, School of Biomedical & Health Sciences, RMIT University, Australia. (masao.nakayama@rmit.edu.au [Presenting author]), (moshi.geso@rmit.edu.au). [2]Division of Radiation Oncology, Kobe University Hospital, Kobe, Japan. (akasaka@harbor.kobe-u.ac.jp). [3]Department of Chemical Science and Engineering, Graduate School of Engineering, Kobe University, Japan. (ochiaki@port.kobe-u.ac.jp). [4]Division of Radiation Oncology, Graduate School of Medicine, Kobe University, Kobe, Japan. (rsasaki@med.kobe-u.ac.jp)

Introduction High Z nanoparticles have been well investigated in their roles as radiosensitizers. The outcome has been showing that they can be effective dose enhancing agent. Our recent results indicated that titanium peroxide nanoparticles (TiO_xNPs) induced reactive oxygen species (ROS) when expose to X-rays and enhanced radiation cytotoxic effects *in vivo* experiments [1]. In this study, the type and amount of ROS generated from TiO_xNPs was investigated and compared to those generated by gold nanoparticles (GNPs).

Method The TiO_xNPs were synthesized from titanium oxide nanoparticles by hydrothermal methods and coated by polyacrylic acid. The GNPs of almost same size as TiO_xNPs were purchased from BBI solutions Co. Ltd. (Cardiff, UK). Using chemical probes, the three types of ROS generation were confirmed without cells; hydroxyl radical (•OH), superoxide anion (O_2^-), and hydrogen peroxide (H_2O_2). In addition, tumour growth inhibition assay was performed to evaluate the effects of generated ROS on the radiation enhancement in vivo.

Results At the high concentration of TiO_xNPs and GNPs, the generation rates of •OH with 10 Gy of radiation were increased by 2.2 and 3.9 fold, respectively. For TiO_xNPs, O_2^- signal with radiation was decreased, and the H_2O_2 was increased regardless of X-ray irradiation. No increase of O_2^- and H_2O_2 signals for GNPs with X-rays was observed. In the in vivo experiments, the combination of TiO_xNPs and X-rays induced significantly stronger tumour inhibition compared to the combination of GNPs and the same level of X-rays.

Conclusion Our results show that the amount of ROS generated from TiO_xNPs under X-ray irradiation is less than that of GNPs, however TiO_xNPs have the ability to release H_2O_2 regardless of X-ray irradiation. The released H_2O_2 is assumed to be acted as a strong radiosensitizing agent of TiO_xNPs in the in vivo set up.

Reference

1. Nakayama M, Sasaki R, Ogino C, Tanaka T, Morita K, Umetsu M, Ohara S, Tan Z, Nishimura Y, Akasaka H, Sato K, Numako C, Takami S, Kondo A (2016) Titanium peroxide nanoparticles enhanced cytotoxic effects of X-ray irradiation against pancreatic cancer model through reactive oxygen species generation in vitro and in vivo. Radiat Oncol 11(1):91. https://doi.org/10.1186/s13014-016-0666-y

P48 Comparison of radiotherapy in-vivo doses measured using MOSFET and thermoluminescent dosimeters (TLDs) for high energy photon and electron external beam radiation therapy.

V. K. Nelson[1,2], P. Narayanan[1,2], S. B. Rajapakse[1,2]

[1]Liverpool & Macarthur Cancer Therapy Centres. [2]Macarthur Health Service, Campbelltown, NSW, Australia. (Vinod.Nelson@health.nsw.gov.au), (Pradush.Peethambaran@health.nsw.gov.au), (Satya.Rajapakse@health.nsw.gov.au)

Introduction In vivo dosimetry is an essential quality assurance tool to assess discrepancies in the planned and delivered dose. Metal oxide semiconductor field effect transistors (MOSFETs) have been proposed as suitable dosimeters this purpose [1–3]. The aim of this work was to ascertain the suitability of MOSFETs as a viable replacement of TLDs for in-vivo dosimetry of high-energy photon and electron external beam radiation therapy.

Method Characterization of five TN502RD-H MOSFETs (Best Medical, Canada) for in-vivo dosimetry in radiotherapy was carried out in terms of reproducibility, linearity, dependence on incident beam angle, beam energy, temperature, source to skin distance and field size. Doses measured simultaneously in solid water using an ion chamber and MOSFETs for a number of field sizes and beam energies were compared. Clinical dose measurements were performed using both TLDs and MOSFETs simultaneously and compared with the planning system doses to assess the suitability of MOSFETs as an alternative to TLDs for in-vivo dosimetry.

Results Table 1 shows the doses measured in solid water phantom by ion chamber and MOSFETs and the %age differences in the measured doses. All MOSFET measured doses are within ± 3% of the doses calculated by the planning system. Figure 1 shows the difference in patient doses measured using MOSFETs and TLDs and doses calculated by the planning system. Measurement no. 11 was for the treatment of ear with a compound shield. The large difference in the

MOSFET-TLD dose is probably due to enhanced TLD response as a result of backscattering from compound shield.

Table1. Comparison of Doses measured in solid water phantom.

Beams	Field Size (cm)	Measured Dose (cGy)			%age Difference		
		Chamber	MOSFET	TPS	Chamber/ MOSFET	Chamber/ TPS	MOSFET / TPS
6X	5x5	92.5	94.4	94.3	-2.1	-1.9	0.1
	20x20	106.8	108.3	109.6	-1.5	-2.5	-1.1
18X	5x5	93.4	92.0	92.7	1.5	0.8	-0.8
	20x20	104.7	103.0	106.1	1.6	-1.3	-2.9
6E	5cm Dia	94.7	95.2	97.2	-0.5	-2.6	-2.1
	6cm Dia	96.9	99.4	98.2	-2.6	-1.3	1.2
10E	8x4	94.2	94.5	96.1	-0.3	-2.0	-1.7
	6x4	88.5	93.1	91.8	-5.2	-3.6	1.4
15E	5x5	96.1	99.6	97.6	-3.6	-1.5	2.0
	4x4	92.9	96.5	96.2	-3.9	-3.4	0.3

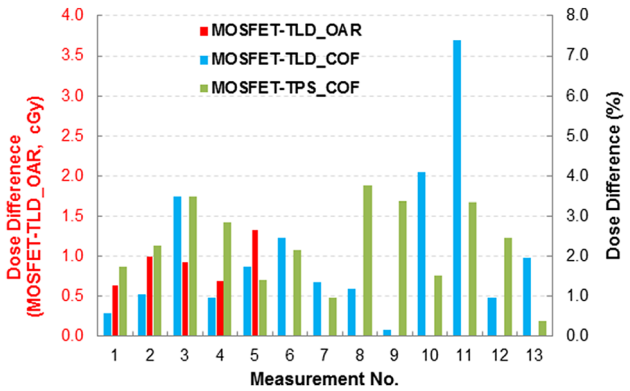

Figure 1. Differences in the clinical doses measured by MOSFETs, TLDs and TPS (OAR – organ at risk, COF-centre of field).

Conclusion The TN502RD-H MOSFETs provide an adequate alternative to TLDs for in-vivo dose assessment for EBRT entrance dose measurements for both megavoltage photon and electron beams. Further testing is planned to assess their suitability for low dose measurements, dosimetry in rotational radiotherapy techniques and kilovoltage superficial radiotherapy.

References

1. V Vassiliki et al (2010) Peripheral dose measurement in high-energy photon radiotherapy and the implementation of MOSFET. World Jour Radiol 28; 2 (11): 434–439:114–125.
2. M. Dybek et al (2005) MOSFET detectors as a tool for the verification of therapeutic doses of electron beams in radiotherapy, Rep Pract Oncol Radiother 10 (6): 301–306
3. R Ramani, S. Russell and P. O'Brien (1997) Clinical Dosimetry using MOSFETS, Radiation Oncology Biol. Phys 37:959–964

P49 Beam modelling and evaluation of an Elekta Agility head in RayStation treatment planning system

S. Nilsson, S. M. Heng, D. Inwood, S. Corde, S. J. Downes

Nelune Comprehensive Cancer Centre, Prince of Wales Hospital, Randwick NSW. (sanna.nilsson@health.nsw.gov.au [Presenting author]), (soomin.heng@health.nsw.gov.au), (dean.inwood@health.nsw.gov.au), (stephanie.cordetehei@health.nsw.gov.au), (simon.downes@health.nsw.gov.au)

Introduction RayStation 7 (RaySearch Medical Laboratories AB, Stockholm, Sweden) was recently acquired at the NCCC, Prince of Wales Hospital, as a new external beam planning system in addition to previously commissioned XiO and Monaco treatment planning system by Elekta (Elekta AB, Stockholm, Sweden). At the NCCC there are currently three clinical beam matched Elekta linear accelerators, with Agility heads, used routinely for conformal, IMRT, VMAT and electron treatment delivery. The clinical dose engines in RayStation 7 are based on the two well-known algorithms, the collapsed cone convolution superposition (CCC) for photons and the Monte Carlo for electrons. This study presents beam modelling and dosimetric evaluation of an Elekta Agility head in RayStation 7.
Method Beam modelling and validation of the model was performed in RayPhysics which is a separate physics module incorporated in RayStation 7. RayPhysics uses the same dose engines as the clinical treatment module uses for patient planning. Measured data for input was collected with appropriate selection of detectors and Gafchromic EBT3 film, for field sizes ranging from 1x1 up to 40x40 cm2. The output in RayPhysics Beam Commissioning module is convolved to account for detector size to enable a good agreement between measured and computed data. Final evaluation of the beam model was performed within the clinical module of RayStation.
Results A good match could be achieved between the Agility model and measured data. Different tolerances were set for different regions of the analysed data. The largest difference could be observed in build-up regions, out of field dose, and the tails.
Conclusion The overall performance of the beam model is satisfactory and released for clinical use. Future work will include implementation of other treatment techniques like TBI.

P50 Evaluation of photon dose calculation in Raystation TPS in heterogenous media

S. M. Heng, S. Nilsson, S. Corde, S. J. Downes

Nelune Comprehensive Cancer Centre, Prince of Wales Hospital, Randwick NSW. (soomin.heng@health.nsw.gov.au [Presenting author]), (sanna.nilsson@health.nsw.gov.au), (stephanie.cordetehei@health.nsw.gov.au), (simon.downes@health.nsw.gov.au)

Introduction Raystation(RaySearch Laboratories, Sweden) was recently acquired at the NCCC, Prince of Wales Hospital. This TPS requires a CT-to-Mass Density (MD) calibration curve for inhomogeneity correction. All CT numbers above the maximum value of 4000 are attributed to the MD value corresponding to this last point of the curve. However, the user can segment an ROI and overrides the MD with one from a predefined list of elements for values exceeding this range. This work aims at (1) comparing the photon dose calculated in heterogenous media between XiO v5.10 (Superposition), Monaco v5.11 (Monte Carlo) and Raystation v7 (Collapse Cone), and (2) experimentally validating the assigned MD for the extended range.

Method Dose profiles were calculated and compared for two different inhomogeneity materials (bone and lung equivalent) placed inside the Scanditronix Wellhofer I'MRT phantom.. Point dose were measured using a CC04 chamber placed in the phantom. The accuracy of the steel and titanium MD assignment on photon dose calculation was checked by performing transmission measurement using the Sun Nuclear Mapcheck 2 diode array.
Results For dose profiles across inhomogeneity materials, Raystation agreed well with XiO, while Monaco, as expected for a Monte-carlo based planning system, exhibits differences. The doses computed with the assigned MD agrees relatively well with measurements for materials with CT numbers higher than the allowable range.
Conclusion Dose calculations in heterogenous media in Raystation are comparable to XiO. Both have known limitations, which are highlighted with experimental measurements and comparison with Monaco using Monte-carlo algorithm. Assigning MD value for the metals inserts led to satisfactory results however it is suggested that extended CT to MD curve to be implemented in future versions of Raystation without the need of segmenting them.

P51 VeriSoft 7.1 commissioning

S. F. E. Liu[1], C. Noble[1], B. Perrett[1], P. O'Connor[1], P. Charles[1]

[1]Radiation Oncology, Princess Alexandra Hospital, Brisbane, Australia. (Saufan.liu@health.qld.gov.au), (Christopher.Noble@health.qld.gov.au [Presenting author]), (Ben.Perrett@health.qld.gov.au), (Patrick.OConnor2@health.qld.gov.au), (Paul.Charles@health.qld.gov.au)

Introduction VeriSoft (version 6.2) is software used to analyze patient specific measurements using the Octavius 4D phantom with either the 1000 SRS array or the 1500 array (PTW, Freiburg, Germany). New software, VeriSoft 7.1 (PTW, Freiburg, Germany), was launched in 2017 and required commissioning for clinical use. A reference field, off-axis fields, and IMRT/VMAT fields were all measured using both VeriSoft 6.2 and VeriSoft 7.1 to evaluate the new software's performance.
Method A 10x10 reference CAX field and 8 off-axis fields were measured using the Octavius 4D phantom with 1500 array on three different days. IMRT/VMAT fields were measured using both arrays. 3 % / 1 mm gamma criteria were used for stereotactic 1000 SRS array analysis while 3 % / 3 mm of gamma criteria were used for the analysis of measurements performed with the 1500 array. 25x25 fields were measured with different array orientations to check the calibration of the 1500 array.
Results For the reference 10 × 10 field, 3D reconstruction of both versions showed a lack of horned profiles at shallow depths. However, for some off-axis fields, VeriSoft 7.1 generally had pass rates greater than 95% while VeriSoft 6.2.had pass rates less than 95%. Slight errors in the 1500 array were detected. The pass rate of IMRT/VMAT measurements using VeriSoft 7.1 was similar to 6.2.
Conclusion VeriSoft 7.1 showed better 3D reconstruction calculations for off-axis fields compared to VeriSoft 6.2. Since IMRT/VMAT measurements using VeriSoft 7.1 were comparable to 6.2, we use VeriSoft 7.1 3D reconstruction for IMRT/VMAT with high dose in the central region and low peripheral dose. For instance, pelvis region, head region, and spine region. However, we do not use VeriSoft 7.1 3D reconstruction in breast VMAT and chest wall VMAT which are high dose in peripheral and low dose in central region.

P52 Commissioning of High Definition Motion Management on the Leksell Gamma Knife Icon

P. O'Connor[1], B. Perrett[1]C. Jones[1], V. Seshadri[1], T. Markwell[2]

[1]Radiation Oncology, Princess Alexandra Hospital, Brisbane, Australia. (Patrick.OConnor2@health.qld.gov.au [Presenting author]), (ben.perrett@health.qld.gov.au), (Catherine.jones3@health.qld.gov.au), (Venkatakrishnan.seshadri@health.qld.gov.au). [2]Radiation Oncology PA Raymond Terrace, Brisbane, Australia. (Tim.markwell@health.qld.gov.au)

Introduction The Leksell Gamma Knife Icon (Elekta, Stockholm, Sweden) includes a real-time infrared patient tracking system. A stereoscopic infrared camera mounted on the couch, a pair of reference reflectors attached to the mask adapter, and a reflector placed on the patient's nose are used to monitor intra-fraction motion. Measured position deviations can be used as a beam interlock.
Commissioning tests were performed to assess the accuracy of measured deviations, and the operation of interlocks during treatment.
Method A reflector, representing the patient, was mounted on a jig used for Winston Lutz type tests. Micrometer adjustments were performed in order to assess the accuracy of the indicated position offset. The reflector was then mounted on a motorised platform so that the reflector could be moved during treatment in order to test the functionality of the beam interlock. In addition, a phantom containing an ion chamber was set up in order to assess any change in dose induced by activating the interlock multiple times during a shot.
Results The average difference between reflector position indicated by the micrometer scales, and reflector position indicated by the infrared system was 0.05 mm, with a maximum difference of 0.11 mm. The motorised platform enabled a simple check for the functionality of beam interlocks once the marker deviation exceeded a set tolerance. Ion chamber measurements indicated that there was negligible change in measured dose caused by activating the interlock on 3 occasions during a single 2.3 min shot.
Conclusion This method was able to assess the accuracy and functionality of the Gamma Knife's infrared system, and can be easily adapted for other types of infrared tracking systems.

P53 3D Printing for rapid prototyping in the radiation oncology environment

J. Wolf[1], S. Baddock[1], T. Ostwald[1]

[1]Department of Radiation Oncology, Calvary Mater Newcastle, Australia. (joshua.wolf@calvarymater.org.au [Presenting author]), (shane.baddock@calvarymater.org.au), (shane.baddock@calvarymater.org.au)

Introduction The use of 3D printing in the radiation oncology environment, specifically Fused Deposition Modelling (FDM) technology, has been increasing in popularity in recent years. 3D printers are generally used for the creation of either bolus or phantoms and other miscellaneous objects. This work investigates the applicability of, and issues involved with, the latter of these use cases.
Method The Calvary Mater Newcastle (CMN) has acquired two Ultimaker 3 Extended FDM printers which are capable of printing in a range of materials including: Polylactic Acid (PLA), Copolyester (CPE), Thermoplastic Polyurethane (TPU), Polycarbonate (PC) and Polyvinyl Alcohol (PVA). The dosimetric performance of these materials was assessed via both CT and irradiation. It should be noted that PVA is only used as dissolvable support and was not investigated further. Three examples are given of the use of the printers in the

clinical environment to resolve encountered issues. Finally learnt lessons are discussed around the implementation of 3D printers in the clinic.

Results It was found that all four materials investigated (PLA, CPE, TPU and PC) had relative electron densities of $\sim$ 1.09, physical densities of $\sim$ 1.2 g/cm^3 and $\sim$ 1% dose enhancement compared to the same thickness of solid water. 3D printing proved useful in quickly producing clinically useful items including: a water tank chamber spacer, a levelling Roos chamber holder and a kV pin-hole camera. The use of 3D printing allowed rapid iteration in all cases where design flaws could be investigated and rectified in a new print, generally within 24 h. Printing issues (such as adhesion) can initially present roadblocks to implementation however with experience these can be overcome.

Conclusion FDM 3D printers have been found to provide a viable way to quickly produce items of need within the clinical environment compared to traditional methods.

P54 Effects of acrylic beam spoilers in MRI-Linac skin Dosimetry

E. Patterson[1], U. Jelen[2], D. Cutajar[1], B. Oborn[1], P. Metcalfe[3]

[1]Centre of Medical Radiation Physics, University of Wollongong, Australia. (ep958@uowmail.edu.au [Presenting author]), (deanc@uow.edu.au), (boborn@uow.edu.au). [2]MRI-Linac Physicist, Ingham Institute, Sydney NSW, Australia. (urszula.jelen@health.nsw.gov.au). [3]School of Physics and Centre of Medical Radiation Physics (CMRP), Wollongong, Australia. (metcalfe@uow.edu.au)

Introduction MRI linac components produce a Lorentz force on secondary electron paths. For some inline designs, this has been termed the electron focusing effect (EFE) and introduces unique challenges for radiotherapy dosimetry, particularly at the entry surface (skin) region. During radiation therapy, excess dose to the skin can cause erythema, desquamation, and necrosis[1]. To provide skin sparing, air generated electrons can be attenuated with the use of acrylic beam spoilers[2].

Method The effects of varying the position of an acrylic beam spoiler to reduce skin dose on an inline MRI linac was investigated. Shallow depth-dose measurements were performed with a high spatial resolution MOSkin dosimeter which is based on MOSFET technology. The MOSkin is suitable for use in the high gradient fields found within the MRI-Linac, with the ability to provide a depth of measurements of 0.07mm, giving a skin dose equivalent depth when placed on a surface during radiation therapy[3]. Measurements were performed at the Ingham Institute research bunker housing an Australian prototype MRI-linac, which consists of a split bore 1 T MRI unit coupled with a 6 MV Varian linac. A 20mm acrylic block was placed 15cm upstream from the isocentre where surface measurements were performed.

Results The electron focusing effect caused a skin dose of 200% relative to Dmax. With the use of the spoiler, the energy deposited in the MOSkin positioned in shallow layers of solid water was notably smaller than measurements performed with no perturbing material, reducing the surface dose to 125% relative to Dmax, as shown in Figure 1.

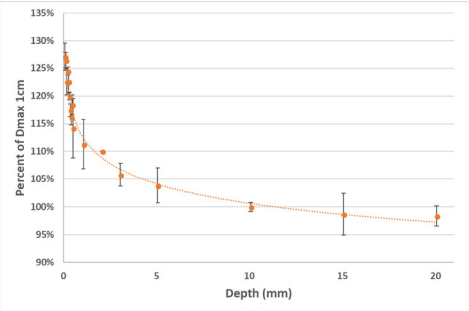

Fig 1. Shallow depth-dose measurements of MRI-linac beam entry when incorporating an acrylic beam spoiler (as measured by a MOSkin dosimeter)

Conclusion The use of an acrylic beam spoiler has a significant dosimetric impact by reducing additional dose concentrated at the skin with inline MRI-linac configurations. This study demonstrates the potential use of spoilers in radiation therapy performed in an MRI-linac system to maintain skin sparing. While the skin dose is less, there is still no build up region, hence more sophisticated methods such as magnetic field purging may need to be implemented.

References

1. I. Turesson and H. Thames, Repair capacity and kinetics of human skin during fractionated radiotherapy: erythema, desquamation, and telangiectasia after 3 and 5 year's follow-up." *Radiother Oncol.*, vol. 15, no. 2, pp. 169–88, 1989.
2. Oborn, B., Kolling, S., Metcalfe, P., Crozier, S., Litzenberg, D. and Keall, P. (2014). Electron contamination modeling and reduction in a 1 T open bore inline MRI-linac system. *Medical Physics*, 41(5), p.051708.
3. P Metcalfe, et al, (2013). Review of four novel dosimeters developed for use in radiotherapy. *Journal of Physics: Conference Series*, 444, p.012008.

Acknowledgements This research has been conducted with the support of the Australian Government Research Training Program Scholarship and the Ingham Institute for Applied Medical Research.

P55 Remote dosimetric auditing for clinical trials using EPID and DVH patient dose analysis

T. S. Pedersen[1,2], N. Miri[2], R. David[3], J. Lehmann[1,2], P. B. Greer[1,2]

[1]Department of Radiation Oncology, Calvary Mater Newcastle Hospital, Newcastle. (Therese.Pedersen@calvarymater.org.au [Presenting author]), (Joerg.Lehmann@calvarymater.org.au), (Peter.Greer@newcastle.edu.au). [2]School of Mathematical and Physical Sciences, University of Newcastle, Newcastle. (Narges.Miri@uon.edu.au). [3]Central Coast Cancer Centre, Gosford Hospital, Gosford. (Rajasekar.David@health.nsw.gov.au)

Introduction This study investigated the novel use of DVH patient dose analysis in remote dosimetric auditing for clinical trials IMRT credentialing. The sensitivity of the DVH analysis method was compared to gamma analysis for delivery errors artificially introduced into a post-prostatectomy (PP) plan and a head and neck (HN) plan. A pilot study was conducted by performing DVH analysis on eleven previously audited radiotherapy centres and comparing to past gamma results [1].

Method A novel method reconstructed the dose delivered to the patient CT model from EPID images acquired in air. This was compared to the planned dose distribution and DVH metrics were used for analysis. Artificial delivery errors (monitor units, collimator angle, and MLC leaf positions) were introduced into the two IMRT plans to investigate the sensitivity of DVH analysis. This was compared to the sensitivity of 2D gamma analysis of planned and measured (EPID-derived) dose distributions in a virtual flat water phantom. Audit data from the radiotherapy centres were analysed using the DVH method and compared to previous gamma analysis results.
Results The DVH analysis method has comparable or better sensitivity than the gamma method to the simulated delivery errors using a ± 2% dose difference threshold for DVH metrics and 90% gamma pass rate threshold with 2%/2 mm and 3%/3 mm gamma criteria. Higher sensitivity was observed for the DVH method for deviations in MLC leaf positions and collimator rotation angles. The pilot study gave more consistent audit results when using DVH analysis with all centres performing within ± 3% dose difference in all PP DVH metrics.
Conclusion Based on the comparable sensitivity of DVH and gamma analysis methods and pilot study results, DVH patient dose analysis shows great promise for use in remote IMRT dosimetric auditing. The use of DVH analysis offers added benefit due to consideration of radiobiological effects.

Reference

1. Miri N, Lehmann J, Legge K, Zwan BJ, Vial P, Greer, PB (2017) Remote dosimetric auditing for intensity modulated radiotherapy: A pilot study. Physics and Imaging in Radiation Oncology 4:26–31.

P56 The feasibility of streamlined small-field dosimetry using EPID imaging

K. Kandasamy[1], B. Zwan[1], A. Cullen[1], R. Poldy[1], M. Barnes[2], C. Lee[1], P. B. Greer[3]

[1]Radiation Oncology, Central Coast Cancer Centre, NSW. (kankean@gmail.com [Presenting Author]), (benjamin.zwan@health.nsw.gov.au), (Ashley.Cullen@health.nsw.gov.au), (rachel.poldy@health.nsw.gov.au), (Christoper.Lee@health.nsw.gov.au). [2]Radiation Oncology, Calvary Mater Newcastle, NSW. (Michael.Barnes@calvarymater.org.au). [3]School of Mathematical and Physical Sciences, University of Newcastle, NSW. (peter.greer@newcastle.edu.au)

Introduction Small Field Output Factors (SFOF) have a high degree of uncertainty inherent in their measurement [1] and requires the use of multiple detectors with time/labour intensive procedures. A recent survey found that inconsistencies in measurement techniques used across centres lead to significantly divergent estimates of the same output factor [2].
The on-board electronic portal imaging device (EPID) is ubiquitous across clinical centres and its high spatial resolution allows for small field measurements. In this cross-institutional study we attempt to determine if the correlation between SFOFs measured by the EPID and those measured by a traditional dosimeter holds across independent machines in a step towards demonstrating the feasibility of using the EPID to acquire and verify small-field dosimetry data.
Method SFOFs for square MLC fields down to 5 × 5 mm and cone defined fields down to 5 mm diameter were measured using the Gafchromic EBT3 Film using three different Varian Clinac iXs at two centres for use as ground truth. SFOFs were then measured using the on board EPID (AS1000) available at these centres. All factors were normalised to the 30 × 30 mm MLC defined field.
Results The ratio of EPID output factors on the film measured factors are plotted below with their attendant uncertainties in measurement. Aside from one exception (L3 6X Cones) they show a consistency of correlation independent of the delivery machine. The EPID acquisition time for all fields was approximately 1.5 h for each machine.

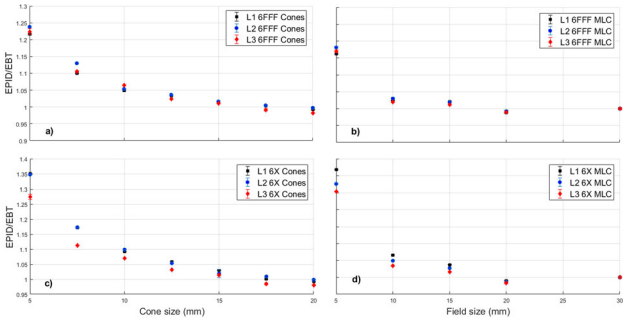

Figure 1 : EPID output factors as a ratio of film output factors. a) 6FFF Cones, b) 6FFF MLC, c) 6X Cones, d) 6X MLC

Conclusion Further work is required to confirm these preliminary results by extending the measurements to additional centres and to Elekta model EPIDs; culminating with Monte Carlo modelling of the interaction of small fields with the EPID architecture. A confirmation of the initial trends discovered would indicate that EPIDs can indeed be used for dosimetric measurements at fields sizes smaller than previously supported by literature.

References

1. Das, I.J., G.X. Ding, and A. Ahnesjö, *Small fields: nonequilibrium radiation dosimetry.* Medical physics, 2008. **35**(1): p. 206–215.
2. Oliver, C.P., et al., *Survey of 5 mm small-field output factor measurements in Australia.* Journal of applied clinical medical physics, 2018. **19**(2): p. 329–337.

P57 Genipin-gelatin reusable 3D dosimeter for verification of small radiosurgery dose distributions

D. Ramm[1,2]

[1]Royal Adelaide Hospital, Adelaide, South Australia. [2]University of Adelaide, Adelaide, South Australia. (daniel.ramm@sa.gov.com [Presenting Author])

Introduction A radiochromic genipin-gelatin dosimeter has previously been proposed for true 3D measurement of radiotherapy dose distributions [1]. There have been few reports of practical application, likely due to challenges presented by the relatively low dose sensitivity and high levels of optical density of the dosimeter. In this work, the utility of genipin gel was demonstrated by verification of treatment planning for small SRS targets.
Method The gel dosimeter was prepared with final concentrations; 2% gelatin, 0.001% genipin and 100mM sulphuric acid in de-ionised water. For reuse, the gel samples were melted and stirred at 35°C and then re-poured. Irradiations using a 6 MV FFF IMRT multi-target treatment plan were followed by optical CT scanning at 594 nm with a previously described scanner [2]. Prescription isodoses were 20 Gy

and gel size was 5 cm diameter. Gel measured absolute dose distributions were compared to treatment planning computed distributions.
Results A dosimeter size of 5 cm gave sufficient optical transmission for optical CT scanning while maintaining reasonable dose sensitivity. The gel bleaches in proportion to the dose delivered, thus reuse is not limited by excessive darkening from accumulated doses. The quality of the measured dose distribution was suitable to verify prescription isodoses for small targets in the range of 5 to 10 mm using 3 % dose difference and 1 mm distance to agreement criteria.
Conclusion Genipin gel was found to be effective for true 3D dosimetry of small SRS dose distributions. The gel could be reused, therefore enhancing the practicality of true 3D dosimetry compared to single use dosimeters.

References

1. Jordan K 2008 Zero diffusion radiochromic genipin–gelatin dosimeter *Med. Phys.* **35** 3413
2. Ramm D 2018 A fast dual wavelength laser beam fluid-less optical CT scanner for radiotherapy 3D gel dosimetry II: dosimetric performance *Phys. Med. Biol.* **63** 045020

P58 Self optical attenuation effects in beryllium oxide ceramic fibre coupled luminescence detectors

A. Chrisanthakopoulos[1], A.M.C. Santos[1,2]

[1]School of Physical Science, University of Adelaide, Adelaide. (a1686927@student.adelaide.edu.au). [2]Department of Medical Physics, Royal Adelaide Hospital, Adelaide (alexandre.santos@adelaide.edu.au [Presenting author])

Introduction Beryllium oxide (BeO) ceramics are a near water-equivalent material recently being investigated for fibre-coupled luminescence dosimetry. Unlike some other common scintillators, BeO ceramics are highly self optically attenuating. The purpose of this study was to investigate the effect that the self optical attenuation from BeO ceramics has on the response of a BeO ceramic fibre-coupled luminescence dosimetry.
Method Using a superficial X-ray unit (SXR), the energy dependence of the radioluminescence from the BeO ceramic was measured in parallel and perpendicular alignment to the radiation field. This setup was utilised to emphasise any response differences due to the self optical attenuation of BeO ceramics. The 3D light collection from the BeO ceramic was modelled via ray optics [1], and the 3D dose distribution modelled using geant4. The effect of the differing light collection due to the self optical attenuation of the BeO ceramic and the differing dose distribution within the scintillator were combined and compared to the response measured.
Results Little energy dependence is measured from the BeO ceramic above SXR energies of 50kVp. The measured energy dependencies with the two setups showed a reduced lower energy response for the parallel aligned detector of $> 25\%$ with a 30 kVp beam. Once the effect of the self optical attenuation and non-uniform dose distribution are accounted for, the difference between the two energy dependencies are $< 6\%$.
Conclusion A difference in energy dependence of the BeO ceramic fibre-coupled luminescence dosimeter was measured. The effect of the self optical attenuation from BeO ceramics was modelled and shown to account for the measured discrepancy. Therefore in gradient dose regions the self optical attenuation of BeO can lead to discrepancies.

References

1. Alexandre Santos, Mohammad Mohammadi and Shahraam Afshar V, Optimal light collection from diffuse sources: Application to optical fibre-coupled luminescence dosimetry, Optics Express, 22(4), 2014.

P59 Investigation into coincidence of Gamma Knife® Icon™ frame based and cone beam CT (CBCT) defined isocenters

V. Seshadri[1], C. E. Jones[1], T. Markwell[2], B. Perrett[1]

[1]Radiation Oncology, Princess Alexandra Hospital, Brisbane, Queensland, Australia. (Venkatakrishnan.seshadri@health.qld.gov.au [Presenting author]), (Catherine.jones3@health.qld.gov.au), (ben.perrett@health.qld.gov.au). [2]Radiation Oncology PA Raymond Terrace, Brisbane, Queensland, Australia. (Tim.markwell@health.qld.gov.au)

Introduction The Gamma Knife® Perfexion at the Gamma Knife® Center of Queensland was upgraded to the Icon™ enabling positioning of patients using CBCT. A technique was developed to independently check the coincidence of the frame based (via fiducial markers) and CBCT defined coordinate systems.
Method The Leksell Gamma Knife® spherical solid water phantom with film inserts is dockable to the frame adapter, and can be imaged with a localizer box containing fiducial markers. Therefore film irradiations can be performed where the stereotactic coordinate system can be defined from either CBCT imaging or via fiducial markers (i.e. a frame based coordinate system).
Gafchromic RTQA films (Ashland Inc., New Jersey) were irradiated with a 4 mm collimator isocentre shot in both the axial and coronal orientations, providing the isocentre location in the three spatial dimensions. This isocentre shot was delivered where the coordinate system was defined by CBCT, and by fiducial markers (i.e. four films were irradiated). Each piece of film was also irradiated with two frame-based 8 mm diameter shots located 2.64 cm from the isocentre. This pair of 8 mm shots acted as a localizer in order to align each CBCT-based with its corresponding frame-based film in order to compare the position of the exposure at the isocentre.

Films were digitized with an Epson Expression 10000XL flatbed scanner with 400 dpi resolution and no colour correction. By analysing the film profiles in the VeriSoft® radiotherapy plan verification software (PTW-Freiburg, Breisgau, Germany), we were able to identify the coincidence of the isocentres.
Results Initial results coincidence of the isocentre coordinates were within 0.3 mm between the localizer box coordinates and CBCT stereotactic coordinates
Conclusion The method was found to be easy to implement and provides reproducible results to serve as a periodic check on the isocenter coordinates.

P60 A comparison between EPSON V700 and EPSON V800 scanner for film dosimetry

T. J. Shameem[1], N Bennie[1], M Butson[2,3], D Thwaites[2]

[1]Radiation Oncology Medical Physics Specialist, NCCI, Lismore, NSW. (Tarafder.shameem@ncahs.health.nsw.gov.au [Presenting Author]), (nick.bennie@ncahs.health.nsw.gov.au). [2]Institute of Medical Physics, School of Physics, University of Sydney. (Martin.Butson@lh.org.au), (David.thwaites@sydney.edu.au). [3]Chris O'Brian Life house

Introduction Radiochromic film is a good dosimeter choice for patient QA for complex treatment techniques (IMRT, VMAT, SABR, SBRT) because of its near tissue equivalency, very high spatial resolution and established method of use [1]. One of its significant problems is the lateral response artefacts (LRA) effect, defined as the differences of response from middle to side of the film orthogonal to the scanner's light source travel direction. This results from the film composition itself and the scanner's construction elements [2, 3, 4]. An LRA effect correction factor is needed, depending on dose range involved and size (and position on film/scanner) of irradiated region of interest. EPSON scanners are commonly used for film dosimetry. NCCI have used an EPSON V700 scanner, but recently acquired a new model EPSON V800 scanner [1]. The purpose of this work was to evaluate any differences between these two scanners to consider whether they can be used interchangeably or not.
Method EBT3 films were irradiated with 40 × 40cm^2 field size and scanned in both the scanners and the differences in LRA effect were compared. The scanned images were read and plotted in ImageJ V1.49 software. To compare calibration curves, 3 × 3cm^2 film pieces were irradiated for doses of 1–60 Gy and ImageJ and MS Excel were used to plot and compare the curves. Repeated scan effects were also compared.
Results The response of the V800 scanner is lower in optical density than for the V700 scanner for the same films and irradiations and the calibration curves are different from each other. The V700 scanner shows about 2% increase in optical density after 10 scans in EBT3 film, whilst the V800 scanner shows less than 1% increase
Conclusion The scanners cannot be used interchangeably. The correction factors for LRA effect and the calibration curves are different. Further characterisation and evaluation is required.

References

1. Nick Bennie, Peter Metcalfe (2016) Practical IMRT QA dosimetry using Gafchromic film: a quick start guide. Australas Phys Eng Sci Med 39(2):533–45 https://doi.org/10.1007/s13246-016-0443-0
2. Hani Alnawaf, Martin J Butson, Tsang Cheung, peter K.N. Yu (2010) Scanning orientation and polarization effect for XRQA radiochromic film. Physica Medica 26:216–219. https://doi.org/10.1016/j.ejmp.2010.01.003
3. Andreas A Schoenfeld, Daniela Poppinga, Dietrich harder, Karl-Joachim Doerner, Bjoern Poppe (2014) The artefacts of radiochromic film with flatbed scanners and their causation by light scattering from radiation-induced polymers. Physics in Medicine and Biology 59:3575–3597 https://doi.org/10.1088/0031-9155/59/13/3575
4. L J van Battum, H Huizenga, R M Verdaasdonk, S Heukelom (2016) How flatbed scanners upset accurate film dosimetry. Physics in Medicine and Biology 61: 625-649 https://doi.org/10.1088/0031-9155/61/2/325

P61 Initial clinical experience and commissioning of the catalyst HD system

A. Snjegota[1], N. Campbell[1]

[1]Radiation Oncology, Auckland City Hospital, Auckland, New Zealand. (asnjegota@adhb.govt.nz [Presenting author]), (ncampbell@adhb.govt.nz)

Introduction The radiation oncology department at Auckland District Health Board (ADHB) recently installed the Catalyst HD system on the new Elekta VersaHD. This system uses real time optical imaging to determine whether the patient is in the correct treatment position, both inter- and intra-fractionally. The commissioning tests that were performed to ensure that the system can be used clinically are described, along with the initial clinical experience for prostate treatments at our department using Catalyst HD for patient positioning.
Method The commissioning tests followed the TG147 [1] recommendations for testing non-radiographic positioning systems. The tests included, but were not limited to, the determination of the maximum field of view, determination of the system warm up time, spatial reproducibility of the system, localisation displacement accuracy, and an end-to-end test following the current clinical workflow. Some of these tests were performed using the Daily Check QA device provided by C-RAD, and some of the tests used a whole body phantom PBU-60.
Results The total field of view using all three cameras is 712mm x 1030mm x 898mm. The warm up time of the system was found to take 35 min with maximum deviation in the spatial drift of 0.8 mm within the first 35 min. Spatial reproducibility measurements over 3 h after the warm up show a maximum deviation of 0.2mm. This falls within the manufacturer's long term stability specification of 0.3 mm.
Conclusion The Catalyst HD system was tested thoroughly during the commissioning process and was found to meet the manufacturer's specifications. The system has been used clinically for prostate treatments and was found to be reliable in positioning the patient correctly.

Reference

1. Willoughby T, Lehmann J, Bencomo JA, Jani SK, Santanam L, Sethi A, Solberg TD, Tomé WA, Waldron TJ (2012) Quality assurance for nonradiographic radiotherapy localization and positioning systems: Report of Task Group 147. Med. Phys., 39:1728-1747. https://doi.org/10.1118/1.3681967

P62 Dose variations in exclusion volumes observed in ACDS IMRT and VMAT audits

J. Supple[1], A. Alves[1], C. Davey[1], F. Kadeer[1], J. Kenny[1], M. Shaw[1], J. Lye[1]

[1]Australian Clinical Dosimetry Service, ARPANSA. (Jeremy.Supple@arpansa.gov.au [Presenting author]), (Andrew.Alves@arpansa.gov.au), (Cate.Davey@arpansa.gov.au), (Fayz.Kadeer@arpansa.gov.au), (John.Kenny@arpansa.gov.au), (Maddison.Shaw@arpansa.gov.au), (Jessica.Lye@arpansa.gov.au)

Introduction Sufficient data for IMRT and VMAT cases in ACDS LII and LIII audits has now been collected to begin analysing the behaviour of various planning systems and dose calculation algorithms. Of particular interest is their performance in challenging situations where there is an OAR with a low dose constraint adjacent to the target volume.

Method The cases included were the 'C-Shape' (both LII and LIII) adapted from AAPM: TG119 [1] (target: D95 $\geq$ 50 Gy, D10 $\leq$ 55 Gy; exclusion: D5 $\leq$ 32 Gy) and the 'Complex' case (LIII only) which consists of two adjacent target structures (D90 > 50 Gy, D10 < 55 Gy and D95 > 40 Gy) and an exclusion sphere fully encompassed by the higher dose target (D5 $\leq$ 32 Gy). The LII audits were measured using a PTW Octavius 1500 2D ion chamber array (PTW, Freiburg, Germany) in both homogeneous and inhomogeneous cubic phantoms. The mean local dose variation of the elements falling within the exclusion volume was calculated. The LIII audits were measured in an inhomogeneous custom thorax phantom (CIRS, Norfolk, VA). A single CC13 chamber was used to measure the dose to the exclusion volume. The local dose difference was calculated using:

Results Figures 1 and 2 show the local dose variations for the exclusion volumes in LII and LIII audits respectively. Significant differences between algorithms was observed and the general trends between them were quite similar for both LII and LIII audit data. The exception to this is Xio Superposition and is likely due to there only being a single audit for each level making it statistically weak.

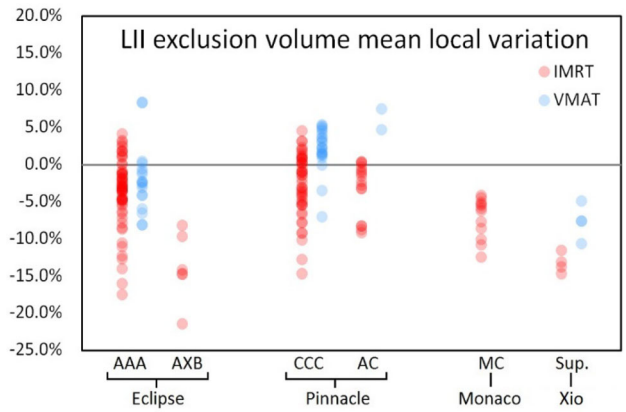

Figure 1: Mean local variation in exclusion volume for all IMRT and VMAT cases in LII audits.

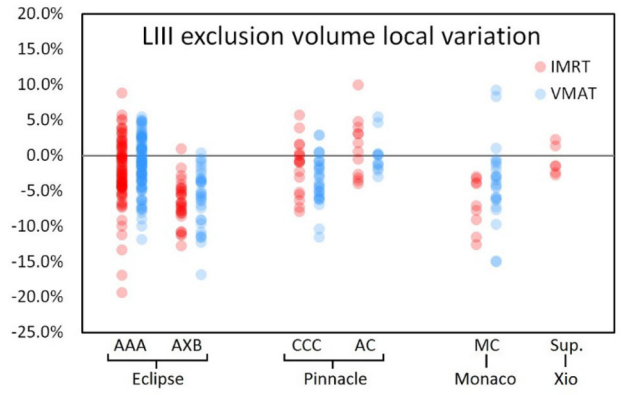

Figure 2: Local dose variation in the exclusion volume for all IMRT and VMAT cases in LIII audits.

Conclusion The ACDS LII and LIII audits both demonstrate that there are measurable differences in the way dose calculation algorithms behave when calculating doses to exclusion volumes.

References

1. Ezzell GA, Galvin JM, Low D, Palta JR, Rosen I, Sharpe MB et al (2003) Guidance document on delivery, treatment planning, and clinical implementation of IMRT: report of the IMRT Subcommittee of the AAPM Radiation Therapy Committee. Med Phys 30(8):2089–115. https://doi.org/10.1118/1.1591194

P63 Implementation of AAPM TG61 kilovoltage dosimetry protocol at Central West Cancer Care Centre

S. J. Tan, A. K. Mishra, D. P. Banjade, G. B. Warr

Central West Cancer Care Centre, Orange Health Service, Orange, Australia. (shiaw.tan@health.nsw.gov.au [Presenting author]), (ajeet.mishra@health.nsw.gov.au), (dilli.banjade@health.nsw.gov.au), (george.warr@health.nsw.gov.au)

Introduction Central West Cancer Care Centre (CWCCC) has implemented the AAPM TG61 [1] protocol for kilovoltage dosimetry, as recommended by ACPSEM [2].

Method The CWCCC kilovoltage system uses 100 kV, 120 kV, 180 kV and 220 kV for clinical treatment. Clinical applicators used are (1) FSD = 20 cm, 2 cm to 10 cm diameter circular open-ended applicators (2) FSD = 50 cm, 4 $\times$ 4cm^2 to 20 $\times$ 20cm^2 square close-ended applicators. The reference applicator is the open-ended 10cm diameter applicator. Farmer and CC13 cylindrical chambers are used for all clinical in-air measurements including HVLs, applicator factors, and absolute dose measurement. A PPC40 parallel plate chamber in solid water is used to measure the applicator factors for applicators with dimensions larger than 5cm. Clinical beam data from the previously used IPEMB protocol [3, 4] are compared to TG61.

Results The HVLs of the 100 kV, 120 kV, 180 kV, and 220 kV were determined to be 2.644 mm Al, 4.93 mm Al, 0.555 mm Cu, and 2.192 mm Cu respectively. The comparison of the IPEMB and TG61 protocols showed that there was less than 0.5% difference in patient monitor unit (MU) calculation using data in the two protocols for all CWCCC clinical beams except for 120 kV with 8cm diameter applicator, which has a discrepancy of 1.1%. This discrepancy is mainly due to the lack of backscatter factor (BSF) in TG61 protocol for applicator diameter when the BSF changes rapidly with applicator diameter between 5cm and 10cm, as shown in Figure 24. This discrepancy can be reduced to 0.2% if a 4th-order polynomial curve fitting method is used instead of linear interpolation to obtain the BSF for the 120kV 8cm diameter applicator.

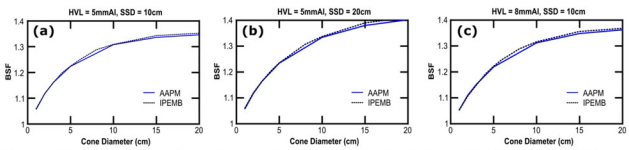

Figure 1 BSF as a function of cone diameter for (a) HVL=5mmAl, SSD=10cm; (b) HVL=5mmAl, SSD=20cm; (c) HVL=8mmAl, SSD=10cm

Applicator factors measured using the PPC40 in solid water are within 3% of those obtained using in-air measurement and applying the BSF.

Applicator factors measured using the PPC40 in solid water are within 3% of those obtained using in-air measurement and applying the BSF.

Conclusion The TG61 and IPEMB protocols are both consistent and appropriate for clinical use. Curve fitting can be used to reduce uncertainty when extracting BSF for clinical use. The TG61 protocol has been implemented clinically at CWCCC.

References

1. Ma C-M, Coffey CW, DeWerd LA, Liu C, Nath R, Seltzer SM, Seuntjens JP (2001) AAPM protocol for 40–300 kV X-ray beam dosimetry in radiotherapy and radiobiology. Med Phys 28:868–893
2. Hill R, Healy B, Butler D, Odgers D, Gill S, Lye J, Gorjiara T, Pope D, Hill B (2018) ACPSEM kilovoltage dosimetry working group recommendations for quality assurance in kilovoltage radiation therapy. [To be published]
3. Klevenhagen SC, Aukett RJ, Harrison RM, Moretti C, Nahum AE, Rosser KE (1996) The IPEMB code of practice for the determination of absorbed dose for x-rays below 300kV generating potential (0.035mm Al – 4mm Cu HVL; 10 – 300kV generating potential). Phys Med Biol 41:2605–2625
4. Aukett RJ, Burns JE, Greener AG, Harrison RM, Moretti C, Nahum AE, Rosser KE (2005) Addendum to the IPEMB code of practice for the determination of absorbed dose for x-rays below 300kV generating potential (0.035 mm Al – 4 mm Cu HVL). Phys Med Biol 50:2739–2748

P64 Validation of 3D printed bolus for external beam radiation therapy

E. Ungureanu, A. Yeo, R. Antony, L. Zhu, V. Geddes, B. Hay, M. Wright, R. Showler, T. Kron

Peter MacCallum Cancer Centre, Melbourne, Australia.
elena.ungureanu@petermac.org (Presenting Author)

Introduction 3D printers have been used to manufacture patient specific bolus for external beam radiation therapy in our department since early 2017. This work summarizes the validation process for the printed bolus prior to clinical implementation, the verification process of the first patient boluses and the ongoing quality assurance procedures.

Method The 3D Printer purchased after market research was a CreatBot DX series printer using Polylactic acid.

Sample printed boluses have been assessed in terms of density, homogeneity, geometrical accuracy, reproducibility and stability. The same sample was CT scanned at weekly intervals, before and after irradiation with typical treatment radiation doses.

The first fifty clinical boluses were assessed prior to the first treatment fraction. The conformity of the bolus to the patient's skin was verified by using the treatment unit's on board imagers. In vivo dose measurements have been performed in order to verify the skin dose under the bolus.

Following the evaluation of the initial clinical boluses, a routine quality assurance program for the printed bolus was developed.

Results Printed bolus was created in 5 and 10mm thickness and found to be geometrically accurate and homogeneous in density. Mean CT numbers were 120 ± 40 (mean ± 2SD). Its physical properties remain consistent throughout the radiotherapy treatment. On board imaging showed an improved conformity to the patients' skin for the printed bolus when compared to other boluses used in our department. In vivo dosimetry confirmed that the delivered radiation doses are in good agreement with the planned doses (ratio measured vs planned 0.98 ± 0.13 (mean ± 1SD)).

The routine quality assurance program includes continuation of measurements for all electron bolus and a monthly verification of density and thickness of geometric samples.

Conclusion 3D printed bolus provides a reliable and superior alternative to more established boluses used in radiotherapy treatments.

P65 Experience with high performance computing in enhancing regional radiotherapy

G. B. Warr, A. Mishra, D. Banjade, S. J. Tan, T. L. Molloy, S. McDonell, G. Dillion, R. Hammond, M. Fuller, S. Piggott, G. Stevens, K. Thuraisingam

[1]Central West Cancer Care Centre, Orange, NSW, Australia.
(George.Warr@health.nsw.gov.au [Presenting author])

Introduction

The Central West Cancer Care Centre (CWCCC) in Orange provides radiotherapy services to patients in the Western NSW Local Health District, an area of 246,676 km^2 (31% of NSW) and population of ~278,000. The centre uses an integrated Varian ARIA Oncology Information System and Varian Eclipse Treatment Planning System (TPS) running on a Citrix environment, facilitating ease of access across the district. The centre has two Varian high-energy linear accelerators (Trilogy and iX), a Gulmay orthovoltage unit and a Toshiba 4D CT Simulator. Both linacs are used for 3D conformal, electron, IMRT and VMAT treatments. The Trilogy linac is used for DIBH treatments and is being commissioned for SABR treatments.

Method The centre is the first NSW public centre to upgrade its TPS to enable Graphical Processor Unit (GPU) treatment planning calculations of the linear Boltzmann Transport Equation to Monte-Carlo class accuracy with the Varian Acuros algorithm (v15.5) [1]. Calculations are performed on the centre's new high-performance computing cluster of three Framework Agent Servers (FAS), each with dual GPU cards (Tesla P100-PCIE-16GB, 3584 cores). The combined GPU performance of the system is 27.9 Double-Precision Tera (10^{12}) Floating Point Operations Per Second (DP-TFLOPS). The FASs complement a suite of 6 planning workstations to make up the Distributed Calculation Framework of 144 Central Processor Unit (CPU) cores, with a combined CPU performance of 5.2 DP-TFLOPS. The planning system has been enhanced with Varian RapidPlan Knowledge Based Planning and Multi-Criteria Optimisation, which are currently being commissioned.

Results Acuros GPU calculations of 3D conformal, field-in-field and IMRT/VMAT plans are typically calculated in around 20 seconds, five times faster than CPU calculations and at about the same speed as the older AAA algorithm CPU calculations, enabling greater use of the higher accuracy Acuros algorithm to improve treatment plans.

Conclusion The CWCCC is the first NSW public radiotherapy centre to implement GPU calculations with the Varian Acuros v15.5 algorithm, enabling faster accurate planning to benefit patients in the Western NSW region.

References

1. Vassiliev ON, Wareing TA, McGhee J, Failla G (2010) Validation of a new grid-based Boltzmann equation solver for dose calculation in radiotherapy with photon beams. Phys Med Biol 55:581–598. http://iopscience.iop.org/0031-9155/55/3/002/

P66 Conversion of PDDs to TMRs for small radiotherapy fields

Emma Whittle[1], Scott Crowe[2,3], Shadi Khoei[4], Emma Spelleken[5], Tanya Kairn[2,3]

[1]Biomedical Technology Services, Herston, Australia. (emma.whittle2@health.qld.gov.au [Presenting author]). [2]Queensland University of Technology, Brisbane, Australia. (t.kairn@gmail.com), (sb.crowe@gmail.com). [3]Royal Brisbane & Women's Hospital, Herston, Australia. [4]Genesis Cancer Care Queensland, Auchenflower, Australia. (shadi.khoei@genesiscare.com.au). [5]Genesis Cancer Care Queensland, Rockhampton, Australia. (emma.spelleken@genesiscare.com.au)

Introduction The calculation of dose in a radiation therapy patient in treatment planning and dose checking software requires the measurement of variation of dose with depth and surface distance. There are two radiation dosimetry quantities, percentage depth dose (PDD) and tissue phantom ratios (TPR) that are commonly used for this purpose. The conversion between PDD and TPR data has not been widely investigated for small-field flattening filter free (FFF) beams. This study investigated and compared measurements of TPRs in small fields (ranging from 0.5 cm x 0.5 cm to 3 cm x 3 cm) to PDD-converted TPRs for both flattening filter (FF) and FFF beams.

Method A Sun Nuclear Corporation (SNC) cylindrical water tank and IBA BluePhantom 3D water tank were used to measure TPRs and PDDs for small field sizes with comparisons to measurements using the Varian TrueBeam linear accelerator. Previously published PDD-TPR conversion methods [1–3] were applied to the PDD data acquired from the TrueBeam linac and then compared with TPR measurements.

Results The best agreement between the practical measurements and conversion methods was the PDD to TPR conversion [2] empirically determined for small fields using different fitting parameters. This was followed by a standard peak-scatter- factor and inverse square law corrected conversion [1] which were in good agreement with the empirical conversion. A functional conversion [3] yielded the greatest. Increased uncertainty was found for the 0.5 cm x 0.5 cm field size. It was concluded that all conversion methods failed to correctly convert PDD data for small FFF fields.

Table 1: Comparing measured TMR data to converted TMR data using RMSE (6X beam

Field Size	BJR [1]	Ding and Krauss [2]	Sauer [3]
0.5 x 0.5 cm^2	0.14 ± 0.02	0.03 ± 0.0008	0.32 ± 0.11
1 x 1 cm^2	0.07 ± 0.01	0.07 ± 0.01	0.27 ± 0.07
2 x 2 cm^2	0.08 ± 0.01	0.08 ± 0.01	0.26 ± 0.06
3 x 3 cm^2	0.08 ± 0.01	0.08 ± 0.01	0.27 ± 0.06

Table 2: Comparing measured TMR data to converted TMR data using RMSE (FFF beam)

Field Size	BJR [1]	Ding and Krauss [2]	Sauer [3]
0.5 x 0.5 cm^2	0.04 ± 0.01	0.04 ± 0.01	0.33 ± 0.11
1 x 1 cm^2	0.08 ± 0.01	0.08 ± 0.01	0.27 ± 0.07
2 x 2 cm^2	0.08 ± 0.01	0.08 ± 0.01	0.27 ± 0.07
3 x 3 cm^2	0.07 ± 0.01	0.07 ± 0.01	0.27 ± 0.06

Conclusion This study highlighted that novel conversion factors are needed for fields less than 1 cm x 1 cm and for FFF beams. It is concluded that when using TPR data for independent dose checking software, measurements for comparisons to other data are used instead of conversion methods.

References

1. British Institute of Radiology. 1996: a survey of depth doses and related data measured in water or equivalent media. *British Journal of Radiology - 25*, *BJR supplement*, page 188, 1996.
2. G. Ding and R. Krauss. SUET544: An Empirical Formula to Obtain Tissue Phantom Ratios From Percentage Depth Dose Curves for Small Fields. *Medical Physics*, 40(6):330, 2013.
3. Otto A. Sauer and J. Wilbert. Functional representation of tissue phantom ratios for photon fields. *Medical Physics*, 36(12):5444–5450, 2009.

P67 Consistency and efficiencies in external brachytherapy training

L. Wilfert[1,2], J. Poder[3], E. Enari[3]

[1]Department of Radiation Oncology, Calvary Mater Newcastle Hospital, Newcastle, NSW, Australia. [2]School of Mathematical and Physical Sciences, University of Newcastle, Newcastle, NSW, Australia. [3]St George Cancer Care Centre, Sydney, NSW, Australia. (lisa.wilfert@calvarymater.org.au [Presenting author])

Introduction Brachytherapy has always been a challenging module in ACPSEM's Training, Education and Assessment Program (TEAP) due to the fact that only 7 out of 17 NSW Departments with public Registrars have a clinical brachytherapy service. Nearly half of our Registrars reside outside Sydney. Further complications include the variation in role of a brachytherapy physicist and variation of case mix and patient numbers over time.

ACPSEM implemented Version 3.6 of the TEAP Clinical Training Guide (CTG) for ROMPs in 2013. Eight broad competencies at level 2 evolved in to 16 learning outcomes with increased scope and more detailed assessment criteria based on Blooms Taxonomy[1]. Techniques on the "would-like-to-see" list were now mandatory, such as low dose rate (LDR) prostate, LDR eye plaque and HDR prostate brachytherapy. LDR techniques are only offered by one specialist service. Visits to departments needed to be formalised due to the volume and critical timing of Registrar visits. Brachytherapy physicists were now asked to train and assess learning outcomes and contribute to the Registrar's submission of best work. Due to the workload involved and cost of travel and accommodation from rural areas, consistency and efficiencies needed to be found.

Results and Conclusion Training and assessment templates were written for all level 2 learning outcomes.

Each template included tables listing:

- pre-requisite knowledge
- pre-requisite clinical experience
- required items of training
- required evidence
- a Registrar log of relevant knowledge and training received elsewhere, co-signed by their Supervisor
- expanded assessment criteria with tick boxes for 'meets expectation' or 'below expectation'
- Assessor feedback ± recommended Comet grading

These templates have been successfully implemented at 4 NSW brachytherapy services. An additional service is about to start. Completed templates are uploaded in to Comet as evidence. Services that support extended brachytherapy rotations grade directly in to Comet.

References

1. Bloom BS, Engelhart MD, Furst EJ, Hill WH, Krathwohl DR (1956) Taxonomy of educational objectives: the classification of educational goals. Handbook I: cognitive domain. David McKay Company, New York

P68 Evaluation of the quality and complexity of IMRT and VMAT plans generated by an automated inverse planning tool

D. Wilkinson[1], K, Shannon[1], D. Novy[1], F. Beaven[2], J. McNamara[2], R. Bailey[2], M. Currie[1], E. Nasser[1]

[1]Illawarra Cancer Care Centre, Wollongong, NSW, AUSTRALIA. (Dean.Wilkinson@health.nsw.gov.au [Presenting author]), (Kelly.Shannon@health.nsw.gov.au), (Dean.Novy@health.nsw.gov.au), (MichaelPeter.Currie@health.nsw.gov.au), (Elias.Nasser@health.nsw.gov.au). [2]Shoalhaven Cancer Care Centre, Wollongong, NSW, AUSTRALIA. (Frances.Beavan@health.nsw.gov.au), (Joanne.McNamara@health.nsw.gov.au), (Renee.Bailey@health.nsw.gov.au)

Introduction The Pinnacle[3] auto-planning (AP) package is an automated inverse planning tool employing a multi-sequence algorithm that fine-tunes a plan's objective function during optimisation based on overlapping volumes, dose coverage and the presence of hot and cold isodose regions. The progressive optimisation algorithm creates small 'dummy' volumes during the optimisation progress in order to improve the plan. The nature of this optimisation can lead to highly modulated fields potentially increasing the complexity of a plan and subsequently pushing the delivery capabilities of a linear accelerator.

Method A retrospective planning study was performed on 30 prostate patients who had previously received IMRT to the prostate and seminal vesicles, prostate and pelvic lymph nodes, or prostate bed. The AP techniques developed for step-and-shoot IMRT (AP-IMRT) and VMAT (AP-VMAT) were applied to these planning cases and compared in terms of target volume coverage and organ at risk (OAR) dose objectives. In addition, each case in the study cohort was also planned with VMAT (without AP).

Plan complexity was assessed for each plan based on the modulation complexity score index proposed by McNiven et al. [1] and later adapted for VMAT by Masi et al. [2]. This index is calculated on plan parameters such as field aperture shape and size, total MLC leaf travel and the total number of plan MU per control point.

Results Plans produced with AP provided comparable dose coverage to the target volumes but with significant reduction in OAR doses for the bladder and rectum when compared to the non-AP IMRT and VMAT plans (Figure 1).

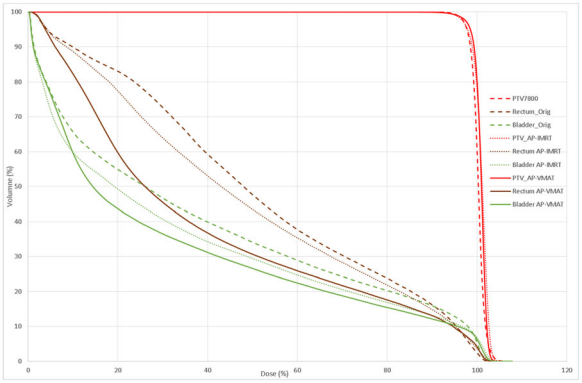

(Figure 1: Mean DVH curve comparing original, AP-IMRT and AP-VMAT plans)

Modulated complexity scores were found to be dependent on the number of beams used for IMRT but were not significantly different between AP and non-AP VMAT plans. Correlation between plan complexity and plan verification gamma index scores are currently being evaluated.

Conclusion An automated planning tool has been evaluated for IMRT and VMAT treatment planning and found to produce plans of equal or superior plan quality without a significant change to plan complexity.

References

1. McNiven A., Sharpe M. and Purdie T. (2010) A new metric for assessing IMRT modulation complexity and plan deliverability. Med Phys Vol. 37 (2): 505–515.
2. Masi L., Doro R., Favuzza V., Cipressi S. and Livi L. (2013) Impact of plan parameters on the dosimetric accuracy of volumetric modulated arc therapy. Med Phys Vol. 40 (7): 071718-1–11.

P69 Validation of a non-invasive beam monitor at a 60 MeV proton therapy beamline

R. Schnuerer[1], J. S. L. Yap[1], H. Zhang[1], C. P. Welsch[1], T. Szumlak[2], A. Kacperek[3]

[1]University of Liverpool and Cockcroft Institute, UK. (Roland.schnuerer@cockcroft.ac.uk [primary author]), (Jacinta.yap@cockcroft.ac.uk [presenting author]), (Hao.zhang@cockcroft.ac.uk), (carsten.welsch@cockcroft.ac.uk). [2]Akademia Górniczo-Hutnicza, Physics, Krakow, Poland (szumlak@agh.edu.pl). [3]The Clatterbridge Cancer Centre NHS Foundation Trust, Wirral, UK. (andrzej.kacperek@nhs.net)

Introduction Online beam monitoring in medical accelerators is essential in assuring patient's safety as well as high quality and efficacy of cancer treatment. In clinical practice for proton therapy, currently used ionization chambers are interceptive devices, degrading both the beam profile and its energy spread. Therefore, a new non-interceptive approach of online beam monitoring is highly desirable.

Method The Vertex Locator (VELO) detector is a multi-strip silicon detector used in the LHCb experiment at CERN. The semi-circular design and position of its sensitive silicon detector offers a non-invasive way to measure the beam intensity through a precise measurement of the beam halo without interfering with the beam core. The adapted standalone VELO detector is integrated at the 60 MeV proton therapy beamline at the Clatterbridge Cancer Centre

(CCC), UK. Synchronised with a Faraday Cup and the RF cyclotron frequency, the quality of the beam monitor is assessed by measuring the beam current at different dose rates and by monitoring the beam halo profile at different positions along the beamline.
Results The integration zone of the VELO detector is after the double scattering foils, range shifter and modulation wheel. The detector can move along 15 cm along the beamline. The beam current is measured for the dose rate of 10 Monitor Units (MU)/min to 60 MU/min at position 0 cm, 8 cm and 15 cm each. Also, 2D and 3D beam profile measurements are presented for non-skewed and skewed beams. The results are benchmarked against GEANT4 simulations.
Conclusion The full setup optimized for implementation in the proton beam line at CCC is described. The capability of VELO as a beam monitor is assessed by measuring the beam current at different dose rates and by monitoring the beam profile. Further measurements in other proton therapy facilities with scanning systems are desirable.
Acknowledgements Work supported by the EU under grant agreements 215080 and 675265, as well as the Cockcroft Institute core Grant No. ST/G008248/1.

P70 Optimisation of multiple-source X-ray imaging systems with Monte Carlo methods

T. Primidis[1], J. Yap[1], C. P. Welsch[1], J. R. López[1], G. Travish[2]

[1]Cockcroft Institute/University of Liverpool, UK. (Thomas.Primidis@liverpool.ac.uk), (jacinta.yap@liverpool.ac.uk [Presenting author]), (welsch@liverpool.ac.uk), (jrestalo@liverpool.ac.uk). [2]Adaptix Ltd, Oxford, UK. (gil.travish@adaptiximaging.com)

Introduction Optimisation of X-ray medical imaging systems requires detailed simulations of their performance in silico. Monte Carlo simulations is one of the methods to achieve this and not only can they describe with great detail the performance of a system including all possible parameters that effect it but they also successfully reproduce the resulting images by simulating the detector response [1]. This work is a comparison between the Monte Carlo codes FLUKA [2, 3]/Flair [4] and GATE [5]/Geant4 [6–8] which proves that different codes successfully reproduce the performance of a multiple-source, X-ray medical imaging system and they produce similar results. This increases confidence on results before design realisation.
Method Monte Carlo methods are used to simulate an X-ray emitter array with 45 sources placed at a 7 × 7 configuration without the four corners and with 1cm pitch. All sources are disks, emitting 60keV monochromatic beams, having Gaussian beam spot radius with σ = 1.2mm and Gaussian divergence with σ = 6.67°. A PMMA block is used as an energy deposition detector and at a 1mm distance lie 3 trapezoid frustums representing teeth. The plane of the sources is at a 120mm distance from the detector.
Results As expected, the teeth cast shadows due to attenuation. The resulting images have minor differences but the overall quality is the same. Finer adjustment of each simulation parameter can decrease those differences.

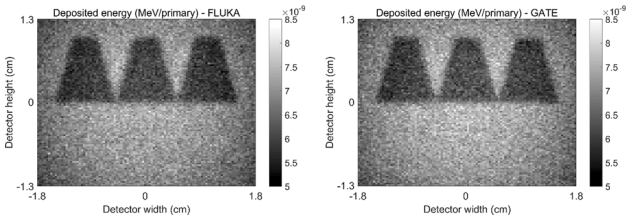

Conclusion Different Monte Carlo codes have been used and benchmarked against each other. Both system performance and detector response are described in detail, enhancing the system optimisation capabilities. Known 3D geometries were simulated to yield the resulting X-ray image from emitter array and the resulting images and errors were analysed to assess code performance.
Acknowledgements This project is funded by the Science and Technology Facilities Council (STFC) within the Accelerators for Safety, Healthcare and Environment project (ASHE) and it is a collaboration between the University of Liverpool and Adaptix Ltd. Finally, the Cockcroft Institute facilities are where research took place.

References

1. Skordis E, Vlachoudis V, Welsch CP (2017) A Monte Carlo Approach to Imaging and Dose Simulations in Realistic Phantoms Using Compact X-Ray Source. Proc. 8th Int. Particle Accelerator Conf. (IPAC'17). https://doi.org/10.18429/JACoW-IPAC2017-THPVA137
2. Böhlen TT et al. (2014) The FLUKA Code: Developments and Challenges for High Energy and Medical Applications. Nuclear Data Sheets 120:211–214
3. Ferrari A, Sala PR, Fasso' A, Ranft J (2005) FLUKA: a multi-particle transport code. CERN-2005-010, INFN-TC-2005-11, SLAC-R-773
4. Vlachoudis V (2009) Flair: A powerful but user friendly graphical interface for FLUKA. United States: American Nuclear Society - ANS.
5. Strulab D, Santin G, Lazaro D, Breton V, Morel C (2003) GATE (geant4 application for tomographic emission): a PET/SPECT general-purpose simulation platform. Nuclear Physics B - Proceedings Supplements 125:75–79. ISSN 0920-5632, https://doi.org/10.1016/S0920-5632(03)90969-8
6. Allison J et al., Recent developments in Geant4 (2016) Nuclear Instruments and Methods in Physics Research Section A: Accelerators, Spectrometers, Detectors and Associated Equipment 835:186–225. ISSN 0168-9002, https://doi.org/10.1016/j.nima.2016.06.12
7. Allison J et al. (2006) Geant4 developments and applications, IEEE Transactions on Nuclear Science 53:1:270–278. https://doi.org/10.1109/tns.2006.869826
8. Agostinelli S. et al. (2003) Geant4—a simulation toolkit. Nuclear Instruments and Methods in Physics Research Section A: Accelerators, Spectrometers, Detectors and Associated Equipment 506:3:250–303. ISSN 0168-9002. https://doi.org/10.1016/S0168-9002(03)01368-8.